In vivo/in vitro investigation of alphaxalone PK/PD sex differences in rats and other species

By
Mohammed Aldurdunji
PharmD, MSc

Thesis submitted for the degree of Doctor of Philosophy

University of Nottingham

2021

Abstract

Alphaxalone is an anaesthetic agent from the neurosteroids class and is currently licensed for cats, dogs and rabbits, while it is also being considered for human use. However, it has been reported that alphaxalone has PK/PD sex differences in rats. The cause of this difference is most likely to be sex related PK differences as has been observed by White, *et al.*, (2017). In general, the primary cause of PK differences tends to be related to sex-based differences in drug metabolism which is usually a reflection of sex differences in the expression of liver metabolism enzymes. This is most pronounced in rodents but has also been observed in humans, rabbits, dogs and monkey.

The aim of this study was to investigate the source of alphaxalone PK/PD sex differences in rats and whether this translates to dog, rabbit, monkey and human. An *in vivo* population PK analysis and *in vitro* investigation of alphaxalone metabolism were conducted in rats to determine sex specific optimal dosing and the major metabolism pathways for alphaxalone, respectively.

Thus, an *in vivo* rat comparison study for alphaxalone was conducted which consisted of two groups using a total of 56 rats (17 male and 23 female) with either Lewis (n=16) or Sprague Dawley (n=24) strains. Alphaxalone PK parameters in rats were determined via deterministic PK models and showed female rats to have significantly lower alphaxalone clearance in comparison to male rats (36.8±20 and 98.3±32 mL/min/kg respectively). This led female rats to have higher alphaxalone plasma exposure resulting in cardiovascular inhibition. A population PK model was developed for alphaxalone in male and female rats for both strains. Initially, strain and sex were the most significant covariates influencing the population typical PK parameter values. However, it was later shown that sex and body weight were most significant with a larger population set. Furthermore, Monte Carlo simulations were performed to address the variability in alphaxalone exposure in rats among the population. Analysis showed

that SD female rats need a 45% reduction in alphaxalone infusion rate in order to have equivalent plasma concentrations to SD male rats.

Furthermore, alphaxalone was investigated *in vitro* using fresh rat hepatocytes in male (n=9) and female (n=6). The sex bias was also observed *in vitro* as male intrinsic clearance for disappearance of alphaxalone was approximately 5-fold larger than female rats. In addition, the male rats had significantly larger V_{max} compared to female (135±54 versus 12±6 nmol/min), whereas K_m was only marginally larger in male (170±106 versus 64±85 μM). Furthermore, the extrapolated *in vivo* hepatic clearance (Cl_H) compared to the estimated clearance from the *in vivo* study were in close agreement.

In addition, alphaxalone metabolite and metabolism pathway identification in rat showed the identification of two distinct alphaxalone metabolites (Keto-alphaxalone and beta-alphaxalone) and the observation of an unidentified third alphaxalone (M3) metabolite and sex differences for the rate of metabolite formation were demonstrated. Using the knowledge acquired for alphaxalone metabolite formation in rats a mathematical kinetic model was created that described the metabolic pathway and estimated the metabolism conversion rate constants. This allowed the magnitude of sex differences to be determined for alphaxalone in rats, human, dog, rabbit, and monkey. Rats showed the largest difference in alphaxalone in vitro clearance between the sexes as well as sex differences in the alphaxalone metabolism kinetic rates and direction of the pathways. While the other species did not show clear sex differences in alphaxalone in vitro clearance each species showed different preferences in the direction of alphaxalone metabolism pathways as well as producing alphaxalone metabolites that were different to rats.

The work presented in this thesis showed a clear PK sex difference for alphaxalone exposure in rats which consequently allowed the optimisation of a new dosing regimen for alphaxalone in female rats so as to mitigate the differences in

alphaxalone exposure and reduce cardiovascular effects. Furthermore, as rats are a major laboratory species the in vitro studies have rationalised the understanding of clinical alphaxalone exposure differences between male/female rats as well as a mechanistic understanding of differences in resulting cardiovascular effects.

Declaration

I declare that the work presented in this thesis was carried out in accordance with the requirements of the Nottingham University Regulations.

The work is original except where indicated by specific reference in the text and has not been submitted for any other academic award at the University of Nottingham or any other institution.

Name: Mohammed Aldurdunji

Signed: 

Date: 06/02/2021

Dedication

This thesis is dedicated to the memory of my father, Maher Aldurdunji, who passed away in June 2015 while I was completing my Master of Science Course. I could not attend his funeral at the time, and I miss him every day. I wish that he could have seen this process through to its completion. Furthermore, to the memory of my friend, Khaled Shibany, who passed away in Sep 2020 due to COVID-19 complications. May both of their souls rest in peace.

Publications and poster participation

- Postgraduate Research Conference - 2017 poster (1st place prize)
- Postgraduate Research Conference - 2018 oral presentation
- Postgraduate Research Conference - 2019 oral presentation
- Symposium – Dx Toxicology: Strategies for Success in Discovery and Development – 2019 poster (1st place prize)
- 48th DMDG Open Meeting 2019 – poster and oral presentation
- Shibany, K. A., Pratt, S. L., Aldurdunji, M., Totemeyer, S., & Paine, S. W. (2020). Prediction of pharmacokinetic clearance and potential Drug-Drug interactions for omeprazole in the horse using *in vitro* systems. Xenobiotica, 50(10), 1220–1227. https://doi.org/10.1080/00498254.2020.1764131
- Paine, S. W, Aldurdunji M,. Hincks P. R, (2021). Plasma and urine pharmacokinetics of hydroxyzine and cetirizine following either repeated oral administrations of hydroxyzine or cetirizine to exercised horses. (submitted)

Table of contents

Abbreviations

BSA	Bovine serum albumin
°C	Degree Celsius
Cl_H	Hepatic clearance
CL_{int}	Intrinsic clearance
CYP	Cytochrome P450
DMSO	Dimethyl sulphoxide
EGTA	Ethylene glycol-bis (β-aminoethylether)-N, N, N', N'-tetraacetic acid
f_{up}	unbound fraction in plasma
g	Gram
g	Relative Centrifugal Force
HPGL	Hepatocellularity Per Gram of Liver
HBSS	Hanks' Balanced Salt solution
l	Litre
mg	milligram
µg	microgram
ml	millilitre
µl	microliter
mM	millimolar
µM	micromolar
nmol	nano mole
MPPGL	Microsomal Protein per Gram of Liver
nm	nanometre
NADPH	Nicotinamide adenine dinucleotide phosphate (reduced)
NMDA	N-methyl-D-aspartate
PBS	Phosphate buffered Saline
SD	Standard deviation
WEM	Williams' medium E
$GABA_A$	Gamma aminobutyric acid receptor type A
3α-HSD	3-alpha hydroxy steroid dehydrogenase
3β-HSD	3-beta hydroxy steroid dehydrogenase
17β-HSD10	17β-hydroxysteroid dehydrogenase type 10
PK	Pharmacokinetics
PD	Pharmacodynamics
popPK	Population pharmacokinetics

Chapter 1

General introduction

1. Chapter 1: General introduction

Brief Introduction

The process of discovering and developing new drugs is a difficult and tedious procedure with a high failure rate. Through the years there has been a decline in the launch of new drugs while at the same time there has been an increase in research and development (R&D) costs. The vast majority of drug attrition in clinical trials is the lack of therapeutic response or the development of unexpected toxicity that led to failure. Usually when a drug candidate reaches the stage of clinical trials, the pharmaceutical company has already spent millions of dollars on research and development. However, the biggest cost is conducting human trials. Unfortunately, drug candidates' attrition rate in the human trials stage is not necessarily therapeutic class or target specific. However, some therapeutic areas have a higher level of attrition rate than others. For example, the failure rate in oncology and women's health is as high as 30% and 42%, respectively (Kola & Landis, 2004).

The most predominant cause of attrition has been due to poor understanding of the pharmacokinetics (PK) and pharmacodynamics (PD) of candidate drugs. In 1991, the pharmacokinetics of a drug was the most significant cause of drug attrition with an estimated fail rate of 40% (El-Kattan & Varma, 2012). After targeting pharmacokinetic issues in the drug discovery stage, the failure rate decreased to less than 10% by 2000. In addition to poor PK, drug efficacy (pharmacodynamics) was and still is another major cause of attrition (Kola & Landis, 2004). As such, a full understanding of the PK and PD during drug discovery will assist in reducing the attrition rate in development and clinical trials.

New Chemical Entities (NCEs) with novel mechanisms of pharmacological action show high reward as a first in class drug but have higher rates of attrition than NCEs that work via established mechanisms. This might explain the higher rate of

oncology drug failures, as each company competes to create compounds that act on a novel target (Kola & Landis, 2004).

Two key questions should be answered in the drug development and selection process. Firstly, has the best drug been chosen, and secondly has the optimal dosage regimen been established. In order to answer these questions an integrated (PK/PD) model approach would assist in formulating the answers. However, in most preclinical and clinical studies, male participants are predominantly used in order to test the NCEs (Liu & Dipietro Mager, 2016) which bias the selection process. There are physiological differences between males and females, and these sex differences have the potential to lead to differences in PK and PD.

These sex differences are more apparent in drugs that are either used for chronic diseases, such as, hypertension and epilepsy or administered continuously such as during anaesthesia. In these cases, frequent dose monitoring is usually used for long-term treatments and dose sensitive diseases. However, dose monitoring is difficult to apply on single long exposure medications, such as, anaesthetic drugs and most of the dose adjustment process is based on physiological observations to reach stable conditions. Unfortunately, some of these drugs have a narrow therapeutic index, which in the case of an incorrect administration can lead to fatal cases (Blix et al., 2010).

Sex differences in anaesthesia

It is well documented that there are dose ranges for anaesthetic drugs, and differences in outcome measures such as recovery times between males and females for humans (Ciccone & Holdcroft, 1999) and animals (Zambricki & D'Alecy, 2004). Using an integrated (PK/PD) model approach would assist in detecting the causes of these differences and determine the adjustment needed to have ideal conditions for both PK and PD.

Thus, the focus of this introduction will be solely on sex differences related to neurosteroidal anaesthetic agents and how PK/PD modelling would assist in identifying the causes of these differences in the physiological body of animals and ultimately humans.

1.1. Anaesthesia

The term Anaesthesia means loss of sensation, which can be in a state of unconsciousness (for general anaesthesia), or it can be reduced sensitivity and response to a small area of the body (local anaesthesia)(Flecknell P, 2016). General anaesthesia is a broad term encompassing the use of drugs to induce a safe and controllable loss of consciousness, lack of movement and pain responses to noxious stimulation coming from the medical procedure (Billard, 2015).

In preparation for the procedure, one or more anaesthetic agents may be used. Anaesthetic agents are a diverse group of drugs that are made of markedly different chemical structures that ranges from inert gases and simple inorganic agents (xenon, ether, and nitrous oxide) to more complicated organic agents like barbiturates and benzodiazepines. General anaesthesia has been used for almost 175 years to facilitate surgery procedures and to relieve pain and suffering (Garcia et al., 2010).

Theory of anaesthesia

Despite the technological advancement in perioperative medicine, some anaesthetics are still being used without a precise understanding of their mode of action. There has been however more recent advancement in understanding the inhaled anaesthetics which conclude that inhaled anaesthetics bind and disrupt the lipid rafts which will activate an ion channel in a two step mechanism (Pavel et al., 2018). Whilst, the widely accepted theory for injectable general anaesthetic is the protein theory (Uwe Rudolph & Antkowiak, 2004). According to the theory, anaesthetic agents interact with protein targets in the central synaptic transmission. At clinical concentrations, several anaesthetics have been shown to

alter the activity of protein receptors and ion channels by synaptic transmitters. Moreover, these agents are able to reduce the presynaptic neurotransmitter release via voltage-gated calcium channels while inhibiting postsynaptic effects by decreasing the excitatory neurotransmitters or increasing the inhibitory neurotransmission (Uwe Rudolph & Antkowiak, 2004).

GABA and its subtypes

The main inhibitory neurotransmitter in the central nervous system is γ-aminobutyric acid (GABA). GABA mediating receptors are estimated in approximately 33% of the synapses in the cerebral cortex of mammalians. As such, inhibiting them can be essential in both the short and long term inhibition of synaptic transmission (Wang, 2011). Two major types of GABA receptors have been identified: $GABA_A$ and $GABA_B$ receptors (Bormann, 2000). $GABA_B$ receptors are G protein-coupled receptors and are mainly unaffiliated in general anaesthesia. In contrast, $GABA_A$ receptors are ligand-gated ion channels which are responsible for chloride channel release. They are pentameric proteins that consist of two α-subunits, β-subunits and one subunit of either δ, γ, ε, π, θ or ρ subunits (U Rudolph et al., 2001; Wang, 2011). This makes $GABA_A$ receptors heterogenic and they possess a high degree of variability in their structural features and subunit composition. Due to this, a wide range of endogenous agonists and antagonists for these receptors are present and each ligand has its distinct affinity and efficacy (Mitchell *et al.*, 2008).

$GABA_A$ importance

Neuropharmacologists over the last 25 years have revealed that the most important target site for general anaesthesia is the $GABA_A$ receptor (Garcia et al., 2010). Activation of the postsynaptic $GABA_A$ receptors cause an increase in chloride conductance which results in cellular hyperpolarisation, which depresses the neuronal function and firing rate (Uwe Rudolph & Antkowiak, 2004). Enhancing

or prolonging the activation of $GABA_A$ receptors appears to be a common mode of action for several anaesthetic agents of either the injectable or inhaled type.

$GABA_A$ substrates

The most commonly known $GABA_A$ acting anaesthetics are barbiturates, benzodiazepines, propofol and neurosteroids (Garcia, *et al.*, 2010). Due to their pharmacological mode of action on $GABA_A$ receptors, these compounds can be used as anticonvulsants and anxiolytic agents in addition to their sedative and hypnotic effect. Moreover, these drugs act as positive allosteric modulators for the $GABA_A$ receptors and can bind to other receptors. However, the neurosteroidal group binds almost exclusively to $GABA_A$ receptors and at a site distinct from the barbiturates and benzodiazepines (Paul & Purdy, 1992; Wang, 2011).

1.2. Neurosteroids

Neurosteroids are steroids synthesized in the brain and can rapidly modulate neural excitability by binding to an extracellular binding site with no genomic action (Lambert *et al*, 2003). The term neurosteroids applies to both synthetic and endogenous steroids that rapidly alter CNS excitability (Reddy & Kulkarnia, 1999).

1.2.1. History of steroids in anaesthesia

It has been recognised for a long while, that steroidal hormones have anaesthetic and sedative activity in animals and humans. It was first reported over 70 years ago that the metabolic reduced form of progesterone and deoxycorticosterone, which are allopregnanolone and allotetrahydro-deoxycorticosterone (THDOC) respectively, were extremely potent anaesthetic agents (Majewska et al., 1986; Doodipala S. Reddy, 2003; Selye, 1941). Soon after, both THDOC and allopregnanolone proved to be among the most potent known ligands for $GABA_A$ receptors. Their affinities are equal to benzodiazepines and a thousand times higher compared to pentobarbital (Paul & Purdy, 1992). Furthermore, allopregnanolone at nanomolar concentrations enhances the affinity of GABA towards its receptor, modulates 5-HT_3 receptors, neuronal nicotinic acetylcholine

receptors and voltage-activated calcium channels though at micromolar concentration. Hence, the neurosteroids at lower doses produced anxiolytic, analgesic, anticonvulsant, sedative and hypnotic effects. Due to this activity, they provide tremendous opportunities for developing therapeutics approaches in anaesthesia and other brain disorders (Rupprecht, 2003).

1.2.2. Neurosteroids structure and biosynthesis

Both steroids and neurosteroids are synthesised from cholesterol by a series of enzymes (Figure 1.1) mediated by CYP450 and non P450 enzymes (Carver & Reddy, 2013). The idea of steroidogenic glands such as the gonads, adrenals cortex and placenta being the only source of the neurosteroids was believed in the past. However, the converting enzymes responsible have now been documented by mRNA and protein analysis to be present in the nervous system of the rat, human and other vertebrate species (Do Rego et al., 2009; Mellon & Deschepper, 1993; Doodipala Samba Reddy, 2010). Neurosteroid synthesis is controlled by various families of enzymes including P450 side-chain cleavage, oxo-reductase (dehydrogenase), sulfotransferase and sulfuryl transferase (Figure 1.1). Most of these enzymes are involved in de novo steroidogenesis in the brain. The sulphated derivative of pregnenolone (dehydroepiandrosterone sulphate (DHEAS) and pregnenolone sulphate) inhibits GABA release, binds and promotes the activity of N-methyl-D-aspartate (NMDA) receptors hence producing excitatory action (Porcu et al., 2016).

The first and rate-limiting step for steroid biosynthesis is cleaving the extra side chain attached for cholesterol by the P450 side-chain cleavage enzymes ($P450_{scc}$); this leads to the formation of pregnenolone which is the cornerstone of steroid biosynthesis. Several enzymes then take over based on which direction the bioreaction is moving, however for neurosteroid synthesis, pregnanolone and androstenediol are oxidised by 3β-hydroxysteroid dehydrogenase (3β-HSD) and converted to progesterone and testosterone, respectively. Furthermore,

progesterone can also undergo chain modification by CYPC21 and generate deoxycorticosterone (DOC). The three generated products are catalysed by 5α-reductase (5α-R) enzyme that reduces the C_4-C_5 double bond. The 5α-R enzyme is a microsomal enzyme that is most known for its irreversible catalytic activity (Compagnone & Mellon, 2000). Furthermore, it is active only on steroids that contain ketone groups at the C_3 position and unsaturated double bonds at C_4-C_5 (Do Rego et al., 2009). The products, dihydro-progesterone (dihydroPROG), DHT and dihydroDOC, are then reduced via 3α-hydroxysteroid dehydrogenase (3α-HSD) to generate all the active neurosteroids.

Based on the parent steroids, the neurosteroids can fall into three different classes (Figure 1.1). The first class and the most active group is the pregnane neurosteroids, such as allopregnanolone and allotetrahydrodeoxycorticosterone (THDOC). The second class is the androstane neurosteroids, such as androstanediol and etiocholanone. The final class is the sulphated neurosteroids, such as, dehydroepiandrosterone sulphate (DHEAS) and pregnenolone sulphate (Wang, 2011).

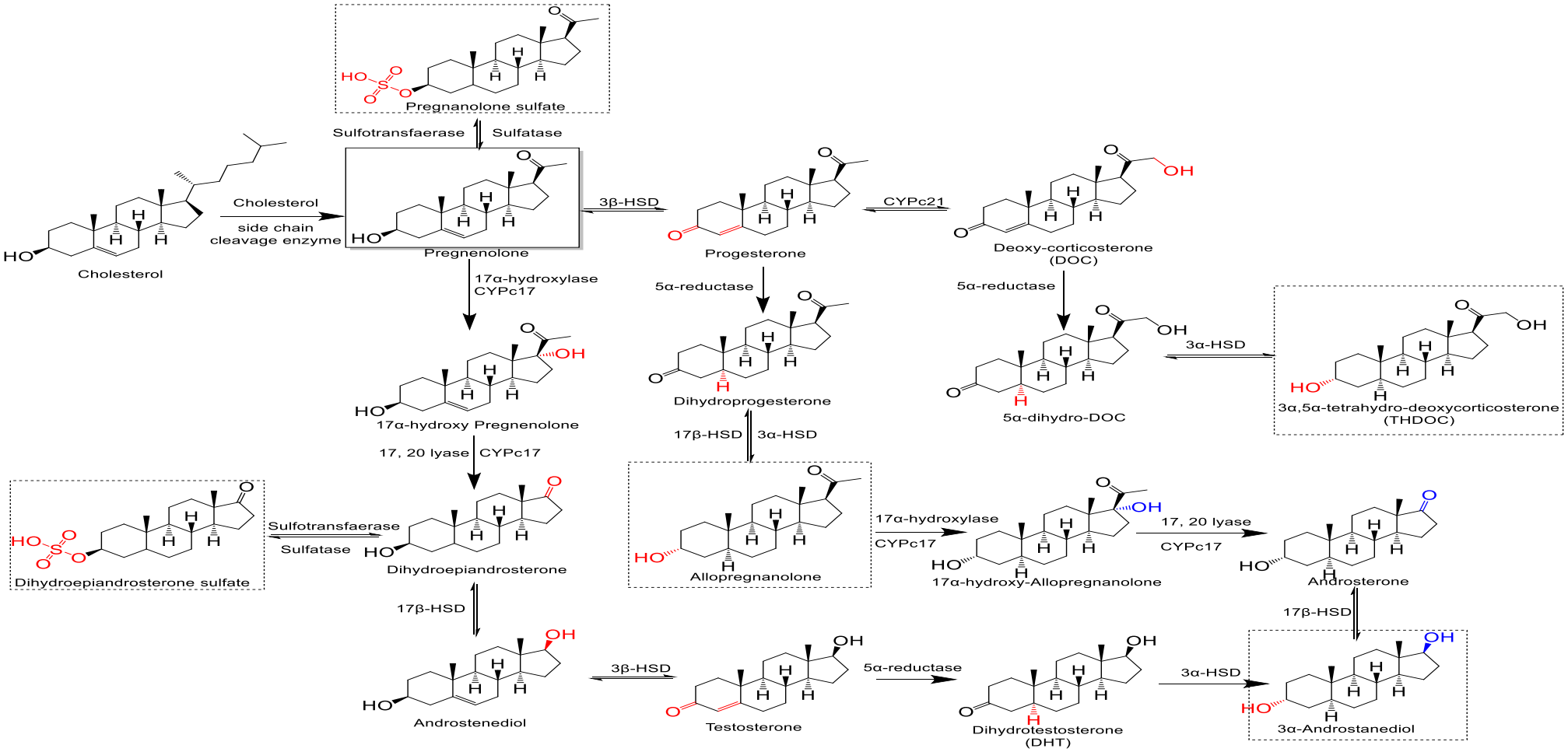

Figure 1.1. Neurosteroid synthesis pathway from each representative steroid branching from the basic building block cholesterol. P450C17, cytochrome P450 17α-hydroxylase/C17,20-lyase; P450c21, 21-hydroxylase; 3α-HSD, 3α-hydroxysteroid dehydrogenase; 3β-HSD, 3β-hydroxysteroid dehydrogenase; 17β-HSD, 17β-hydroxysteroid dehydrogenase.

1. 3β-hydroxysteroid dehydrogenase (3β-HSD) enzyme

The 3β-HSD is a membrane bound enzyme that reversibly catalyses the conversion of Δ^5-3β-hydroxysteroids into Δ^4-3-ketosteroids utilising NADPH as cofactor (Figure 1.1). This enzyme is one of the oxo-reductase enzymes that play a crucial role in the biosynthesis and regulation of steroids hormones. The enzyme has been identified in humans, primates, rodents, birds, fish and amphibians (Do Rego et al., 2009; Rhéaume et al., 1991; Vaudry et al., 2011). The enzyme is expressed in the placenta, adrenal gland, gonads and skin as well as in the liver (Rhéaume et al., 1991).

2. 3α-hydroxysteroid dehydrogenase (3α-HSD) enzyme

The 3α-HSD is similar to 3β-HSD in which both are NADPH dependent and both can reversibly reduce and oxidise the C_3 of steroids. The enzyme is expressed all around the body, including the brain and liver. However, its oxidation ability is 7-fold less than its reduction capability (X. Y. He et al., 2005). Moreover, it has been reported that type 10 of 17β-hydroxy steroid dehydrogenase (17β-HSD10) is more active in oxidation at C_3 compared with 3α-HSD (X. Y. He et al., 2019) and it is also known as 3-hydroxyacyl-CoA dehydrogenase type-2 (Shafqat et al., 2003).

1.2.3. Neurosteroid substrates

Several synthetic neurosteroids were created as general anaesthetics. The well-known agents of this group are hydroxydione, alphaxalone, alphadolone, minaxolone and ganaxolone (Korpi & Sinkkonen, 2006). Hydroxydione proved to be a safe and reliable anaesthetic drug. However, it caused pain and irritation at the injection site, which led to refinement and development of alphaxalone/alphadolone. This mixture was very lipophilic and was solubilised via Cremophor-EL, which is a poly-oxylated castor oil-based surfactant and was marketed for human and veterinary use as Althesin® and Saffan®, respectively. However, it was withdrawn due to cases of anaphylactic reactions from the presence of Cremophor-EL (Clarke et al., 1973). In the mid-1990s Althesin® was

withdrawn from the medical market for humans. Minaxolone which has shown more significant activity than the previous agents (Mitchell et al., 2007), also failed to gain market authorisation as it failed to show clinical advantages due to a prolongation of recovery time in comparison to propofol and thiopental (Korpi & Sinkkonen, 2006; Tang et al., 1997). Ganaxolone is being tested as a potential new treatment for human neonate seizures (Yawno et al., 2017) and is currently undergoing Phase III trials.

Recently, a newer formulation of alphaxalone (with no alphadolone) in 2-hydroxypropyl-β-cyclodextrin (HPCD), as the solubilising agent, has been developed for small animals (cats and dogs) and marketed as Alfaxan® by Jurox Pty Ltd. The newer formulation lacks the histamine release associated with the solubilising agent Cremophor-EL while maintaining the same pharmacological properties (Flecknell, 2016).

1.3. Alphaxalone (alfaxalone):

Alphaxalone (3α-hydroxy-5α-pregnane-11, 20-dione) is a synthetic progesterone analogue neurosteroidal anaesthetic agent (Carver & Reddy, 2013). Structurally, alphaxalone and its class resemble endogenous steroidal hormones by having the same core structure of four fused rings (Figure **1.2**). The interest in alfaxalone is increasing in the biomedical sciences and clinical veterinary medicine as it is able to offer some selective advantages over other anaesthetic combinations (Santos González *et al.*, 2013). In clinical studies it has been demonstrated to have good safety and a large therapeutic window, minimal pain on injection and low cardiopulmonary depression and reflex suppression while having satisfactory muscle relaxation effect (Goodwin et al., 2012; Tammisto et al., 1973; Tamura et al., 2015). Furthermore, it has a rapid onset of action and offset which allows rapid recovery from anaesthesia without any signs of accumulation after repeated doses; allowing alphaxalone to be titrated for an effective dose and maintaining anaesthesia without prolonging the recovery time (West, 2017; Whittem et al.,

2008). This would make alphaxalone a promising alternative candidate to the already existing arsenal of intravenous anaesthetics.

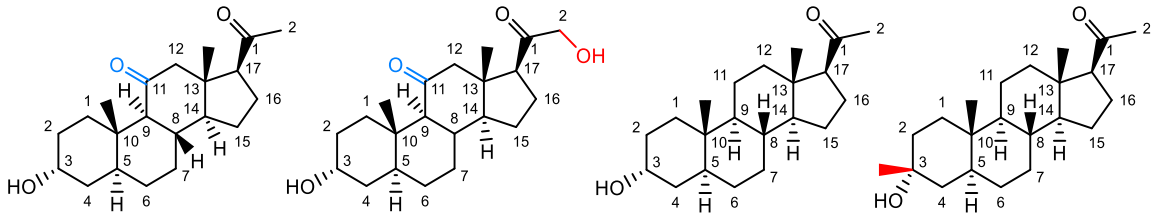

Alphaxalone Alfadolone Allopregnanolone Ganaxolone

Figure 1.2: **Alphaxalone chemical structure comparison with alfadolone and allopregnanolone.** Structural similarities and dissimilarities are highlighted in blue and red respectively.

Alphaxalone's controversial history

Alphaxalone was first launched in 1971 as Althesin®, as a combination of alphaxalone and alphadolone (Figure **1.2**) (0.9 and 0.3% respectively) suspended in 20% cremophor for injection for veterinary anaesthesia. Due to alphaxalone hydrophobicity, the early formulation required the addition of castor oil (Cremaphor-EL) to enhance solubility. However, the alphaxalone-castor oil formulation induced anaphylactic reaction in many species, including cats and dogs (Warne et al., 2015). Althesin was also reported to cause anaphylactic reactions in people who received the the old formulation at the time. The reported reactions were one of the highest between the intravenous anaesthetic agents available at the time and led to voluntary withdrawal from the market (Haworth et al., 2019; J. Sear, 1996).

Recently, a newer formulation of alphaxalone in 2-hydroxypropyl-β-cyclodextrin (HPCD), as the solubilising agent has been developed. The cyclodextrin vehicle is a cyclic oligosaccharide molecule with a hydrophilic surface and hydrophobic core that allows a hydrophobic molecule (alphaxalone) to reside and be delivered to target cells. It is also a common substance approved by the US Food and Drug Administration, frequently used as a solubilizing agent to improve delivery of several low solubilising drugs (Loftsson et al., 2005).

Currently, alphaxalone is registered for intravenous (IV) administration for induction and maintenance of anaesthesia in dogs, cats and rabbits in most of the world (Warne et al., 2015). It has also been used in pigs (Keates, 2003), horses (Goodwin et al., 2011), sheep (Andaluz *et al.*, 2012), monkeys (Bertrand, et al., 2017) and other exotic species (McMillan & Leece, 2011; Villaverde-Morcillo *et al.*, 2014). The registration of the new formulation started in the Australian market during 2001, later the UK and Europe adopted it in 2007 and 2008 respectively and lastly Canada and the USA in 2011 and 2012 (Haworth et al., 2019). However, the world adoption rate of alphaxalone in the new formulation was slow, possibly due to the previous reaction observed from the older formulation.

Alphaxalone pharmacology:

Enhancing or prolonging the activation of $GABA_A$ receptors appears to be a common mode of action for several anaesthetic agents of either the injectable or inhaled type. Alphaxalone and the neurosteroidal class of agents bind almost exclusively to $GABA_A$ receptors at a site distinct from the barbiturates and benzodiazepines (Figure **1.3**) (Paul & Purdy, 1992; Wang, 2011).

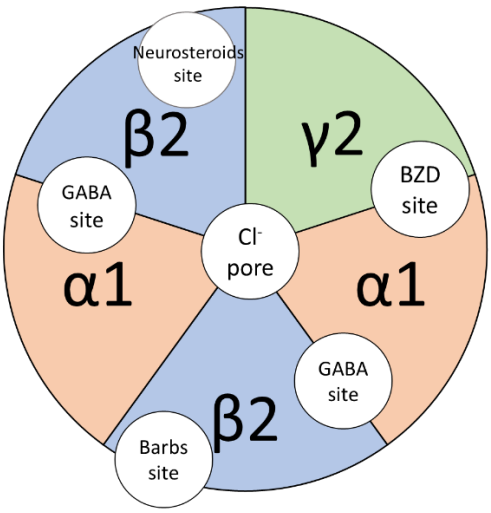

Figure 1.3: Schematic diagram of $GABA_A$ receptor and the location of various ligand-binding sites. The channel has multiple receptor sites where GABA, barbiturates (Barbs), benzodiazepines (BZD) and neurosteroids bind to exert their effects. The binding site of each of these groups is in a distinct location from each other.

Detailed mechanistic investigations of alphaxalone has revealed that it has a dual mechanism of action. At low concentration, it allosterically modulates the $GABA_A$ receptor; and at higher concentration (≥1μM) alphaxalone can directly activate the $GABA_A$ receptors as an agonist (Paul & Purdy, 1992). Hence, similarly to the benzodiazepines and the barbiturates, there has been a renewed interest in the neurosteroids as novel treatments of anxiety, insomnia, depression and seizure disorders (Visser et al., 2002). In addition, unlike the benzodiazepines and the barbiturates, neurosteroids are reported to increase the expression of $GABA_A$ receptors which make them less susceptible to develop tolerance (Martinez-Botella et al., 2014).

$GABA_A$ receptors and neurosteroid interaction

$GABA_A$ receptors are pentameric proteins that consist of two α-subunits, the β-subunits and one subunit of either δ, γ, ε, π, θ or ρ subunits (Rudolph et al., 2001; Wang, 2011). Due to this variability, a wide range of endogenous agonists and antagonists for these receptors are present, and each ligand has a distinct affinity and efficacy (Mitchell *et al.*, 2008). However, $GABA_A$ receptor sensitivity to neurosteroids is modulated by several factors including receptor subunit composition. Although neurosteroids bind to most $GABA_A$ subunit configurations, unlike benzodiazepines, different isoforms of α and γ subunits influence their efficacy and potency level (Brown et al., 2002; Carver & Reddy, 2013; Lambert et al., 2003). For instance, the synaptic strength of $GABA_A$ receptors comprised of $\alpha_1\beta_2\gamma_2$ subunits (female dominant) possesses faster and prolonged activation in comparison to those made of $\alpha_2\beta_1\gamma_2$ subunits when bound to allopregnanolone (endogenous neurosteroid) (Lavoie et al., 1997). These differences in neural excitability are due to sexual dimorphism (Galanopoulou, 2005; Wang, 2011), as progesterone and allopregnanolone were able to decrease the neural activity of male and female mice, however, greater effects were observed in females

compared to males (Reddy et al., 2004). This sex-specific polymorphism might explain the PD response differences observed between sexes.

Alphaxalone pharmacokinetics

The pharmacokinetic properties of alphaxalone have been determined in dogs (Ferré et al., 2006), cats (Muir et al., 2009), rats (Visser et al., 2002; Lau et al., 2013; White, et al., 2017) and horses (Goodwin et al., 2011; Goodwin et al., 2012). In general, alphaxalone is characterised by fast and smooth induction of anaesthesia and rapid recovery.

Dogs

Alphaxalone demonstrated excellent short term anaesthesia in dogs and dose dependent cardiovascular inhibition effect as well as apnoea and hypoventilation correlated to dose (Muir et al., 2008; Tamura et al., 2015). Furthermore, the clearance and volume of distribution values reported for IV bolus injection of alphaxalone to dogs were 65 and 54 mL/min/kg and 2.2 and 2.5 l/kg for female and male dogs, respectively. (Ferré et al., 2006).

Cats

Similarly to dogs, alphaxalone demonstrated good to excellent anaesthesia in cats characterised by muscle relaxation and unresponsiveness to noxious stimuli (Muir et al., 2009). Following a bolus IV dose of 5 mg/kg, the anaesthesia was characterised by a stable plane of anaesthesia with infrequent hypoventilation and apnoea, normal heart rates and a smooth and uneventful recovery. In cases where the premedication component is inadequate or omitted the recovered cats can be excitable. The reported clearance and volume of distribution values of alphaxalone in un-premedicated cats were 25 ml/min/kg and 1.8 L/kg respectively (Whittem et al., 2008)

Horse

The induction of anaesthesia by alphaxalone in horses was also smooth, with little to no muscle rigidity (Goodwin et al., 2011). The reported clearance was 37 mL/min/kg while volume of distribution was 1.6 L/kg (Goodwin et al., 2011). The PK values however, were comparatively lower in foals as they were almost half the reported values for the adult horses (Goodwin et al., 2012). This observation for foal metabolism is consistent with other drugs that reportedly have increased clearance with horse age (Norman et al., 1997)

Human

Most studies in human were conducted using the old formulation of alphaxalone (Althesin). However, there should not be a significant difference between this and the new formulation for the PK parameters of alphaxalone (Monagle et al., 2015). The reported PK values for alphaxalone using the old formulation as an IV bolus administration were 20.57-22.42 mL/min/kg for the clearance and 0.69-0.77 L/kg for the volume of distribution (J. Sear, 1996). A newer alphaxalone formulation made for humans (PHAXAN^{TM}) is being investigated and the outcome of the phase 1 trial has been recently published by Goodchild *et al*., (2020). The reported study outcomes were for male humans using IV bolus injection of alphaxalone with values of 0.37 L/kg for Vd and 15.71 mL/min/kg for clearance. However, the reported PK parameters are slightly lower compared to previously reported human data using Althesin formulation.

Rats

In rats, alphaxalone has been administered intraperitoneally (IP) and intravenously (IV). The IP administration required less restraint, however, the effects of alphaxalone were more unpredictable compared to the IV route, as 30% of rats failed to achieve complete immobilisation in one study (Lau et al., 2013). Furthermore, alphaxalone was shown to have low bioavailability due to first pass metabolism in the liver and a prolonged effect as well as requiring 2-3 times the doses used for IV administration (J. W. Sear & McGivan, 1981). Alphaxalone PK

parameters using IV infusion were 48 and 92 mL/min/kg for clearance while for the volume of distribution values were 3 and 2.8 L/Kg for female and male SD rats respectively (White et al., 2017). Other groups reported alphaxalone PK parameters for Wistar rats (Lau et al., 2013; Visser et al., 2002) with clearance values of 158 and 55 ml/min/kg for male and female, respectively. However, the clearance reported by Visser *et al.* was based on body weight covariates and corrected for blood clearance using the equation: 158 x $BW^{1.67}$ ml/min/kg. Furthermore, alphaxalone clearance in males was approximately equal to rat liver blood flow which is approximately 20 ml/min for a rat weighing 300g. This make alphaxalone clearance in male Wister rats very close and limited by liver blood flow, which make it blood flow dependent and thus suggesting that rat body weight is a covariate for alphaxalone clearance.

Interestingly, pure alphaxalone administration to male rats showed a slightly faster clearance than alphaxalone formulated in cyclodextrin (ALPHAX®) (Visser et al., 2002). While in comparison, alphaxalone's old formulation (Althesin) has a slightly slower clearance rate for IP administration. The cause of the clearance differences for the old formulation may be due the presence of alfadolone (Figure **1.2**) which is structurally very similar to alphaxalone but less effective. The existence of alfadolone may have caused competitive inhibition at the drug metabolising enzyme site leading to a lower clearance.

Alphaxalone metabolism

Alphaxalone is metabolised rapidly in the liver, and a small amount is metabolised in the lung and kidneys (Sear & McGivan, 1981; Warne et al., 2015). Due to its rapid metabolism it does not accumulate in the tissues (Suarez et al., 2012). It has a large margin of safety as it required 28 times the clinical dose in cats to cause a toxic effect (Warne et al., 2015). Studies in humans, dogs, cats and rats showed that alphaxalone metabolites are primarily excreted in urine and a small amount is excreted in bile (Sear, 1996; Warne et al., 2015).

In most species, alphaxalone was found to be liver metabolised through phase-I (CYP450 dependent) and phase-II (glucuronidation and sulphate dependent conjugation) pathways, although the only metabolite identification study was conducted in-house by Jurox Pty Ltd (Warne et al., 2015). In cats and dogs, both species produced the same metabolites (Figure 1.4) (Warne et al., 2015). Phase-I metabolites were allopregnatrione, 3β-alfaxalone, 20-hydroxy-3β-alfaxalone, 20-hydroxy-alfaxalone and 2α-hydroxy-alfaxalone, whilst phase-II metabolites observed were alphaxalone-glucuronide (major in dog and cat), 20-hydroxy-alphaxalone-sulphate (minor in dog and major in cat), 2α-hydroxy-alfaxalone-glucuronide (dog only) and 3β-alfaxalone-sulphate (cat only) (Warne et al., 2015). Due to its rapid metabolism alphaxalone is only available in an injectable formulation.

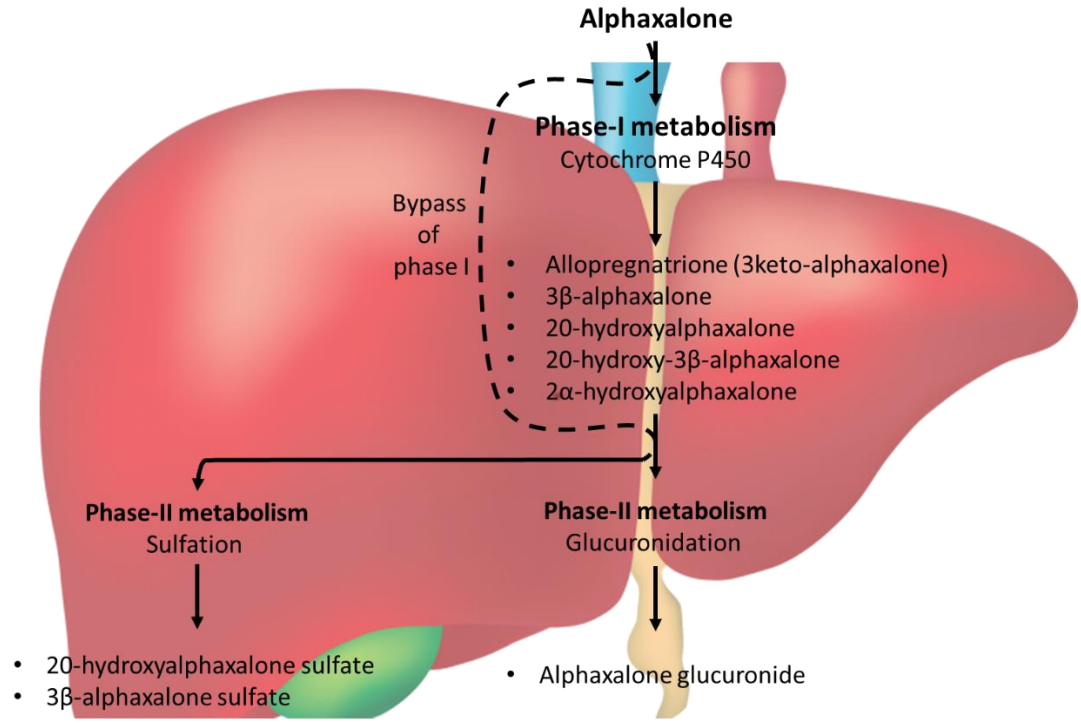

Figure 1.4: Alphaxalone metabolic pathway in the liver of feline and canine.

It has been hypothesised that the reason for the high *in vivo* clearance and low bioavailability of the neurosteroids is due to rapid primary and secondary catalytic reactions at the C_3 position, which in alphaxalone case, it starts with oxidation to

a ketone and then a conjugation reaction follows to the alcohol formed in the beta position by reduction (Martinez-Botella et al., 2014). The responsible converting enzyme for 3α-oxidation has been reported to be catalysed by microsomal 3α-hydroxysteroid dehydrogenase (3α-HSD), which also acts as a 3-keto-steroid reductase (He et al., 2005). While the formed ketone product may be reduced by either 3α- or 3β-HSD enzymes

Sex differences in effects and kinetics

Sex related differences in anaesthetic effects have been reported with old and new formulations of alphaxalone (Arenillas & Gomez de Segura, 2018; Fink et al., 1982). The old formulation required four times the dose for male SD rats to achieve the same plane of anaesthesia as female rats using IP administration. Furthermore, it required three times the dose for male compared to female SD rats using IV administration with the new formulation. The cause of the sex difference for IP administrations was attributed to the presence of oestrogenic hormones which potentiate the anaesthetic effects (Fink et al., 1982), while others have suggested that differences of allopregnanolone concentration may increase the clinical sensitivity of alphaxalone after dosing in female rats (Estes et al., 1990). However, the latest findings suggest that the sex differences observed for alphaxalone in rat is PK dependent with female having a lower clearance than male rats (White et al., 2017). Furthermore, the clearance differences between male and female rats were also evident from other groups using Wister rats (Lau et al., 2013; Visser et al., 2002). However, there was no clear understanding of the factors that cause these findings in rats and whether it was present in other species.

1.4. General sex differences

Sex differences are evident throughout mammals, even at the most basic cellular level. Every cell in the human body carries either of the male chromosomes (XY) or the female chromosomes (XX) but not both (Arnold & Burgoyne, 2004). Sex

differences extend beyond the level of size and shape differences. It is a vast area which is difficult to cover in this review. Sex differences in PD and PK has been observed in the field of general anaesthesia, such as barbiturates (Hoffman & Levy, 1989), midazolam (Sun, et al., 2008) and ketamine (Lees, et al., 2004). It is well documented that in order to attain comparable level of anaesthesia or recovery time there are differences in dose administration between male and females in humans (Ciccone & Holdcroft, 1999) and animals (Zambricki & D'Alecy, 2004).

Sex hormones have an impact on the development of physiological structure, which lead to permanent differences in several distinct areas between males and females. During growth, sex hormones induce differentiation of distinct brain regions that range from neuronal composition to differences at the cellular level. This differentiation would lead to variations in structural volume, connectivity and neurotransmitter distribution between genders (Reddy, 2010). Furthermore, sex hormones have been documented to have a direct link in genomic regulation of the enzymes responsible for the synthesis and degradation of neurosteroids (Matsui et al., 2002; Mitchell et al., 2008; Mitev et al., 2003), as well as being precursors for the neurosteroids, as shown in their synthesis (Figure 1.1). Thus, gender differences will determine the level of sex hormones and influence the neurosteroid concentration in the plasma and brain (Wang, 2011).

1.4.1. PD sex differences

$GABA_A$ receptor sensitivity to neurosteroids is modulated by several factors including receptor subunit composition. Although neurosteroids bind to most $GABA_A$ subunit configurations, unlike benzodiazepines, different isoforms of α and γ subunits influence their efficacy and potency level (Brown *et al.*, 2002; Carver & Reddy, 2013; Lambert *et al.*, 2003). For instance, the synaptic strength of $GABA_A$ receptor $\alpha_1\beta_2\gamma_2$ subunit is faster and a more prolonged activation in comparison to $GABA_A$ receptor $\alpha_2\beta_1\gamma_2$ subunit when bound to allopregnanolone (Lavoie *et al.*,

1997). This difference in neural excitability is more evident between genders as there is evident sexual dimorphism differences (Galanopoulou, 2005; Wang, 2011). Progesterone and allopregnenolone were able to decrease neural activity of male and female mice, although they showed greater effects in females compared to males (Reddy *et al.*, 2004).

1.4.2. PK sex differences

Sex differences in PK, if present, do influence a small number (e.g. 6-7%) of marketed drugs (Anderson, 2005). However, these drugs showed approximately 40% change in their PK profiles between men and women. Sex differences in PK can impact upon bioavailability, distribution, metabolism and excretion. Sex hormones influence the bioavailability by affecting the gastrointestinal motility and gastric emptying rate, which is inhibited by oestrogens.

Furthermore, PK differences can result from sex differences in drug distribution. The overall body composition between males and females may be different as the amount of fat and muscle and organ sizes are significantly regulated by the sex hormones which in turn would majorly influence the PK profiles between genders. For example, the total body fat for an adult male is 13.5 kg while in females it is 16.5 kg (Soldin & Mattison, 2009). This larger proportion of body fat in women may increase the burden on the body from lipophilic compounds as they might accumulate in the fat compartments based on the degree of their lipophilicity and polarity. Another factor would be the plasma volume and blood flow to organs as females have lower plasma volume than males, and blood flow in several regions of the body, such as kidney, liver, muscles, heart and adipose tissue (Soldin & Mattison, 2009). Due to differences of body fat percentage and blood flow some highly lipophilic neuromuscular blocking drugs (e.g. vecuronium and rocuronium) have shown faster onset and prolonged duration of action in women compared to men, while diazepam has shown differences in distribution due to protein binding differences (Soldin & Mattison, 2009).

1.4.3. Sex differences in hepatocellularity

Furthermore, recent quantitative evaluation of hepatocytes for sex difference comparison have been conducted and shown significant sexual dimorphism in favour of females when assessing the hepatocellularity (number of hepatocytes per gram of liver), although the total number of hepatocytes when scaled for liver weight were similar (Marcos et al., 2016). Hepatocellularity is also important for direct comparisons between studies, because it is extensively used when *in vivo* drug clearance prediction is needed (Barter et al., 2007). For drug clearance prediction, there are three essential components required: intrinsic clearance, hepatocellularity and liver weight. Measuring the intrinsic clearance of a drug determines the capacity of the individual cells to metabolise a drug, however, this requires scaling to a complete liver. Unfortunately, most intrinsic clearance studies use hepatocytes from male subjects, which might lead to inaccurate predictions of clearance in females if there is a sex difference.

1.4.4. Hormonal differences in hepatocellularity

A possible cause of the high hepatocellularity in females may be because of oestrogen. It has been demonstrated from *in vitro* studies that hepatic proliferation can be induced up to seven-fold, although no induction in CYP activity was observed (Vickers & Lucier, 1996). Sexual dimorphic expression of P450s genes and liver related genes have been shown to be regulated by the hormone release pattern from the pituitary glands which is also regulated by sex hormones (Waxman & Holloway, 2009). The plasma hormone release and concentration in males is pulsative which can lead to undetectable levels between the next pulse, whereas it is nearly continuous in females and subsequently influences the expression of CYP450 enzymes. The variability of hormone release adds extreme challenges for studying sex differences, as hormonal changes might enhance or decrease the sex differences depending on the situation. Furthermore, the biggest variable factor that would influence the hormone release is the female hormonal cycle (McCarthy, *et al.,* 2012).

1.4.5. Sex differences in metabolism

Liver clearance is very important in anaesthesia as the liver metabolism is considered the major organ for metabolism for most of the intravenous anaesthetic drugs (Pleym et al., 2003). One of the factors that limits a drug's clearance is the liver blood flow. Females in general have a reduced total liver blood flow per kg compared to males due to lower cardiac output (Soldin & Mattison, 2009). This sex-linked effect is more apparent for drugs with a high extraction ratio from the blood where liver blood flow is the rate-limiting step. However, for drugs with a low extraction ratio they are limited by the hepatic oxidative and conjugation systems (phase-1 and phase-2 respectively); sex differences in the expression and activity of these enzymes are more important than the liver blood flow differences.

1.4.6. Cytochrome P450 (CYP450) enzyme super family

The cytochrome superfamily is divided into families (e.g. CYP1, -2, -3 etc.), and subfamilies (labelled by letters A, B, C etc.) and denoted with a number to represent a specific enzyme. These CYP families appear to be responsible for the metabolism of drugs and other xenobiotics, in addition to their involvement in the metabolic conversion of a variety of endogenous compounds, particularly hormonal biosynthesis and conversions (Nebert & Russell, 2002). The cytochromes P450 (CYP450) are considered the major enzymes responsible for the phase-I oxidation reaction (Knights, et al., 2016). This group of enzymes bind two atoms of oxygen, which result in the formation of a water molecule in addition to the production of a metabolite. The most common reactions are hydroxylation, de-alkylation or oxidation reactions; however, ring reduction or opening can also take place.

Sex differences in liver metabolism are the major reason for sex related PK differences where most of the drug biotransformations occur. These differences were found to be present for many drugs in general and was recognised for general

anaesthesia in rats as early as 1932 with respect to different rates of barbiturates metabolism(Nicholas & Barron, 1932). These sex differences in metabolism are now known to reflect sex differences in the expression of specific individual hepatic P450 enzymes (Waxman & Holloway, 2009).

Sex-linked differences in P450-dependent drug and steroid metabolism are most predominately found in rats (Martignoni, et al., 2006). They are also found in hamsters, dogs, chickens, rabbits, monkey and fish (Czerniak, 2001; Waxman & Holloway, 2009). Furthermore, sex differences in human CYP450 are well documented but are less dramatic than in the rat. However, 6 to 7% of marketed drugs commonly used in humans are reported to demonstrate at least 40% differences in PK between men and women (Gandhi, et al., 2004).

1.4.7. Hormone regulation of CYP enzymes

Sex hormones have been documented to have a direct link in genomic regulation of the CYP450 enzymes responsible for metabolism of drugs (Matsui et al., 2002; Mitchell, et al., 2008; Mitev et al., 2003). The differences are more observable in rats, as many CYP450 enzymes are regulated by increasing or decreasing the expression of certain CYP450 enzymes such as CYP 2A2, 2B1, 2C11, 2C13, 3A1, 3A2 which are male-specific, whilst CYP 1A2, 2C7, 2C12 are female rat specific (Waxman & Holloway, 2009). While in humans, the males have a higher drug metabolism activity in comparison to females for CYP1A2 and potentially CYP2E1, while females have a higher activity for CYP2D6 and some enzymes have no differences such as CYP2C19 (Meibohm et al., 2002). Sex differences in CYP450 enzyme expression and activity have also been observed with higher expression levels of CYP3A4 and CYP2D6 in females compared to males (Anderson, 2002; Diczfalusy et al., 2008). Hence certain CYP3A4 drug substrates such as steroids show a higher clearance rate in females than males. For instance cortisol, which is metabolised by CYP3A4 and used as its activity biomarker, is metabolised faster in women than in men (Inagaki et al., 2002; Raven & Taylor, 1996). Additionally,

although reports are inconsistent, midazolam showed differences in clearance rates ranging from no difference (Kharasch, et al., 1999; Raven & Taylor, 1996) to 50% (Quinney et al., 2008) and 90% (Tsunoda, et al., 1999) higher in women compared to men. An experimental drug for heart conditions named tirilazad has also demonstrated to have a 50% higher clearance rate in women in comparison to men (Hulst et al., 1994), which required a two to three fold dose increase in comparison to males to reach positive effects on the clinical outcome (Lanzino & Kassell, 1999). Incidentally, other drugs metabolised by the same CYP3A4 enzyme (e.g. alfentanil), fail to demonstrate PK sex differences. However, one of the unique characteristics shared by tirilazad and steroids is that they share the steroidal ring structure (Figure 1.5). This may suggest that steroid like compounds, such as alphaxalone, and hormonal steroids are metabolised via specific metabolic pathways influenced by sex hormones.

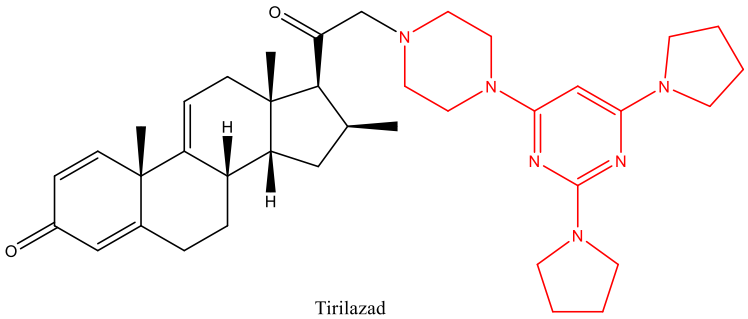

Figure 1.5. The chemical structure of tirilazad. The chemical structure highlighted in black is the steroidal scaffold. The area highlighted in red is an attachment that is used for its activity.

Oestrus cycle

The oestrous cycle causes endocrine changes in oestrogen and progesterone levels. These hormone changes are most noticeable in rats. In the rat's oestrous phase, the concentration of oestrogen is high while the progesterone concentration is low. In contrast, the dioestrous phase has heightened levels of progesterone which induce its metabolite, allopregnanolone, in plasma and the brain (Reddy, 2009). Furthermore, the duration of the rat oestrus cycle is three days, which results in the hormonal concentrations fluctuating during the same day. The

fluctuation in hormonal synthesis and circulation from the ovarian cycle would be expected to affect the synthesis and function of $GABA_A$ receptors and the resulting neurosteroidal activity; as well as induce changes in liver metabolism activity. Unfortunately, most animals used in pain and anaesthesia research are male laboratory rats or mice of a particular strain, while female rats being excluded due to hormonal fluctuations from the osestus cycle. However, is has been shown that female rats do not show more variation compared to male rats and in some cases male rats can show more variability on nervous system measurements (Becker, *et al.*, 2016; Beery, 2018). Hence, adding female rodents, despite the complexity of the oestrus cycle, is important to facilitate the translation to other species.

1.5. Sex differences and its effect on PK and PD

Sex differences in pharmacokinetics are straightforward to measure as it is a relatively simple procedure to inject the drug and measure its concentration from the plasma. Hence, more data are available on sex differences in PK than PD. However, the data from isolated PK studies are of less value if they are not accompanied by measurements of clinical response and this is also true for the PD, as studying *in vivo* PD alone can also be of limited value. As such, injecting a fixed dose of a drug to both sexes and measuring the outcome is one way to determine sex differences in PD, as the response is driven by the drug concentration at the site of action.

However, drug concentration at the site of action can be significantly influenced by sex differences in PK parameters. For example, reaching the steady state of a drug means that the concentration of the drug is equalised between plasma and the site of action, however, the steady state is mainly driven by drug clearance. As clearance is the principal parameter which determines the concentration of a drug at steady state, any sex differences in clearance can alter plasma concentration and ultimately influence clinical outcomes.

In vitro and *in vivo* PK models

An integrated PK/PD model describes the time course of a drug effect in relation to the dose over time. Investigating alphaxalone in an *in vivo* PK/PD model in this context is the best way to describe the individual parameters for each subject and combine the data in a future step. However, the downside is the economical and ethical consequences, as it needs many samples per subject during and after drug administration. Using an *in vitro* system on the other hand, will provide insight into cellular behaviour in an environment isolated from other physiological parameters. For instance, studying drug metabolism *in vitro* would provide the metabolic rate of hepatocytes only (the intrinsic clearance, CL_{int}), and although it may not represent the true physiological metabolic rate of a drug, it will provide other important information about the cellular metabolic capacity and the metabolic pathways taken by the drug. Moreover, using mathematical models to compensate for the absence of physiological conditions has proven to be effective in numerous cases in the process of *in vitro*/*in vivo* extrapolation (IVIVE) (Houston, 1994; Ito & Houston, 2004; Barter et al., 2007).

Furthermore, the population pharmacokinetic analysis approach considers samples from all patients together, in such way that takes the pharmacokinetic data from every subject and utilises them in the model even if the subject only had a single sample from a steady state or early time point. It combines sparse data with subjects of full profiles which enhances the sample size and allows a more comprehensive assessment of PK and PD properties. The population model provides the typical values of the PK/PD parameters, in addition to an estimation of inter- and intra-individual variability of the parameters and predicted concentration (Mould & Upton, 2013). Moreover, it allows the addition of different types of covariates such as physiological (i.e. sex, age, weight) or unconventional (i.e. drug formulation or site of injection) to the model calculation, which can improve its model fit and consequently its predictability. Hence, population analysis can determine if a covariate (i.e. sex) has a significant influence on either PK or PD parameters.

1.6. PK/PD

1.6.1. Pharmacodynamics

Pharmacodynamics (PD), which is the other half of PK/PD modelling, is the area that studies all the physiological and biochemical effects of a drug. It can be simplified to "what the drug does to the body" (Holford & Sheiner, 1982). PD also describes the relationship between drug concentration at the targeted site and the resulting effect, including the time course and the intensity of therapeutic and adverse effects. In addition, for any drug the resulting pharmacodynamics can have a wide range of endpoints, from mRNA, protein, cellular to tissue and organs or whole body responses.

Ligand receptor interaction

The molecular targets of a drug can be classified into four types: (1) Receptors, which are usually protein molecules that exist on the cell membrane, in the cell cytoplasm, in the nucleus or other organelles and can interact with endogenous neurotransmitters and hormones. (2) Enzymes, which may be intra or extracellular. (3) Ion channels, which are present on the cell membrane or organelles. Type (4) is transport proteins which are present in the cell membrane. Each of these types have their unique characteristics and response time which is crucial with regard to measuring the physiological responses for a drug.

Drugs and endogenous compounds binding to their receptors are called ligands. With a few minor exceptions for some drugs the majority of drugs produce their effect solely dependent on their chemical structure. These compounds aim to enhance or inhibit the normal physiological process or in some cases inhibit a vital process for microbial organisms. There are two main types of ligands, agonists and antagonists. The agonists can bind to a receptor and produce a conformational change that leads to a traditional mechanistic pathway which then gives a cellular and biological response. While antagonists bind to their receptors but cause no conformational change and no signal transduction. These ligands, if they have the

same receptor occupancies at the target site can compete against each other. Moreover, there is a range of categories for ligand activity e.g. full agonists are ligands that express a maximum response whilst a partial agonist is a ligand that has intermediate properties between a full agonist and antagonist. Another type of ligand is known as a biased ligand, which demonstrates activation for certain signal transduction mechanisms but not others.

Response time

In general, normal physiological effects are produced from endogenous compounds interacting with receptors forming a ligand receptor complex and biological consequences would follow as a result of this binding.

$$Drug + Receptor \leftrightharpoons Drug - receptor\ complex \rightarrow \left(^{Transduction}_{pathway}\right) \rightarrow Response$$

In order for a ligand to produce a pharmacodynamic response the process requires time, and different molecular targets have different response times. Excluding any pharmacokinetic reason, response time is dependent on the receptor location or transduction pathway. Thus, there is a time lag for a response between an extra and intracellular located receptor. Extracellular targets are more exposed and accessible to ligands while intracellular receptors are hidden and the ligand requires more steps to be transferred to the receptor location. To put the time lag difference between molecular targets into perspective, a response from an ion channel would take milliseconds while the activation of an intracellular receptor and messaging system would take seconds to minutes and for DNA transcription from a nuclear hormonal receptor would take hours to measure a response. Norepinephrine is a great example to illustrate the rapid onset of a drug in the body, which makes it an excellent drug for emergency therapy e.g. cardiac arrest and severe allergic reactions used as a bronchodilator. While hormonal therapy is an example from the opposite spectrum of time lag e.g. some steroidal drugs are used in asthma management, although these drugs are not used for urgent cases as they have a slow onset of action.

Biomarker endpoints

Marketed drugs have a range of physiological effects on the body. A drug such as norepinephrine from the previous example induces several biological and sympathetic pathways leading to pupillary dilatation, hyperglycaemia and piloerection. These biological responses are considered as a biomarker for the clinical response which is a translation of the pharmacological pathway of the investigated drug (Derendorf & Meibohm, 1999). Furthermore, biomarkers can be used to give an insight on the drug behaviour, even if they are not directly related to the clinical outcome and may give a qualitative prediction.

The norepinephrine example illustrates the interaction complexities between a drug and the physiological systems and the overlapping signal transduction pathway for the central nervous system which make these biomarkers unavoidable. Fortunately, they can be used as observed clinical endpoints to measure the potency and specificity of a drug by measuring the magnitude of these biomarkers e.g. physical sign, blood analytes or physiological measurement. Therefore, it is more common to have a drug with a main endpoint and several biomarkers to be assessed in an *in vivo* study. In addition, the PD effect of ultimate interest in a PK/PD trial may be used as a substitution for the clinical endpoint. This will be a biomarker that is objectively measured and validated as an indicator of a pathogenic process, or a pharmacological response to a therapeutic intervention.

1.6.2. Pharmacokinetics (PK)

The term Pharmacokinetics (PK) originates from ancient Greek "*pharmakon*" and "*kinetikos"* which mean drug and moving or setting in motion, respectively. A very simple definition for pharmacokinetics is "What the body does to the drug" (Holford & Sheiner, 1982). Another elaborated definition for PK would be to describe it as the study of the time course of a drug through the absorption, distribution, metabolism and elimination phase (ADME).

Absorption:

Absorption is the passing of a drug through the gut membrane into the blood stream. For drug administration there are several routes of administration such as enteral (oral and rectal route) and parenteral (all types of injection and inhalation routes). The process of absorption is greatly affected by several complexities due to physiological and physio-chemical factors that may cause significant variation in the absorption process. Physiological factors include gastric acidity and empting rate, the blood flow at the absorption site, age and sex (Fletcher et al., 1994). While the physico-chemical factors are the solubility, degree of ionisation, size and the lipid-water partition coefficient (LogP) of the compund (Lipinski, 2004).

Moreover, unless a drug is given by IV injection, for every other route of administration the drug is required to pass through the cell membrane to reach the circulation (Consortium et al., 2010). These membranes act as a type of biological barrier to selectively reduce the passage of any unwanted foreign material including drugs. Usually, compounds can pass through the membrane through passive diffusion or active transportation or the para-cellular route. Compounds with incompatible properties would have a lower and slower absorption rate (Consortium et al., 2010).

Distribution:

After a drug is absorbed, it passes into systemic circulation which will distribute it to the body's tissues. However, on entering the circulation the drug does not instantly distribute to the whole body. As a PK parameter, the volume of distribution (Vd) represents the apparent volume in which the drug is distributed to represent the same concentration that is currently in blood plasma. The larger the Vd, the more the drug has been distributed in the body. The process of distribution requires time to reach equilibrium at the targeted tissues. For instance, for some parts of the body and for certain drugs, the speed of distribution occurs at various rates and extents. There are several factors that affect the

distribution pattern for a drug. These factors include the movement of drug to the tissues (perfusion), the ability to cross the tissue membrane (permeability), the degree of binding and partitioning in the blood, tissue and fat (Rostami-Hodjegan, 2012). In addition, physico-chemical properties of the drug influence the level of drug distribution, especially if the compound is a weak acid or base. Understanding these factors enables prediction of the distribution of a specific compound within the body.

Metabolism:

Metabolism is the body's way of deactivating any exogenous or endogenous compounds. The process of metabolism occurs in several areas of the body, such as the small intestine, kidneys and liver. However, the liver is the most important organ as it has the largest quantity of metabolising enzymes. The body bio-transforms any chemical structure of the compounds by introducing different functional groups or splitting the original compound to smaller parts converting them into metabolites. Every metabolic pathway aims to inactivate the drug and increase the polarity of the compound in order for it to be excreted. Thus, most polar compounds will be eliminated directly, however, for less polar compounds, which represent the majority of drugs, the process of metabolism produces a more hydrophilic inactive metabolite. However, metabolites are not always inactive; some metabolites have a greater pharmacological activity than the original compound e.g. morphine glucuronide. Many of the marketed drugs have been designed as prodrugs to be less potent or have no potency in favour of optimizing their physio-chemical properties leading to increased absorption and then be activated by metabolism (El-Kattan & Varma, 2012). Moreover, some metabolites have other pharmacological activity, which may be undesirable or toxic. In this case, it is necessary to undertake metabolic analysis and toxicology studies for any lead compound in the preclinical stages in order to exclude candidates with a toxic profile. As the liver is the main organ of metabolism most metabolism studies

use liver tissues to measure the compounds ability to be metabolised and characterise the metabolites produced.

Drugs are metabolised in the body through two main phases. Firstly, the Phase-I reaction involves modifying or forming a new functional group, or cleavage of the compound and this occurs mainly by oxidation, reduction, hydrolysis, acetylation or O/N-dealkylation. These processes yield more polar compound derivatives, such as alcohols, phenols or carboxylic acids. The major phase-I enzymes are the cytochromes P450 (CYP450), and to a lesser extent the Flavin monooxygenase (FMO) (Krueger & Williams, 2005). Phase I is followed by phase-II conjugation where endogenous hydrophilic moieties, such as glucuronic acid, sulphate or glycine, are conjugated to either the original compound or phase I metabolite significantly increasing the hydrophilicity (Knights, et al., 2016). For example, glucuronide metabolites, which are the most common for phase-II metabolism, are secreted into the bile or excreted via the kidneys leading to rapid elimination from the body. Additionally, some compounds undergo either phase-I or phase-II reactions depending on their functional chemical group and degree of polarity.

Excretion

As previously mentioned, some drug metabolites can have pharmacological activity and if they accumulate in the body may cause toxicity or side effects. Thus, there is a need to remove these metabolites from the body and this often occurs via excretion. This process can occur after metabolism or directly via excretion through the kidneys if the drug is a highly polar compound. The principle pathways of excretion are through the kidneys, biliary system, lungs, saliva, sweat and breast milk (Meletiadis, et al., 2006). The kidneys are the major excretion route and the biliary system has a moderate role, while the other pathways have minor contributions.

Membrane transporters

Membrane transporters can be a major factor in the pharmacokinetics of a drug as they can affect the drug absorption, disposition and elimination. There are more than 400 membrane transporters from two major super-families: the ATP binding cassette (ABC) and solute carrier (SLC). These transporters are distributed all around the body, however, in drug development, attention is focused on epithelia of the intestine, kidneys, liver and the endothelial of the blood brain barrier (Zhang, et al., 2006). These four sites represent the foundation of drug PK and activity. However, certain transporters are more important than others with regards to clinical relevance, such as, P-glycoprotein (p-gp also known as MDR1 or ABCB1, breast cancer resistance protein (BCRP; also known as ABCG2), organic cation transporters (OCTs), organic anion transporters (OATs) and organic anion transporting polypeptides (OATPs)) (Zhang, et al., 2006). If a drug is a substrate or inhibitor for one or multiple transporters, experiments should be conducted that identify each transporter and assess the risk of DDIs including the impact on bile salt excretion from the liver. The discovery of transporter protein structure via crystallography and the advancement of computer prediction of transporter-drug interactions through quantitative structural activity relationship (QSAR) studies is advancing drug discovery (Consortium et al., 2010).

1.6.2.1. Pharmacokinetics studies

The process of drug discovery and development for new drugs is expensive and time consuming (Dimasi, 1994). At the clinical stages a high number (>90%) of drugs fail to make it through the trials. A major causes of this attrition are unacceptable pharmacokinetic properties (El-Kattan & Varma, 2012). Thus, the application and development of reliable methods to predict human drug disposition, will reduce the number of drug candidates that fail. This can be achieved by improving the selection process for development compounds by optimising the PK properties in parallel with efficacy for the intended therapeutic use.

1.7. Prediction of pharmacokinetics parameters

The most described technique for the prediction of human pharmacokinetics is allometric scaling (Obach et al., 1997). Allometry is a pharmacokinetic tool used for extrapolating human PK parameters from preclinical species (Riviere *et al.*, 1997). Originally, allometry was a technique developed to explain the observed relations between mammals' body weight and their organ size (Mordenti, 1986). However, further studies demonstrated additional relationships between body weight and physiological parameters, such as hepatic blood flow and glomerular filtration rate. This led to the application of allometric scaling to human PK parameters from other preclinical species (Boxenbaum, 1984). When the hepatic blood flow and glomerular filtration rate of the preclinical species were plotted against their weight on a log-log scale, a linear relationship was obtained. The PK parameters would be expected to be linked to hepatic blood flow and glomerular filtration rate, such as, clearance and half-life, which in turn would be corelated to the body size (Ritschel *et al.,* 1992). Typically, allometric scaling of PK parameters focuses on interspecies relations between their body weight and Vd and clearance. After establishing a relationship between these parameters in the preclinical species, it can then be extrapolated to humans allowing a prediction for human clearance and Vd. However, allometric scaling has a major drawback due to its empirical nature. For instance, scaling plasma clearance using allometry does not explain any species differences in metabolic clearance pathways, which might have a substantial impact on accurately extrapolating to human clearance. Fortunately, combining the knowledge of species differences from *in vitro* metabolism data with allometric scaling improves the prediction for compounds that are prone to significant species difference in metabolism (Ings, 1990; Lave et al., 1996; Mordenti, 1986).

Prediction method and scaling

Methods for predicting *in vivo* clearance from *in vitro* data were first described around 40 years ago (Rane et al., 1977). It was demonstrated that the level of liver extraction of many drugs could be estimated from the enzyme kinetics of the biotransformation of these drugs by microsomal enzymes. This introduced and henceforth applied to practice the concept of an *in vivo/in vitro* correlation (IVIVC) that uses data from human and preclinical species. The most commonly used systems for estimating hepatic intrinsic clearance are liver microsomes and hepatocytes. Each of these methods has their advantages and disadvantages in the ease of use and accuracy and the completeness of the data. However, given the destructive nature of microsomes preparations, which results in loss of both cellular integrity and most of the non-CYP450 metabolising enzymes, it is often assumed that hepatocytes usage is the superior choice in regard to accurate prediction of *in vivo* data (Ito & Houston, 2004; Obach, 1999; Soars, 2002; Zomorodi et al., 1995).

There are several approaches for kinetic studies and data collection that can be used to define a PK profile of a drug, including *in vitro, in vivo* and ex-vivo studies. *In vitro* studies incorporating scaling and correction factors are used to predict *in vivo* clearance. Whilst, *in vivo* and *ex vivo* studies require multiple blood samples at different time points, the resulting concentration time data can be used to create non-compartmental and multiple compartmental models. For the *in vitro* studies, there are several methods for predicting the liver clearance. Hence the most common methods will be described briefly.

Methods for human clearance prediction

Biotransformation is an essential part of the PK profile and primarily occurs in the liver. This process converts non-polar and lipophilic compounds into polar compounds, which are usually inactive, and can be easily eliminated by the kidney or other organs. As such, it is important to predict the liver metabolic pathways and the clearance rate of a drug from *in vitro* studies before expensive and invasive *in vivo* PK studies are carried out in humans. There are four main *in vitro* systems that can be used to study hepatic metabolism; recombinant metabolising enzymes, microsomes, hepatocytes or liver sections (Brandon *et al*, 2003). Hepatocytes and liver slices give the most comprehensive view of processes in the liver. Liver slices are used for models that keeps liver structure intact or for studying liver enzyme induction (Edwards et al., 2003). However, liver slices have decreased in usage since the 1970s due to difficulties in handling and maintaining viability (Ekins *et al*, 2001). In contrast, hepatocytes can be used fresh, cryopreserved or cultured, though each has their own imperfections. For example, fresh hepatocytes can lose their viability after a few hours and while cultured hepatocytes can maintain viability over days they gradually decrease their activity (George *et al,* 1997). The use of microsomes is another popular method for liver drug metabolism studies as it contains a variety of phase-I and phase-II metabolising enzymes such as, CYP450 and UGT (Zhang *et al*, 2012). Lastly, recombinant enzymes are the best system for investigating isoform specific drug metabolism.

As mentioned earlier, clearance prediction from preclinical species is essential for predicting the drug exposure to the human body. Intrinsic clearance is the cornerstone for the extrapolation of *in vitro* data to the *in vivo* situation. The intrinsic clearance is a direct measurement of the enzyme activity to a drug without any interferences by other physiological factors, such as, blood flow and

drug binding to plasma protein. Intrinsic clearance (CL_{int}) can be measured using the following steps:

I. The first step uses the enzyme kinetics since drug metabolism occurs via a variety of metabolising enzymes. However, the reaction should not exceed 50% depletion as metabolite formation may lead to enzyme inhibition and therefore affect the results (Obach et al., 1997). The most direct enzyme kinetic model is the Michaelis-Menten model (Cornish-Bowden, 2012). This model is characterised by a hyperbolic concentration velocity function (Figure 1.6), which is represented by Equation 1.1.

$$\mathbf{v} = \frac{\mathbf{V_{max}} \times [\mathbf{S}]}{\mathbf{K_M} + [\mathbf{S}]}$$

Equation 1.1

v is the velocity at a given compound concentration [S], V_{max} represents the maximum velocity achieved by the system at maximum substrate concentration, while K_m, which is the Michaelis constant, is the concentration at 50% of the maximum reaction speed (V_{max}), and in most cases approximates to the substrate's affinity for the enzyme.

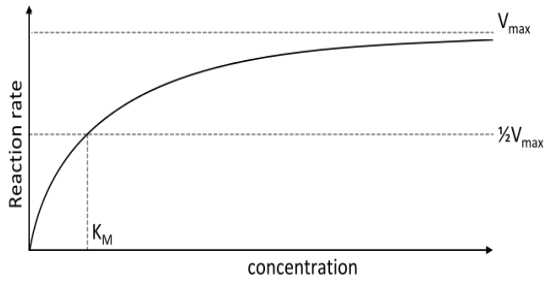

Figure 1.6 kinetics of drug metabolising enzymes.

This model acts in a constant linear manner when the substrate concentration is less than 10% of the K_m and CL_{int} in this concentration range would be equal to V_{max}/K_m ratio. This is analogous to dose linear pharmacokinetics of the *in vivo* situation where the therapeutic drug substrate concentration does not exceed the K_m (Venkatakrishnan, et al., 2001), and on the assumption that the substrate

concentration [S] is very low, the substrate can be removed from the formula equation 2.

$$CL_{int} = \frac{V_{max}}{K_m}$$

Equation 1.2

II. The second step is the scaling up of the *in vitro* CL_{int} using a scaling factor that considers the CL_{int} in terms of the physiological size of the liver. The scaling factor used considers the hepatocellularity (number of hepatocytes per gram of liver) and weight of the liver using the following Equation 1.3 (Houston J., 1994).

$$in-vivo\ CL_{int} = (invitro)CLint.\frac{mL\ of\ incubation}{No.of\ hepatocytes}.\frac{Hepatocellularity.}{g\ of\ liver\ weight}.\frac{g\ of\ liver\ weight}{Kg\ of\ body\ weight}$$

Equation 1.3

Where each value could be obtained from an individual experiment or by using published values from the literature. However, age and sex may influence these values and subsequently on hepatic drug-metabolising capacity (Kwak, et al., 2015; Mennecozzi, et al., 2015).

III. In order to scale from *in vivo* CL_{int} to blood hepatic metabolic clearance (CL_h) other physiological processes such as blood flow (Q_H), plasma protein and incubation binding must be incorporated. This requires the use of liver models in order to represent the relationship between blood clearance and *in vivo* CL_{int}. The most established models are the well-stirred and parallel tube models. The well-stirred method is the most commonly used model due to its mathematical simplicity (Ito & Houston, 2004). As the name implies, the well-stirred model assumes that the liver is a single compartment, and the concentration of the unbound drug is in equilibrium with the liver. Hence, the hepatic clearance can be calculated using the following Equation 1.4:

$$CL_H = \frac{Q_H.\frac{F_{ub}}{F_{u\ inc}}.CL_{int}}{Q_H + \frac{F_{ub}}{F_{u\ inc}}.CL_{int}}$$

Equation 1.4

Where $F_{u.inc}$ and F_{ub} are the fraction unbound in the incubation and blood respectively. Q_H is the liver blood flow and CL_{int} is the *in vivo* intrinsic clearance.

On the other hand, the parallel-tube method considers the physiological architecture of the liver and assumes that it is composed of identical parallel tubes with evenly distributed enzymes in each cross section of sinusoidal vascular space (Pang & Rowland, 1977). Thus, hepatic clearance can be estimated through the following Equation 1.5:

$$CL_H = Q_H.\left(1 - e^{\frac{-CL_{int} * \frac{F_{ub}}{F_{u\,inc}}}{Q_H}}\right)$$

Equation 1.5

There is no major distinguishable difference between both models (Ito & Houston, 2004). However, the parallel tube model has shown better predictability for highly hepatically cleared compounds (Ito & Houston, 2004). The well-stirred model gives similar results to the parallel tube model for drugs with low hepatic clearance. The scaling process is summarised in Figure 1.7.

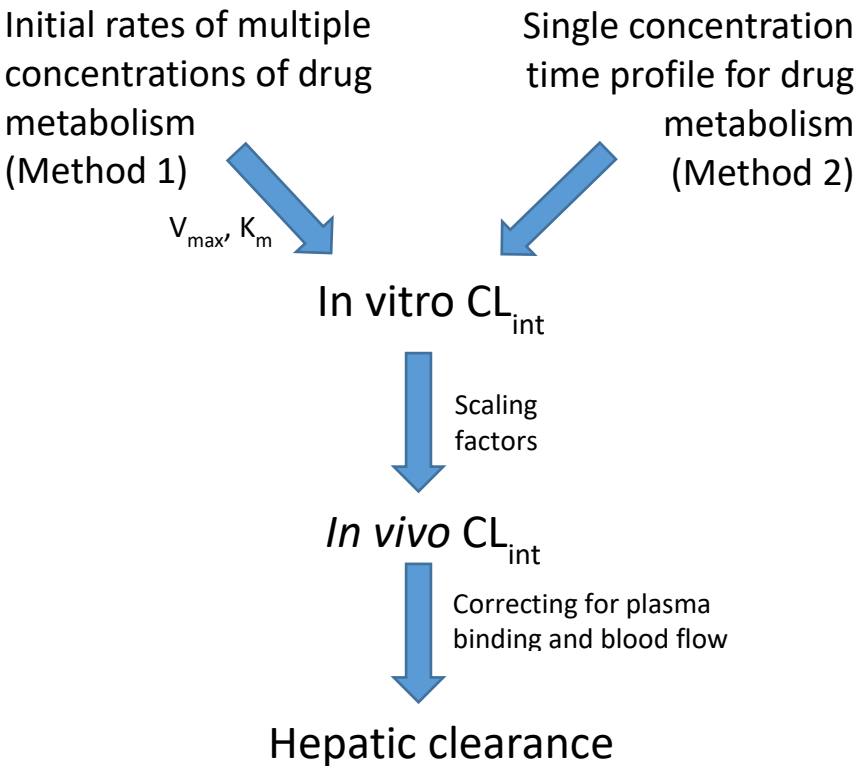

Figure 1.7: Schematic diagram that shows methods for determining the intrinsic clearance and how ultimately hepatic clearance is predicted.

1.7.1. PK/PD modelling

The decision for proposing a new drug and designing an effective dosage treatment is derived by understanding the relationship between the dose administered, the resulting concentration in the body and the pharmacological effect strength (Meibohm & Derendorf, 1997). This relationship can be acquired by understanding the drug's PK and PD properties. The PK/PD modelling integrates and combines both areas and establishes new models that link them together. Consequently, the newly developed PK/PD model describes and predicts the pharmacological effect over time directly resulting from a given dose (Figure **1.8**). This offers insight into the underlying biological process involved with the flexibility to extrapolate the model to other clinical situations. Furthermore, PK/PD modelling provides general structure for extrapolation between species and from *in vitro* to *in vivo*. In addition, the PK/PD method is useful for rational drug selection and confirming the relevancy of the endpoints to predict the efficacy or side effects.

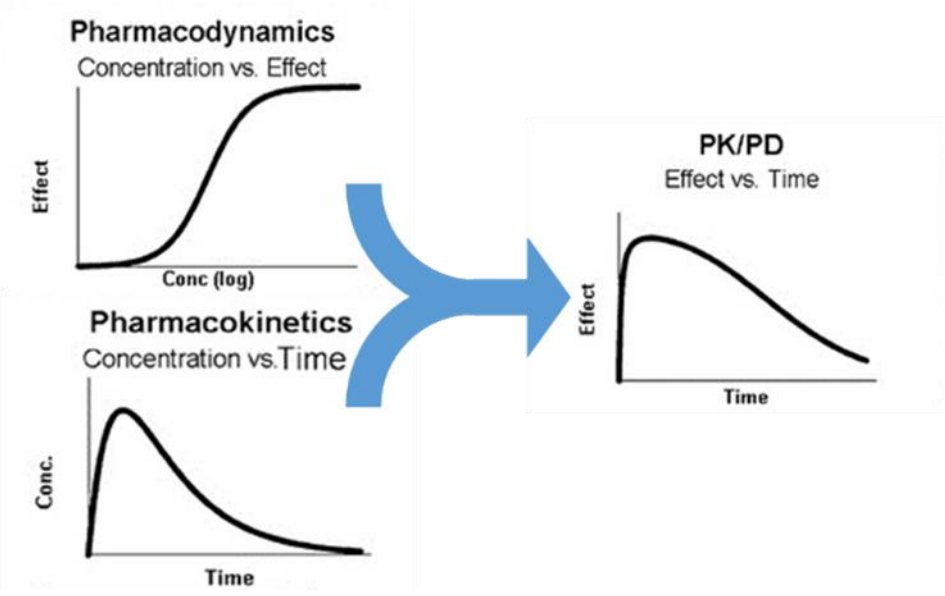

Figure 1.8: Interrelationship between pharmacokinetics, pharmacodynamics and PK/PD modelling.

Background (Historical)

Pharmacological effect and drug disposition relationships have been described over the last 50 years since the early evolution of pharmacokinetics (Holford &

Sheiner, 1982; Wagner, 1968). It has been shown that the intensity and the time course of action for numerous direct and indirectly acting drugs are related, and mainly determined by the time course of the drug concentration in the body. Furthermore, when both the concentration-time and the concentration-effect courses are known, it is often possible to predict the pattern of their pharmacological effect including intensity and duration of action. However, many other drugs are believed to have no relationship between drug concentration in plasma and the time course of action and is based on the observation that the pharmacological effect lags behind the concentration in plasma. The pharmacological effect increases in intensity even though the drug plasma concentration decreases and therefore maintains its effect beyond the time where drug concentration can no longer be detected in plasma. Though, this apparent dissociation was managed by the introduction of hypothetical BioPhase compartments by Segre in 1968 to account for the lag between concentration and effect (Csajka & Verotta, 2006). The concept of BioPhase compartments and the increased availability and ease of use of computational resources, allows the mathematical calculations to be more manageable and has advanced the field of PK/PD modelling from a classic dose–response concept to an expanded and sophisticated modelling technique (Derendorf & Meibohm, 1999).

PK/PD model classification

PK/PD models are usually used to simplify the real physiological process, and in some cases, it can give insight into the underlying biological process. This can make these models purely descriptive by only combining the observed time course of effect and concentration and neglecting the physiological mechanisms; or it can be more sophisticated by developing mechanism-based models, which would

consider the physiological events involved in the appearance of the observed effect. The (Holford & Sheiner, 1982).

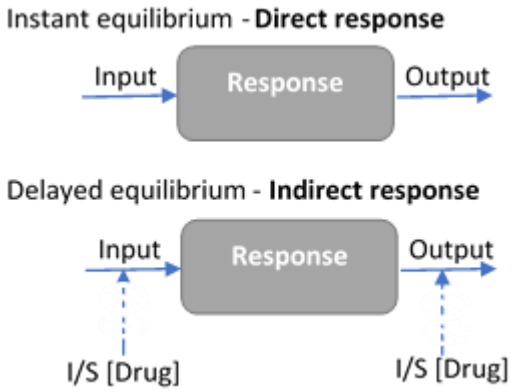

Figure 1.9: A schematic representation of the difference between instant (direct) and delayed (indirect) equilibrium. [Drug] indicate sites of potential inhibition (I) or stimulation (S). In the direct model, the response is rapid with no time delay. In the indirect model the [Drug] will act on either of the input or output which will lead to time delay in response hence the indirect effects.

The simplest way to describe the relationship between concentration and observed response is by determining if they have a direct or indirect relationship. Knowing this would influence the modelling process entirely. A direct model would make a direct link with instant synchronisation between plasma concentration and observed effect. This is used when a drug effect is directly related to plasma concentration where the PD model at a given time would be directly dependent on plasma concentration. Otherwise, the relationship between drug concentration and effect may be delayed and desynchronised leading to an indirect relationship (Figure 1.9) (Gabrielsson & Weiner, 2016). However, for most drugs, it is fairly uncommon to have plasma concentration and effect synchronicity with time (Toutain, 2002) as numerous drugs have a distribution lag from the PK perspective or slow response time from the PD perspective. For instance, while drug concentration is measured from plasma, the response effect is affected by the concentration at the action site. As this is a separate location to plasma then the relationship between drug concentration in plasma and at the site of action may be either instantaneous or controlled by compartmental distribution which may be rate limiting time dependent change. In the latter case the maximal plasma concentration for a drug would occur before having a maximum effect or the effect to hysteresis (Figure 1.10).

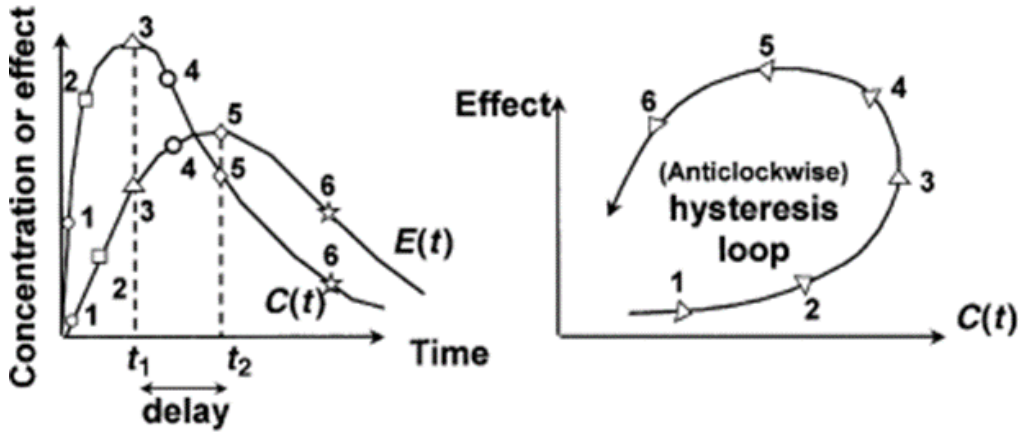

Figure 1.10. Plots of concentration vs. time and effect vs time relationships. The concentration and effect desynchronise creating a hysteresis loop when effect is plotted against concentration (Adapted from Toutain, (2002).

1.7.2. Population pharmacokinetics

Several factors can affect the dose-concentration relationship, including species, race or strain, sex, therapeutic and environmental factors. Population pharmacokinetics is a method to identify the measurable factors and the clinical extent that can affect the dose-concentration relation in order to develop an appropriate dosage regimen to be utilised for individuals (Sparreboom & Figg, 2006). Conducted PK studies usually consist of homogeneous subjects fixed to certain criteria which can create an artificial condition that does not represent the relevant population in real situations for drug usage (Aarons, 1991). This however creates an obstacle for finding the relevant population as traditional pharmacokinetics studies will require rigorous sampling that may be difficult to conduct on some sensitive populations such as paediatrics, pregnant women and elderly. Hence, population pharmacokinetics take and utilise data from the intensive sampling method as well as unbalanced observations from difficult to acquire group subjects, which enables pharmacokinetic studies to be conducted in target patient population.

The concept of population pharmacokinetics modelling is not new, as it was first introduced in 1972 by Sheiner *et al.* (Mould & Upton, 2012; Sheiner et al., 1972) to handle sparse data collected during therapeutic drug monitoring and then expanded upon to include integrated PK/PD models. Subsequently, modelling has

grown to be an important tool in drug development. There are several approaches to conduct population pharmacokinetics, which are naïve pooled data analysis, two stage approach, Bayesian estimation and non-linear mixed effects modelling approach. Originally, the population pharmacokinetics started by estimating parameters by fitting the combined data from all the individuals and ignoring individual differences, this is termed the naïve pooled approach. Alternatively, a two-stage approach can be used where the parameter estimates can be obtained by fitting each individual set of data separately and combining them to generate an average and standard deviation for the population parameters. Both approaches have disadvantages which become exacerbated when inadequacies such as missing samples or other data errors are present which will result in biased PK parameter estimates. The Bayesian approach uses the actual data and prior distribution of the PK parameter estimates to estimate individual parameters from the obtained posterior distribution of parameters. The results of this method, however, depends on uncertainty of prior distribution. Nonlinear mixed effects models are a one stage approach that estimates population parameters and variability concurrently using data from all individuals. The latter approach is arguably the most common method used for population pharmacokinetic analysis due to it producing accurate and precise estimates of population mean and variability (Mould & Upton, 2012).

The nonlinear mixed-effects modelling is a statistical model that incorporates both fixed and random effects hence the name mixed-effects. The fixed effects are population parameters which are assumed to be equal for data collected at the same time, while random effects are random variables which are associated with each sample (subject) from a population (inter individual variability). Furthermore, since many drugs are being eliminated in an exponential fashion, it requires nonlinear functions to calculate it, as such it was named nonlinear mixed effects modelling (NLME).

NLME structure

The nonlinear mixed effects (NLME) model consists of three sub models (points of evaluation) known as the structural model, statistical model and covariate model. The structure model conveys the trend of the data and gives estimates of pharmacokinetics parameters in the absence of covariates, whilst the covariate model describes the estimated parameters relation with the used covariates. Finally, several statistical model outcomes obtained from a combination of several criteria, such as, maximum likelihood, Akaike information criterion (AIC) and Bayesian information criterion (BIC), are used for evaluating and selecting the optimal base model and the influence of covariates based on statistical models (Mould & Upton, 2012).

Monte Carlo simiulation

A population PK model can characterise the typical population parameter values among subjects and the interindividual variability and covariate influences on the pharmacokinetics. This knowledge can be used to support the decision for the appropriate drug dosage administered. Monte Carlo simulation can be applied using the popPK model outputs to obtain the probability to achieve a desired target exposure under different dosing administrations. Monte Carlo simulation repeatedly simulates the model each time drawing different values from the sampling distribution of the model parameters which results in a set of possible outcomes (Bonate, 2001)

Model evaluation

The final model must be assessed for its stability, goodness of fit and reliability and if needed can also be validated for its predictive purposes by statistical techniques that include data splitting, bootstrap, and visual predictive check.

Diagnostic plots

Some of the commonly used diagnostic plots for model evaluation are: the plot between the observed concentration versus population predicted concentration (PRED) and the observed concentration versus individual predicted concentration (IPRED). For these plots the concentration should be equally distributed around the line of unity without any trends and should show no bias of model prediction. Furthermore, conditional weighted residual (CWRES) versus PRED and CWRES vs time plots are also important which represent the goodness of the fit and the values for CWRES should be equally distributed around the zero line. Values significantly above 3 or below –3 are questionable and may indicate poor fit.

1.8. Aims and objectives

Alphaxalone's better safety profile, lower receptor interaction in the pain pathway and less pain on injection have led to an increase in its popularity within biomedical research and clinical veterinary medicine. Furthermore, these applications may require using animals from both sexes and therefore any sex differences in the pharmacokinetics or pharmacodynamics may impact on the clinical outcome if dosed improperly.

Based upon recent literature, it is hypothesised that the sex difference observed for alphaxalone exposure in rats is due to sex differences in the rate of metabolism and may extend to other species where alphaxalone is licenced or being considered for authorisation such as, humans, dogs, rabbits and monkey.

Therefore, the main aim of this research is to investigate the source of this alphaxalone sex difference in rats and apply this information using *in vitro* studies to investigate the following species: humans, cats, dogs, rabbits and monkeys to see if there are similar sex differences.

For this several objectives have been employed: first, *in vivo* pharmacokinetic analyses (both deterministic and population) in order to understand alphaxalone sex differences in rats and the influence of gender, strain and body weight on the PK parameters in a larger model. Furthermore, recommend an optimal dosing regimen for alphaxalone administration in both sexes. Second, rationalise the observed sex differences in pharmacokinetic clearance using enzymology and differential metabolism pathways using *in vitro* tools such as hepatocytes and liver microsomes in conjunction with kinetic modelling for the major metabolic pathways of alphaxalone. Finally, a mathematical kinetic model for alphaxalone NADPH dependent metabolism will be developed and used to quantify and compare the alphaxalone metabolism pathways between the previously mentioned species.

Chapter 2

Materials and methods

2. Chapter 2: Materials and methods

2.1. Chemicals and materials

Alphaxalone (Alfaxan) used for *in vivo* experiments was purchased from Jurox® (UK) while alphaxalone (CAS: 23930-19-0) used for *in vitro* experiments and *in vivo* standard curves was obtained from LGC standards (UK). The internal standard lansoprazole (CAS: 103577-45-3), oestradiol (CAS: 50-28-2) and 3β-glucuronide oestradiol (CAS: 14982-12-8), in addition, to both alphaxalone metabolites 3β-alphaxalone (beta-alphaxalone) (R198242) and allopregnatrione (keto-alphaxalone) (CAS: 2089-06-7) were purchased from Sigma (UK) as well as enzyme inhibitors clotrimazole (CAS: 23593-75-1), indomethacin (CAS: 53-86-1) and trilostane (CAS: 13647-35-3). All other chemicals are reagent grade chemicals.

Isolation reagents

Calcium-free Hanks' Balanced Salt Solution (HBSS) ×10, HEPES (4-(2-hydroxyethyl)-1-piperazineethanesulfonic acid) buffer and foetal bovine serum (FBS) were purchased from Thermo Fisher Scientific (UK). Williams' medium E, no phenol red from Gibco® and lastly, two collagenase type IV were purchased from Thermo Fisher Scientific and Sigma (UK).

Cofactors and enzymes

The initiating enzyme for phase-I reaction: NADPH (β-Nicotinamide adenine dinucleotide 2'-phosphate reduced tetrasodium salt hydrate) (CAS: 2646-71-1) phase-II related enzymes: UDPGA (Uridine 5'-diphosphoglucuronic acid) CAS: 63700-19-6, alamethicin (CAS: 27061-78-5) and PAPS (3'-Phosphoadenosine-5'-phosphosulfate) (CAS: 109434-21-1) were obtained from sigma (UK).

Biological materials

Human liver microsomes for male and female (each pooled from 10 donors), beagle dog liver microsomes for male and female (each pooled from 5 donors), Australian rabbit liver microsomes for male and female (each pooled from 5

donors), and rhesus macaque monkey liver microsomes for male and female (each pooled from 3 donors) were obtained from BioIVT (UK).

2.2. Animals used for *in vivo* and *in vitro* alphaxalone study

Lewis rats (Normal dose administration group).

Sixteen adult (8-12 weeks) Lewis rats, nine male (308±49 g) and seven females (222±9 g) (Charles River Laboratories, Margate, UK) were used for the investigation of the alphaxalone PK/PD study.

Sprague Dawley rats (Adjusted dose administration group)

Twenty-four adult (9-12 weeks) SD rats (8 male rats (422±41 g) and 16 female rats (304±15 g) (Charles River Laboratories, Margate, UK) were used in this study.

Rat liver hepatocyte samples and source

13 male and 6 female (9-12 weeks) Lewis Rats were obtained from Charles River Laboratories (UK) and used for hepatocyte isolation experiments.

2.3. *In vivo* alphaxalone plasma samples

Plasma samples taken from alphaxalone administrations to male and female Lewis and Sprague Dawley rats were generously provided by Prof. Kate White and were adapted for this study (White et al., 2017). The study was conducted according to the Animal (Scientific) Procedures Act 2013 (EU Directive 2010/63/EU) UK Home Office regulations and local ethics approval, Project Licence PPL30/3156. The animals were housed in single-sex groups of 4 in double layer, ventilated cages given access to food and tap water *ad libitium*. Moreover, all cages had play tubes, bedding material and chew blocks for enrichment and maintained a 12-hour light/dark cycle (including 1-hour dawn and 1-hour dusk) while all experiments started at 10:00 h each day.

2.3.1. Study design

The study was conducted to obtain alfaxalone pharmacokinetics, and to monitor the pharmacodynamic endpoints (measures of arterial blood pressure). Two separate *in vivo* trials occurred to investigate alphaxalone gender differences and to adjust the alphaxalone dose for females. Hence, the first study had a fixed alphaxalone loading dose and constant rate infusion for males and females while the second study had an adjusted infusion of alphaxalone in the females to match alphaxalone plasma concentration in the male rats, based on the outcomes of the first trials. Furthermore, the first experiment was conducted using Lewis rats and the latter incorporated the Sprague Dawley strain.

2.3.2. Drug administration and sampling

The *in vivo* methodology has been reported before by (White, et al.,2017). In brief, the rat was placed in a custom-built Perspex anaesthesia chamber (Vet-Tech Solutions, Congleton, UK) and anaesthesia was induced using 3% isoflurane (Isoflo, Abbott, Maidenhead, UK) delivered via a Tec 3 precision vaporizer in oxygen (1 L/min) and nitrous oxide (2 L/min). Anaesthesia was maintained using 2-2.25% (vaporizer setting) isoflurane in nitrous oxide and oxygen delivered via

a nosecone for maintenance of anaesthesia. Respiratory rate and effort were assessed by observing chest excursion and measuring end-tidal carbon dioxide (CapStar 100, Linton, Diss, UK). In animals exhibiting respiratory depression as judged by a low respiratory rate and rising end-tidal carbon dioxide values, intermittent positive pressure ventilation was initiated (Harvard 683 ventilator, Harvard Apparatus, Cambridge, UK) at 60-80 breaths per minute to maintain end-tidal carbon dioxide 35-45 mmHg. The left jugular vein was cannulated using 0.63 mm OD polyethene tubing (Portex, Fisher Scientific, Loughborough, UK) for the administration of the intravenous anaesthetic. The arterial pressure was monitored using 1 mm OD polyethene tubing (Portex, Fisher Scientific, Loughborough, UK) cannulated in the left Carotid artery. This was also used for blood sampling for the pharmacokinetic studies, arterial blood gas analysis and haematology and biochemistry.

An infusion of alfaxalone was started at time 0 with a loading dose followed by constant alphaxalone infusion via a calibrated syringe driver (SP100iz, WPI, Hitchin, UK). As there were two trials the preparations, the pre-alphaxalone administration phase was identical for both studies. The main differences were alphaxalone infusion rate and two separate strains of rats were used (Table 2.1). The isoflurane and nitrous oxide were stopped 2.5 minutes after starting the alfaxalone infusion or, prior to this if arterial blood pressure decreased sharply or apnoea occurred as described previously (White *et al.,* 2017).

For the pharmacodynamic parameters for each study, arterial blood pressure was monitored by an arterial pressure transducer (SensoNor 840; SensoNor, Horten, Norway) and recorded using a PC running Spike2 software (Cambridge Electronic Design (CED) Ltd, Cambridge, UK). Blood pressure measurements were analysed offline. Systolic, diastolic, and the mean blood pressure measurements were taken immediately prior to sampling.

Table 2.1. Alphaxalone dose used for the administration of each group.

Test group		Loading dose	Constant rate infusion (CRI)		Reduced CRI
			Phase I	Phase II	
	Duration / strain & gender / Rat	0 - 2.5 min	2.5-60 min	60 min - until the end of electrophysiology trial	end of electrophysiology trial to termination
Trial 1 **Normal dose group**	**Lewis**	Loading dose	Constant rate infusion (CRI)		Reduced CRI
		(mg/kg/min)	(mg/kg/min)		(mg/kg/min)
	Male	1.67	0.75	0.75	0.57
	Female	1.67	0.75	0.75	0.57
Trial 2 **Adjusted dose group**	**Sprague Dawley**	Loading dose	Phase I	Phase II	
		(mg/kg/min)	(mg/kg/min)	(mg/kg/min)	
	Male	1.67	0.75	0.75	
	Female	1.67	0.56	0.42	

2.3.3. Blood plasma sampling

The pharmacokinetic study involved eight samples collected in heparin tubes. The samples were centrifuged at 4000*g* for 10 minutes within 30 minutes of collection. The plasma was harvested and stored at -20°C and later moved to -80 °C freezer until analysis. Blood samples were collected at time 0 (before drug administration) and 2.5 (at the end of loading dose), and at 10, 30, 60, 120 min, as described previously (White *et al.*, 2017) in addition to R1 and T1 for the first study (Lewis rats). The last two samples were taken after reducing the infusion by 30% at 25 and 50 min for male rat experiments, while for female experiments, they were taken at 40 and 80 min. Furthermore, due to using the rats in two concurrent

experiments the R1 and T1 exact time points varied depending on the duration of electrophysiology experiment. Finally, the number of samples remained the same for the second study (SD rat), however, the time points were slightly modified. The plasma samples were taken at time 0, 2.5, 10, 30, 60 ,90, 120 and a final sample before terminating the experiment for both male and female SD rats.

2.3.4. Pharmacokinetic analysis

Pharmacokinetic analyses were conducted using a deterministic one compartment model (WinNonlin) with weight of $1/Y_{pred}$, where C_{obs} is described in terms of the predicted model concentration (C) and residual error (C_{Eps}) as shown in the following equation:

$$C_{Obs} = C+((C^{0.5}) \times C_{Eps})$$

Equation 2.1

Furthermore, the population PK (popPK) analysis used nonlinear mixed-effects modelling (NLME). Both models were conducted using Phoenix WinNonlin 8.3 software (Pharsight Corporation, Cary, NC).

2.3.4.1. Alphaxalone population PK analysis

The NLME population PK models were applied to the plasma concentration data using a one compartment pharmacokinetic model with zero order dose input and first order elimination, which provided a significantly better fit to the concentration time profiles compared to other multi compartments models. The rat populations used are shown in Table 2.2.

Table 2.2. Rat population distribution used in the popPK model. Small set model used 32 rats from group A and B while full set popPK model used A, B and C groups.

Strain	Lewis rats (A)		Sprague Dawley rats (B) (White et al., 2017)		Sprague Dawley rats (C) (modified dose/new study)	
No. of rats	16		16		24	
Gender	Male	Female	Male	female	Male	female
No. of rats	9	7	8	8	8	16

The residual error was estimated using a proportional residual error model. An exponential random effect model was chosen to describe inter-individual variability *i.e. parameter = typical parameter * exp(eta).*

Categorical covariates for sex (male and female) and strain (Lewis and Sprague Dawley rats) were implemented on the model parameters using a multiplicative exponential methodology. In addition, weight was added as a continuous covariate after normalising for the mean population weight using the following equation:

$$\boldsymbol{Rat\ normalised\ body\ weight = Log\left({}^{\boldsymbol{Rat\ weight}}/_{\boldsymbol{Mean\ population\ weight}}\right)}$$

Equation 2.2

The model analysis started with the basic compartmental models without the covariates. Next, the contribution of the covariates to the PK parameters was assessed by a reduction in the objective function (OBF) using stepwise forward inclusion. Selection of the best model was based on the change in the objective function to produce the lowest values in the Akaike and Bayesian Information Criteria (AIC and BIC), chi-square p-value based on the likelihood ratio test, and visual inspection of the population predicted concentration versus the observed concentrations and the resulting conditional weighted residual errors.

2.3.4.1.1. Candidate model validation

The chosen best model that described the data was statistically significant ($P<0.05$) on the likelihood ratio test in comparison to the basic model. The model was then checked for its adequacy and robustness using a bootstrap resampling method with stratification. This, in brief, is a repeated random sampling method from the original dataset of rats in order to produce another dataset of the same size but with a different sample combination of individuals, and the number of repeats can be determined before the start. The parameters obtained with the bootstrap replicates (500 times) were compared with the estimates obtained from the original model to check the validity of the tested model.

2.3.5. Alphaxalone dose adjustment using simulation

Dose simulations were performed using the final population PK model outputs to select which dose, infusion rate and duration for alphaxalone would be used in female rats in order to mimic the concentration-time profile of male rats and reach similar steady state levels.

2.4. Rat hepatocyte isolation procedure

2.4.1. Pre-isolation preparation

The hepatocyte isolation procedure (chelating and collagenase perfusion) is based on a modified protocol from Shibany *et al.*, (2016) and Shen *et al.*, (2012). The rats were euthanised according to Home Office procedures by cervical dislocation. Following confirmation of death, a U-shape incision was made starting at the caudal abdomen extending up to the diaphragm to expose the liver and portal vein. An over the needle catheter (size 20G) was inserted into the portal vein approximately 7-10 mm from the liver and secured in position with silk sutures. The perfusion was initiated within 10 minutes of the rats being euthanised to ensure effective infusion and cell viability. Once the catheter was secured, a small volume of buffer solution (buffer 1) was used to flush the liver and to make sure there was no leakage from the catheter insertion point. The liver inflated with pressure hence a cut in the inferior vena cava was made to let the flush solution escape. All buffer solutions were maintained at 37 °C and infused at the slowest possible pump speed (20 ml/min).

Figure 2.1. Hepatocyte isolation process. The picture shows catheter insertion and sutures fixing its location. The liver (yellow/cream) is inflated from the perfusion process.

2.4.1.1. Hepatocyte perfusion steps

Several buffer solution arrangements and optimisations were used in the hepatocyte isolation process. Furthermore, several perfusion buffer combinations were used for the optimisations, but the contents remained constant (Table 2.3). The sequence of buffers is as follows: solution 1 was for flushing the blood from the liver vasculature, solution 2 was a chelating solution (non-recirculation) to disrupt cell-matrix adhesion, solution 3, which contains calcium, was used to washout any remaining EGTA buffer. This third solution will also reintroduce the calcium into the liver to increase the activity of the collagenase enzyme for the next step. Solution 4 contains the collagenase enzyme which was used to dissociate the liver. The activity of this enzyme is mainly dependent on the presence of calcium in the liver. The decision to stop the perfusion was based on liver consistency, as the liver will lose its ability to maintain its structure. The different combinations are listed in Table 2.4. Lastly, method 7 was the most successful providing a large yield with high cell viability. This method was subsequently used for hepatocytes preparation.

Table 2.3. Description of each buffer solution

Perfusion solutions	Contents
Solution 1	Hanks' Balanced Salt Solution without Ca^{2+} and Mg^{2+} HEPES 20mM + $NaHCO_3$ 0.5mM
Solution 2	Solution 1 + EGTA 1 mM
Solution 3	Solution 1 + Ca^{2+} 5mM
Solution 4	Solution 3 + Collagenase IV (0.1, 0.5, 0.35 or 0.01%w/v)
Solution 5	William E medium + Foetal calf serum (10%)

Table 2.4. Different buffer combinations used for each method of hepatocytes isolation.

Method used	Solutions used				
	Solution 1	**Solution 2**	**Solution 3**	**Solution 4**	**Solution 5**
				Collagenase conc. (w/v)	
1	√	√	√	0.1% (Type IV fisher)	√
2	√	√	√	0.035% (Type IV fisher)	√
3		√		0.05 % (Type IV fisher)	√
3		√		0.05 % (Type IV fisher)	√
4		√		0.01 % (Type IV fisher)	√
4		√		0.01 % (Type IV fisher)	√
5		√		0.02% (Type IV sigma)	√
6		√		0.01 % (Type IV fisher) + Oxygenation	√
7	√	√	√	0.025 % (Type IV sigma)	√

2.4.1.2. Purification of the initial cell suspension

The digested liver was transferred to a sterile 10 cm Petri dish whilst perfused with solution five. It was then manually disrupted gently, using pointed scissors and tissue forceps. The liver capsule released the hepatocytes from the undigested tissue and formed a hepatocyte suspension. The suspension was passed through a sterile steel mesh of 250 µm (Metal Sieve, US Standard 60 mesh (250um), Fieldmaster®) followed by a 100 µm nylon mesh into 50 ml centrifuge tubes. Next, the cell suspension was centrifuged and washed twice for 5 min at a speed of 50 g at 4 °C. Then, the cell pellets were resuspended using solution 5 to a volume of 30-50 ml and placed on ice.

2.4.1.3. Determination of hepatocytes viability and yield

The yield and viability of freshly isolated hepatocytes were assessed with Trypan Blue dye exclusion test (Tennant, 1964). A volume of 15 µl of the cell suspension was diluted 1:5 in solution five and then a further 15 µl of the diluted mix was mixed with the same volume of the trypan Blue dye. The dye stains non-viable cells while viable cells will remain unaffected and were counted in a haemocytometer. Therefore, the viability (%) was determined as a percentage of live cells to total cell count. While the yield was determined by counting the number for viable cells multiplied by the dilution factor and the total suspension volume in the flask.

2.4.2. Preparation of rat liver microsomes

2.4.2.1. Rat liver tissue

A total of four male and four female Lewis rat livers were used for liver microsome preparation. Both inferior and superior right lobes of rat liver were tied and then excised (approximately 2g) during the hepatocyte isolation process, between solution 1 and 2, and stored at -80 °C.

2.4.2.2. Homogenisation of liver samples

On the day of preparation, the liver samples were thawed on ice and weighed accurately. The liver samples were finely cut and homogenised in 0.15 M potassium chloride solution (pH 7.4) at a volume of 10 ml/g of liver for 1 minute using a homogeniser (Witeg®, HG-15D, 27000 rpm, digital external controller). The homogenate was then filtered through nylon mesh (pore size = 250 µm) (Fisher scientific, UK). Aliquots (2 ml) of the filtered homogenate were stored at -80 °C for later use.

2.4.2.3. Preparation of S9 fraction and liver microsomes

The remainder of the homogenate was centrifuged at 10,000g for 20 minutes (Beckman® Coulter) at approximately 4 °C and the supernatant (S9 fraction) retained. Portions (3 ml) of the S9 fraction from each male rat were pooled together and centrifuged at 70,000*g* for 60 minutes (Hitachi® ultracentrifuge CP100NX) and the resulting supernatant discarded. The generated pellet was re-suspended in ice cold 0.1 M phosphate buffered saline (PBS) before being centrifuged again at 70,000*g* for a further 60 minutes. The final pellet was then re-suspended again in a volume of phosphate buffered saline equivalent to two times the weight of the original tissue. The samples were aliquoted and stored at -80 °C for CYP P450 and total protein determination.

2.4.3. Measurement of hepatocellularity

2.4.3.1. Hepatocyte suspension homogenisation

Tubes containing freshly isolated hepatocytes (3-5x10^6 cells/ml) for male and female rats were homogenised by multiple freeze-thaw cycles to rupture the cells, and then stored at -80°C until CYP450 content determination.

2.4.3.2. Cytochrome P450 content measurement and hepatocellularity determination

The method of Matsubara et al. (1976) was used for determining CYP 450 content of hepatocytes (homogenate), microsomes and homogenate (liver homogenate). This method used the dithionite difference in the Unicam UV/Vis Spectrometer UV4. Each sample was divided in two cuvettes that contained 1-2 mg of dithionite each. Then, one of the cuvettes was exposed to carbon monoxide (CO) for one minute, at the rate of one bubble per second. The baseline was recorded from the unexposed cuvette (no CO) and the spectral difference between the other samples (exposed to CO) was determined. The CYP450 content in hepatocytes, microsomes and homogenate was calculated using (equation 1).

$$nmol\ P450\ per\ ml = \frac{(A450 - A490)}{0.091}$$

Equation 2.3

Where 0.091 mL/nmol/cm is the CYP450 molar extinction coefficient, A450 is absorbance at 450 nm and A490 is absorbance at 490 nm

After measuring the CYP450 content in hepatocytes and its matched liver homogenate, hepatocellularity for each rat was determined using Equation 2.4

$$\text{Hepatocellularity per gram of liver } (HPGL) = \frac{nmol\ CYP450_{homogenate}\ per\ gram\ liver}{nmol\ CYP450\ per\ 10^6\ cells}$$

Equation 2.4

2.4.4. Protein content determination for rat liver microsomes

The protein content of liver homogenate and microsome samples (both diluted 10 and 20-fold) were measured for the total concentration, according to the Bradford method (1976). The calibration curve used for protein determination was made from Bovine Serum Albumin (BSA) in Phosphate Buffer Solution (PBS). The concentrations used for the calibration curve ranged from 0, 0.1, 0.5, 1.0, 1.4 and 2 mg/ml. Twenty µl of each standard dilution, the homogenate and liver microsomes were mixed with 1 ml of Bradford reagent (Sigma Aldrich, UK). The samples were left for 5 min at room temperature, and then transferred to cuvettes to determine the Optical density (OD) at 595 nm using a Spectrophotometer (PLS, UK). The total concentration of the protein was determined by comparing the OD of the liver microsomes against the standard calibration curve. Then, multiplying the determined protein concentrations in the diluted samples with the dilution factor.

2.5. Alphaxalone incubations

2.5.1. Linearity of initial reaction rate with respect to number of hepatocytes per ml

Male and female rat fresh hepatocyte concentrations were varied (0.1, 0.2, 0.5, 1, 2, 3, 4 × 10^6 cells/ml) for incubations with 10 µM of alphaxalone (final incubation concentration). Lastly, the incubations were carried out as described below (2.5.2).

2.5.2. Fresh rat hepatocyte incubation

The incubations were performed in 1.2 ml cluster tubes (Sigma, Dorset, UK) in a 96-well heater block (BioShake iQ), at 37 °C with a total incubation volume of 1 ml and cell concentration of 1 x10^6 cells/ml. Alphaxalone stock concentrations were prepared in Dimethyl sulfoxide (DMSO) at 100-fold the final incubation concentration (2 to 250 µM).

The isolated hepatocytes were diluted to 1 million cells/ml, using WEM with 0.125 % Bovine serum albumin. The hepatocytes were pre-incubated for 30 minutes at 37 °C with 5% CO_2. The reaction was initiated by adding the hepatocytes to cluster tubes containing alphaxalone giving final incubation concentrations of 2, 5, 10, 25, 50, 75, 100, 150, 200 and 250 µM. The incubation involved agitating the cells at 750 rpm at 37 °C. Due to the rapid rate of metabolism observed in male hepatocytes from section 2.5.1 the incubation sampling times used for male were 0, 0.5, 1, 1.5, 2, 4, 6 min while the female sampling times were 0, 1, 3, 6, 10, 14, 20 min. At each pre-determined time point 50 µl aliquots were removed from the incubation and quenched in 100 µl of ice cold methanol containing internal standard (3 µM). The samples were frozen at -20 °C and stored for later use.

2.5.2.1. Rat liver microsome incubations for NADPH dependent metabolism and inhibition studies

For determining NADPH dependent alphaxalone metabolism and metabolite appearance, alphaxalone was incubated in male liver microsomes. The incubation contained a microsomal concentration of 1 mg/ml, 10 µl alphaxalone (final incubational concentration of 15 uM), NADPH 10 mM and saline/phosphate buffer (pH 7.4) to make a total volume of 1 ml for each incubation. However, for the inhibition study, alphaxalone concentration was 15 µM while the inhibitors' concentrations (clotrimazole, indomethacin and trilostane) were 150 µM. Efforts were made to have no more than 1% of DMSO with in the incubation. Liver microsomes in PBS and NADPH were initially kept separate. Then, they were mixed for approximately 5 min at 37 °C to reactivate the liver microsomal protein before the start of the experiment. After 5 minutes, the test drugs with or without inhibitor were mixed into the microsomes, while the cluster tubes were agitated at 500 rpm at 37 °C. The incubation sampling time points for male rat liver microsomes were at 0, 1, 2, 3, 4, 7, 14, 24 minutes. At each time point 50 µl aliquots were removed from the incubation tubes, and then quenched in 100 µl of

ice-cold methanol containing internal standard (3 µM). Post incubation, the samples were frozen at -20 °C and stored for later use.

2.5.2.2. Alphaxalone and metabolites incubation for other species

Male and female rat, human, dog, rabbit and rhesus monkey liver microsomes were used to investigate sex and species variation for alphaxalone metabolism. Alphaxalone, keto-alphaxalone and beta-alphaxalone were incubated in 1 mg/ml liver microsomes and the initial concentration of each substrate was 15 µM. The incubations were carried out as described in Sec. 2.5.2.1 above.

2.5.2.3. Phase -II metabolism

2.5.2.3.1. Glucuronidation study

The method of incubation was modified from Fisher, et al. (2000). Briefly, 1 mg/ml of male or female liver microsomes, 0.1 M potassium phosphate buffer (pH 7.4), and 50 µg of alamethacin were mixed and placed on ice for 15 min. Magnesium chloride (1 mM in incubation) and either alphaxalone (25 µM in incubation) or oestradiol as a positive control (25 µM in incubation) were added, and the mixture was pre-incubated at 37 °C for 3 min. The reaction was initiated by adding uridine diphosphate glucuronic acid (UDPGA) (sigma) (3 mM in incubation) to make a final volume of 500 µl and shaken at 500 rpm. The incubation lasted 30 minutes and samples taken (100 µl) for each time point (0, 15 and 30 minutes) were quenched in 200 µl of ice-cold methanol containing internal standard (3 µM). Post incubation, the samples were frozen at -20 °C and stored for later use.

2.5.2.3.2. Sulfation using S9 fraction

The incubation method was modified from Richardson *et al.* (2016). The male rat S9 fraction was used at a concentration of 1 mg protein/ml and diluted with tris buffer solution (200 mM, 7.4 *p*H) containing 2 mM magnesium chloride. Alphaxalone was incubated at 25 µM and the reaction started by adding 100 ml of PAPS (0.1 mM) in tris buffer. The S9 fraction was preincubated for 5 min at 37 °C and then the drug and cofactor were added to initiate the reaction. The incubation lasted 30 minutes and the samples taken (100 µl) for each time point (0, 15 and

30 minutes) were quenched in 200 µl of ice-cold methanol containing internal standard (3 µM). Post incubation, the samples were frozen at -20 °C and stored for later use.

2.5.3. Sample preparation for analysis

The samples that were frozen were kept at least overnight at -20 °C but not more than two weeks. The samples were then centrifuged at 1000*g* for 15 min at 4°C. Then, the supernatant was transferred to LC-MS vials ready for analysis.

2.5.4. Enzyme Kinetic Analysis

Peak area ratio of alphaxalone and its respective internal standard lansoprazole was determined by integration of chromatograms produced using Analyst 1.7.1 (A B Sciex UK Ltd, Macclesfield , UK) The data were plotted as the natural logarithm (Ln) of substrate peak area over internal standard peak area against time. K_{dep} is represented by the slope of the line and the initial reaction rates (V_0) in alphaxalone incubations were determined using the following Equation 2.5:

$$V_0 = -k_{dep}[D]_0$$

Equation 2.5

The initial reaction velocity (V_0) for the different substrate concentrations were calculated by multiplying the initial substrate concentration $[D]_0$ with the corresponding K_{dep} value. The initial reaction rate (V_0) is related to the Michelis constant (K_m) and the maximal reaction velocity (V_{max}) via Equation 1.1. For the determination of intrinsic clearance, V_0 was plotted against initial substrate concentration to produce a Michaelis-Menten graph (Figure 1.6) using Graph Pad Prism 8.1. Intrinsic clearance (CL_{int}) was calculated using (Equation 1.2).

2.5.5. Rat liver clearance *In vitro/In vivo* extrapolation (IVIVE)

2.5.6. Estimating hepatic metabolic clearance

The hepatic metabolic clearance was calculated using the following equation:

$$Hepatic\ CL_{int} = (invitro)CLint.\frac{mL\ of\ incubation}{No.of\ hepatocytes}.\frac{Hepatocellularity.}{g\ of\ liver\ weight}.\frac{g\ of\ liver\ weight}{Kg\ of\ body\ weight}$$

Equation 2.6

Where both male and female Lewis rat hepatocellularities (determined in sec. 2.4.3 above) were used in the equation for each specified gender. Rat liver weight was determined by deducting the total weight of the rat from its weight after removing the liver which ranged from 2.5–3 % of total rat body weight.

2.5.6.1. Plasma protein binding (PPB)

For determining male and female Lewis rat PPB of alphaxalone a single-use Rapid Equilibrium Dialysis (RED) device, Thermo Fisher Scientific (UK), with 48 equilibrium membrane inserts was used. Each insert consists of two sides (plasma side and buffer side) and is connected by a membrane. Furthermore, the buffer side contained 400 µl of PBS sample, containing 100 mM sodium phosphate and 150 mM sodium chloride at *p*H 7.4, while 200 µl of plasma containing drug sample was used in the plasma chamber. Three replicates of 10 µM alphaxalone and diclofenac as positive control were used for the study. The dialysis system was agitated at 800 rpm for 4 hours at 37 °C to reach equilibrium. Plasma and buffer samples (50 µl) were taken, and an equal volume of its blank counterpart was added to each sample in order to have an equivalent matrix. Then, 200 µl of ice-cold methanol containing internal standard (3 µM) was added to the samples and stored at -20 °C for at least 24 hours. The samples were then prepared as described in section 2.5.3 above.

2.5.6.2. Alphaxalone incubational binding

The value of the fraction unbound in hepatocytes incubation ($f_{u\ inc}$) was predicted using lipophilicity base model by Kilford *et al.*, (2008) and is described as follow:

$$f_{u,inc} = \frac{1}{1 + 125 * V_R * 10^{0.072*(LogP)^2 + 0.067*LogP - 1.126}}$$

Equation 2.7

Where VR is the ratio of the cell and incubation volumes which is 0.005 for 10^6 cell/ml incubation.

2.5.6.3. Blood:plasma ratio determination

Separate male and female Lewis rat blood (pooled n=5), obtained from Charles River Laboratories (Margate, UK), were used for blood plasma ratio determination of alphaxalone. The experiment consisted of three (0.5 ml blood) test samples and vehicle only sample for each gender. Diclofenac was used as positive control to validate the experiment procedure. No more than 0.1 % of DMSO was used in the experiment so as to reduce any haemolysis and a concentration of 10 μM were used for both alphaxalone and diclofenac. After the addition of the drug to the blood, the vials were covered from light and kept at room temperature for 30 minutes. The samples were then centrifuged at 2000g for 15 min at 4°C. The vehicle only sample was checked to make sure that no haemolysis had occurred and then 50 μl of the supernatant for each remaining sample was also checked and transferred to another vial. 100 μl of ice-cold methanol containing internal standard (3 μM) was added to the samples and stored at -20 °C for at least 24 hours. The samples were then prepared as described in section 2.5.3 above. The ratio was then calculated using the following equation:

$$\text{B:P ratio} = \frac{\text{Peak Area of directly spiked plasma (references plasma)}}{\text{Peak Area of plasma from spiked blood (plasma sample)}}$$

Equation 2.8

2.5.6.4. Estimating blood hepatic metabolic clearance

For estimating the blood hepatic metabolic clearance (CL_H) both well stirred and parallel-tube models were used following Equation 2.9 and Equation 2.10. The

hepatic blood flow used was 72 ml/min/kg (Davis & Ward, 2015) and the plasma protein binding for alphaxalone was 96% for male and female Lewis rats.

Well-stirred model

$$CL_H = \frac{Q_H \cdot \frac{F_{ub}}{F_{u\,inc}} \cdot CL_{int}}{Q_H + \frac{F_{ub}}{F_{u\,inc}} \cdot CL_{int}}$$

Equation 2.9

Parallel-tube model

$$CL_H = Q_H \cdot \left(1 - e^{\frac{-CL_{int} * \frac{F_{ub}}{F_{u\,inc}}}{Q_H}}\right)$$

Equation 2.10

2.6. Alphaxalone metabolic pathway modelling

A simple model was designed in order to model the metabolic pathway and metabolite formation. The alphaxalone metabolism modelling was performed using Phoenix 8.3 NLME with a multiplicative or additive residual error model. The rats metabolic pathway modelling was conducted using population modelling to account for inter individual variability. While, the human, rabbit, dog, monkey data analysis was conducted without population analysis as all data was produced from of a single pooled sample in triplet.

Alphaxalone was shown to be reversibly converted to keto-alphaxalone and then beta-alphaxalone as well as metabolised to other metabolites. Hence, a simplified model was created Figure 2.2. The model considers the reversable nature of alphaxalone conversion to keto and beta alphaxalone and any unknown metabolites (A_0, K_0 and B_0) that can also be reversibly converted back to the original substrate.

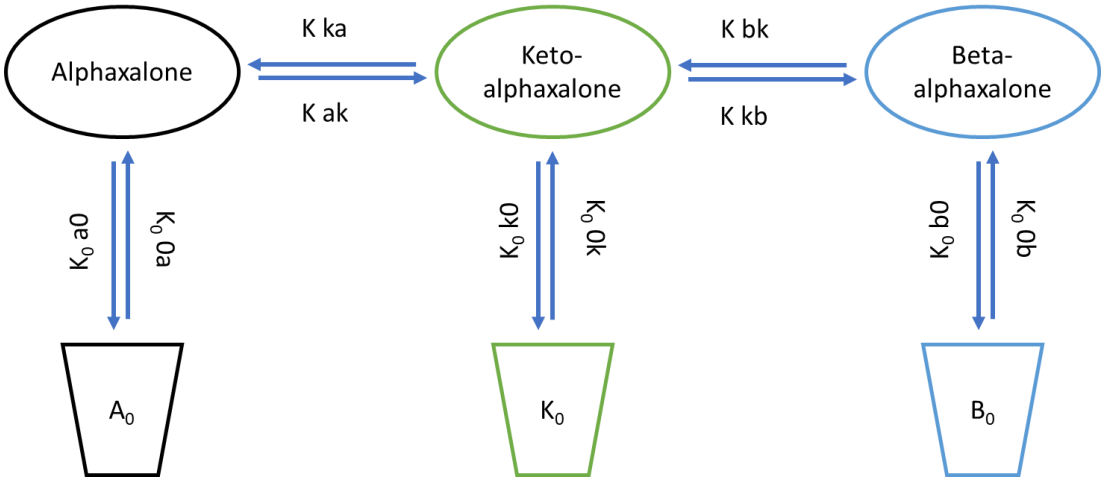

Figure 2.2 Model used for the simultaneous modelling of alphaxalone and its metabolites concentration data. Parameter definitions are listed in table 2.5.

Table 2.5. Rate constant definitions used in the alphaxalone metabolism model.

Parameter	Description
Alphaxalone (µM)	Alphaxalone compartment
A_0	Alphaxalone elimination compartment
Keto-alphaxalone (µM)	Keto-alphaxalone compartment
K_0	Keto-alphaxalone elimination compartment
Beta-alphaxalone (µM)	Beta-alphaxalone compartment
B_0	Beta-alphaxalone elimination compartment
K_ak (1/min)	Conversion rate constant for alphaxalone to keto-alphaxalone
K_ka (1/min)	Conversion rate constant for keto-alphaxalone to alphaxalone
K_kb (1/min)	Conversion rate constant for keto-alphaxalone to beta-alphaxalone
K_bk (1/min)	Conversion rate constant for beta-alphaxalone to keto-alphaxalone
K_0_a0 (1/min)	Conversion rate constant for alphaxalone elimination
K_0_0a (1/min)	Conversion rate constant for alphaxalone reversable elimination
K_0_k0 (1/min)	Conversion rate constant for keto-alphaxalone elimination
K_0_0k (1/min)	Conversion rate constant for keto-alphaxalone reversable elimination
K_0_b0 (1/min)	Conversion rate constant for beta-alphaxalone elimination
K_0_0b (1/min)	Conversion rate constant for beta-alphaxalone reversable elimination

2.7. Standard (STD) quantification curve and plasma sample preparation

Standard quantification (STD) curves for *in vivo* plasma samples quantification were generated using authentic alphaxalone standard samples giving concentrations from 0.6 to 120 μM in addition to the use of quality controls (QC). Spiking solutions for standards and QCs were made from separate accurate weighing of drug compounds. The methanol standard curve and QCs were prepared by spiking 10 μL of a known concentration spike solution into a solution of 40 μL methanol + 100 μL methanol containing 3 μM of lansoprazole as internal standard + 50 μL of either male or female blank plasma (Charles River, Margate, UK), which was used for matching the *in vivo* samples. Alphaxalone *in vivo* plasma samples were prepared by adding 50 μL of the plasma samples + 50 μL methanol + 100 μL methanol containing 3 μM of lansoprazole as internal standard.

Samples, standards and QCs were then vortexed, stored in a freezer at -20 °C overnight prior to centrifugation at 4000*g* for 20 minutes at 4 °C. The supernatant was then transferred into LC-MS vials for analysis and concentration determination. Finally, the STD curves were analysed at the beginning of the run and at the end of the run to determine any variation or deterioration of LC/MS performance. The analytical methods were validated to ensure suitable precision and accuracy, lower limit of quantification (LLOQ), linearity, calibration range and selectivity.

While the STD curves for the metabolic pathway determination were generated using a single curve that contained the three substrates together (alphaxalone, Keto-alphaxalone and beta-alphaxalone) and IS with a substrate concentration ranging from 0.2 to 60 μM, in addition to the use of quality controls (QC). The preparation process is similar to the plasma STD curve preparation but with the use of inactivated rat liver microsomes instead of plasma for matrix matching.

2.7.1. STD curves used for quantification

Two linear standard curves were measured, at the start and the end of each run and an average of two curves were used to calculate drug concentrations. This was true for both *in vivo* and *in vitro* quantification process. Furthermore, the lower limit of quantification (LLOQ) was (0.2 µM) and at least r^2>0.9 for both male and female standard curves while the variation at LLOQ was <20%.

2.7.2. LC-MS method for analysis

The initial liquid chromatography-mass spectrometry (LC-MS) machine used was retired and the new samples had to be analysed on an alternative machine. Due to this, the plasma samples have been analysed at several sites and using different machinery, as such, there will be three methods of analysis for alphaxalone plasma samples described.

Analytical method 1: Plasma samples for Lewis male and female rat *in vivo* studies.

The method was developed on a Micro mass Quattro Ultima mass spectrometer (Waters, Wilmslow, UK) using electrospray positive mode with an Agilent 1100 HPLC (Cheadle, UK). Tandem mass (MS/MS) analysis was used on alphaxalone and lansoprazole as the internal standard. The mass spectrometer for alphaxalone and lansoprazole was operated in positive ion mode, with a source temperature of 140 °C, a spray voltage of 3.5 kV and collision energy of 18eV and 25eV, while the mass transition of alphaxalone and lansoprazole were m/z 333.2 ➔ 315.2 and 297.2 and 370 ➔ 252.1, respectively.

The solvent flow rate was kept constant at 0.4 ml/min and the solvent gradient is described in table 2.6. Solvent (A) was 10% methanol, 90% water and 0.02% formic acid and Solvent (B) was 100% methanol and 0.02% formic acid. Compounds were separated at 60 °C on Ascentis® C18 column (2.1 × 50 mm, 3 µm) (Sigma, UK) protected by a Phenomenex C18 guard cartridge (Phenomenex, UK).

Table 2.6. Alphaxalone solvent gradient for liquid chromatography analysis

Time	% Solvent B	Flow rate
0.00	30	0.4
1.80	80	0.4
3.00	99	0.4
3.60	99	0.4
3.75	30	0.4

Analytical method 2: Plasma samples for male and female SD rat *in vivo* studies.

To have accurate representation of alphaxalone plasma concentrations, the plasma samples were not allowed to be stored for longer than two months from sampling. As such, all male SD plasma samples and some female SD plasma samples were analysed by an external contractor (Xenogesis) using a different LC-MS/MS method. Those rats were coded as 1001 to 1008 for male SD rats and 2001 to 2008 for female SD rats.

The Xenogesis method was developed on a Thermo TSQ Quantiva with Thermo Vanquish UPLC system. Tandem mass (MS/MS) analysis was used on alphaxalone and imipramine as the internal standard. The mass spectrometer for alphaxalone and imipramine was operated in positive ion mode RF Lens (V) at 67 and 56, with a source temperature of 365°C, a spray voltage of 4.25 kV and collision energy of 18eV and 40eV, while the mass transition of alphaxalone and imipramine were m/z 333.2 →, 297.1, 223.1 and 281.18 → 193.04 respectively.

The solvent flow rate was kept constant at 0.8 ml/min. Solvent (A) was 100% water and 0.1% formic acid and Solvent (B) was 100% methanol and 0.1% formic acid. Compounds were separated at 65°C on Phenomenex Luna Omega 1.6µm, C18 100Å, 50 x 2.1mm protected by a Phenomenex C18 guard cartridge (Phenomenex, UK). The initial gradient started at 35% of solvent B and reached 100% at 1.15 min. Then, the solvent concentration returned to 35% at 1.4 min.

Analytical method 3: plasma samples for female SD rats

The remaining part of the female batch were analysed inhouse using a method developed on a Sciex Qtrap 4000 mass spectrometer (A B Sciex UK Ltd, Macclesfield , UK) using electrospray mode combined with Shimadzu Liquid Chromatography. The female SD rats are coded 2201 to 2208.

Tandem mass (MS/MS) analysis was used on alphaxalone and lansoprazole as the internal standard. The mass spectrometer for alphaxalone and lansoprazole and other metabolites and their specific masses and collision energy are listed in

Table 2.7. In addition, all compounds were analysed in positive ion mode, the ion source temperature was 450 °C, the ionisation voltage was 5.0 kV, source gas 1 and 2 were 30 and 40 psi respectively, and finally the curtain gas used was 30 psi. Oxidation metabolism is a common metabolic pathway for steroids and steroid like structures. Thus, for alphaxalone metabolite investigation a mass of +16 was added to both alphaxalone and keto-alphaxalone m/z to determine any other unidentified oxidative metabolites. A list of alphaxalone, internal standard and alphaxalone metabolites MS conditions as well as the parent and daughter ions are in Table **2.7**.

The solvent flow rate was kept constant at 0.3 ml/min with an upper pressure limit of 350 bar. Solvent (A) was 10% methanol, 90% water and 0.02% formic acid and Solvent (B) was 100% methanol and 0.02% formic acid. The gradient started at 30 % of solvent B and reach nearly 100 % at 5 minutes which then was kept for a full minute before reducing the concentration back to 30 % (Table **2.8**). The compounds were separated at 60 °C on Ascentis® C18 column (2.1 × 50 mm, 3 µm) (Sigma, UK) protected by a Phenomenex C18 guard cartridge (Phenomenex, UK). The run time for alphaxalone and metabolite separation in the liquid chromatography was an 8.5-minute.

Table 2.7. Mass spectrometry method for alphaxalone, lansoprazole, keto-alphaxalone, and oxidised metabolites.

Drug	Ion mode (+/-)	Main mass (m/z)	Fragment mass (m/z)	Dwell time (Sec)	Cone voltage (volts)	Collision energy (CE)	Collision cell exit potential (CXP)	Retention time (min)
Lansoprazole	+	370.1	252.1	0.1	56	17	20	4.24
Alphaxalone	+	333.2	315.2-297.1	0.05	90	21	14-20	5.60
Keto-alphaxalone	+	331.2	313.3	0.05	90	21	14	5.21
Beta-alphaxalone	+	333.2	315.2-297.1	0.05	90	21	14-20	5.13
Product X	+	331.2	301.2	0.05	90	21	15	4.99
Beta-oxidised alphaxalone	+	349.2	289.2	0.05	90	21	8	
Oxi-alphaxalone	+	349.2	331.2	0.05	90	15	18	

Table 2.8. Solvent concentration gradient for alphaxalone separation from other metabolites.

Time	% Solvent B	Flow rate
Min		**ml/min**
0	30	0.3
5	90	0.3
5.2	99	0.3
6.2	99	0.3
6.3	30	0.3
8.5	30	0.3

2.7.3. Statistical analysis

Statistical tests were performed using GraphPrism version 8.3 (GraphPad Software, CA, USA). The pharmacokinetic parameters were tested using unpaired t-test and two way analysis of variance test (ANOVA) followed by Sidak test for multiple comparisons and a p value of <0.05 was considered statistically significant. Data are reported as mean ± standard deviation (SD) unless stated otherwise.

Chapter 3

Alphaxalone PK/PD in vivo investigation

(male and female rats)

3. Chapter 3. Alphaxalone PK/PD *in vivo* investigation (male and female rats)

3.1. Introduction

The neurorsteroidal drug, alphaxalone, is one of the better options available for quick and safe induction of anaesthesia in domestic species such as dogs, cats and rabbits. It has been reported that alphaxalone demonstrates sex differences; initially these were thought to be from an oestrogen related response that potentiated the alphaxalone response (Fink et al., 1982) and later reported to be caused by pharmacokinetic differences (White, *et al.*, 2017). The White *et al.* group studied alphaxalone pharmacokinetics in male and female Sprague Dawley rats by administering a constant rate infusion and then measured alphaxalone plasma concentrations and resulting PK parameters were compared. The group concluded that alphaxalone clearance was greater in male rats compared to female rats with the latter having greater exposure. Furthermore, the female rats were more profoundly anaesthetised as observed from the lower measured arterial pressures as the alphaxalone infusion progressed. This difference was most likely due to alphaxalone plasma concentration differences as alphaxalone reportedly has dose dependent cardiovascular inhibition (Muir et al., 2008).

The pharmacokinetics investigation of alphaxalone has been reported by several groups who unfortunately only investigated single sex in their studies (Lau et al., 2013; Visser et al., 2002). However, the combined reports showed that female clearance was at least two-fold smaller than the male in Wistar rats. Furthermore, the Visser group concluded that bodyweight is a significant covariate in alphaxalone clearance and needs to be considered when alphaxalone is being investigated. Larger rats tend to have bigger organs and larger blood flow to all organs including the liver.

Rat weight can greatly vary by its gender and in some cases strain. For gender, the adult male rat is approximately 1.5 to 2 fold heavier than female for the same

age group (Charles River). Following the conclusion by Visser *et al*., a two fold difference in bodyweight may truly affect the rate of alphaxalone clearance. However, the question arises whether there is a difference in clearance between male and female rats of the same weight. Another rat strain used for research is the Lewis rat which are mostly used for induced inflammation and arthritis studies. This strain is characterised by their small size and weight in comparison to other strains such as Sprague Dawley and Wistar rats. Matching the weight for both male and female in PK studies can be used to remove weight as a covariate for clearance and therefore unmasks any intrinsic differences between genders such as metabolism or renal excretion. However, fixing weight for male and female usually introduces an age covariate which may also impact on clearance.

Hence, the aim of this chapter is to use PK population modelling and incorporate these covariates (sex, strain and weight) for the PK parameters and draw conclusions about their significance. Furthermore, as reported by White *et al.,* female rats showed more cardiovascular inhibition compared to male rats for the same dosing regimen. Therefore, the creation of a population PK model may be used to produce a modified alphaxalone administration for female rats providing the same plane of anaesthesia as male rats while minimising detrimental cardiovascular inhibition. A summary of the investigation approach is presented in figure 3.1.

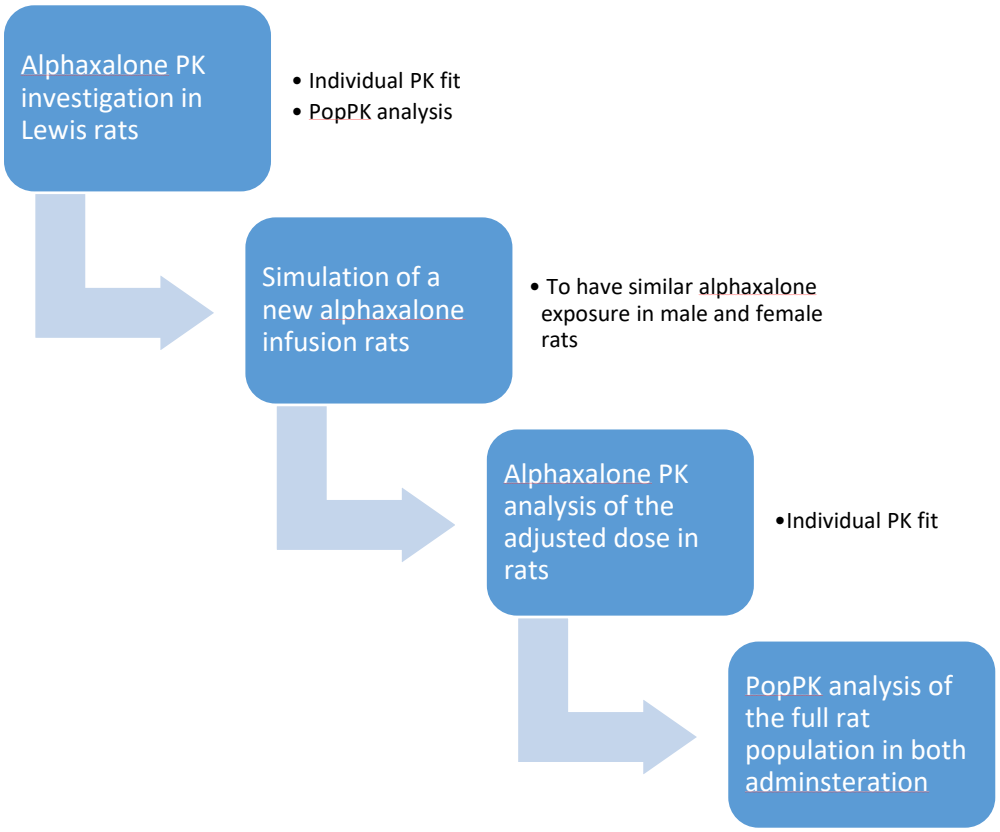

Figure 3.1. Schematic diagram summaries the investigation process taken in the present chapter.

3.2. Results

3.2.1. *In vivo* alphaxalone investigation using Lewis rats: Deterministic PK compartmental analyses

Alphaxalone plasma concentrations for Lewis male and female rats were best fitted to a one compartmental IV infusion model. Adding additional compartments to the model did not improve the fit according to the Akaike Information Criteria (AIC). The model fit along with alphaxalone concentrations for the male and female Lewis rats are presented in Figure 3.2 Figure 3.3, respectively. The data showed that the model fit and PK parameter estimations were greatly influenced by some time points more than others due to the limited number of plasma samples for each rat and some missing time points some extrapolation has been used in order to fir the curves. When all the *in vivo* data overlapped together (Figure **3.4**), the comparison showed a clear higher alphaxalone exposure in female rats compared to the male rats.

Two rats, one of each sex, died and concentrations for these were only determined up to the point of death. Two experiments, one of each sex, were terminated in the herein study. Both causes of termination were due to problems with breathing due to mucus accumulation in the endotracheal cannula.

The male Lewis rat plasma concentrations reached steady state concentrations earlier than female rats. In fact, it appears that some of the female rats have not reached steady state concentrations as alphaxalone plasma concentrations were still increasing at later time-points. The pharmacokinetic parameters calculated by the one compartment IV infusion model for the male and female Lewis rats are presented in table 3.1. An unpaired two tailed t-test showed statistically significant differences between male and female rats for all PK parameters.

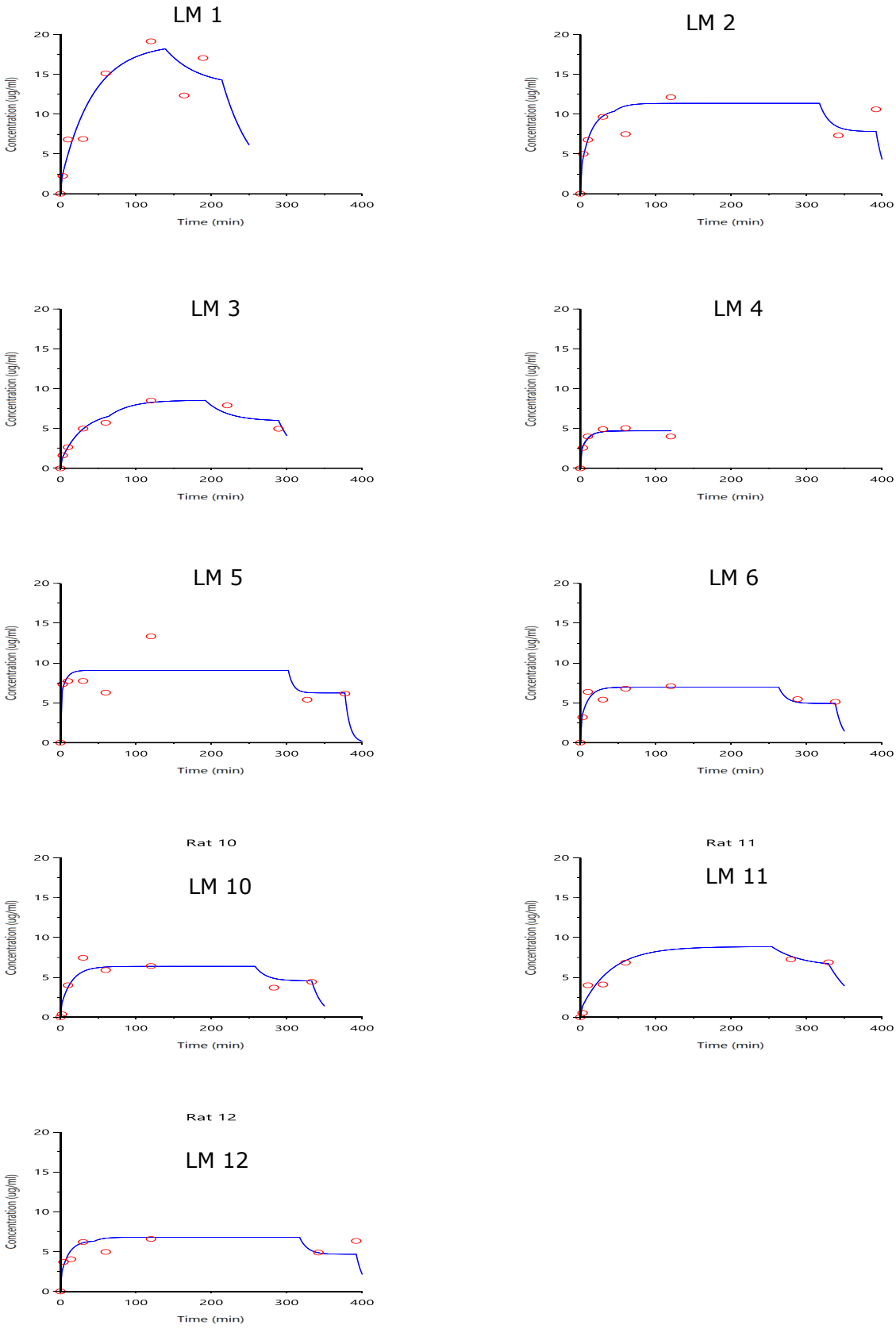

Figure 3.2: **Alphaxalone plasma concentration-time plots for Male Lewis rats.** Blue line represents one compartment model fit. Red circles represent measured concentrations. Alphaxalone IV administration at a rate of 1.67 mg/kg/minute for 2.5 minutes followed by 0.75 mg/kg/minute until the end of the electrophysiological stage, then by 0.52 mg/kg/minute for the end of the experiment.

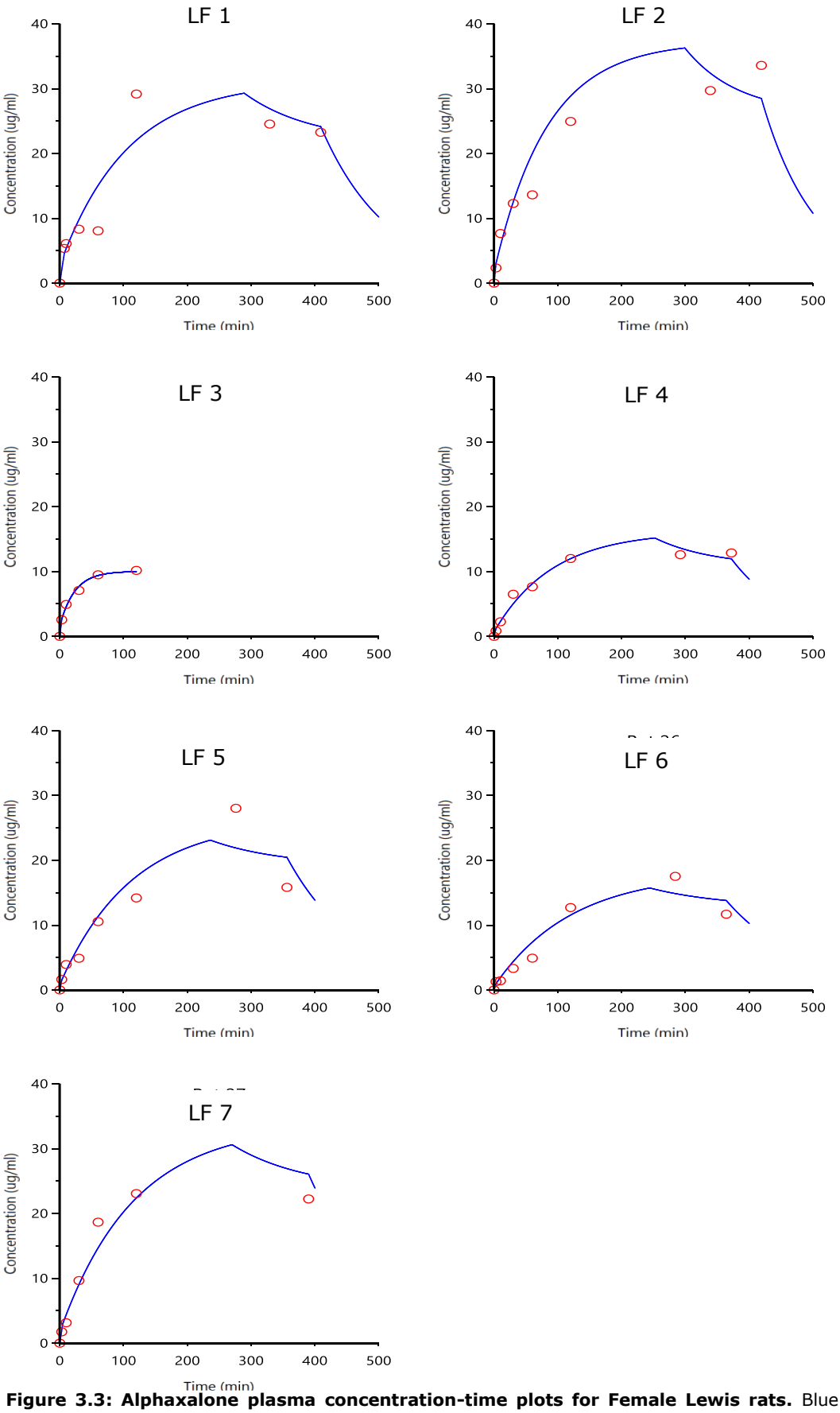

Figure 3.3: Alphaxalone plasma concentration-time plots for Female Lewis rats. Blue line represents one compartment model fit. Red circles represent measured concentrations. Alphaxalone IV administration at a rate of 1.67 mg/kg/minute for 2.5 minutes followed by 0.75 mg/kg/minute until the end of the electrophysiological stage, then by 0.52 mg/kg/minute for the end of the experiment.

Table 3.1: Estimated PK parameters of male and female Lewis rats. PK parameters for 16 (9 male & 7 female) Lewis rats after IV administration of alphaxalone at a rate of 1.67 mg/kg/minute for 2.5 minutes followed by 0.75 mg/kg/minute until the end of the electrophysiological stage, then by 0.52 mg/kg/minute for the end of the experiment.

Rat name	**CL**	**$T_{½}$**	**MRT**	**Vd_{ss}**
	(mL/min/kg)	**(min)**	**(min)**	**(L/kg)**
Male group				
LM 1	41.2	29.5	42.6	1.76
LM 2	70.1	9.4	13.6	0.95
LM 3	107	20	28.9	3.10
LM 4	150	6.4	9.2	1.39
LM 5	81.6	4.5	6.4	0.52
LM 6	110	6.8	9.8	1.08
LM 7	122	10	14.4	1.75
LM 8	85.3	27.3	39.3	3.36
LM 9	117	7.2	10.3	1.21
Mean	**98.3**	**13.5**	**19.4**	**1.7**
SD	**32.2**	**9.6**	**13.8**	**1.0**
Female group				
LF 1	23.5	73.2	106	2.5
LF 2	19.5	57.7	83.3	1.6
LF 3	75.5	16.2	23.4	1.8
LF 4	44.4	63.6	91.7	4.1
LF 5	29.8	77.9	112	3.3
LF 6	42.7	84.2	121	5.2
LF 7	22.2	80	116	2.6
Mean	**36.8**	**64.7**	**93.3**	**3.0**
SD	**19.7**	**23.3**	**33.6**	**1.3**
P	**<0.01**	**<0.01**	**<0.01**	**<0.05**

CL, clearance; $T_{½}$, half-life; Cp_{ss}, plasma concentration at the steady state; MRT, mean residence time; Vd_{ss}, volume of distribution. CL, Vd_{ss}, $T_{½}$ and MRT are significantly different between the male and female rats.

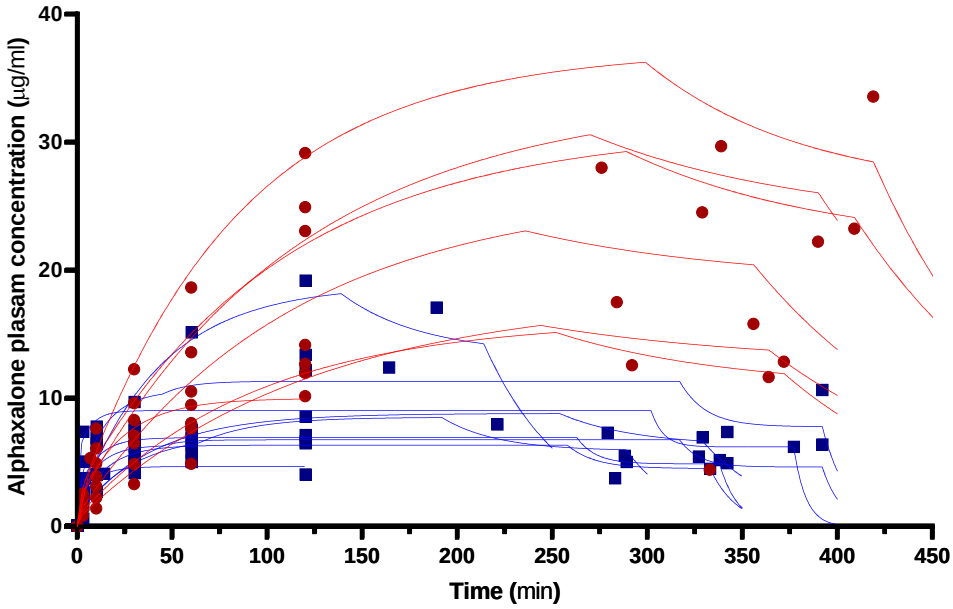

Figure 3.4: Alphaxalone plasma concentration-time curve; comparison between male (blue lines) and female (red lines) Lewis rats for the same dosing regimen: 1.67 mg/kg/minute for 2.5 minutes followed by 0.75 mg/kg/minute until the end of the electrophysiological stage, then by 0.52 mg/kg/minute.

3.2.2. cardiovascular effects of alphaxalone in Lewis rats

The mean arterial pressure (MAP) data during administration of alphaxalone are plotted in Figure 3.5. Inhalant anaesthesia (isoflurane) prior to alphaxalone administration depressed MAP, however, 5-10 min following discontinuation of the inhaled anaesthesia and start of the alphaxalone loading dose, all rats showed an increase in the arterial pressure (Figure 3.5). The arterial pressure then stabilised after 30 min of the start of the main alphaxalone infusion. The MAP peak was maintained until 220 min for males before declining, while females showed early signs of MAP decrease from between 40-75 min. Measurements of MAP showed no significant difference between male and female rats up to 60 min of alphaxalone infusion, however, at 120 min females showed significantly greater cardiac inhibition ($P<0.05$) compared to males.

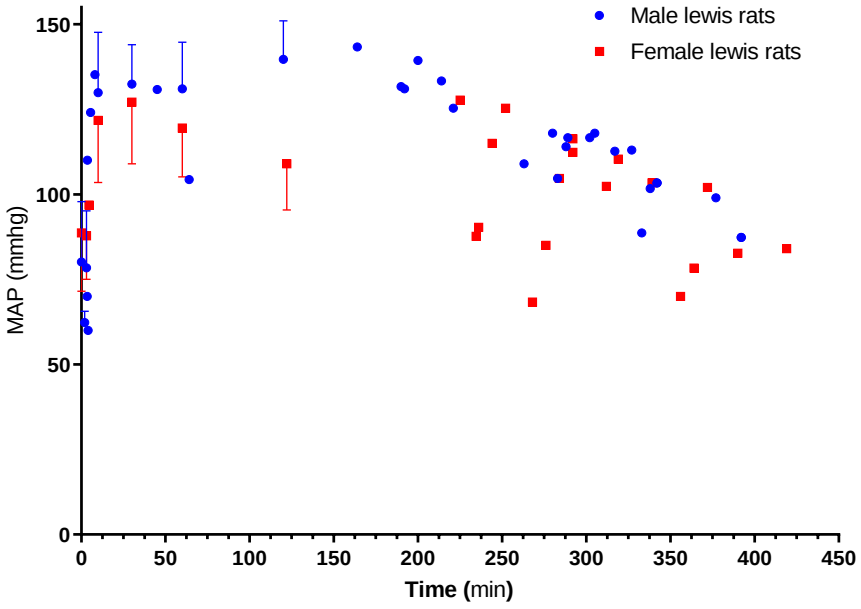

Figure 3.5: MAP versus time plot. Data presented as mean±SD; later time points are presented as single recorded points as they were measured at different times.

3.2.3. Alphaxalone population PK (popPK) analysis (small set)

From the previous results, it was clear that administering the same dose of alphaxalone to male and female Lewis rats resulted in a substantial cardiovascular depression in the females which correlated to higher alphaxalone plasma exposure. Hence, to reduce this cardiac depression to the minimum in female rats while maintaining an appropriate plane of anesthesia, an advanced nonlinear mixed-effects (NLME) model was used to analyse the rats as a population. This popPK model characterizes the concentration-time course of alphaxalone and evaluated the impact of each covariate (strain, gender, weight) on fixed parameter effects while assessing interindividual variability through the inclusion of random effects.

The first dataset (small set) used for the analysis of alphaxalone infusion consisted of 28 animals of both sexes and strains (Table 2.2). The data for the small set was obtained from two studies: 1. Male and female Lewis rats; 2. Male and female SD rats (same dosing regimen as Lewis study) from White *et al.*, (2017). The total number of plasma samples used in the modelling was approximately 200, with an average of 5 to 8 samples for each rat.

A stepwise forward approach were used to create a series of models to find the most parsimonious model, which is presented in (Figure 3.6). The random effects were included on both parameters (Vd and CL) with no correlation. Furthermore, a continuous covariate for body weight was used in the model though it did not reduce the objective function for any of the parameters while categorical covariates (gender and strain) were implemented on the parameters Vd and CL. The influence of the covariates for (gender) male and female rats and (strain) Lewis and Sprague Dawley are as follow:

$$V = tvV \times \exp(-0.0237 \times (Strain = 1)) \times \exp(nV)$$

Equation 3.1

$$Cl = tvCl \times \exp(-0.841 \times (gender = 1)) \times \exp(0.478 \times (Strain = 1)) \times \exp(nCl)$$

Equation 3.2

Where the Typical Value (*tv*) is the population fixed effect value for the parameter, Strain = 1 refers to Sprague Dawley, and gender = 1 refers to females.
The outputted typical values (*tv*) that resulted from the final small set model (Table **3.2**) were encompassed by the 2.5 and 97.5% confidence intervals of the bootstrap resampling analysis. Also included in Table 3.1 are the mean and the SD of the post hoc empirical Bayes estimates (EBE) for the parameters.

Model evaluation

The overall predicted concentrations had a good distribution around the line of unity as observed in both goodness of fit plots of the basic and the optimised small set model for observed concentration against individual predicted concentration (IPRED) shown in Figure 3.6 and observed concentration and predicted concentration (PRED) shown in Figure **3.7**. The conditional weighted residuals (CWRES) for the basic and optimised small are presented in Figure 3.8 and show less spread and an overall improvement over the basic model. A box plot of sex and strain versus CL and Vd of the optimised small set model (Figure 3.9) showed

no diverging random effects after incorporating the covariates into the optimised popPK model.

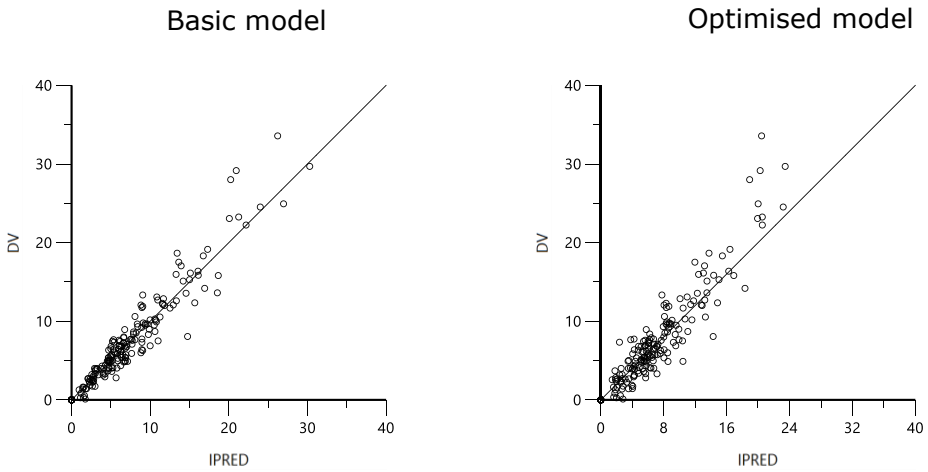

Figure 3.6. The plot of the observed concentrations (DV) versus individual predicted values (IPRED) (DV vs IPRED). Individual prediction obtained by setting random effects to the 'post hoc' or empirical Bayesian estimate of the random effects for the individual from which the DV observation was made. Thus, the plot shows observed vs fitted values of the model function. Ideally, points should fall close to the line of unity y=x. The concentration presented is (µg/ml)

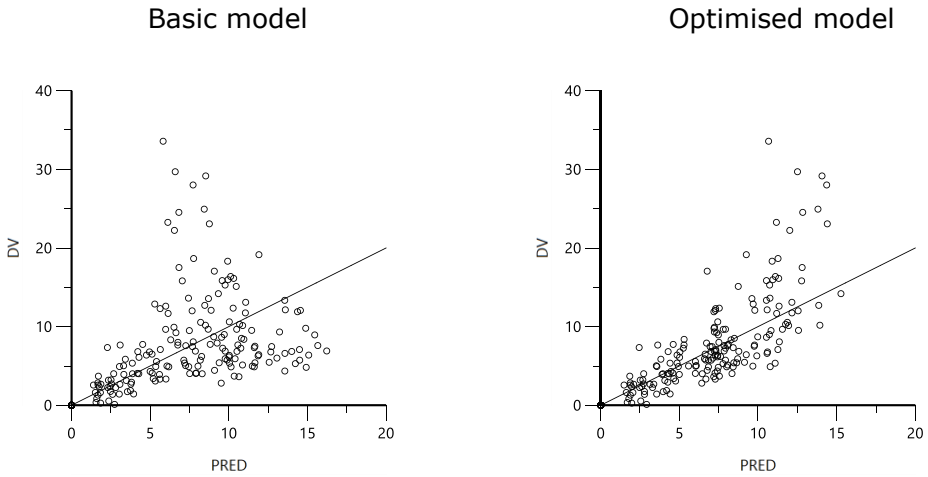

Figure 3.7. Alphaxalone plasma concentration (DV) vs PRED. Population predictions used instead of individual predictions. Since population predictions are typically less accurate, this plot will show larger deviations around the y=x line of unity than DV vs IPRED. The concentration presented is (µg/ml).

Table 3.2. The outputted typical values of the primary PK parameters for the most parsimonious model of small set.

	Typical values		Post hoc (mean±SD)	
Rat groups	Vd (mL)	CL (mL/min)	Vd (L/kg)	CL (mL/min/kg)
Male Lewis rat (♂)	1.90	84.1	1.96 ±1.05	101 ±52.2
Female Lewis rat (♀)	1.90	33.1	1.89 ±0.46	30.1 ±12.9
Male Sprague Dawley (♂)	1.87	135	1.79 ±0.47	138 ±86.9
Female Sprague Dawley (♀)	1.87	58.5	1.83 ±0.44	100 ±80.1

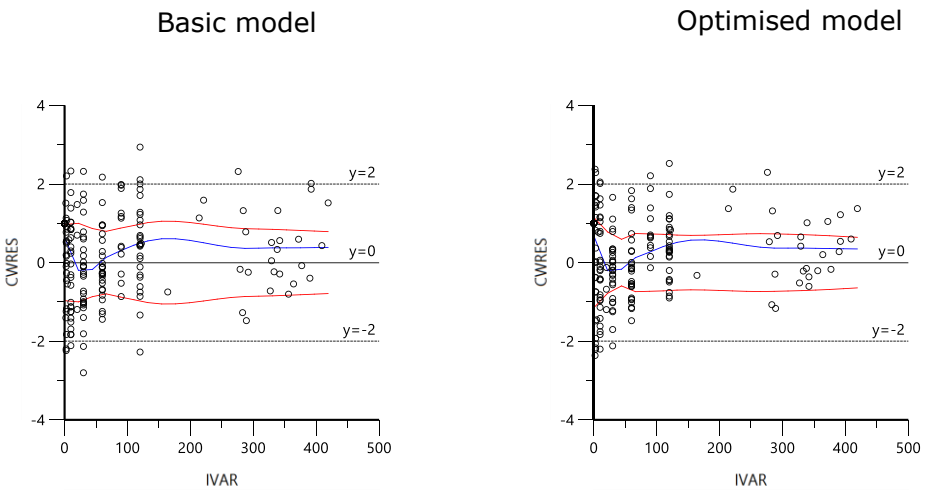

Figure 3.8. Pop CWRES vs IVAR. Plot of CWRES (conditional weighted residuals) versus individually predicted alphaxalone plasma concentration. Values significantly above 3 or below -3 are suspect and may indicate a lack of fit and/or model misspecification.

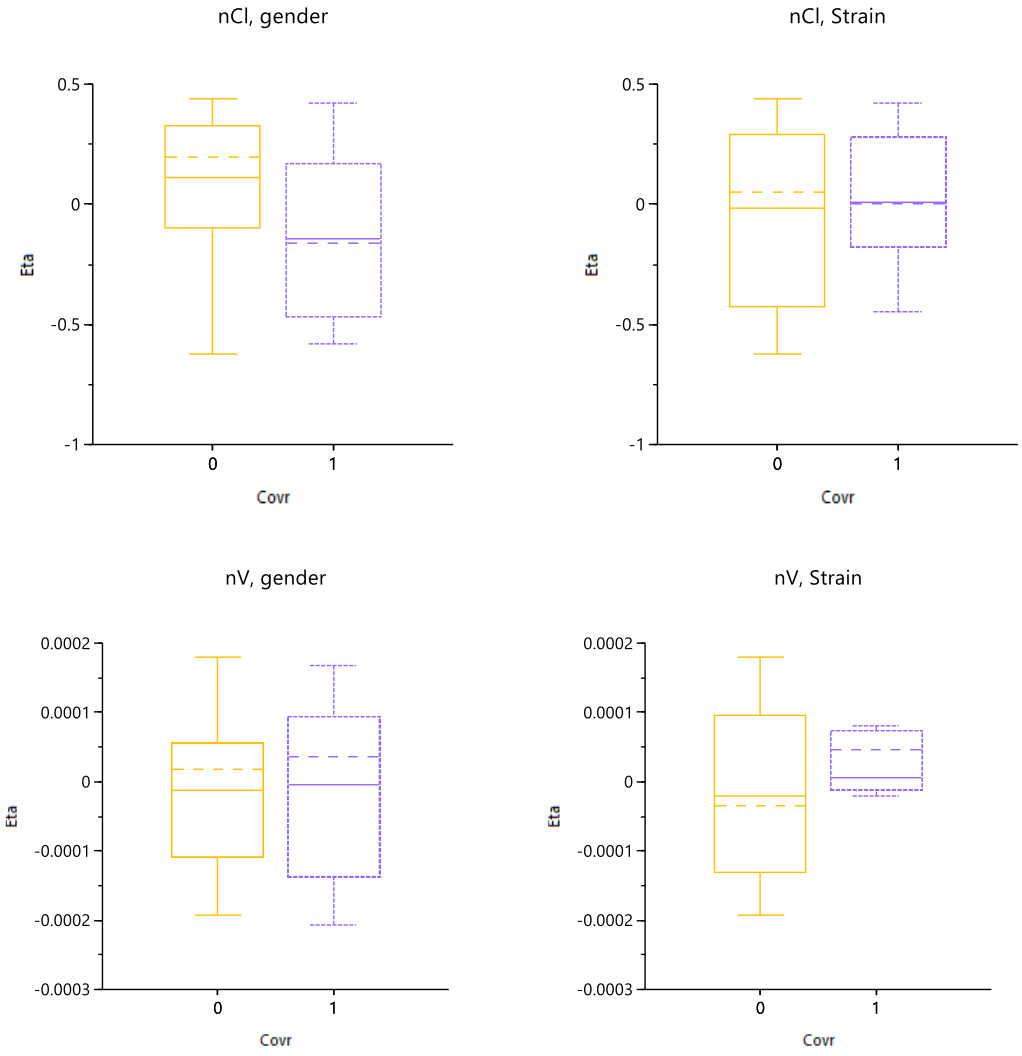

Figure 3.9. Box-plot depicting sex, strain versus distribution of random effect (eta). The covariate groups have a good distribution around the tv(0).

3.2.4. Simulation of adjusted alphaxalone dose for female rats and *in vivo* results of male and female SD rats:

Based on the output of the best popPK model, alphaxalone administration was simulated with a modified regimen for female rats to have a similar alphaxalone steady-state concentration as male rats. The selected dosage regimen for female rats consisted of three phases compared to the 2 phases of infusion rate used in male rats, which was the best regimen to closely match the alphaxalone male rats PK profile which is summarised in Table 3.3. The resultant modified infusion of alphaxalone is presented in Figure 3.10.

Table 3.3: Alphaxalone new dose administration for female SD rats in comparison to the one used for male SD counterparts.

Female dose		**Time (min)**		**Dose**	
3 phases		**Start**	**Finish**	**Duration**	**mg/kg/min**
1	**LD**	0	2.5	2.5	1.67
2	**1st CRT**	2.5	60	57.5	0.56
3	**2nd CRT**	60	End of experiment	N/A	0.42 25-45% reduction
Male dose					
2 phases		**Start**	**Finish**	**Duration**	**mg/kg/min**
1	**LD**	0	2.5	2.5	1.67
2	**1st CRT**	2.5	End of experiment	N/A	0.75

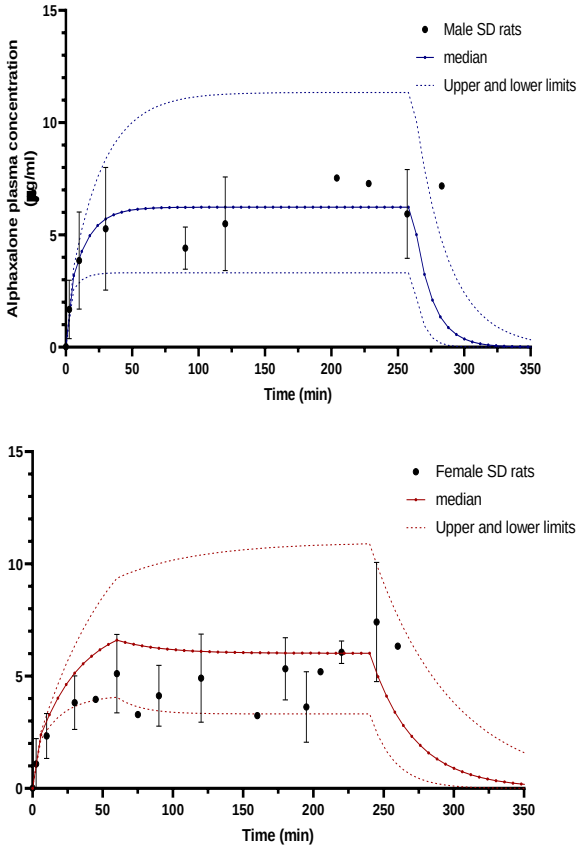

Figure 3.10: Alphaxalone plasma concentration simulated for male and female rats. The graph shows the simulated alphaxalone plasma concentration (solid continuous line) and 5th and 95th percentile (dashed line). Observed plasma concentration of alphaxalone (•) are superimposed over the male and female simulation. The observed data are described in the next section (3.2.5). The male simulation and observed concentrations of alphaxalone are closely matching the median while the observed concentrations in females were slightly lower than the median.

3.2.5. Alphaxalone pharmacokinetics for male and female SD rats (reduced infusion)

Similarly, to Lewis rats, the observed alphaxalone plasma concentrations were modelled to a one compartment IV infusion model. The suggested new administration from the simulation for the female rats was used in a new study that contained 16 female and 8 male SD rats. The graphs of model fitness to the observed concentration are shown in Figure 3.11, Figure 3.12 and Figure 3.13. Upon comparing the observed plasma concentrations with the simulated alphaxalone model, they closely matched the median of the simulated graphs (Figure 3.10) in the male rats, while the female SD rats were having slightly lower alphaxalone plasma concentration in comparison to the simulation. Overall, there was no significant difference between male and female alphaxalone concentration at each matched time point (unpaired two-way ANOVA), and no observed cardiac depression for the female rats when administered using the new administration. The estimated PK parameters (Table 3.4) when compared however, showed significance differences for CL, $T_{½}$ and MRT but not for VD_{ss}.

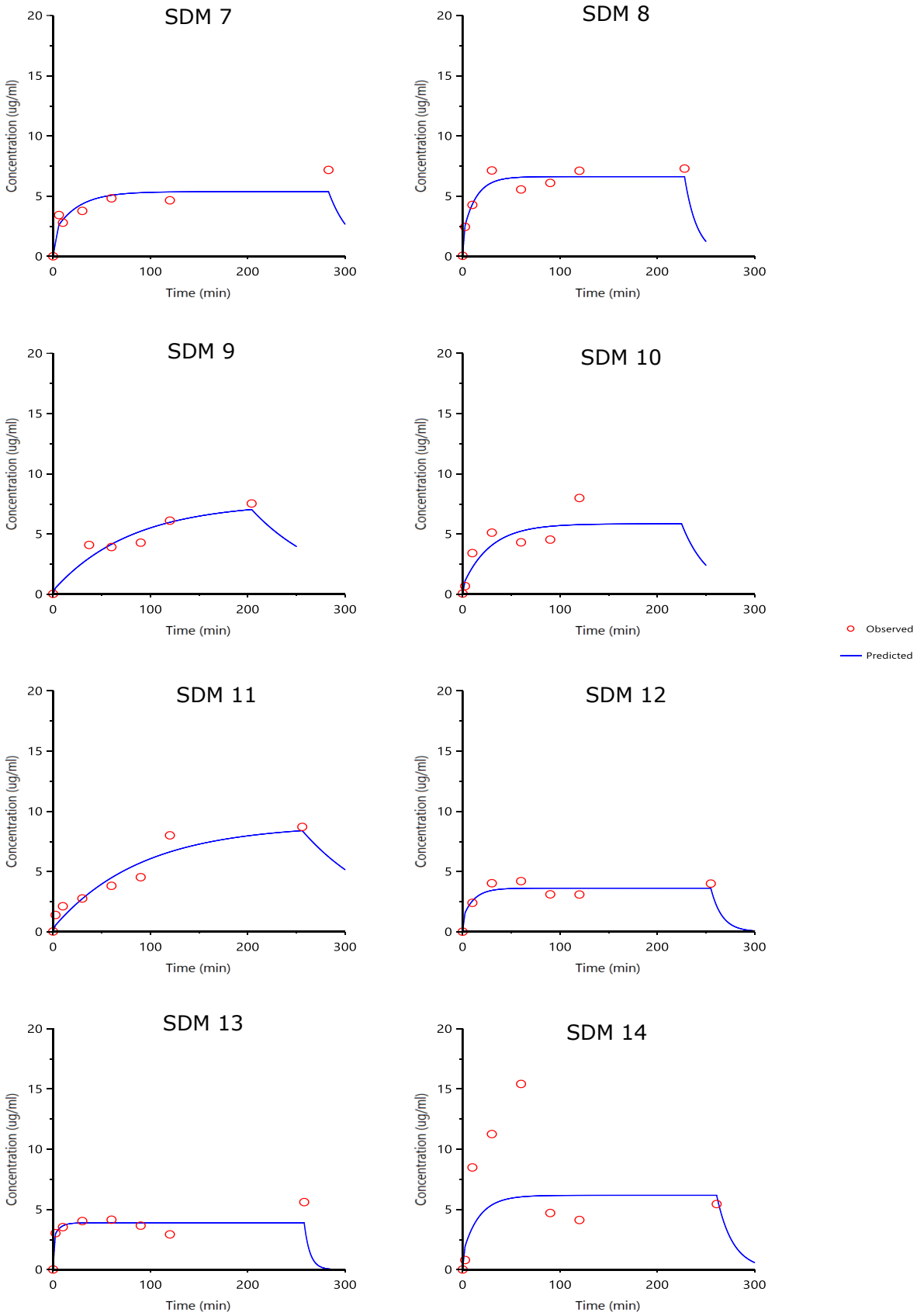

Figure 3.11: Male SD rats PK graphs. A one compartment PK model was also used to fit the male SD rats. All of the male rats completed the experiments. Alphaxalone IV administration at a rate of 1.67 mg/kg/minute for 2.5 minutes followed by 0.75 mg/kg/minute.

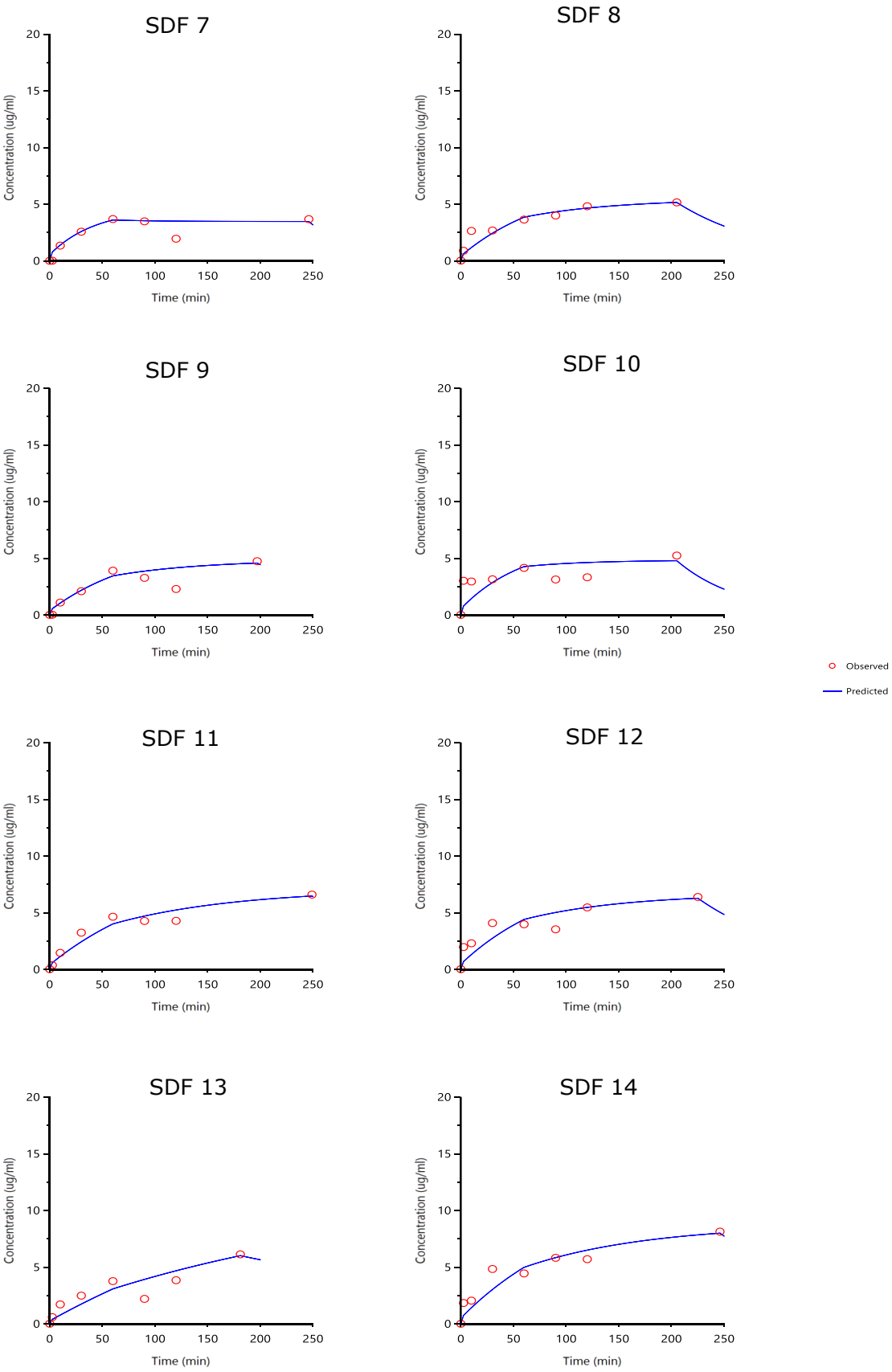

Figure 3.12. Female SD rats PK graphs. A one compartment PK model was also used to fit the female SD rats. All of the female rats completed the experiments. Alphaxalone IV administration used the three phase approach starting with a rate of 1.67 mg/kg/minute for 2.5 minutes followed by 0.56 mg/kg/minute for 60 min and continued with 0.42mg/kg/minute.

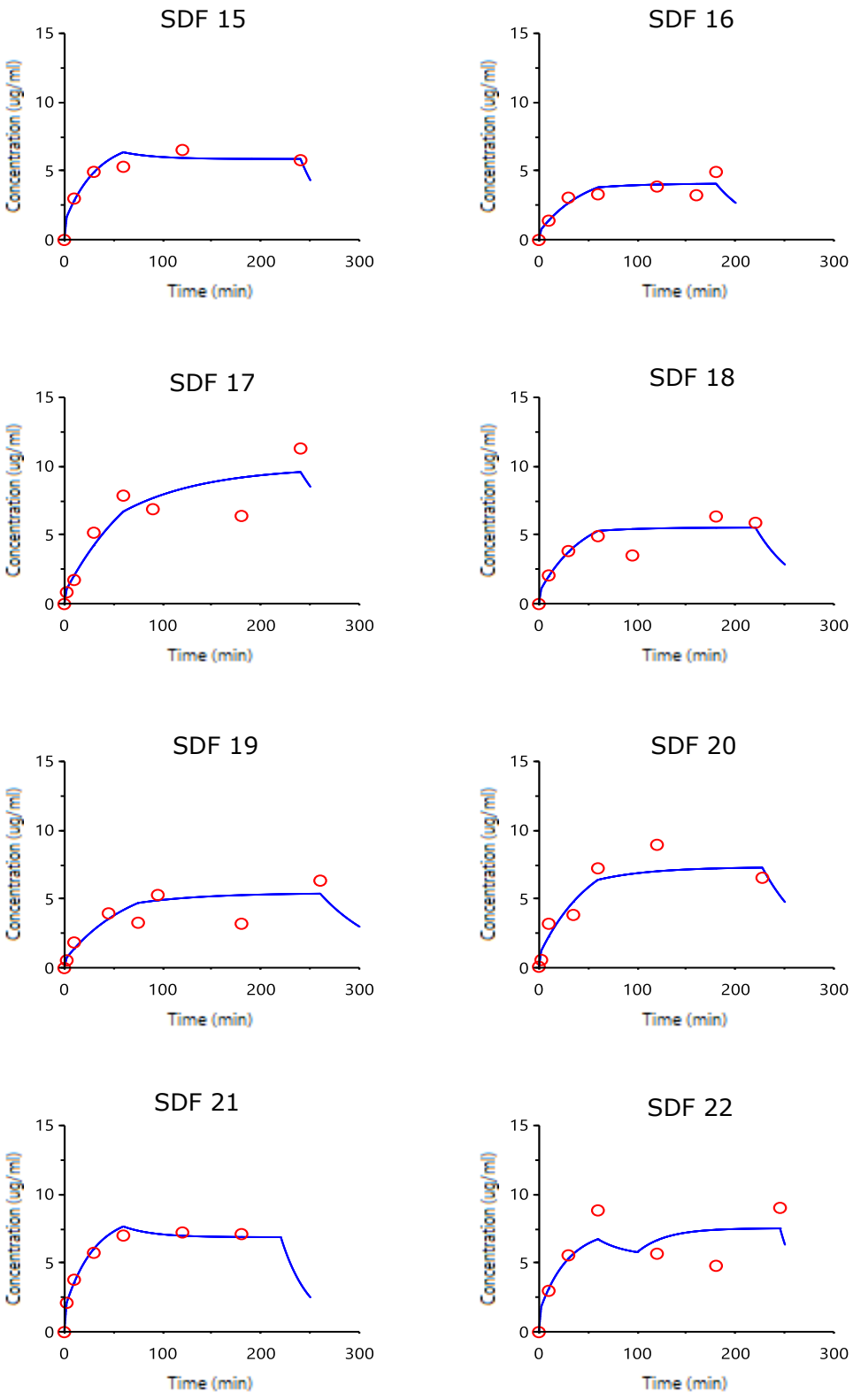

Figure 3.13. Female SD rats PK graphs. A one compartment PK model was also used to fit the female SD rats. All of the female rats completed the experiments. Alphaxalone IV administration used the three phase approach starting with a rate of 1.67 mg/kg/minute for 2.5 minutes followed by 0.56 mg/kg/minute for 60 min and continued with 0.42mg/kg/minute.

Table 3.4: **The new SD rats pharmacokinetic parameters.** The table presents a total of 16 (8 male & 8 female) SD rats after intravenous administration of alfaxalone normal regiment (a rate of 1.67 mg/min/kg for 2.5 minutes followed by 0.75 mg/min/kg) for the male rats; and the modified dosage (a rate of 1.67 mg/min/kg for 2.5 minutes followed by 0.56 mg/min/kg for 60 min and then dose is reduced to 0.42 mg/min/kg for the end of the experiment) for the female SD rats.

Rat name	**CL** (ml/min/kg)	**T½** (min)	**MRT** (min)	**Vd_{ss}** (L/kg)
Male group				
SDM 7	140	16.8	24.3	3.40
SDM 8	113	9.10	13.1	1.50
SDM 9	98.6	55.6	80.3	7.90
SDM 10	128	19.5	28.1	3.60
SDM 11	84.3	62.5	90.1	7.60
SDM 12	208	8.00	11.5	2.40
SDM 13	193	4.10	5.90	1.10
SDM 14	122	11.5	16.5	2.00
Mean	**136**	**23.4**	**33.7**	**3.7**
SD	**43.5**	**22.6**	**32.6**	**2.6**
Female group				
SDF 7	121	30.0	43.3	5.20
SDF 8	77.1	59.9	86.4	6.70
SDF 9	86.3	59.7	86.2	7.40
SDF 10	86.8	41.8	60.4	5.20
SDF 11	59.3	81.8	118	7.00
SDF 12	62.9	66.3	95.6	6.00
SDF 13	34.9	212	305	10.7
SDF 14	47.9	81.4	117	5.60
SDF 15	76.9	12.3	17.8	1.40
SDF 16	107	33.2	47.9	5.10
SDF 17	44.7	58.4	84.3	3.80
SDF 18	83.4	31.4	45.3	3.90
SDF 19	79.0	47.2	68	5.40
SDF 20	58.4	37.9	54.8	3.20
SDF 21	62.5	20.7	29.9	1.90
SDF 22	74.7	20.2	29.2	2.20
Mean	**72.7**	**55.9**	**80.6**	**5.00**
SD	**22.4**	**46.6**	**67.1**	**2.4**
***P* <**	<0.0001	<0.05	<0.05	**ns**

CL, clearance; T1/2, half-life; Cp_{ss}, plasma concentration at the steady state; MRT, mean residence time; Vd_{ss}, volume of distribution. CL, Vdss, t½ and MRT are significantly different between the male and female rats.

3.2.6. Alphaxalone cardiovascular inhibition comparison for original and modified dose

The monitoring of arterial pressure was started before alphaxalone administration. However, due to the influence of the inhaled anaesthesia (isoflurane) on arterial pressure as seen in the early reading on Figure 3.5, all readings before the stabilisation of the mean arterial pressure (any time points before 30min) have been excluded for the analysis, for the concentration-response curve to accurately represent cardiovascular depression (Figure **3.14**, A and B).

The female Lewis rats showed dose dependent inhibition of arterial pressure at higher plasma concentration of alphaxalone. In contrast, neither the male rats nor female SD rats showed any significant signs of cardiac depression.

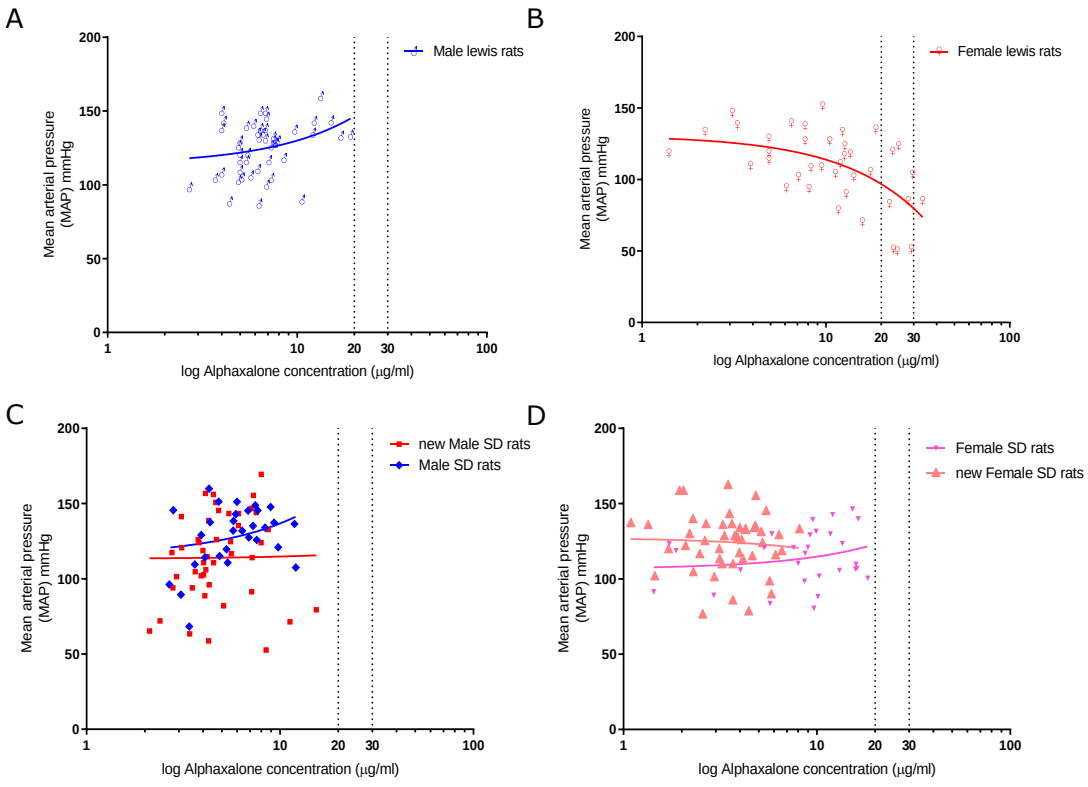

Figure 3.14: The mean arterial response against alphaxalone concentration for each rat group. The data is divided by strain and gender: A represents the male Lewis rats, B represents female Lewis rats, C represents male SD rats and D represents female SD rats. The female Lewis rats show an inhibition trend with high alphaxalone concentrations, while the other rats show no correlation between response and concentration.

3.2.7. Alphaxalone popPK analysis of the large set

Alphaxalone PK data generated from the second study was integrated into the popPK model and created a large set popPK model to optimise it to the fullest. Hence, a 24 rat data set from the second study (full set distribution in Table 2.2) was used for a new popPK analysis model. The conditions and the criteria of this model are quite similar to the small set model. The major improvement is the inclusion of body weight as a continuous covariate in addition to sex and strain. The inclusion of body weight as a covariate, instead of strain, for clearance has improved the model significantly and altered the conclusion of the model slightly (Figure 3.15). The model concluded that body weight in addition to sex were the major factors that affected alphaxalone clearance in rats while strain has the major influence on Vd. The generated data from the large set model is shown in Table **3.5** and the typical values were within the 2.5 and 97.5% confidence intervals of the bootstrap resampling analysis. The influence of the covariates on the new model is described as follows:

$$V = tvV \times exp(0.69 \times (Strain = 1)) \times exp(nV)$$

Equation 3.3

$$Cl = tvCl \times (1 + Weight \times 3.64) \times exp(-0.43 \times (gender = 1)) \times exp(nCl)$$

Equation 3.4

Where the Typical Value (tv) is the population fixed effect value for the parameter, Strain = 1 refers to Sprague Dawley, and gender = 1 refers to females and the weight is logged the body weight and cantered to the mean.

Model evaluation

The overall predicted concentrations had a good distribution around the line of unity as observed in both goodness of fit plots of the basic and the optimised large set model for observed concentration against individual predicted concentration (IPRED) shown in Figure 3.15 and observed concentration and predicted concentration (PRED) shown in Figure 3.16. The conditional weighted residuals (CWRES) for the basic and optimised large model are presented in Figure 3.17 and

show less spread and an overall improvement over the basic model. A box plot for the categorical covariates (sex and strain) versus CL and Vd (Figure 3.18), as well as, a scatter plot for the continuous covariate (weight) Figure 3.19 of the optimised large set model shows no diverging random effects after incorporating the covariates into the optimised popPK model.

Table 3.5: The typical values for clearance and volume of distribution including the average weight of the set while the minimum and maximum impact of weight on clearance is shown between brackets.

	TYPICAL VALUES		**Post hoc**	
Rat group	**VD (L/kg)**	**CL (mL/min)**	**VD (mL/kg)**	**CL (mL/min/kg)**
LM	1.71	113.3 ± (98 – 122)	1.58 ±0.78	103 ±30.6
LF	1.71	63.3 ± (60 – 64)	3.03 ±1.3	40.4 ±17.4
SDM	3.41	126.7 ± (109 – 137)	2.18 ±1.1	111 ±34.9
SDF	3.41	72.3 ± (61 – 76)	3.84 ±1.9	74.6 ±20.4

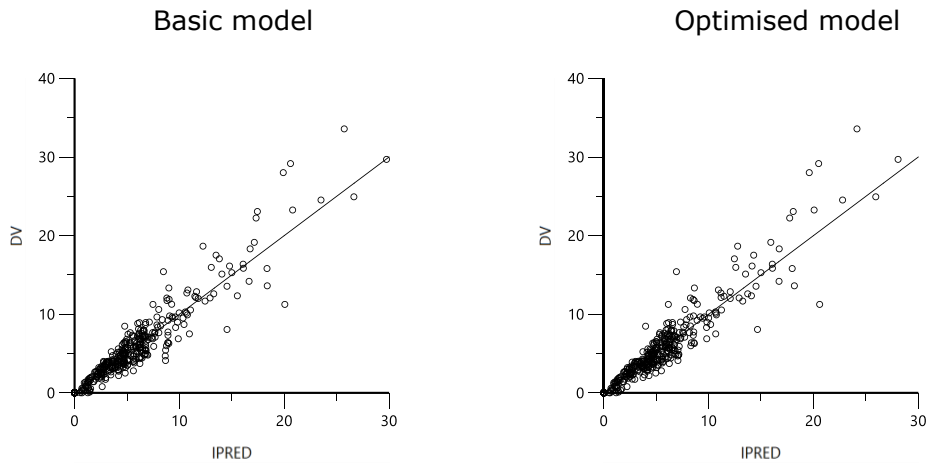

Figure 3.15 DV vs IPRED. Plot of the dependent variable (DV, observed concentrations) versus individual predicted values (i.e., predicted individual concentrations). The concentration presented is (µg/ml).

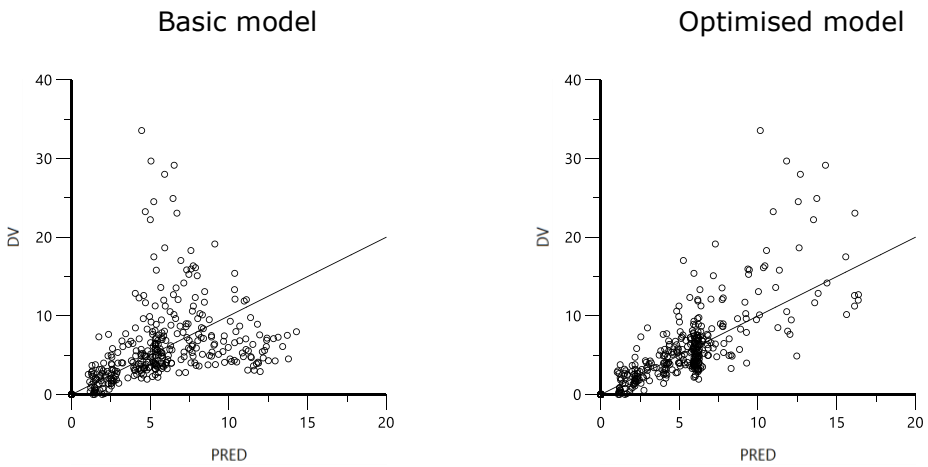

Figure 3.16. Pop DV vs PRED DV vs PRED. Plot of the dependent variable (DV, observed concentrations) versus population predicted values (i.e., population predicted concentrations).

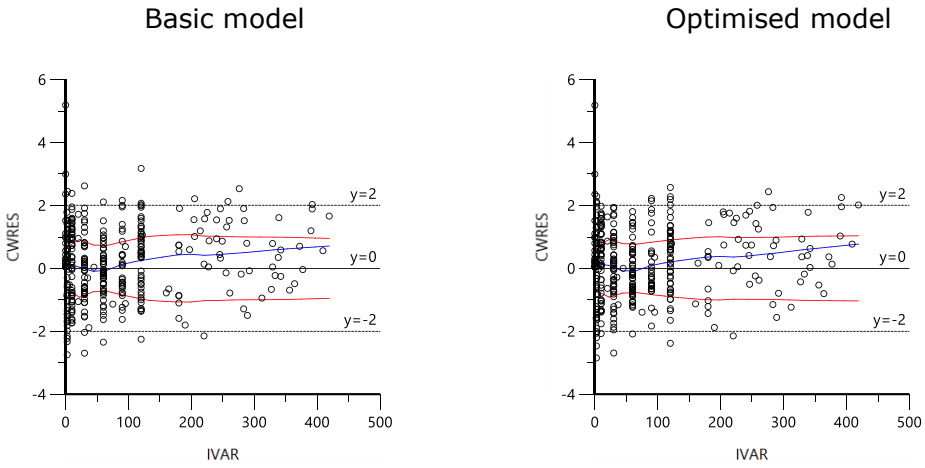

Figure 3.17. Pop CWRES vs IVAR Pop CWRES vs IVAR. Plot of CWRES (conditional weighted residuals), against IVAR, the independent variable (IVAR is time).

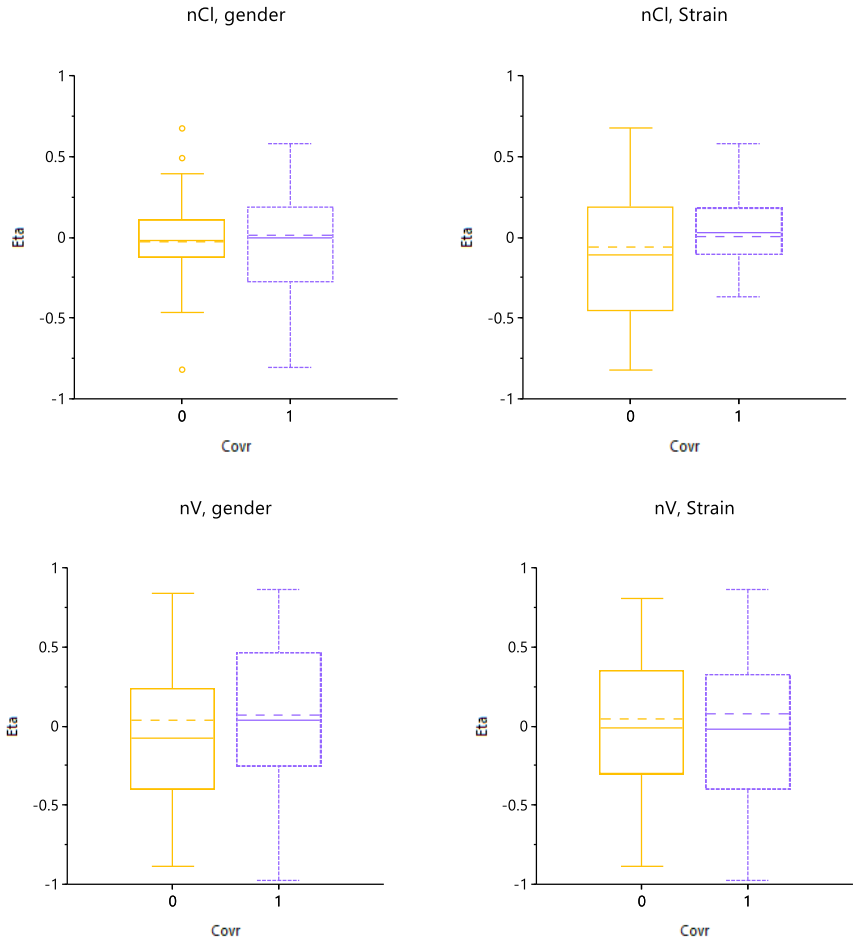

Figure 3.18. Box-plot depicting sex and strain versus distribution of random effect (eta). The covariate groups have a good distributed around the tv(0).

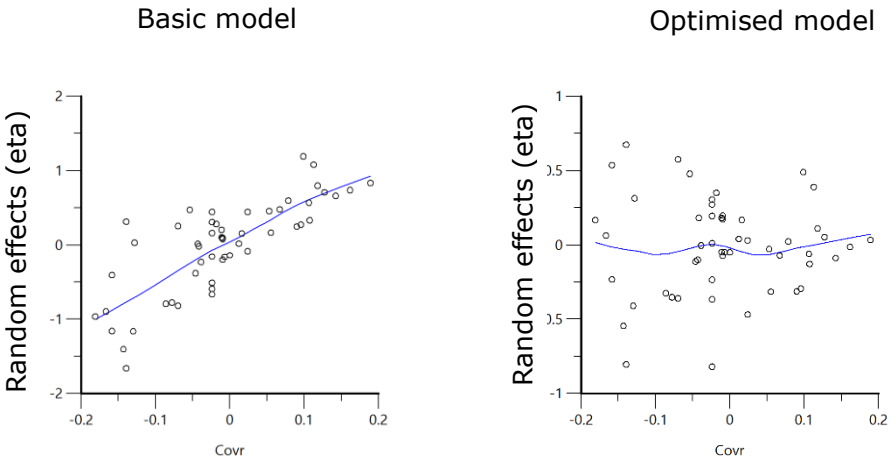

Figure 3.19. Scatter plots of rat weight as continuous covariate vs clearance random effects (Eta). At the basic model there is a clear correlation between random effects and weight. however, after considering weight as covariate in the optimised model the correlation no longer significant.

3.3. Discussion

Chapter Summary

This study evaluated alphaxalone sex differences for both PK and PD using two *in vivo* experiments and combined investigations using population pharmacokinetic models. The first *in vivo* study used a fixed alphaxalone dosing regimen with a reduction in the infusion rate by 30% in the latter half of the experiment to monitor the PD change induced by a reduction in alphaxalone plasma concentration. The second *in vivo* study investigated alphaxalone sex differences by using two different alphaxalone dosing regimens for male and female rats, computed by population model outputs. Furthermore, a finalised population PK (large set) analysis was performed on the data generated from both studies and from previous published studies (White, *et al.,* 2017).

Summary of results

The study demonstrated a sex difference in alphaxalone pharmacokinetics in male and female Lewis and SD rats. The sex difference was observed *in vivo* in Lewis and SD rats and further confirmed in the population analysis as sex is a covariate that significantly impacted rats' alphaxalone clearance. In male rats alphaxalone appeared to be eliminated faster compared to females and an adjustment of a maximum of 45% reduction of the male administration dose rate for the females provided equivalent plasma alphaxalone steady-state concentrations.

Alphaxalone sex related differences in anaesthetic effects have been observed and reported for the old formulation Althesin® (Fink et al., 1982) which required a four-fold higher dose in male compared to female Wistar rats. It was also reported with the new formulation (White, *et al.*, 2017; Arenillas and Gomez de Segura, 2018) which required threefold higher doses in male compared to female SD rats. However, the major difference between this study and other reports is in this study alphaxalone plasma concentration measurements were used to simulate similar

PK profiles while other studies based their dose adjustments on their observation of the depth of anaesthesia in both sexes.

Both the deterministic PK compartmental and popPK analyses in this study suggest that the clearance of alphaxalone is significantly different in male and female rats. Observed alphaxalone clearance differences were reported by the Visser et al., (2002) and Lau *et al.*,(2013) studies where the clearances of alphaxalone were 154±15 and 54.3±6.8 ml/min/kg for male and female Wistar rats respectively. Hence, making a total of three rat strains to demonstrate sex differences in alphaxalone clearance.

The deterministic estimated clearance parameter for Lewis rats for both sexes in the herein study were in the lower range compared to the reported values by the Visser and Lau groups for Wistar rats as well as the reported values by White et al for SD rats (White, *et al.*, 2017). The lower clearance values for Lewis rats are consistent with strain being a significant covariate in the population PK model for the small set. However, the conclusion of the large set population model suggested that weight was a covariate source for clearance. This may be due to body weight having a wider range in the large set model compared to the narrow body weight range in the small set model.

The continuous covariate of body weight replaced the significance of strain for clearance parameters in the large set model, however, the estimated clearance in SD female rats is significantly different to Lewis rats which supports the presence of strain differences. A possible explanation may be related to liver blood flow restriction differences; in general, ultra-fast metabolising drugs are limited by liver blood flow, as the amount of drug in the plasma that reaches the liver will be metabolised instantly. The female SD rats, however, were on average significantly heavier and larger than female Lewis rats which can explain increased liver blood flow. Furthermore, the higher observed alphaxalone plasma concentrations in Lewis female rats was accompanied with cardiovascular depression i.e. mean

arterial pressure depression, which may have assisted in reducing the clearance due to reduction of liver blood flow (negative feedback cycle).

The estimated *in vivo* plasma clearance in male rats showed an overall higher clearance rate than liver blood flow (72 ml/min/kg) (Davis & Ward, 2015). This might indicate either the blood to plasma ratio (B:P ratio) is greater than 1 or there is an additional elimination pathway. Alphaxalone is reportedly mainly metabolised in the liver (Warne, et al., 2014), as such, it is more likely to be due to differences in B:P ratio. There are no reports on the blood to plasma ratio value for alphaxalone, however, sex differences can affect this ratio (Gandhi, et al., 2004).

The present study used arterial pressure measurements as a clinical biomarker for the PD investigation. Cardiovascular effects were chosen as a biomarker because alphaxalone has a dose dependent depression on the cardiorespiratory system i.e. a decrease in blood pressure (Khan et al., 2014; Muir et al., 2009; Sear, 1996) but to a lesser extent compared to other anaesthetics such as thiopental and propofol (Goodchild et al., 2015; Visser et al., 2002). As such, a dose reduction (33%) of alphaxalone near the end of infusion was designed to observe a dynamic change in the cardiovascular effect to determine an IC_{50}. However, there was no noticeable change in the cardiovascular response as a result of the 30% reduction phase. Alternatively, female Lewis rats were the most impacted by the higher alphaxalone plasma concentrations and showed cardiovascular inhibition from the beginning of infusion, while the male rats did not demonstrate a dose dependent relationship but exhibited a stable plane of anaesthesia.

There are some limitations in the present study for the PD measurements. All the rats had a sampling cannula secured in the left carotid artery which required surgery and the use of gaseous anaesthesia i.e., isoflurane and nitrous oxide. Isoflurane, in particular, can cause significant cardiovascular depression in a dose dependent manner (Yang, et al., 2014), as such, no arterial pressure baselines in

conscious rats were available. Furthermore, after discontinuing the gases, most rats' arterial pressure rebounded rapidly to a higher blood pressure. However, in view of the concurrent cessation of the volatile agent and a loading dose of alphaxalone infusion, it is not clear what the value of the real baseline is.

Adverse effects

The previous alphaxalone formulation Althesin is known to cause a severe anaphylactic reaction which ultimately caused its withdrawal from the market. The new alphaxalone formulation was introduced specifically to overcome the reason for this adverse reaction. Interestingly one case has been reported of an anaphylactic reaction associated with Alfaxan® (Jurox) in a cattle dog (Haworth et al., 2019). The dog exhibited diarrhoea, vomiting and acute hypotension immediately after the intravenous administration of Alfaxan. In this study, no anaphylactic reactions were observed, and the alphaxalone was well tolerated.

Chapter 4:

In vitro investigation of PK sex differences in rats

4. Chapter 4. *In vitro* investigation of PK sex differences in rats

4.1. Introduction

The major conclusion of the previous chapter (chapter 3) was that alphaxalone demonstrated sex dependent pharmacokinetic differences in Lewis rats. Furthermore, alphaxalone clearance was significantly larger in male rats which resulted in a dose reduction by 45% for female rats to reach equivalent alphaxalone plasma concentrations and limit cardiovascular depression.

The estimated clearance of alphaxalone in Chapter 3 represents the total body clearance and is the parameter that determines the systemic exposure of a drug for given dose. Thus, alphaxalone clearance is the sum of all processes that eliminate the parent drug from the body predominantly via renal excretion and liver metabolism. However, alphaxalone has been reported to be mainly metabolised by the liver with a minor role of renal excretion in rat, cat and dog (J. W. Sear & McGivan, 1981; Warne et al., 2015).

In vitro systems are important components for drug metabolism and toxicological studies. The use of freshly isolated hepatocytes is the gold standard for these evaluations. Hepatocyte isolation techniques were first established in the late-1960s and followed by significant progress using the two-step enzymatic approach which was introduced by Seglen (Seglen, 1976). This approach made the use of isolated hepatocytes an attractive alternative to *in vivo* studies and allowed drug metabolism investigations in species other than laboratory animals and humans prior to clinical studies (Bakala et al., 2003). Despite the limited viability time of fresh hepatocytes (up to 4 hours), the duration is long enough to establish drug stability and metabolite identification (Soldatow et al., 2013).

The estimated drug metabolic stability and enzyme kinetics data for a drug is routinely used to determine the intrinsic clearance (CL_{int}) of compounds in the discovery phase of drug development. The data is then extrapolated to predict *in vivo* metabolic clearance (CL_H) (Barter et al., 2007). However, this prediction

methodology tends to underpredict when using either liver microsomes or hepatocytes (Foster *et al.*, 2011). The *in vitro* rate of metabolism is usually expressed as per million cells (hepatocytes) and it must scale to the intact liver (organ) to estimate the whole liver clearance. The well stirred and parallel tube methods are mostly used for *in vitro in vivo* extrapolation (IVIVE) (Ito & Houston, 2004). These models require scaling factors such as hepatocellularity, liver weight and blood flow as well as plasma protein binding and blood to plasma ratio. The scaling process, however, will have poor correlation if the drug has other major routes of elimination other than liver metabolism. While for compounds mainly metabolised by the liver, they will have good correlation. Having a good correlation between predicted and the actual observed *in vivo* clearance in one species can give more confidence in finding similar correlations with other species.

The aim of this chapter was to firstly deliver a suite of liver *in vitro* systems. This included the optimisation of a hepatocyte isolation method to generate functional hepatocytes from *ex-vivo* rat livers as well as microsomes and S9 fraction. Also, to investigate alphaxalone metabolism rate within these *in vitro* systems in order to determine and compare intrinsic clearance values in male and female Lewis rats. Furthermore, the results from the two IVIVE models were assessed against the measured *in vivo* clearance (chapter 3) for comparison. Finally, the *in vitro* liver systems will be used to elucidate the mechanism and metabolic pathways responsible for the observed sex differences *in vivo*. A summary of the investigation approach is presented in figure 4.1.

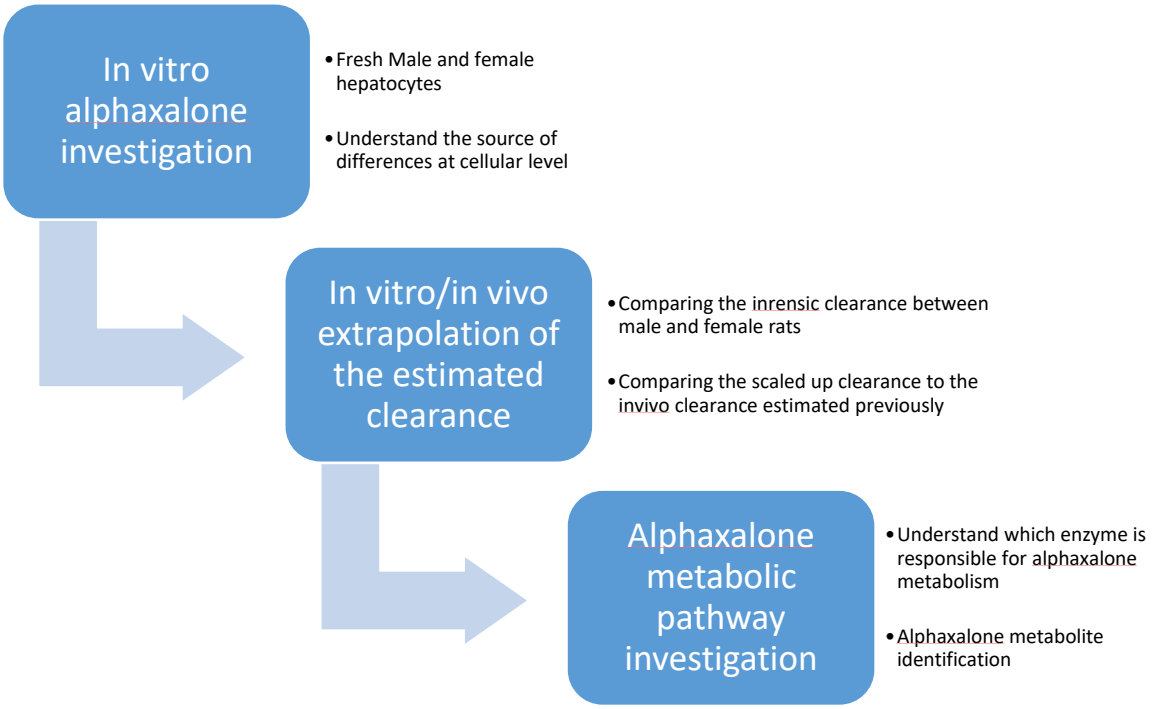

Figure 4.1. Schematic diagram summaries the investigation process taken in the present chapter.

4.2. Results

4.2.1. Rat hepatocytes isolation method

Firstly, it was crucial to develop and optimise a valid method for rat hepatocyte isolation with high yield and viability. The approach started by taking an already established in house protocol for equine, pig and sheep hepatocyte isolated from *ex-vivo* liver (Shibany et al., 2016) and scaling down for rat liver. Several method optimisations were carried out for the isolation of hepatocytes. The results of each method are summarised in Table 4.1. In method 1, rat liver was rapidly over digested and showed low yield and viability. For method 2, the collagenase concentration was reduced in order to slow the digestion rate. Unfortunately, the viability for this method was worse than the first method. There was a possibility that the collagenase concentration was too low and some buffers were possibly not required, therefore, the collagenase concentration was increased slightly (0.035 to 0.05%) and only solution 2 and 4 were kept. Method 3 showed only one successful hepatocyte isolation with viability of 78 %, however, the reproducibility of this method was not consistent. Methods 4-6 showed no signs of improvement even though the collagenase source was alternated between different manufacturers. Finally, method 7 reverted back to the original full set of infusion buffers while using a further collagenase supplier. This method was highly successful and reproducible for hepatocyte isolation in terms of both yield and viability.

Table 4.1: Description of the methods used in hepatocyte harvesting and each method solution content.

Method used	Solutions used					Rats No.	Viability %	Total yield
	Solution 1	Solution 2	Solution 3	Solution 4	Solution 5			(million cells)
				Collagenase conc. (w/v)				
1	√	√	√	0.1% (IV fisher)	√	4	<40%	≈100
2	√	√	√	0.035% (IV fisher)	√	3	<15%	≈100
3		√		0.05 % (IV fisher)	√	2	78% & <30%	≈100
3		√		0.05 % (IV fisher)	√	1	<45 %	≈70
4		√		0.01 % (IV fisher)	√	1	<10 %	≈80
4		√		0.01 % (IV fisher)	√	1	<10 %	≈80
5		√		20 % (IV sigma)	√	1	<10 %	≈80
6		√		0.01 % (IV fisher)	√	1	<10%	≈80
7	√	√	√	0.025% 25mg/100ml (IV sigma)	√	1	94%	200
7	√	√	√	25mg/100ml (IV sigma)	√	1	84%	≈90
7	√	√	√	25mg/100ml (IV sigma)	√	1	94%	≈100

4.2.2. Linearity of alphaxalone hepatocyte kinetics with respect to number of cells

The main assumption of Michaelis-Menten kinetics is that the substrate concentration is much greater that the enzyme concentration. To validate this assumption for alphaxalone, the initial rate of alphaxalone metabolism was determined by measuring its depletion over time with a range of incubational hepatocyte concentrations using Equation 2.5. For both male and female Lewis rat hepatocytes, alphaxalone initial depletion rate was linear with cell concentration

(Figure 4.2). Therefore, it was decided that 1 million cells/ml would be used for alphaxalone depletion kinetics at a range of initial substrate concentrations.

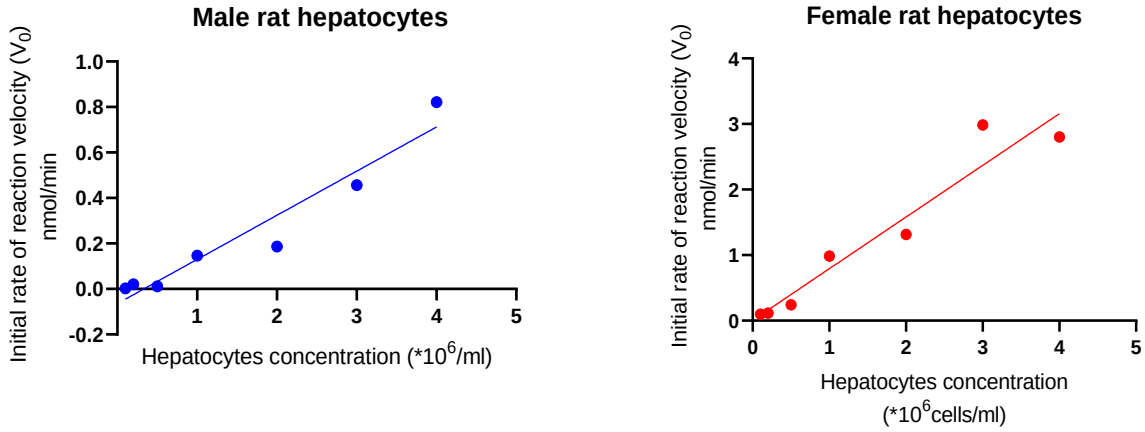

Figure 4.2: Linearity of alphaxalone initial depletion rate *versus* incubational rat hepatocyte concentration.

4.2.3. Initial depletion rate versus initial alphaxalone concentration in freshly isolated hepatocytes (10^6/ml) for male and female Lewis rats

Incubating a range of alphaxalone concentrations with hepatocytes was the first step in determining alphaxalone intrinsic clearance and other enzyme kinetic parameters. These parameters will later be used for *in vitro/in vivo* extrapolation.

Hepatocytes isolated from 9 male and 6 female Lewis rats were used. Metabolism was evident in both male and female rat hepatocytes. However, the rate of alphaxalone depletion was dramatically different between male and female hepatocytes at all initial starting concentrations of alphaxalone. The data presented in Figure 4.3 show a representative example for each sex

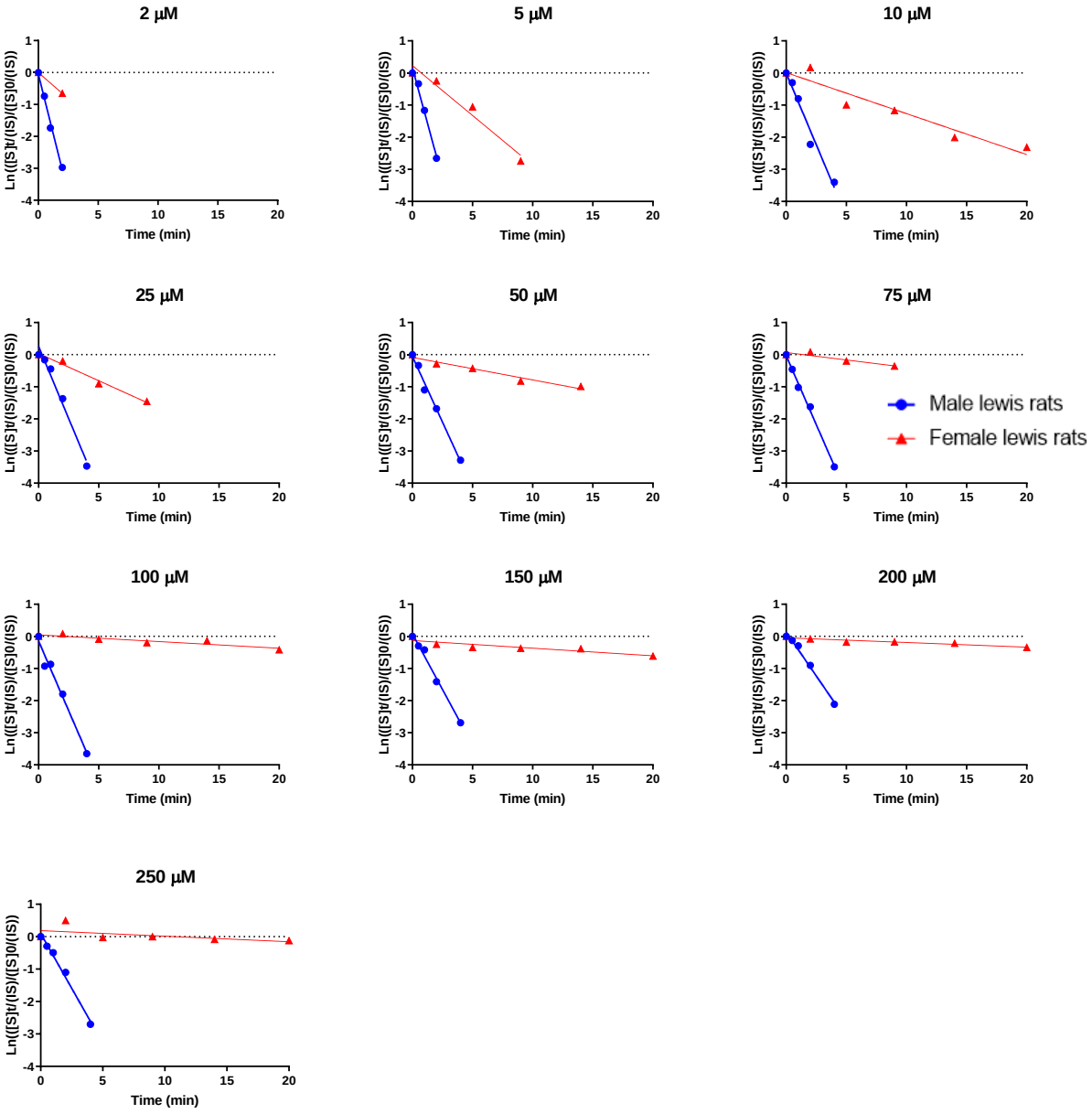

Figure 4.3. comparison between the rate of metabolism of alphaxalone in male (blue circle) and female (red triangle) hepatocytes. Data were plotted as the natural logarithm (Ln) of substrate/internal standard response against time. K_{dep} is represented by the slope of the line.

4.2.4. Michalis-Menten analysis

The acquired V_0 from Equation 2.5 was plotted against drug concentration and fitted to the Michaels-Menten equation for both male and female rats (Figure 4.4 and Figure **4.5**) in order to estimate Michalis constant (K_m) and the maximal reaction velocity (V_{max}).

Both calculated parameters showed that male rats were significantly different (p<0.05) to female rats for alphaxalone metabolism. Furthermore, the males showed three and ten fold higher K_m and V_{max} respectively in comparison to female rats. A summary of the kinetic parameters is shown in Table 4.2

Table 4.2: The estimated values of V_{max} and k_m for male and female Lewis rats.

Female rat			Male rat		
	V_{max}	**K_m**		**V_{max}**	**K_m**
	(nmol/min)	(μM)		(nmol/min)	(μM)
1	5.2	9.3	***1***	48.1	53.9
2	8.9	14.4	***2***	144.1	236.7
3	8.4	7.7	***3***	134.2	391.8
4	14.8	109.1	***4***	232.4	164.1
5	22.7	219.5	***5***	90.6	43.6
6	8.8	24.4	***6***	176.0	113.2
			7	167.7	227.4
			8	93.9	159.1
			9	131.2	138.0
Median	**8.9**	**19.4**	**Median**	**134.2**	**159.1**
Mean	**11.5**	**64.1**	**Mean**	**135.4**	**169.8**
SD	**6.3**	**85.3**	**SD**	**54.2**	**106.6**

Kinetic parameters from fresh hepatocyte incubations at 1 million cells/mL

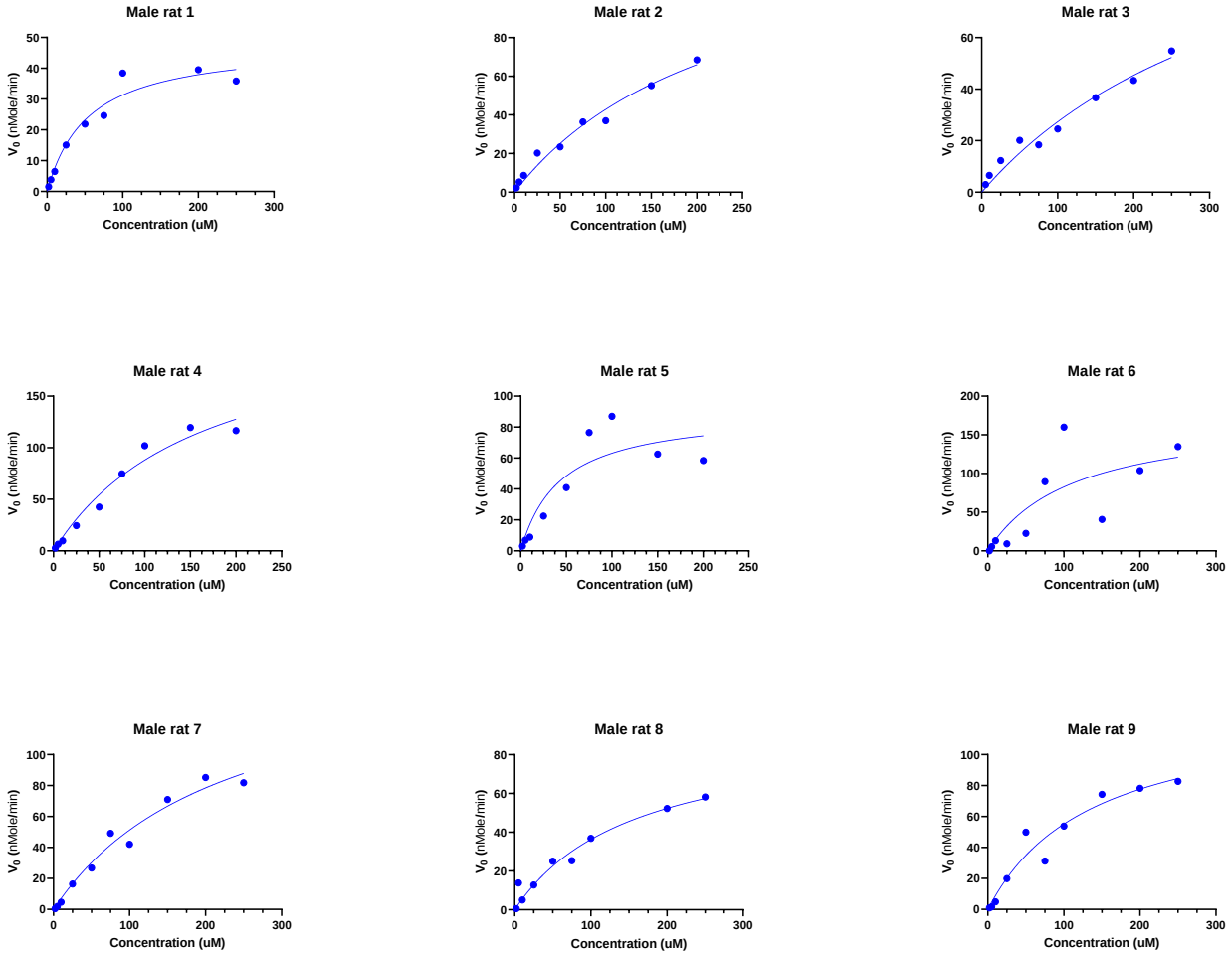

Figure 4.4. Michealis-Menten curves for alphaxalone in freshly isolated male rat hepatocytes. Initial rate (V_0) is plotted against drug concentration.

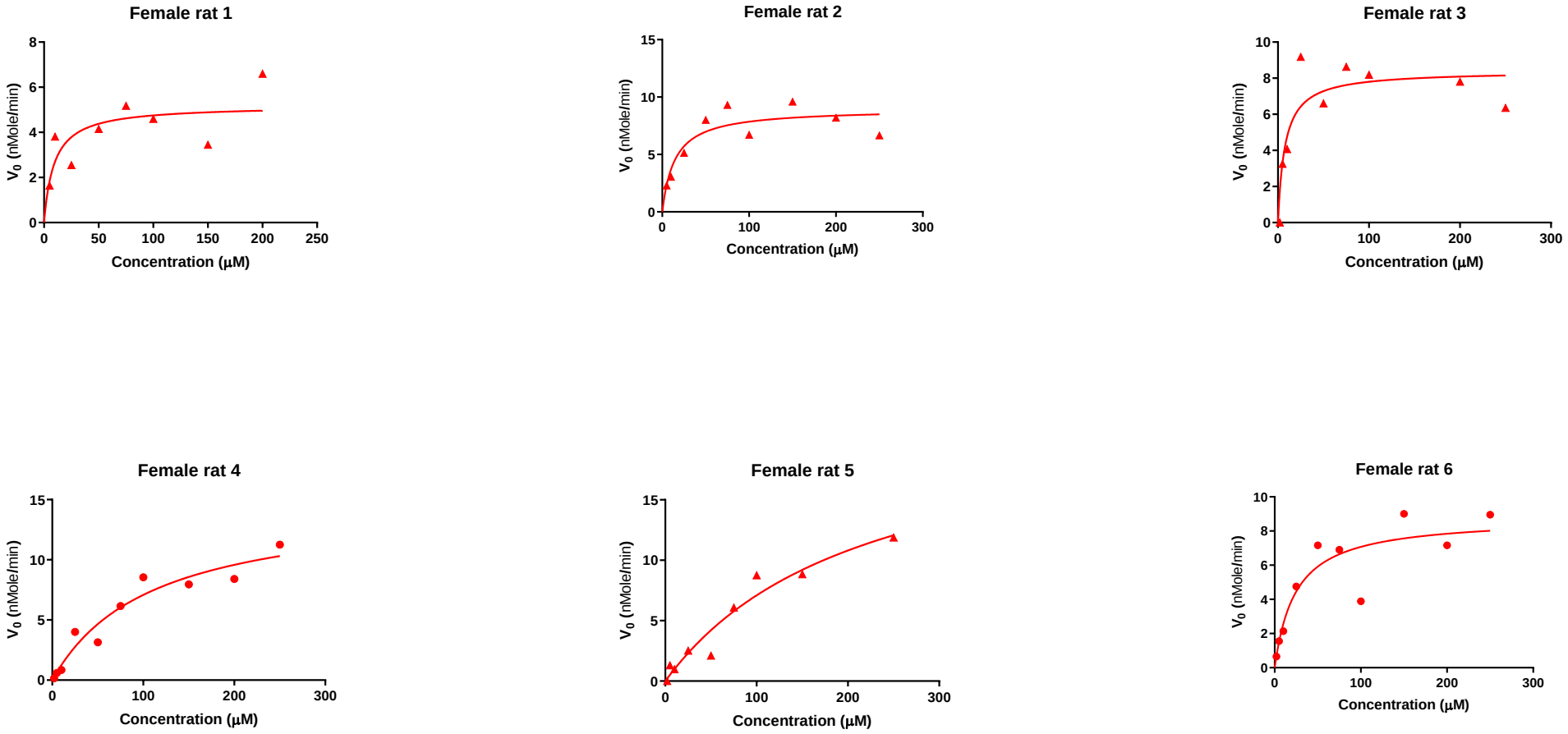

Figure 4.5: Michealis-Menten curves for alphaxalone in freshly isolated female rat hepatocytes. Initial rate (V_0) is plotted against drug concentration

4.2.5. *In vitro/in vivo* extrapolation of alphaxalone in male and female Lewis rats

Knowing intrinsic clearance is important as it is the first step for extrapolating the clearance of alphaxalone to the *in vivo* situation. However, this step requires other parameters unique for alphaxalone which can be determined using simple experiments. The parameters required are plasma protein binding and the blood:plasma ratio for male and female Lewis rats. These parameters were determined and both sexes gave the same value for alphaxalone plasma protein binding (95% binding) and a ratio of 0.65 for the blood:plasma ratio. Other normal physiological parameters are liver blood flow which was assumed to be 72 ml/min/kg (Davis & Ward, 2015) and the hepatocellularity (number of hepatocytes in a gram of liver). Hepatocellularity determined for both male and female Lewis rats were 170.5±73 and 151±20 million cells per gram of liver (n=4, for male and female), respectively. The parameters used for the scaling process are summarised in Table 4.3.

Table 4.3: The male and female Lewis rat physiological parameters used for IVIVE of alphaxalone clearance. both PPB and B:P ratio are presented as mean and SD (n=3)

	Male Lewis rat	Female Lewis rat
Plasma protein binding (PPB)	95±0.3%	95±0.5%
Fraction unbound in the incubation (Fu_{inc})	0.83	0.83
Blood:Plasma ratio (B:P ratio)	0.65±0.03	0.65±0.03
Hepatocellularity (n=4 male/female) (10^6cells/g of liver)	170.5±73	151±20
Liver blood flow (ml/min/kg)	72	72
Average liver weight (g)	9	7.5
Average body weight (Kg)	0.3	0.25

The resulting liver CL_{int} and the *in vivo* $CL_{hepatic}$ are summarised in table 3.8, after factoring in the physiological parameters, using either the parallel tube or well-stirred methods. The scaled $CL_{hepatic}$ values (Table 4.4) showed male Lewis rat hepatocytes to have a five fold larger predicted clearance in comparison to female Lewis hepatocytes for both models. The predicted $CL_{hepatic}$ were comparable with

the *in vivo* clearance values observed from Lewis rats in Table 3.1. Therefore, this suggests that alphaxalone is mainly and extensively metabolised by the liver in rats. To further understand the source of this observable sex difference a more in depth look at metabolites formed is essential to understand the alphaxalone metabolic pathway.

Table 4.4: The intrinsic clearance from enzyme kinetics in fresh hepatocytes and scaling to liver CL_{int} and Cl_H.

	CL_{int}	**Liver CL_{int}**	**$CL_{Hepatic}$ (Blood)**		***In vivo* CL Lewis rats (Plasma)**	***In vivo* CL Lewis rats (Blood)**
	(µl/min/million cells)	(ml/min/kg)	(ml/min/kg)		(ml/min/kg)	(ml/min/kg)
			WSM	**PTM**		
Male Lewis rats	797.4	4066.8	52.1	66.8	98.3±32.2	63.9±21
Female Lewis rats	179.4	813.3	24.8	29.4	36.8±19.7	23.9±13

WSM: well-stirred method, PTM: parallel tube method.

4.2.6. Alphaxalone metabolite identification

Alphaxalone metabolism appears to be sex dependent in rat. Hence it is vital to investigate the identity of the metabolic pathway and the enzymes responsible for metabolism of alphaxalone, as this will uncover the predominant pathway taken by alphaxalone for both sexes.

4.2.6.1. Metabolite 1:

The alphaxalone signal was detected using 1 parent and 3 daughter ions which should increase the selectivity and sensitivity of detecting the drug. Unexpectedly, the first of the alphaxalone metabolites was detected via the same channels used for alphaxalone. In other words, this metabolite shares the same molecular weight and can generate the same fragments (daughter ions) that alphaxalone produced when analysed. This metabolite (Figure 4.6), however, appeared at a different retention time and increased with longer incubation time. Furthermore, the typical retention time for alphaxalone is at 5.61 min while the metabolite appeared at 5.13 min suggesting it is more polar than the parent drug.

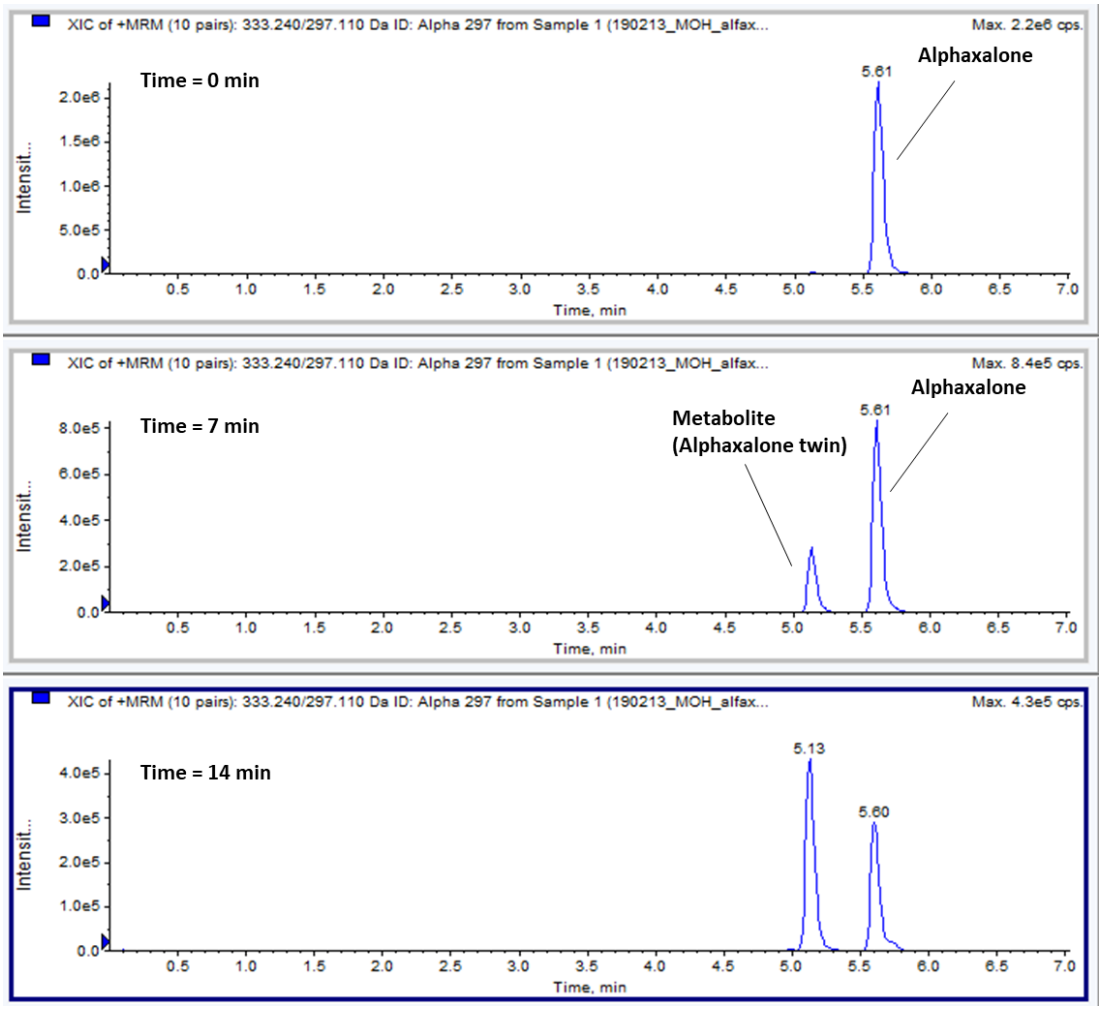

Figure 4.6. chromatographs of alphaxalone across multiple time points in male rat hepatocytes. At time 0 there is only alphaxalone signal/peak at 5.61 min. while, later time points a new peak (metabolite 1) appears at 5.13 min detected at the same MS/MS channel (333.2➔297.1).

4.2.6.1.1. Metabolite 1 identification:

Like other steroids, alphaxalone can undergo phase-I or phase-II metabolism. As most phase-I metabolism consists of oxidation and reduction reactions to stable compounds, the mass of the generated metabolite is most likely to be different to the original compound. Phase-II metabolism involves the attachment of a high polarity moiety (e.g. glucuronide, sulphate) to the drug, however, this conjugation bond is usually temporary and unstable (Gagez et al., 2012). There is a possibility the conjugate can be disintegrated in the mass spectrometer due to high collision energy and temperature which make it hydrolyse and revert back to its parent molecular mass (Figure 4.7). The generated metabolite will give the same mass as alphaxalone but is expected to have a shorter retention time, as such, phase-II metabolism is more likely to be the product of this metabolism.

To confirm this theory two sets of phase-II experiments needed to be performed: firstly, glucuronidation experiments and secondly conducting sulfation experiments.

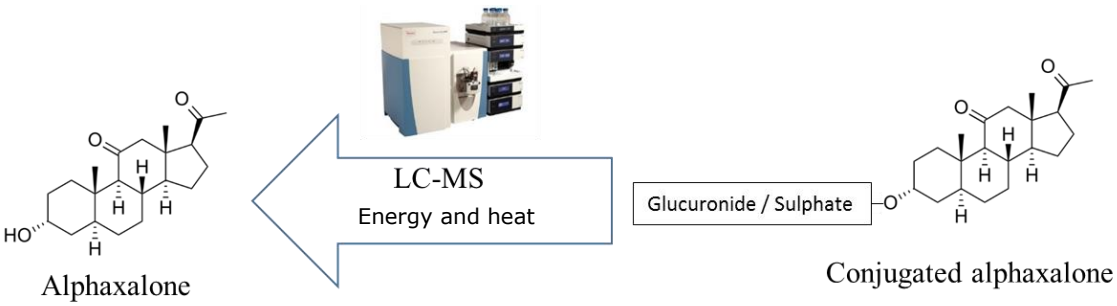

Figure 4.7: Disintegration of alphaxalone conjugate back to parent alphaxalone.

4.2.6.1.1.1. Phase-II Metabolism studies

4.2.6.1.1.1.1. Glucuronidation

The first experiment for metabolite identification was a Phase-II glucuronidation incubation. In this experiment alphaxalone was used as a substrate for phase-II conjugation investigation while oestradiol was used as a positive control. The study occurred on 1mg of male rat liver microsomes prepared inhouse. Furthermore, an authentic 3β-glucuronide oestradiol standard was obtained and used for method development and validation of the retention time of its appearance in the chromatogram. Thus, oestradiol disappearance and the 3β-oestradiol conjugate formation were possible to measure. Moreover, efforts were made to optimise the LC-MS conditions in favour of the metabolite appearance, as a sensitive measure of glucuronidation.

Oestradiol (positive control) glucuronidation

For the positive control (oestradiol), the experiment was successful and there was glucuronidation metabolism, as shown in Figure 4.8. There was no peak of 3β-glucuronide oestradiol at the beginning of the incubation while after 30 minutes there was a very large peak of 3β-glucuronide oestradiol. Furthermore, the oestradiol peak area was greatly reduced from the beginning to the end of experiment.

Time = 0 min

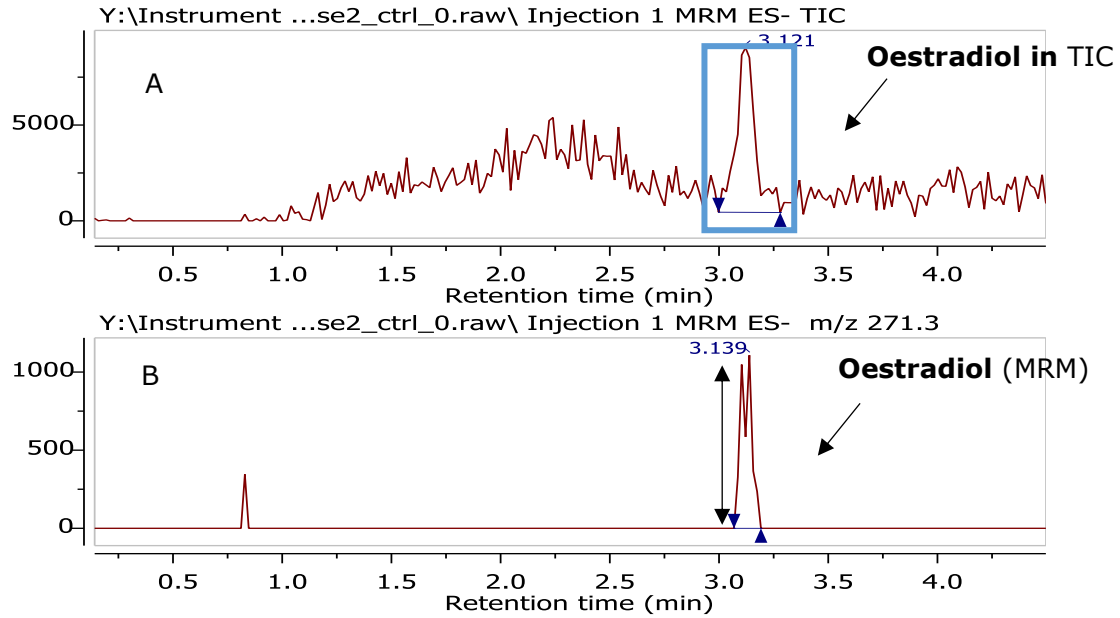

Time = 30 mins

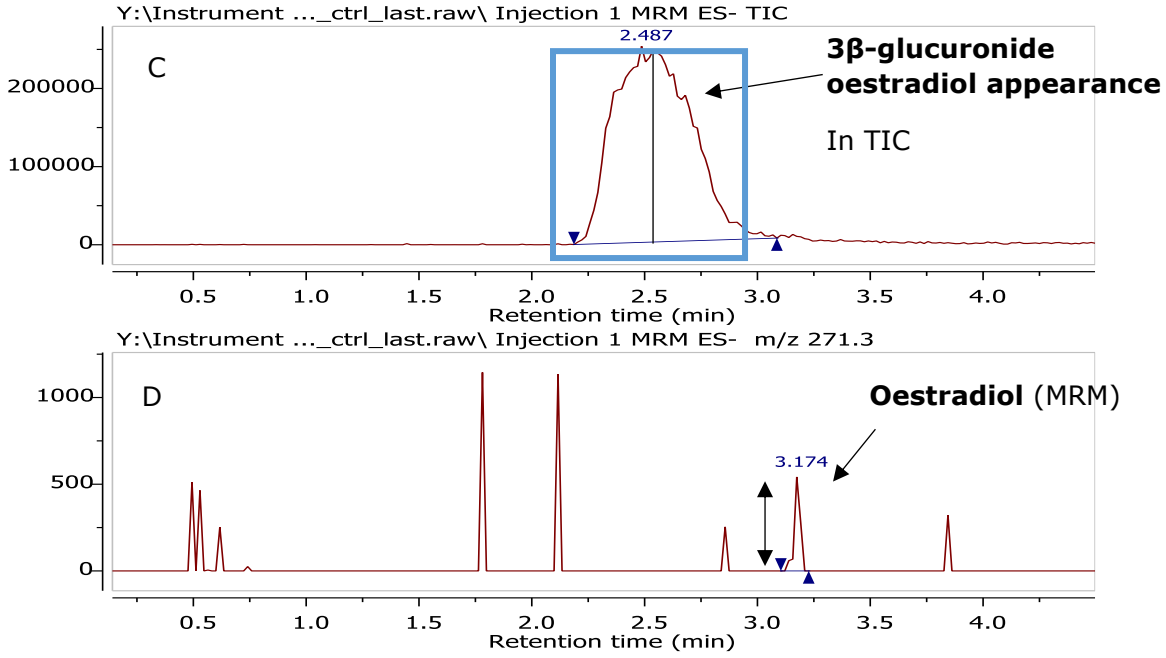

Figure 4.8: The chromatogram of 3β-glucuronide oestradiol appearance from oestradiol after 30 minutes incubation time and disappearance of oestradiol. (A) In total ion current (TIC) there was only oestradiol detectable at t=0 and no presence of any metabolites formed. (B) multiple reaction monitoring (MRM) was performed for selective detection of oestradiol only. (C) after t=30 minutes the metabolite 3β-glucuronide oestradiol was detected while oestradiol peak disappeared. (D) Oestradiol barely detectable using MRM after t=30 minutes.

Alphaxalone glucuronidation

In contrast, alphaxalone did not show any sign of metabolite formation from the glucuronidation reaction as shown in Figure 4.9. This suggests that alphaxalone undergoes very little to no glucironidation in the rat.

Time = 0 min

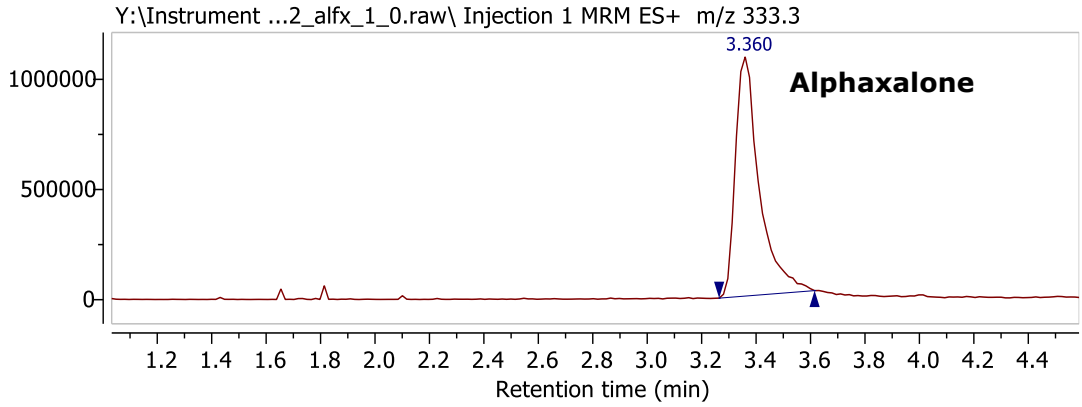

Time = 30 min

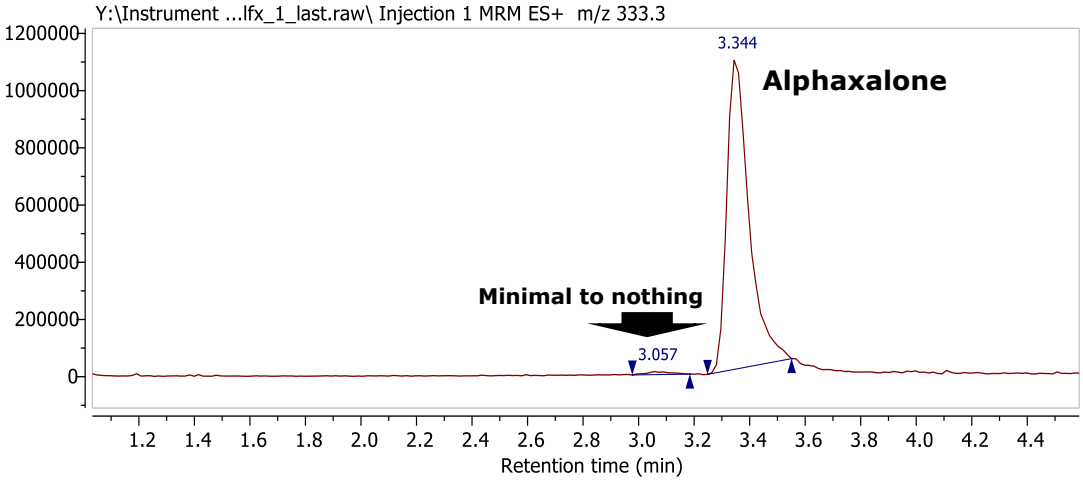

Figure 4.9: Alphaxalone chromatogram at T= 0 and 30 minutes. From incubation showing no signs of metabolism or metabolite formation.

4.2.6.1.1.1.2. Sulfation

The second phase-II study investigated alphaxalone sulfation. Alphaxalone was incubated using pooled S9 preparation and PAPS (3'-Phosphoadenosine-5'-phosphosulfate) cofactor to monitor any sulfation metabolite produced, as well as to measure the disappearance of alphaxalone across time. As shown in Figure 4.10, there was no evidence of alphaxalone being metabolised in the S9 preparation as alphaxalone concentration is stable over the incubation time period maintained at the same concentration as time zero. Furthermore, the metabolite (M1) which had been detected in hepatocytes previously was not detected in the S9 incubation and suggests that M1 is not a sulphation metabolite.

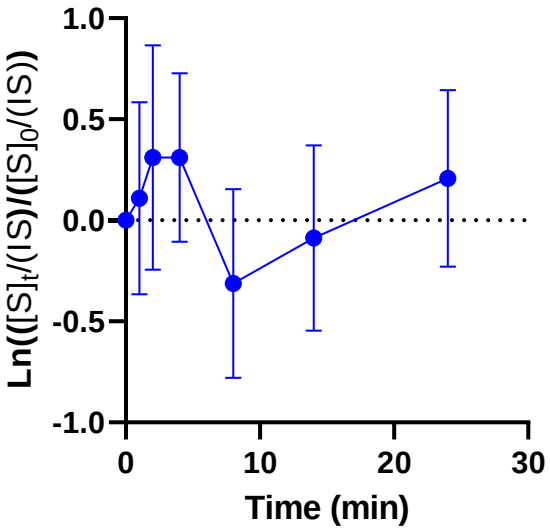

Figure 4.10. Alphaxalone response versus time for male rat liver S9 incubation. Alphaxalone concentration is stable with no sign of depletion (n=4).

4.2.6.1.1.2. Phase-I metabolism

Investigation of 3β-hydroxy-alphaxalone (3β-alphaxalone).

Alphaxalone is reported in cats and dogs to produce 3β-hydroxy-alphaxalone as a metabolite (Warne *et al.*, 2015). The metabolite is a diastereomer of alphaxalone at A-ring carbon 3. This is formed from a possible oxidative-reduction of the alcohol at the 3 position and upon reduction, a different diastereomer is formed. To test this theory, both alphaxalone and an authentic sample of 3β-hydroxy-alphaxalone were obtained and investigated with the same LC-MS/MS conditions as previously used for alphaxalone metabolism in hepatocytes. After running the authentic sample, alphaxalone appeared at the same distinct retention time of 5.60 min and M1 appeared at 5.12 minutes .

Figure **4.11**,A). When the authentic sample of 3β-hydroxy-alphaxalone was analysed it appeared at a retention time of 5.13 min (Figure **4.11**,B) and closely matches the retention time of M1. This strongly suggests that M1 is 3β-hydroxy-alphaxalone.

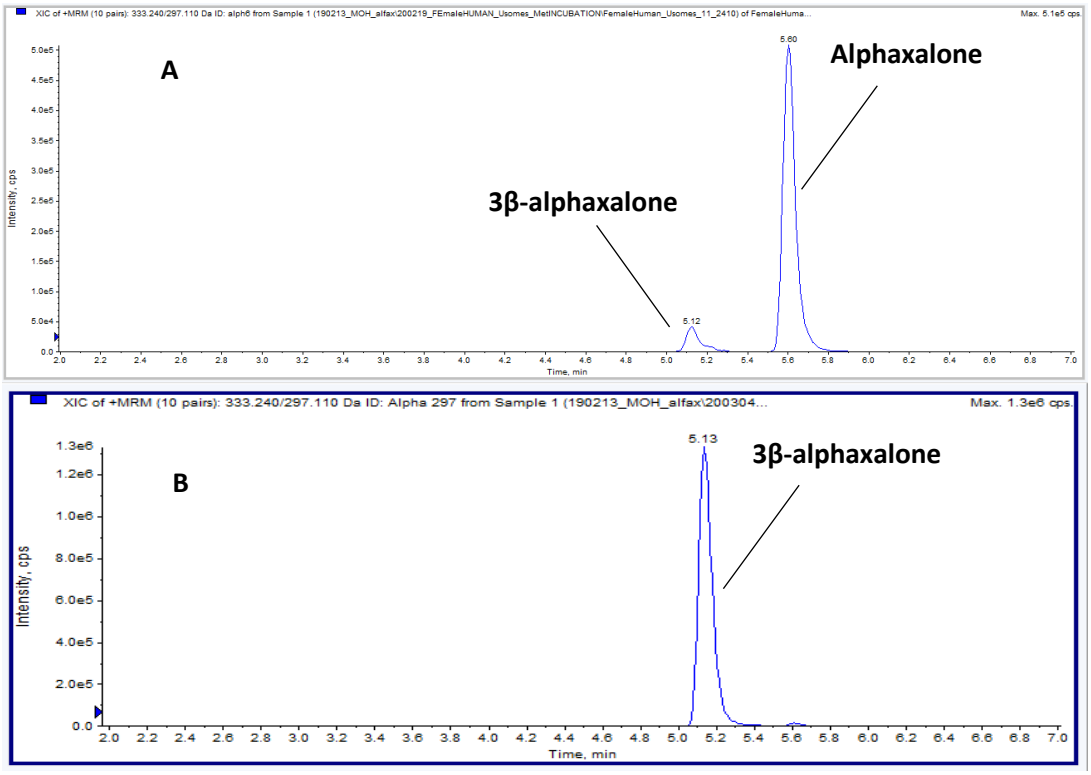

Figure 4.11: Alphaxalone and 3β-alphaxalone chromatograms. (A) Alphaxalone appeared at a retention time of 5.60 min while the metabolite is at 5.12 min. (B) 3β-hydroxy-alphaxalone appeared at a retention time 3.13 min which is different to alphaxalone and similar to M1.

4.2.6.2. Metabolite 2: 3Keto-alphaxalone

The stereo chemical conversion from alphaxalone to its metabolite diastereomer beta-alphaxalone cannot possibly be a direct conversion and there should be a reduced form as a metabolite at the 3 position which acts as an intermediate as shown in Figure 4.12. Hence, an authentic sample of Keto-alphaxalone (i.e. Allopregenatrione) needs to be tested and validated.

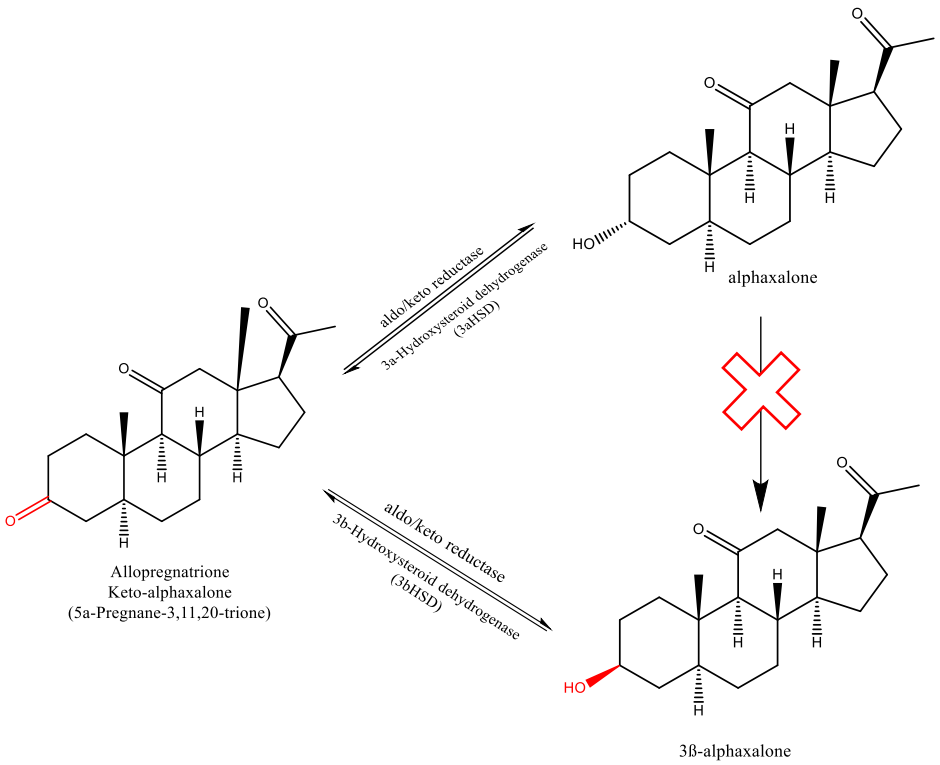

Figure 4.12: Schematic showing the conversion steps of alphaxalone to its metabolite Beta-alphaxalone.

An authentic sample of keto-alphaxalone was sourced and a unique and selective MS/MS method was developed. The authentic sample gave a peak at a distinct retention time of 5.28 min. This MS/MS method was applied to one of the later time points from a male rat hepatocyte incubation and was able to detect the keto-alphaxalone metabolite (Figure **4.13**)

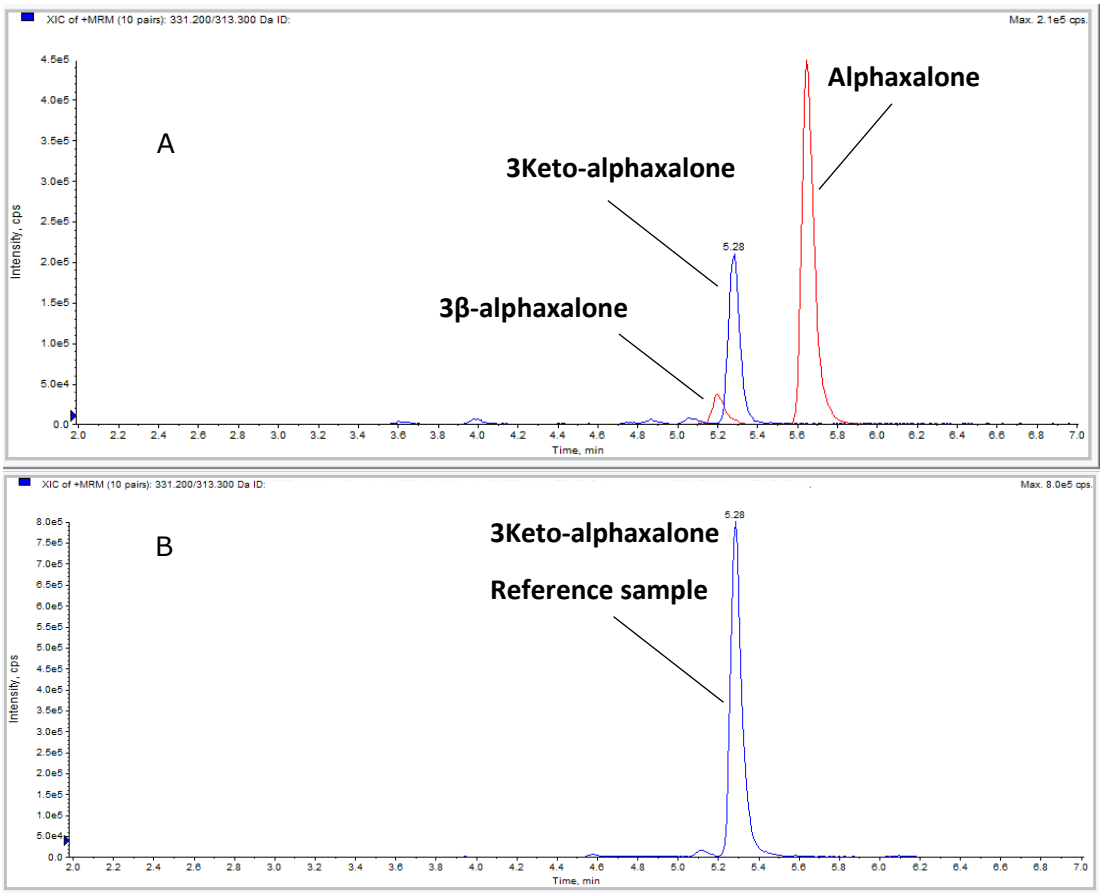

Figure 4.13: Alphaxalone sample from fresh hepatocyte incubation was validated against an authentic reference sample of 3Keto-alphaxalone.

4.2.6.2.1. Inhibition of alphaxalone metabolic pathway and validation of suggested pathway for keto and beta-alphaxalone metabolites.

Two metabolites (3β-alphaxalone and 3keto-alphaxalone) have been identified for alphaxalone. Starting with keto alphaxalone, the direction of conversion is mainly dependent on selective enzymes which are responsible for each stereoisomer conformation as shown in Figure 4.12. These enzymes are reported to be the enzymes responsible for neurosteroids synthesis as well as metabolism.

To validate this conversion pathway, two reportedly selective inhibitors for 3α-HSD and 3β-HSD enzymes, indomethacin and trilostane respectively, were used to inhibit alphaxalone metabolism in male rat liver microsomes. The disappearance of alphaxalone and the production of both keto and beta-alphaxalone were monitored. As shown in Figure 4.14, neither alphaxalone nor keto-alphaxalone

showed any reduction in their metabolism or formation, respectively, by inhibitors of 3β or 3α-HSD. However, beta-alphaxalone formation was clearly inhibited by trilostane (3β-HSD inhibitor) when compared to no inhibitor or the 3α-HSD inhibitor (indomethacin).

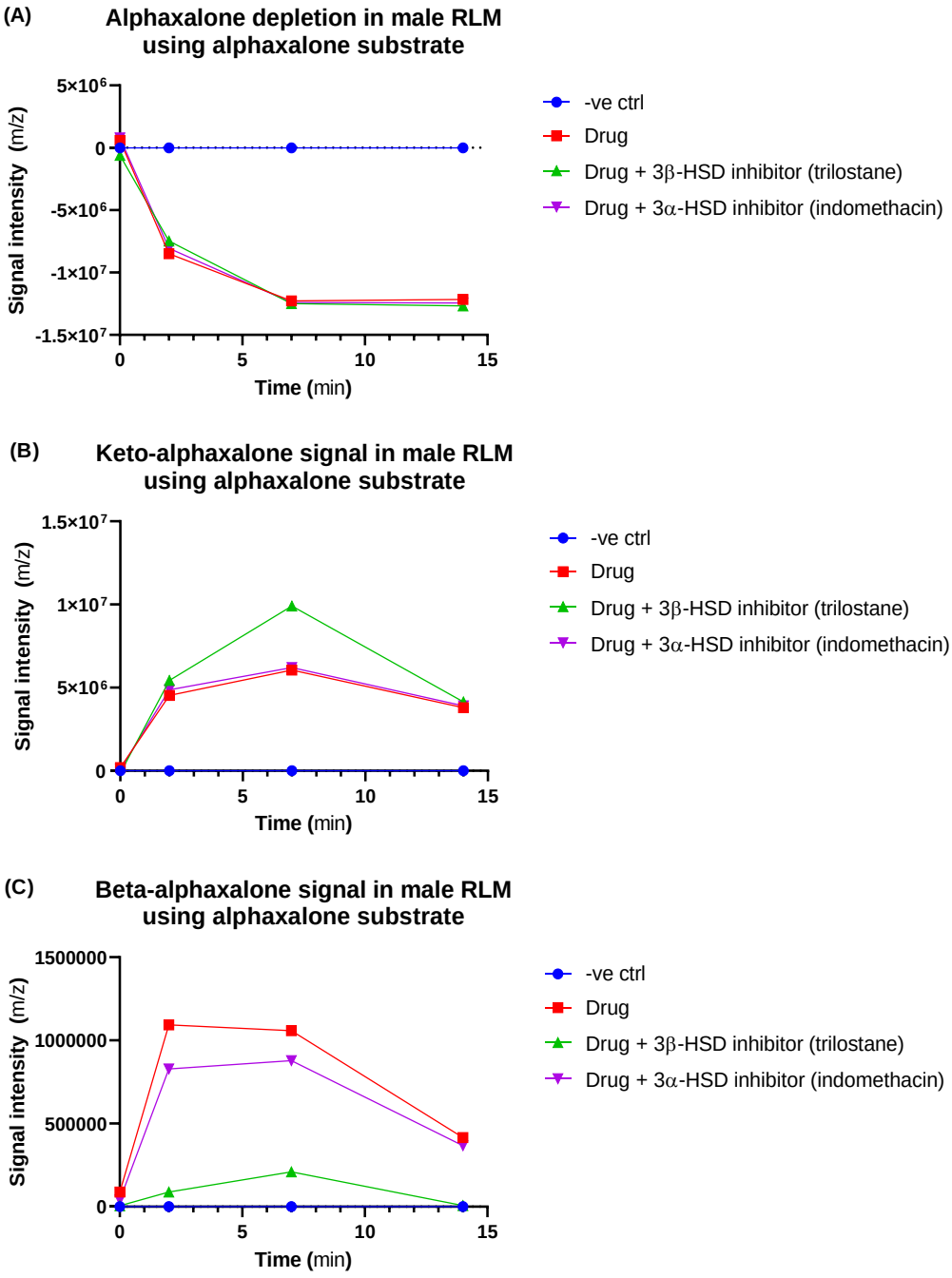

Figure 4.14: Inhibition of 3α- and 3β-HSD pathways for alphaxalone metabolism. (A) There was no change in the rate of alphaxalone disappearance with or without inhibitors. (B) keto-alphaxalone showed a slightly higher level of formation in the presence of 3β-HSD inhibitor (trilostane) in comparison to control or 3α-HSD inhibitor (indomethacin). (C) beta-alphaxalone showed inhibition when 3β-HSD inhibitor (trilostane) was present.

4.2.6.3. Metabolite 3: oxidised form of alphaxalone

The 3keto-alphaxalone was detected at MS/MS transition of 331.2➔313.2 m/z. Surprisingly, another metabolite (M3) was also observed with the same MS-MS of keto alphaxalone (Figure 4.15). M3, however, had a shorter retention time which suggests it is more polar than the other metabolites. Scanning the spectrum of M3 using an oxidised alphaxalone m/z of 349.2 (alphaxalone m/z +16) confirmed M3 to be an oxidised metabolite of alphaxalone. However, the exact position of oxidation could not be confirmed. M3 was very prominent in male rat incubations while negligible amounts were detected in female rat incubations.

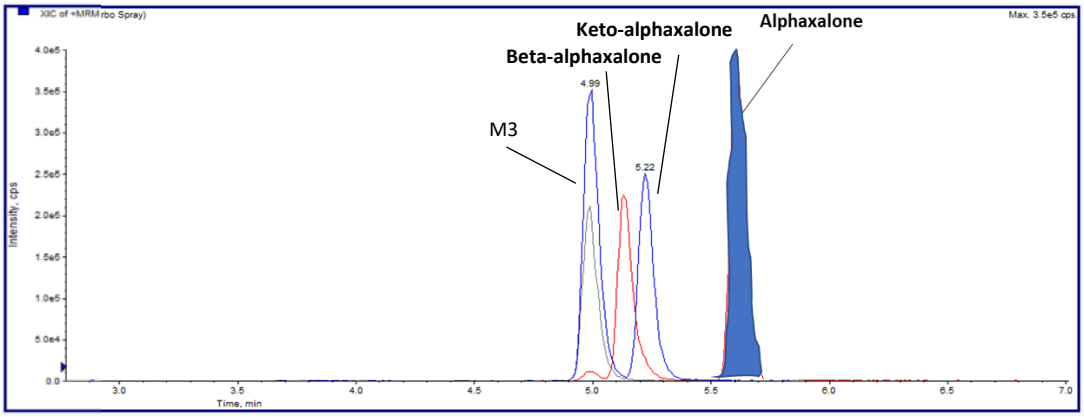

Figure 4.15. Alphaxalone, M1,M2 and M3 identified in fresh male rat hepatocyte incubations

4.2.6.3.1. Alphaxalone metabolism inhibition using a selective CYP 3A inhibitor (Clotrimazole)

The most expressed CYP enzymes in rats are the CYP 3A group. Sex dependent differences in their liver expression in rats have been reported. CYP 3A enzymes may be the metabolising enzymes responsible for the production of M3. As such, alphaxalone was incubated with and without a selective CYP 3A inhibitor (clotrimazole) to detect any change in this metabolite formation using male rat liver microsomes. Alphaxalone showed a significant overall reduction in its rate of metabolism (Figure 4.15) and the M3 level was drastically reduced (Figure 4.16).

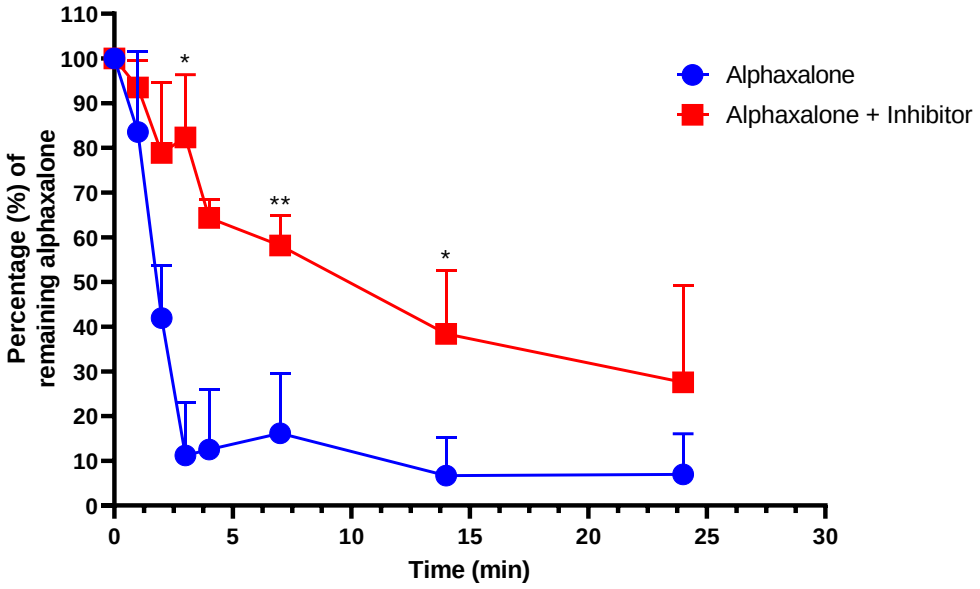

Figure 4.16: Alphaxalone metabolism with and without inhibitor (clotrimazole) (n=5). Data are presented as a mean ± SD. Asterisks denote significant difference * p < 0.05, **p < 0.01 using two-way ANOVA followed by Sidak test for multiple comparisons.

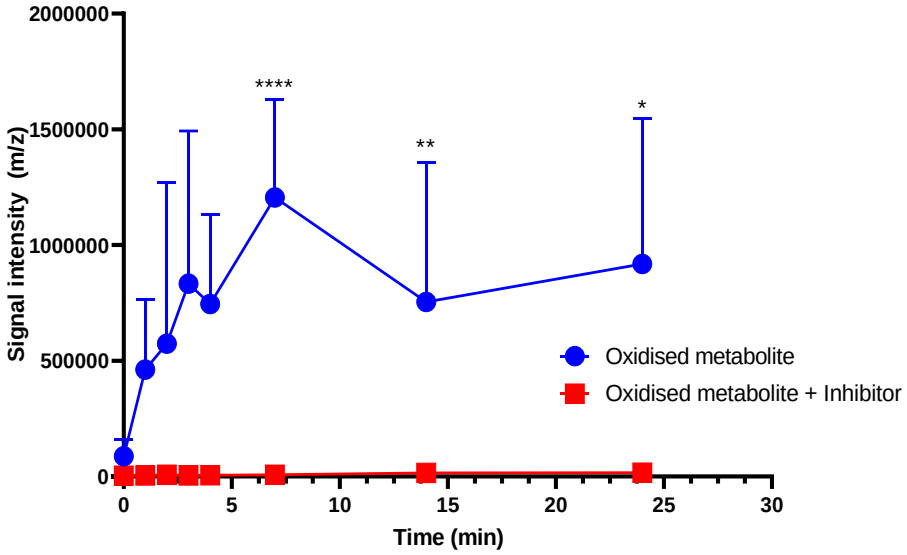

Figure 4.17: M3 formation with and without inhibitor (clotrimazole) (n=5). The metabolite M3 formation is supressed significantly with the presence of inhibitor. Data are presented as a mean ± SD. Asterisks denote significant difference * p < 0.05, **p < 0.01, ****p < 0.0001 using two-way ANOVA followed by Sidak test for multiple comparisons.

4.3. Discussion

Hepatocytes isolation /Liver isolation

Primary hepatocyte isolation is an *in vitro* model that is widely used for various liver physiology and pathology studies. For example, hepatocytes are used to assess drug metabolism, drug-drug interactions and assess the expression and function of drug metabolising enzymes such as CYP450 as well as examining the mechanism of cytotoxicity/genotoxicity (Shen et al., 2012).

Two approaches can be used for hepatocytes isolation, the first would require surgery on a live animal which requires a Home Office licence (in the UK), anaesthesia and skilled personnel. This *in vivo* method gives high hepatocyte yield and viability but higher operational costs. The second approach uses ex-vivo liver lobes from sacrificed animals terminated through schedule 1 killing and does not require an animal research licence. However, the yield tends to be lower in comparison to the former method. The method developed and described herein combined aspects from previous reports of Shen *et al.* (2012) and Shibany *et al.* (2016). The hybrid method resulted in a high yield and viability by digesting the whole liver rather than individual lobes. The average yield for hepatocyte isolation differed between male and female rats, however, no less than 75 $x10^6$ cells/liver was obtained while viability ranged from 80-95%. The acquired yield and viability was comparable to the one reported by Shen *et al.* (2012) with up to 10 $x10^7$ cells/liver and viability of 88-96%. It was also possible for this method to simultaneously harvest a whole liver lobe for subcellular fraction experiments without affecting the isolation process. In this regard, the proposed method has an optimal isolation efficiency and high degree of modularity which made it feasible to minimise the number of experimental animals.

The key factors in successful hepatocyte isolation are the type and concentration of collagenase, and perfusion flow rate. Collagenase invokes architecture break up and perfusion should be long enough to dissociate properly but not excessive to

cause cell damage. A high concentration of collagenase enzyme can be the main reason for cell death (Gonçalves, et al., 2007), while improper flow rate can affect the perfusion of collagenase in the liver. Choosing an effective collagenase with optimum flow rate was challenging in this study as improper flow rate can either rupture the internal liver capillaries for a high flow rate or will not let the collagenase evenly distribute all over the liver. While choosing the right type of collagenase for the isolation of cells is fundamental for the successful outcomes of the isolation. In the process of developing a successful isolation method, we sourced and used collagenase from two suppliers. However, both produced different results and ultimately the choice was made to only use collagenase type II (Sigma). This does not necessarily mean the other collagenase was not functional, just that it requires more optimisation.

The enzymatic activities of bacterial collagenases are extracted as poorly purified mixture of enzymes that could be significantly different within commercialised lots which affects the number and quality of the isolated cells (Berardo et al., 2020). The choice of one collagenase over another can be dependent on the type of investigation that will be carried out on the obtained hepatocytes. Furthermore, both commercial suppliers sourced their product from different manufacturers which may have used different manufacturing process with variable lot activity for this enzyme. Hence, it is advisable to not keep changing the provider as the effectiveness can be different based on the manufacturing process and will require subsequent optimisations processes. In addition, having a tight seal at the inlet area (portal vein) is crucial for successful isolation, as having solution leakage decreases the infusion pressure and will risk having air bubbles trapped inside the liver. Air bubbles if trapped, will hinder buffer flow and collagenase perfusion in the liver, which ultimately will significantly affect the overall yield and viability.

Interpretation of K_m and V_{max} values

Alphaxalone *in vitro* metabolism was investigated using fresh male and female Lewis rat hepatocytes; it was shown that the liver CL_{int} was 4.4 fold higher in male compared to female rats. Furthermore, the sex difference also extended to the Michaels-Menten estimates as the male Lewis rats had 12 and 2.6 fold higher V_{max} and K_m , respectively, in comparison to female Lewis rats. Having higher V_{max} may indicate that the specific CYP enzyme(s) responsible for oxidation of alphaxalone are more dominant in males compared to females. This is consistent with reported sex bias in the expression of CYP450 enzymes in male compared to female rats (Gandhi et al., 2004). It is more likely that the major enzyme(s) responsible for alphaxalone metabolism is highly expressed in male rats. On the other hand, this enzyme(s) may be severely under expressed or not present in the female rats. This rationale was further supported by the inhibition studies where alphaxalone disappearance and M3 formation were significantly reduced in male rats.

***In vitro*/*in vivo* extrapolation** (IVIVE)

Gender differences in hepatic enzyme activity seem to be a major contributor in determining pharmacokinetic variability by sex, (Gandhi, et al., 2004). Hepatic metabolism activity can be affected by the content levels of phase-I and –II metabolic enzymes inside the cells, the hepatocellularity and the size of liver for each sex. Although there are significant differences in hepatocellularity between sexes in Lewis rats, the difference can be dismissed when factoring in the liver size differences between genders as observed in this study and reported by Marcos *et al.* (2016). Thus, making a direct comparison of cellular metabolic activity (CL_{int}) would define the differences at a cellular level.

Both the well stirred (WSM) and parallel tube (PTM) models were able to predict to the *in vivo* values and gave high clearance prediction. However, the PTM model gave a higher clearance prediction and was closer to the liver blood flow. This estimation was close to the estimated plasma clearance for the alphaxalone *in vivo*

Lewis data. This was expected as PTM is known to have a better predictivity with highly cleared drugs (Ito & Houston, 2004).

As mentioned previously in chapter three, the estimated *in vivo* plasma clearance showed an overall higher clearance rate than the literature liver blood flow (72 ml/min/kg) for the rat which required investigation of plasma protein binding and blood:plasma ratio. There were no signs of gender differences for either plasma binding or blood:plasma ratio of alphaxalone. Both PTM and WSM models improved their scaled clearance when corrected for blood:plasma ratio and fraction unbound for incubational binding. Investigating the incubational binding of a drug is also an additional parameter to improve the accuracy of clearance prediction. However, alphaxalone did not show any significant non-specific binding at 1 million cells/ml to be considered impactful.

Interpretation of low *in vivo* alphaxalone clearance for female rats

Some of the estimated K_m and V_{max} values appeared as outliers for some of the rats in both male and female. However, the female K_m showed the most variance in its estimation with a coefficient of variation (CV) of 133%. This variation may be due to the process for isolating hepatocytes and the condition of the hepatocytes during the experiment. However, despite the presence of these variations, the substrate depletion approach is frequently used in the pharmaceutical industry for rapid screening of new drug entities (Jones and Houston 2004; Nath and Atkins 2006).

Furthermore, it was interesting to see that some of the K_m values for the female Lewis rats were surprisingly low in comparison to the male. In addition, these very small K_m values in female were comparable to the highest free alphaxalone plasma concentrations that were observed in section 3.2.1 above (Figure **3.4**) which may have led to the saturation of metabolic enzymes further reducing alphaxalone clearance in females.

Alphaxalone metabolite identification

While conducting the alphaxalone *in vitro* investigation, the M1 alphaxalone metabolite was detected. According to the retention time of its appearance, the metabolite was more polar than the parent drug. Furthermore, as alphaxalone is structurally similar to endogenous steroids, it is reported that the 3α-hydroxy group in the A-ring is more likely to be conjugated with glucuronic acid while 3β-hydroxy is more likely to be sulphated (Schänzer, 1996). Furthermore, since alphaxalone glucuronide is one of the major metabolic pathways observed in cat and dog (Warne, et al., 2014), the observed peak was thought to be indirect evidence of alphaxalone glucuronide. These conjugated metabolites are able to break down and produce the same parent mass and daughter (m/z) of alphaxalone when analysed in the mass spectrometer (Gagez et al., 2012) but will have a shorter retention time.

There was no metabolite detected from the glucuronidation or sulfation incubations conducted on alphaxalone in the present study. In this context, Warne et al. (2015) reported that one of the alphaxalone metabolites observed in both cat and dog was 3-beta-hydroxy-alphaxalone (i,e, M1). This metabolite is a diastereomer of alphaxalone, which is a compound that has different configurations at one (epimer) or more chiral centres but are not mirror images of each other and reportedly have no ability to potentiate $GABA_A$ receptors (Turner & Simmonds, 1989). The retention time difference between alphaxalone and the M1 metabolite in the present study suggests that this metabolite may be the expected epimer, as diastereomers are known to have different physio-chemical properties which makes it possible to have different retention times (Carey & Giuliano, 2011). Moreover, an authentic standard for 3β hydroxy alphaxalone gave the same retention time as the detected metabolite (M1) *in vitro.* In addition, the presence of the intermediate, keto-alphaxalone (M2) further supported M1 being 3β hydroxy alphaxalone.

Gender differences in metabolite formation in rats

The C3 position in steroids is notorious for metabolism and biotransformation as witnessed in neurosteroid synthesis to allopregnanolone from 5α-dihydro-progesterone (Schänzer, 1996). Allopregnanolone is also readily oxidised at the same site (C3 position) resulting in accumulation of the inactive 3-keto metabolite form. The neurosteroids in general are characterised by their rapid clearance due to rapid primary and secondary phase metabolism at the C3 position by either conjugation or the aldo-keto reductase enzymes (Martinez-Botella et al., 2014). A blocking group such as methyl at the C3 position as shown for ganaxolone (Figure **1.2**) has been shown to prevent its rapid metabolism and prolonged its half-life from minutes to hours ($T_{½}$= 19.2±5.2 hour) (Monaghan et al., 1997) and provided greater bioavailability (Yawno et al., 2017) in comparison to alphaxalone.

The 3α-hydroxy steroid dehydrogenase (3α-HSD) and 3β-hydroxy steroid dehydrogenase (3β-HSD) enzymes are responsible for either oxidation or reduction of the C_3 position. Theses enzymes are members of the aldo-keto reductase (AKR) family that catalyse the conversion of 3-keto-steroids to and from 3α and 3β steroids (Dufort et al., 2001). Sex bias in expression of these enzymes can lead to different rates of product formation. Generally, both enzymes are expressed throughout the body, however in rats, they are highly expressed in the liver. In addition, studies that examined the regulation of these enzymes appear to show sex specific isoforms due to the sexually dimorphic regulation of these enzymes. Studies concluded that for female rats there is 2-3 fold higher expression of 3α-HSD (Stolz et al., 1991); while 3β-HSD is 5.8 fold higher in male rats (Naville et al., 1991), which may explain the alphaxalone sex differences observed.

Alphaxalone inhibition studies for both of these enzymes gave conflicting results. The 3α-HSD inhibition study did not show any signs of inhibition with indomethacin. This inhibitor, however, has been reported from multiple studies to selectively inhibit the 3α-HSD enzyme in humans (Blomquist et al., 2005; Byrns

et al., 2008; Penning et al., 1997). On the other hand, 3β-HSD was inhibited with the reported selective inhibitor trilostane (Naville et al., 1991). A possible explanation for the lack of indomethacin inhibition for the 3α-HSD enzyme is that the enzyme is known to have three types, distributed around the body. The non-steroidal anti-inflammatory inhibitor for the 3α-HSD enzyme has been reported to be a potent and selective 3α-HSD inhibitor mainly of the type 3 class within the 3α-HSD enzyme family in humans. However, as there was no observable inhibition by indomethacin it may be the case that the type 3 class is poorly expressed in the rat liver. An alternative explanation is that there are more than one enzymes responsible for this metabolism as the 17β-HSD type10 enzyme has been reported to act in a similar way to the 3α-HSD enzyme (X. Y. He et al., 2019; Shafqat et al., 2003).

The third detected metabolite (M3) was an oxidised form of alphaxalone and was formed mainly in male rat hepatocytes. M3 was also significantly inhibited by the selective rat CYP 3A inhibitor (clotrimazole). The inhibitor not only reduced the formation of the M3 metabolite, but also reduced the depletion of alphaxalone in rat hepatocytes. This suggests that the pathway that leads to M3 is the major pathway in male rats, although there are minor pathways such as alpha to beta isomerisation which are the main pathways used by female rats.

Chapter 5:

Alphaxalone metabolism pathway for rat and other species

5. Chapter 5. Alphaxalone metabolism pathway for rat and other species

5.1. Introduction

Alphaxalone sex differences were observed in hepatocyte metabolism of Lewis rats. This difference was also observed *in vivo* for Lewis, SD and Wistar rats (Visser *et al.*, 2002; Lau *et al.*, 2013; White *et al.*, 2017). The consensus is that alphaxalone is primarily metabolised by the liver and supported via the accuracy of the IVIVE shown in the previous chapter. The metabolism of alphaxalone in the male rat was noticeably faster compared to female rats which might be due to higher expression levels of the relevant metabolic enzymes.

Alphaxalone was found to be converted into keto-alphaxalone which in turn was metabolised to beta-alphaxalone. Each of these metabolites has demonstrated the ability to revert to alphaxalone due to the nature of their converting enzymes. The possibility of having additional metabolism pathways has been reported by Warne *et al.* (2014). The group reported alphaxalone metabolism in both phase-I and phase-II enzymatic systems. The reported alphaxalone metabolites in the phase-I canine hepatocytes were allopregnatrione (keto-alphaxalone), 3β-alphaxalone, 20-hydroxy-beta-alphaxalone, 20-hydroxy-alphaxalone and 2α-hydroxy-alphaxalone. These five metabolites were also observed in cats (Warne et al., 2015). While alphaxalone phase-II metabolites were alphaxalone glucuronide and 20-hydroxy-alphaxalone sulfate detected in both cat and dog. In addition, 2α-hydroxy-alphaxalone glucuronide was observed in dog only while 3β-alphaxalone sulfate was only present in cat. The reported metabolites showed some species differences for phase-II metabolism, however, both dog and cat had the exact same five metabolites for phase-I enzymatic system. The best *in vitro* model to study drug stability is freshly isolated hepatocytes. As discussed previously, the hepatocytes contain all the necessary enzymes and cofactors to metabolise the drugs via phase-I and -II reactions. Liver microsomal enzymes are also used frequently for these studies if the drug is mainly metabolised by phase-I enzymes.

Chapter 5. Alphaxalone metabolism pathway for rat and other species

Alphaxalone has been demonstrated to be metabolised mainly via the phase-I enzymes, mostly by the steroid dehydrogenase enzyme family (3α-HSD/3β-HSD) as well as the CYP 3A enzyme in male rats. However, there was no evidence of alphaxalone phase-II conjugation in rats (Chapter 4).

The metabolic enzymes responsible for phase-I reactions in common steroids were reported to have sex differences in their functionality and expression in rats. For instance, the expression of the steroid dehydrogenase enzymes and their catalytic activity preference are gender dependent while CYP 2B and 3A enzymes are mainly male dominant (Kato & Yamazoe, 1992; Naville et al., 1991; Stolz et al., 1991; Waxman & Holloway, 2009). The CYP 3A sub family is the most important metabolic enzyme in humans and has been detected in rat, rabbit, dog, mini-pig and monkey (Bogaards et al., 2000). Both CYP 3A4 and 2C9 enzymes have shown great catalytic activity for testosterone and steroid like structures in humans (Pasanen, 2004). However, species differences are quite common and must be considered in translation from preclinical species to humans (Martignoni *et al.*, 2006). While other species such as rabbits have more predominant CYP 2C3 enzyme responsible for steroid metabolism (Bogaards et al., 2000).

Thus, understanding alphaxalone metabolism pathways is important as the drug is licensed and used for a variety of species and also being considered and tested in humans (Goodchild et al., 2020). The estimated *in vitro* clearance of alphaxalone is a representation of the total metabolism pathways that have occurred in the liver. However, understanding the differences at the metabolism pathway level gives more insight into our understanding of alphaxalone pharmacokinetics. From the previous findings of alphaxalone metabolism a simple mathematical model can describe kinetically the metabolism pathway of alphaxalone.

Hence the aim of this chapter was to quantify the individual metabolism pathways in kinetic terms in order to discover which are the major components/pathways

responsible for the overall disappearance of alphaxalone *in vitro* and whether there are differences in males and females across the species (human, rabbit, dog, monkey). A summary of the investigation approach is presented in figure 5.1.

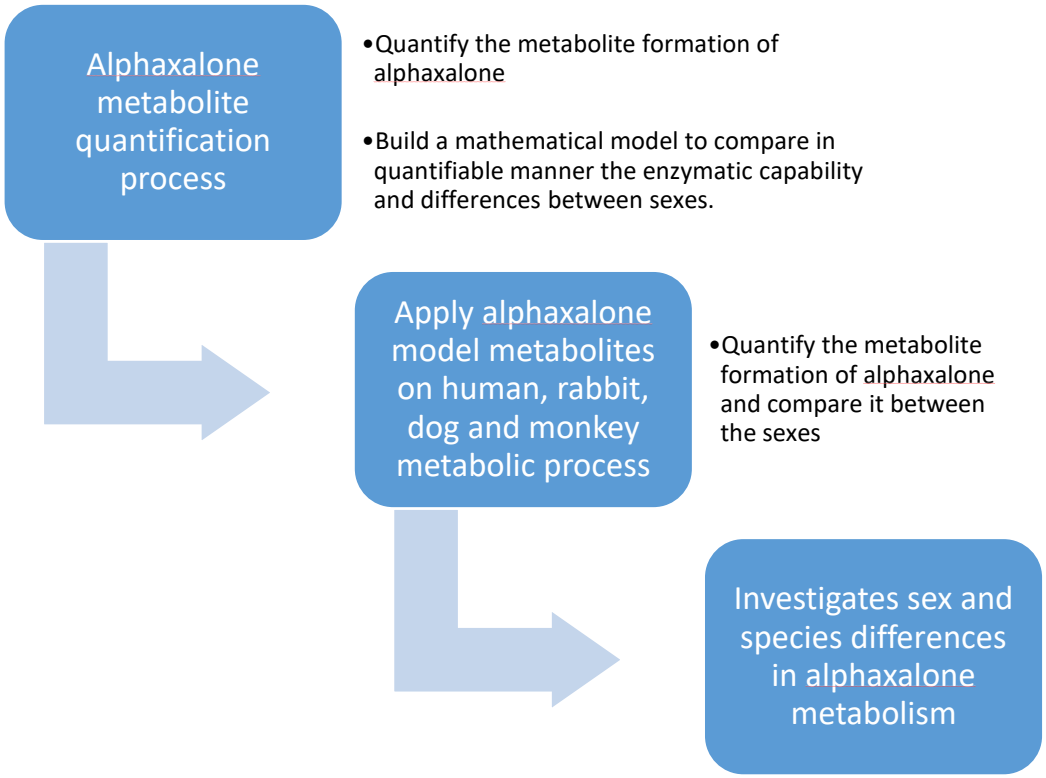

Figure 5.1. Schematic diagram summaries the investigation process taken in the present chapter.

5.2. Results

5.2.1. Alphaxalone metabolism pathway model

Alphaxalone, keto-alphaxalone and beta-alphaxalone were each incubated in liver microsomes for several species and genders to understand the magnitude of gender and species differences for alphaxalone metabolism. The data of the alphaxalone metabolic pathway was fitted to a simple model (Figure 5.2) for each species and gender. The model considers the conversion of alphaxalone to the identified metabolites (Keto-alphaxalone and 3β-alphaxalone); these metabolites were identified previously to be formed by 3α-HSD and 3β-HSD enzymes that act reversibly. Hence, each converting enzyme has a rate constant for each conversion direction. Furthermore, elimination routes (A_0, K_0 and B_0) were added to the model for each substrate which represents the sum of any undetermined metabolism route. The elimination route was considered reversible to account for any unspecific metabolite that could convert back to its original drug.

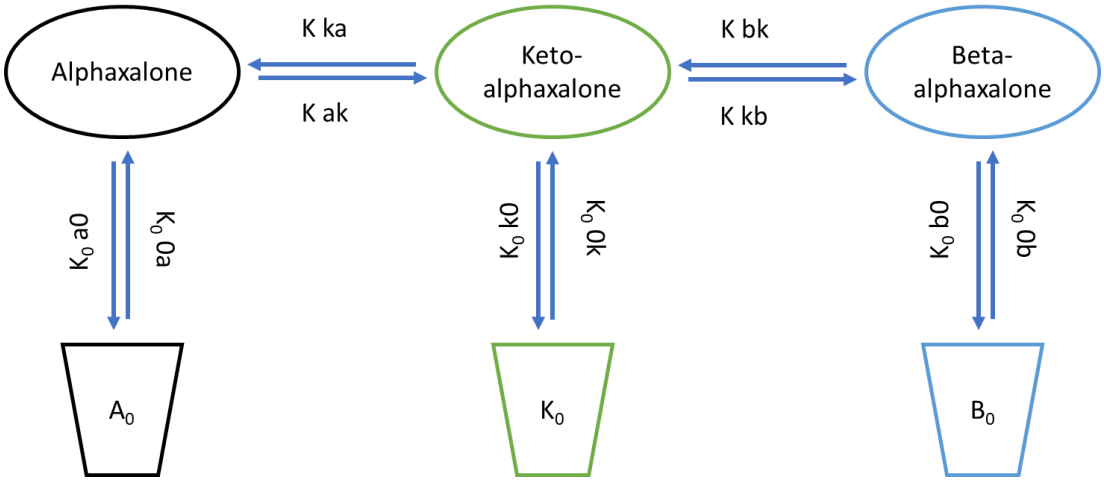

Figure 5.2. Alphaxalone metabolism pathway kinetic model used to analyse alphaxalone metabolism and the formation of its metabolites. The parameter definitions are described in table 2.5 or bellow. K ka and K ak represent the enzyme 3α-HSD while K bk and K kb represnst 3β-HSD.

Table 2.5. Rate constant definitions used in the alphaxalone metabolism model.

Parameter	Description
Alphaxalone (µM)	Alphaxalone compartment
A_0	Alphaxalone elimination compartment
Keto-alphaxalone (µM)	Keto-alphaxalone compartment
K_0	Keto-alphaxalone elimination compartment
Beta-alphaxalone (µM)	Beta-alphaxalone compartment
B_0	Beta-alphaxalone elimination compartment
K_ak (1/min)	Conversion rate constant for alphaxalone to keto-alphaxalone.
K_ka (1/min)	Conversion rate constant for keto-alphaxalone to alphaxalone
K_kb (1/min)	Conversion rate constant for keto-alphaxalone to beta-alphaxalone
K_bk (1/min)	Conversion rate constant for beta-alphaxalone to keto-alphaxalone
K_0_a0 (1/min)	Conversion rate constant for alphaxalone elimination
K_0_0a (1/min)	Conversion rate constant for alphaxalone reversable elimination
K_0_k0 (1/min)	Conversion rate constant for keto-alphaxalone elimination
K_0_0k (1/min)	Conversion rate constant for keto-alphaxalone reversable elimination
K_0_b0 (1/min)	Conversion rate constant for beta-alphaxalone elimination
K_0_0b (1/min)	Conversion rate constant for beta-alphaxalone reversable elimination

5.2.1.1. Alphaxalone kinetic parameters for male and female rat liver microsomes obtained from model

The model was able to fit the data for alphaxalone and its metabolites with an r^2 average of greater than 0.7 for observed concentrations (DV) *versus* individual predicted values (IPRED) (DV vs IPRED) Figure 8.1 and Figure 8.2. However, the model struggled at fitting some of the metabolites formed when the overall concentration was low. The substrate and metabolites data and the model fit are shown in Figure 5.3. The estimated parameters for the conversion rate constants in male and female Lewis rats are listed in Table 5.1.

Alphaxalone conversion rate constants showed an overall larger value in male compared to female rats for the following rate constants: K_ak, K_ka, K_kb and K_bk. In male and female rats, the 3α-HSD enzyme which is represented as K_ak and K_ka preferred the conversion toward the alphaxalone direction (K_ka) over the other. Furthermore, the ratio between K_ak to K_ka is the same between sexes, however, this pattern was not observed in the 3β-HSD enzyme, as male and female rats showed sex differences for the enzyme activity. Female rats did not show tendencies for beta-formation (K_kb) unlike male rats. For the other elimination routes, male rats showed significantly faster rates of metabolism from alphaxalone (K_a0) which was not observed in female rats, while keto metabolism (K_k0) showed faster metabolism in female rats compared to male rats. Lastly, the elimination of beta-alphaxalone is negligible as the dominant direction of the equilibrium is K_0_0b being equal or several times larger than K_0_b0 in male and female rats, respectively. A summary of the results is illustrated in Figure 5.4.

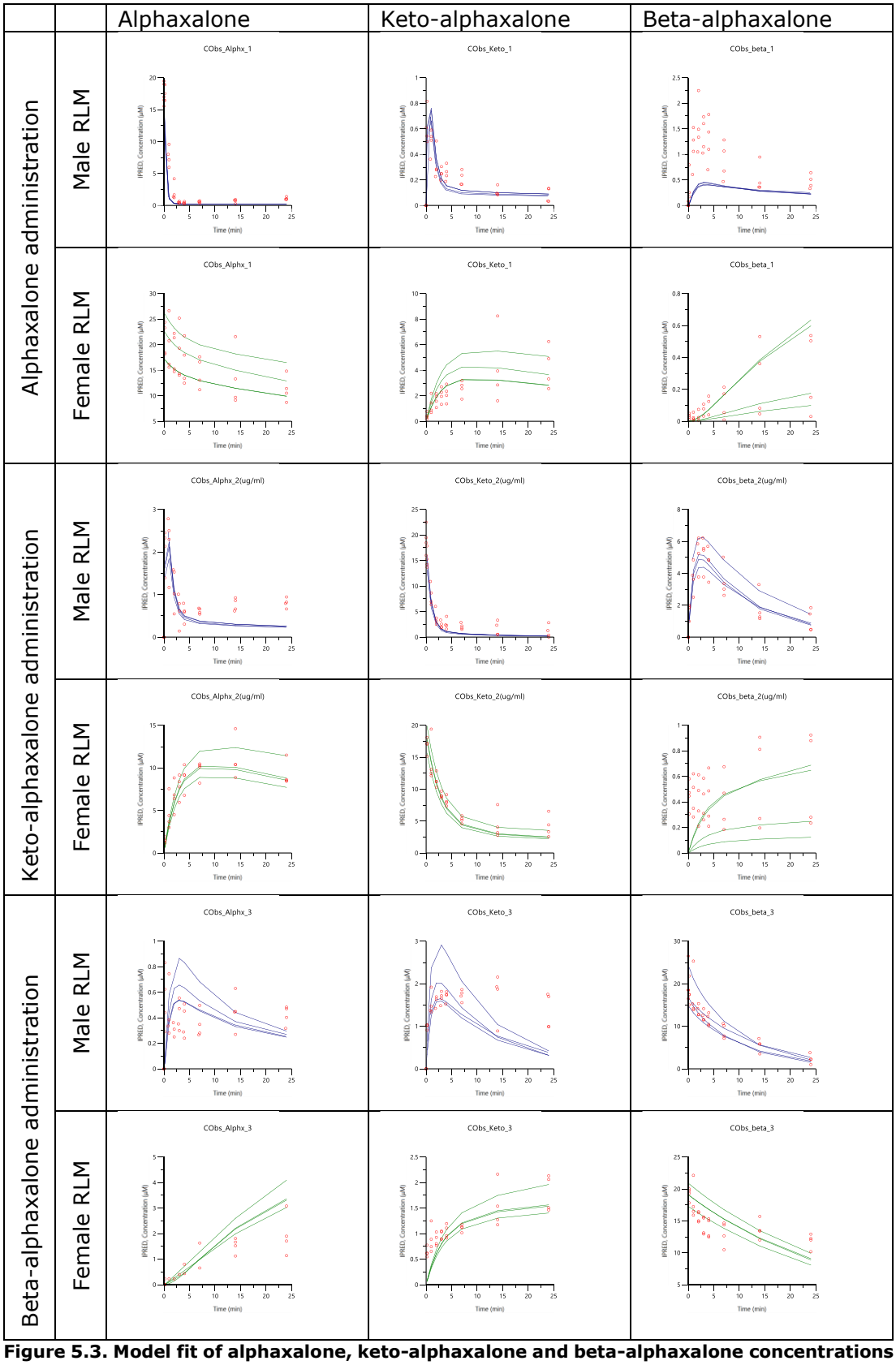

Figure 5.3. Model fit of alphaxalone, keto-alphaxalone and beta-alphaxalone concentrations from male and female rat liver microsomes. The Y axis represent substrate concentration (µM) while the X axis represent time (minutes). n=4 representative. Larger figure images are presented in figure 8.15, 16, 17.

Table 5.1. Estimated rate constants of alphaxalone metabolism and its metabolite in male and female Lewis rat liver microsomes. The data represents the mean and SD (n=4)

Lewis rat - liver microsomes				
	Alphaxalone			
	Male rat		Female rat	
Parameter	**Mean**	**SD**	**Mean**	**SD**
	(1/min)			
K_ak	0.262	6.37E-07	0.0773	1.79E-07
K_ka	0.736	5.19E-08	0.221	6.79E-06
K_kb	0.386	1.08E-07	0.00505	0.00306
K_bk	0.154	0.021	0.0215	7.87E-09
K_0_a0	2.94	0.000266	1.76E-09	2.65E-18
K_0_0a	0.0366	0.000498	0.725	5.76E-08
K_0_k0	4.46E-08	1.72E-13	0.056	0.0137
K_0_0k	0.219	1.42E-11	9.86E-05	5.61E-08
K_0_b0	4.40E-08	4.26E-17	0.0106	2.95E-09
K_0_0b	6.43E-08	7.78E-16	10.3	0.0376

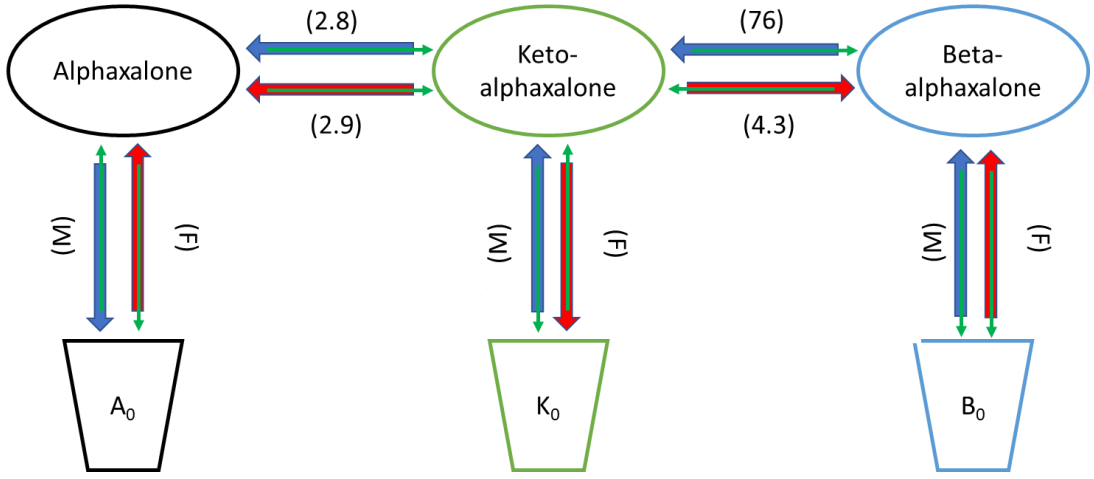

Figure 5.4. Alphaxalone metabolism pathway model fit for rat. The parameters estimated from the model are represented in the schematic. Blue and red arrows represent the male and female dominant metabolism direction. The green arrows are to show that the catalytic conversion of alphaxalone, keto- and beta-alphaxalone are modelled as unidirectional. The numbers above/below arrows represent the ratio of representative rate constants. The details of each directional rate constants are described in Figure **5.2**. The letters M and F represent male and female as the major metabolic direction.

5.2.1.2. Alphaxalone kinetic parameters for male and female human liver microsomes from model fit

The model was able to fit the data for alphaxalone and its metabolites from human liver microsomes as shown in Figure 8.3 and Figure 8.4. However, the model struggled to fit the data when the metabolite concentration was low, such as, beta-alphaxalone formation when it was formed from both alphaxalone and keto-alphaxalone as starting substrates in both sexes. Furthermore, the female data for beta-alphaxalone as starting substrate had poor correlation (r^2<0.7). A complete fitting of the data for each substrate for male and female is shown in Figure **5.5** and the estimated parameters for conversion rate constants in male and female humans are listed in Table 5.2.

Alphaxalone showed an overall faster rate of conversion in male compared to female rats for the following rate constants: K_ak, K_ka, K_kb and K_bk. In male and female humans, the K_ak and K_ka constants preferred the conversion toward Keto-alphaxalone (K_ak). This was also the case for keto-alphaxalone formation from beta-alphaxalone (k_bk) compared to the opposite pathway in both sexes. This made the conversion to keto-alphaxalone the major interconversion metabolism for both male and female humans.

For the other elimination routes, all the elimination back rates (K_0_0a, K_0_0k, K_0_0b) are several times larger than K_0_a0, K_0_k0, K_0_b0 for females indicating negligible elimination by these pathways. On the other hand, the prominent elimination pathway in males was from keto-alphaxalone followed by the beta-alphaxalone route as the dominant direction of the equilibria were towards K_0_k0 and K_0_B0. A summary of the results is illustrated in Figure 5.6.

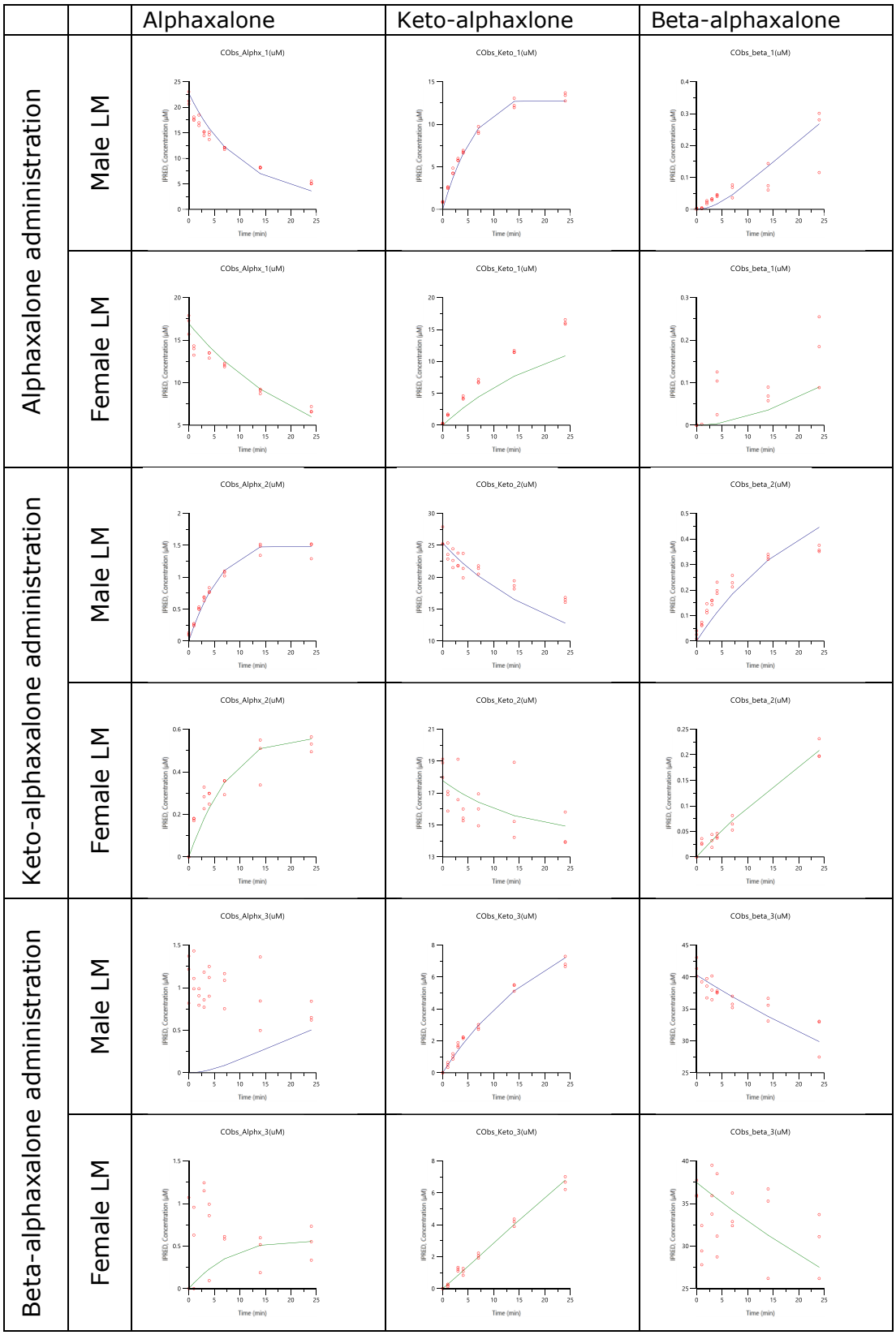

Figure 5.5. Model fit of alphaxalone, keto-alphaxalone and beta-alphaxalone concentrations from male and female human liver microsomes. The Y axis represent substrate concentration (µM) while the X axis represent time (minutes). Larger figure images are presented in figure 8.18, 19, 20.

Table 5.2 Estimated rate constants for alphaxalone metabolism and its metabolites in male and female human liver microsomes.

Human - liver microsomes		
	Alphaxalone	
	Male	Female
Parameter	**(min^{-1})**	
K_ak	0.092	0.043
K_ka	9.59E-03	4.45E-12
K_kb	1.22E-03	6.23E-04
K_bk	0.012	7.24E-03
K_0_a0	1.57E-15	4.25E-03
K_0_0a	0.212	132308
K_0_k0	0.025	0.013
K_0_0k	3.41E-13	4321
K_0_b0	2.37E-04	5.70E-03
K_0_0b	6.89E-09	84.648

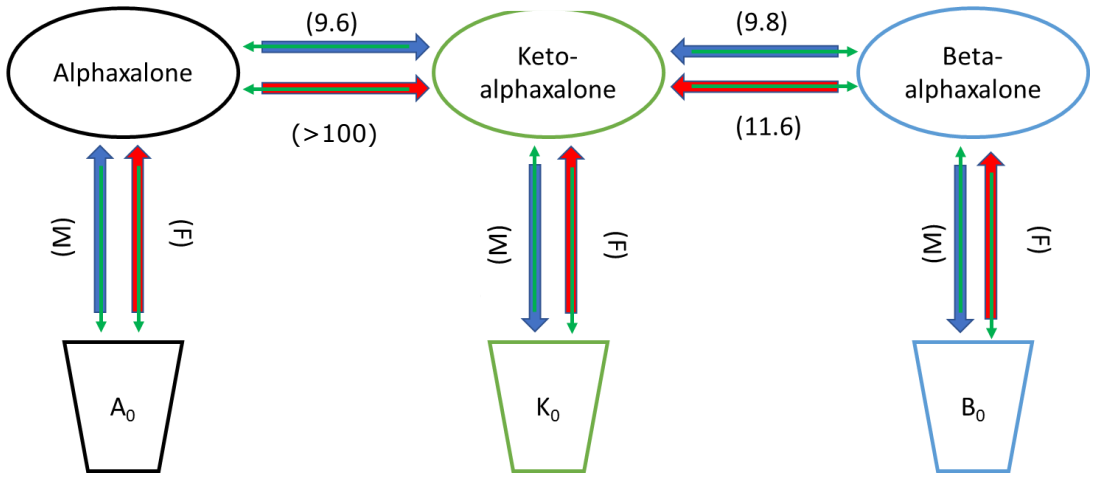

Figure 5.6. Alphaxalone metabolism pathway model fit for human. The parameters estimated from the model are represented in the schematic. Blue and red arrows represent the male and female dominant metabolism direction. The green arrows are to show that the catalytic conversion of alphaxalone, keto- and beta-alphaxalone are modelled as unidirectional. The numbers above/below arrows represent the ratio of representative rate constants. The details of each directional rate constants are described in in Figure 5.2. The letters M and F represent male and female as the major metabolic direction.

5.2.1.3. Alphaxalone kinetic parameters for male and female rabbit liver microsomes from the model fit

The model was able to fit the data for alphaxalone and its metabolites in rabbit liver microsomes as shown in Figure 8.5 and Figure 8.6. Furthermore, similar to the human liver microsomes data fitting, the model showed an overall good fit (r^2>0.7) however, it also struggled to fit the metabolites at low concentration formed from either alphaxalone or keto alphaxalone. Furthermore, the nominal concentration for each substrate was 15 µM, however, the beta-alphaxalone quantified concentration was two-fold higher than the nominal concentration. A complete fitting of the data for each substrate for male and female is shown in Figure 5.7 and there is clear underestimation of alphaxalone clearance. Furthermore, the estimated parameters for conversion of rate constants in male and female rabbits are listed in Table 5.3.

Alphaxalone elimination (K_0_a0) on the other hand was a pathway preferred by male rabbits while the females had several times larger K_0_0a. This was also the case for the beta-alphaxalone elimination route. On the other hand, keto-alphaxalone elimination (K_0_k0) was observed in both male and female as the forward rate was several times larger than the back rate (K0_0k). A summary of the results is illustrated in Figure 5.8.

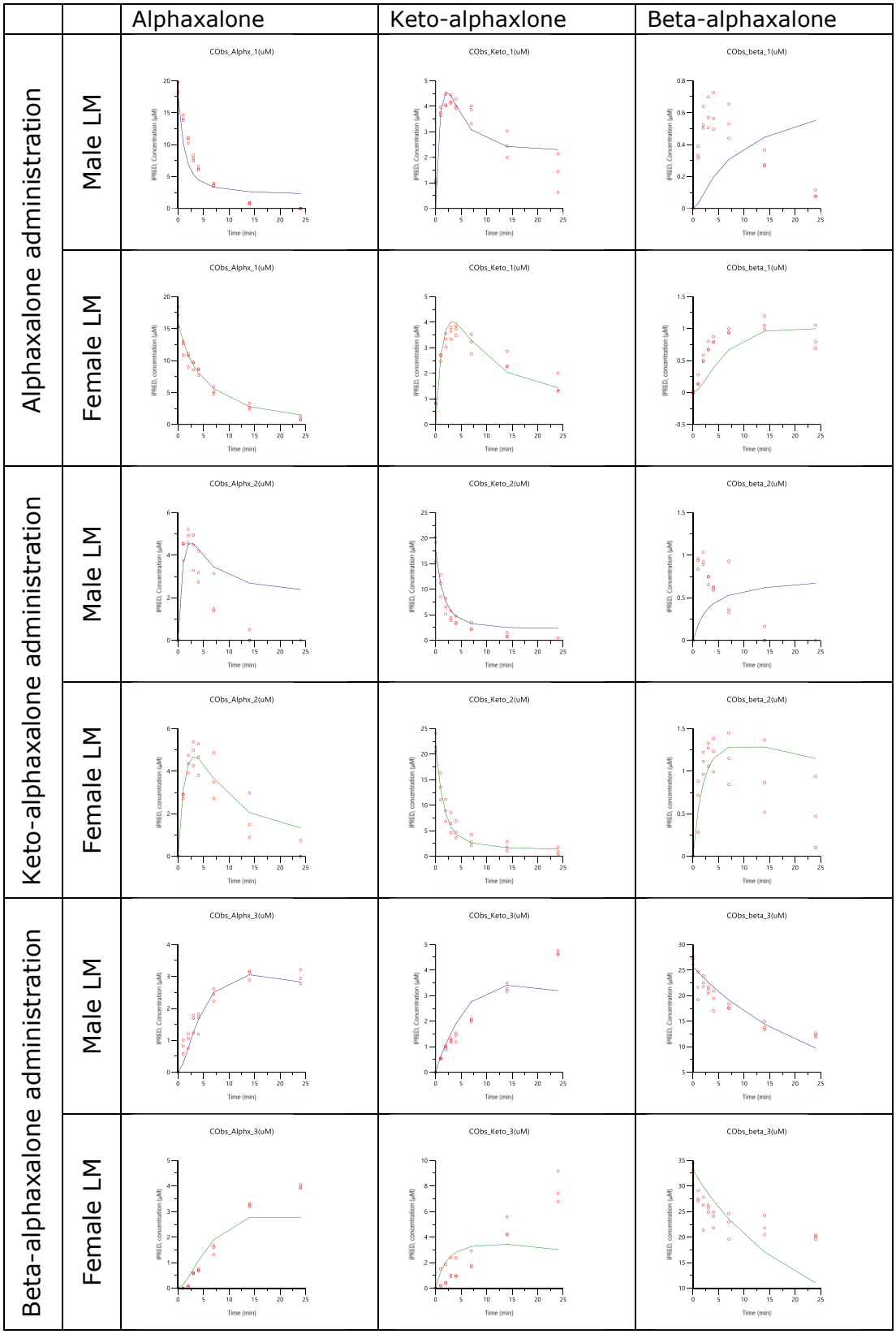

Figure 5.7. Model fit of alphaxalone, keto-alphaxalone and beta-alphaxalone concentrations from male and female rabbit liver microsomes. The Y axis represent substrate concentration (µM) while the X axis represent time (minutes). Larger figure images are presented in figure 8.21, 22, 23.

Table 5.3. Estimated rate constants for alphaxalone metabolism and its metabolites in male and female rabbit liver microsomes.

Rabbit - liver microsomes		
	Alphaxalone	
	Male	Female
Parameter	**(min^{-1})**	
K_ak	0.368	0.235
K_ka	0.335	0.204
K_kb	0.014	0.033
K_bk	0.030	0.052
K_0_a0	0.261	7.01E-10
K_0_0a	0.123	1.426
K_0_k0	0.194	0.304
K_0_0k	0.053	0.028
K_0_b0	0.014	1.68E-11
K_0_0b	3.46E-11	0.967

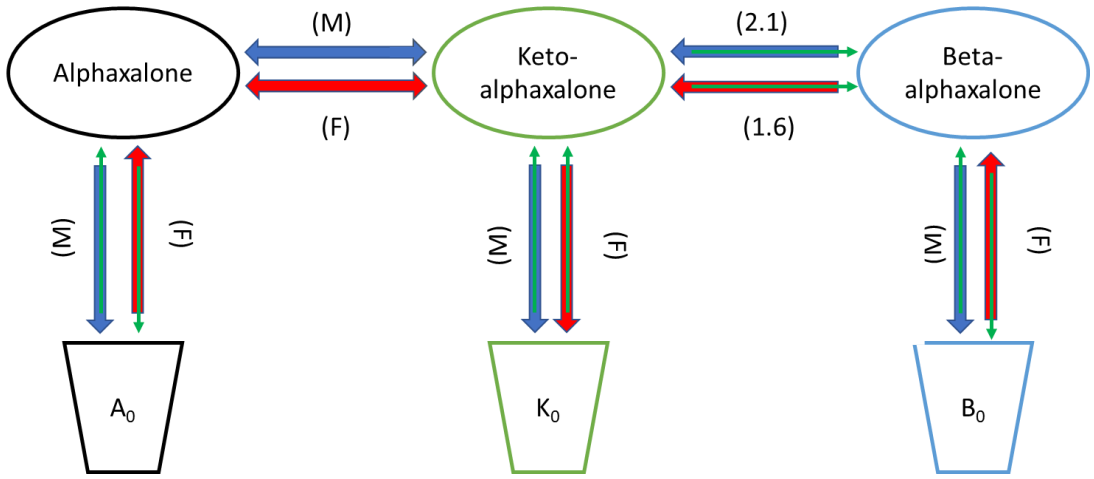

Figure 5.8. Alphaxalone metabolic pathway model fit for rabbit. The parameters estimated from the model are represented in the schematic. Blue and red arrows represent the male and female dominant metabolism direction. The green arrows are to show that the catalytic conversion of alphaxalone, keto- and beta-alphaxalone are modelled as unidirectional. The numbers above/below arrows represent the ratio of representative rate constants. The details of each directional rate constants are described in Figure **5.2**. The letters M and F represent male and female as the major metabolic direction.

5.2.1.4. Alphaxalone kinetic parameters for male and female beagle dog liver microsomes from the model fit

The model was also able to fit the data for alphaxalone and its metabolites in dog liver microsomes as shown in Figure 8.7 and Figure 8.8. The model also showed less optimal fitting for beta-alphaxalone in both formation, which may be due to low concentration (<0.5 μM), and depletion processes. A complete fitting of the data for each substrate for male and female is shown in Figure 5.9 and the estimated parameters for conversion rate constants in male and female dogs are listed in Table 5.4.

Alphaxalone conversion rate constants slightly favoured the keto-alphaxalone formation in male. On the other hand, female had a faster alphaxalone elimination rate compared to male. Keto-alphaxalone elimination rate was negligible in female, as K_0_0k was several times larger than K_0_k0. Both male and female dogs were able to eliminate beta-alphaxalone. Furthermore, there is an overall trend for female dogs to have 4 to 10 fold larger elimination rates compared to male dogs in the elimination processes (K_0_a0, K_0_k0, K_0_b0). A summary of the results is illustrated in Figure 5.10.

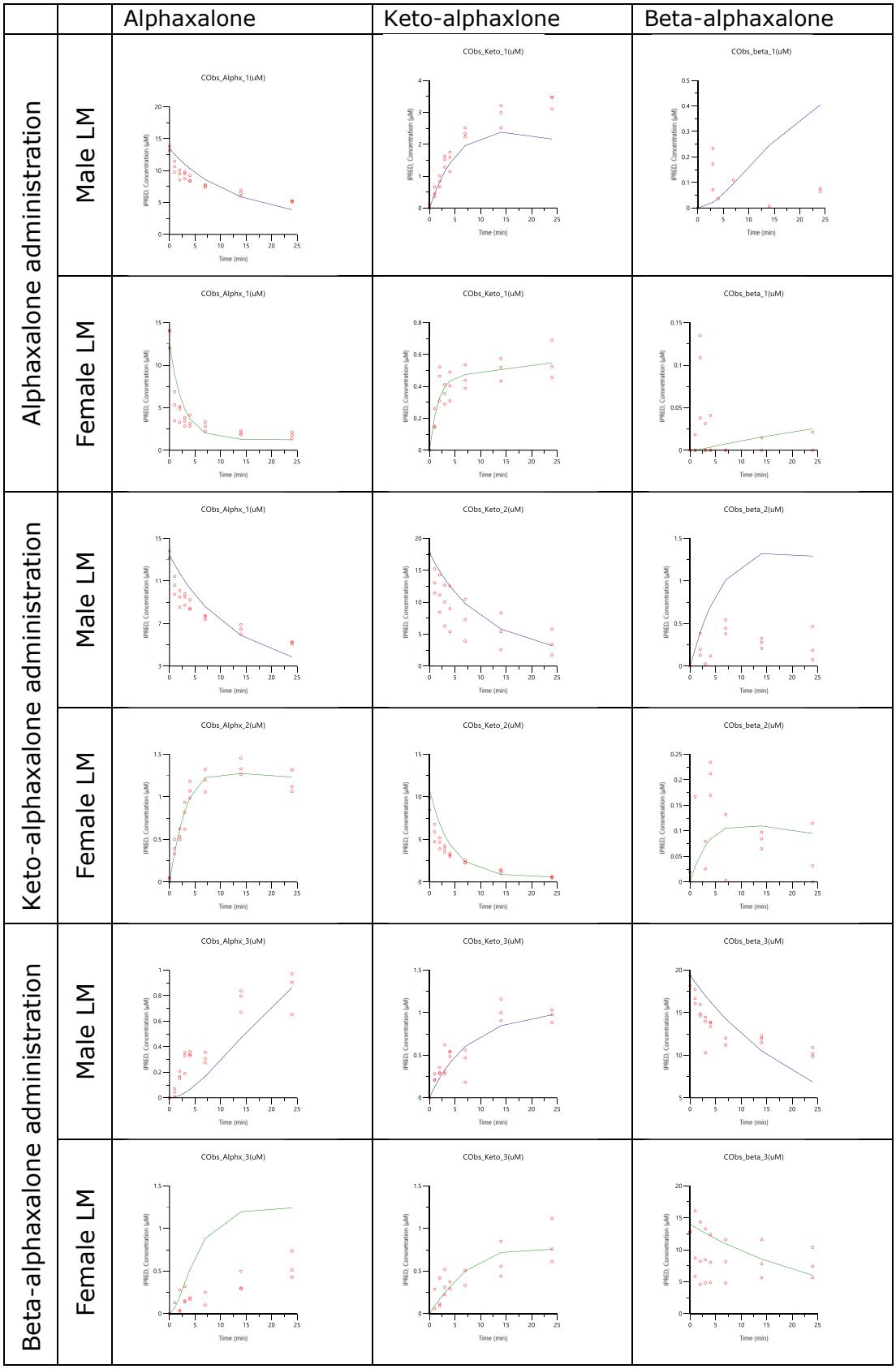

Figure 5.9. Model fit of alphaxalone, keto-alphaxalone and beta-alphaxalone concentrations from male and female dog liver microsomes. The Y axis repressnt substrate concentration (µM) while the X axis represent time (minutes).n=4 representative. Larger figure images are presented in figure 8.24, 25, 26.

Table 5.4. Estimated rate constants for alphaxalone metabolism and its metabolites in male and female dog liver microsomes.

Dog - liver microsomes		
	Alphaxalone	
	Male	Female
Parameter	**(min^{-1})**	
K_ak	0.036	0.022
K_ka	0.029	0.035
K_kb	0.013	3.21E-03
K_bk	6.82E-03	7.12E-03
K_0_a0	0.034	0.320
K_0_0a	0.013	0.039
K_0_k0	0.047	0.194
K_0_0k	8.15E-03	0.294
K_0_b0	0.038	0.028
K_0_0b	9.83E-03	5.73E-11

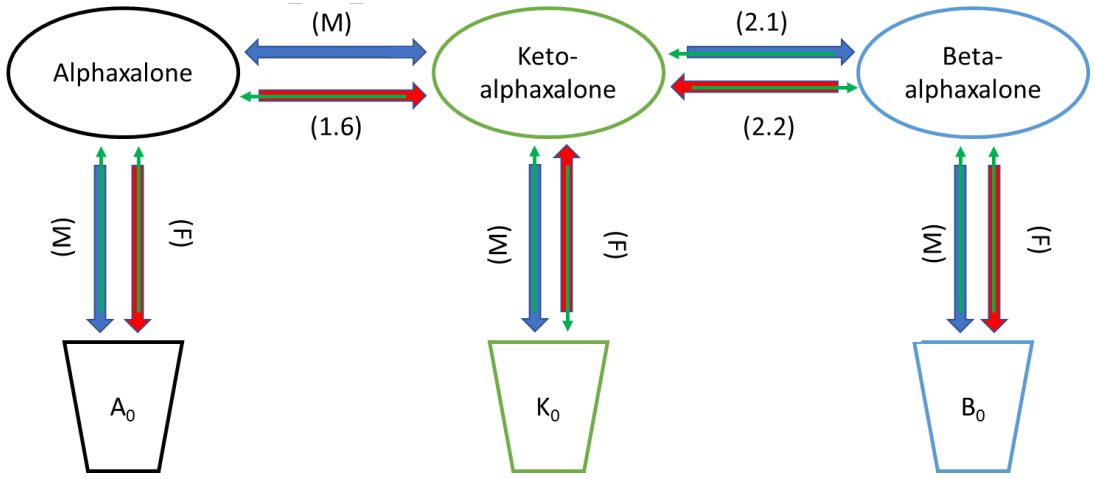

Figure 5.10. Alphaxalone metabolic pathway model fit for dog. The parameters estimated from the model are represented in the schematic. Blue and red arrows represent the male and female dominant metabolism direction. The green arrows are to show that the catalytic conversion of alphaxalone, keto- and beta-alphaxalone are modelled as unidirectional. The numbers above/bellow arrows represent the ratio of representative rate constants. The details of each directional rate constants are described in Figure **5.2**. The letters M and F represent male and female as the major metabolic direction.

5.2.1.5. Alphaxalone kinetic parameters for male and female rhesus monkey liver microsomes from model fit

The model gave the best fit to the data for alphaxalone and its metabolites in rhesus monkey (r^2>0.75) as shown in Figure 8.9 and Figure 8.10. However, the model gave a poor fit for alphaxalone formation from beta-alphaxalone substrate. A complete fitting of the data for each substrate for male and female is shown in Figure 5.11 and the estimated parameters for conversion rate constants in male and female rhesus monkeys are listed in Table 5.5.

There was no apparent difference in alphaxalone conversion rate constants between male and females for the following rate constants: K_ak, K_ka, K_kb and K_bk. In male and female monkeys K_ak and K_ka preferred the conversion toward keto-alphaxalone (K_ak) over the other. This was observable in the 3b-HSD enzyme system as the preferred conversion direction is toward keto-alphaxalone formation (K_bk) and was the major product formed.

For other elimination routes, both male and female elimination routes were negligible as the dominant direction of the equilibria K_0_0a, K_0_0k, K_0_0b ware several times larger than K_0_a0, K_0_k0, K_0_b0. A summary of the results is illustrated in Figure 5.12.

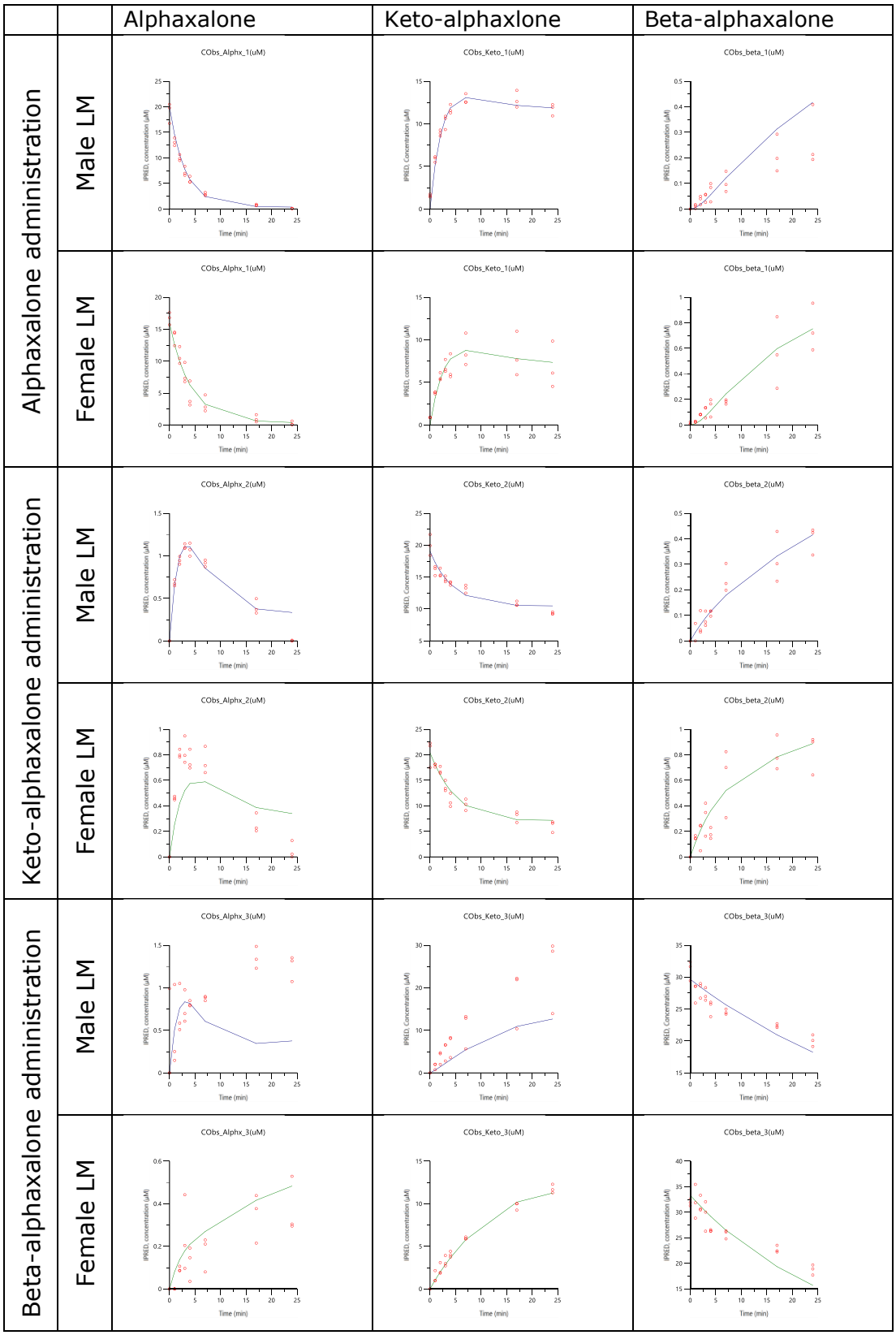

Figure 5.11. Model fit of alphaxalone, keto-alphaxalone and beta-alphaxalone concentrations from male and female monkey liver microsomes. The Y axis repressnt substrate concentration (μM) while the X axis represent time (minutes). n=4 representative. Larger figure images are presented in figure 8.27, 28, 29.

Table 5.5. Estimated rate constants for alphaxalone metabolism and its metabolites in male and female monkey liver microsomes.

Rhesus monkey - liver microsomes		
	Alphaxalone	
	Male	Female
Parameter	**(min^{-1})**	
K_ak	0.320	0.240
K_ka	0.010	0.011
K_kb	1.88E-03	5.98E-03
K_bk	0.021	0.034
K_0_a0	0.041	5.53E-03
K_0_0a	17.388	16108.516
K_0_k0	0.093	0.108
K_0_0k	0.149	0.102
K_0_b0	2.53E-10	5.68E-11
K_0_0b	0.046	0.518

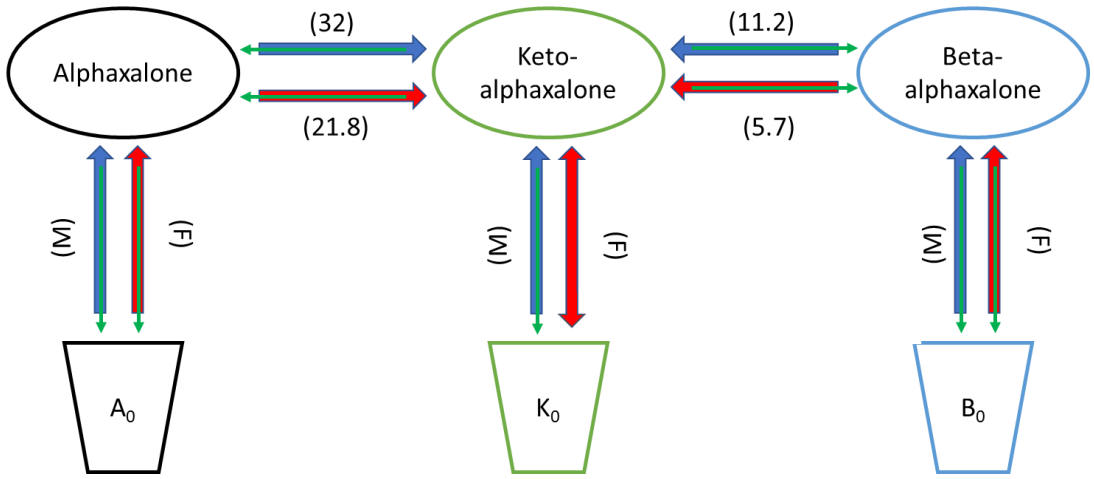

Figure 5.12. Alphaxalone metabolic pathway model fit for monkey. The parameters estimated from the model are represented in the schematic. Blue and red arrows represent the male and female dominant metabolism direction. The green arrows are to show that the catalytic conversion of alphaxalone, keto- and beta-alphaxalone are modelled as unidirectional. The numbers above/below arrows represent the ratio of representative rate constants. The details of each directional rate constants are described in Figure **5.2**. The letters M and F represent male and female as the major metabolic direction.

5.2.2. Metabolite investigation in other species

There were new additional metabolites detected upon investigating alphaxalone metabolism in human, rabbit, dog and monkey compared rat liver microsomes. These metabolites showed less prominent sex differences compared to rats. Furthermore, there were signs of species specificity in metabolite formations as more metabolite variety was detected compared to the major metabolites of alphaxalone found in rats.

Alphaxalone metabolism

The alphaxalone metabolites, beta and keto-alphaxalone, were detected at their distinct retention times in both genders for all the investigated species. However, the metabolite M3, which was more prominent in male rats, while it was too small to be significant in male and female humans. However, the metabolite was present in both genders to a certain degree in all other species (highest in rabbit). All metabolites observed are listed in Table **5.6** and the chromatography of all species' metabolites for males and females are shown in Figure 5.14 and Figure 5.15.

Two new metabolites (M4 and M5) (Figure **5.13**) were observed with the same MS/MS of alphaxalone. These metabolites were adjacent to alphaxalone and beta-alphaxalone with a retention time difference of 10 seconds. These metabolites were not noticeable in rats; however, they were observable in male and female of the other species except rabbits. Furthermore, another major metabolite observed in most species was M6 at 4.74 min. This metabolite was present in all species except rats and presented signs of sex differences in favour of females for human (Figure **5.14** and Figure **5.15**).

The Australian rabbits used in this study demonstrated a variety of alphaxalone metabolism. Some of these metabolites were unique to rabbits and were not seen in other species. The most unique metabolite was M7 (Figure 5.14 and Figure 5.15) which was more abundant in males compared to female rabbits. In addition, both male and female rabbits produced three additional metabolites, M10, M11 and

M12 however, female rabbits produced (based on signal) a larger concentration of these metabolites in comparison to males. On the other hand, male dog showed sex specific formation of M9 sited at 3.95 min which was not observed in the female dog. The rhesus monkey, however, formed M10 only in female while there were two small peaks of both M8 and M12 which were detected for both genders. A summary of all the detected metabolites and their comparison across the investigated species is listed in Table **5.6**

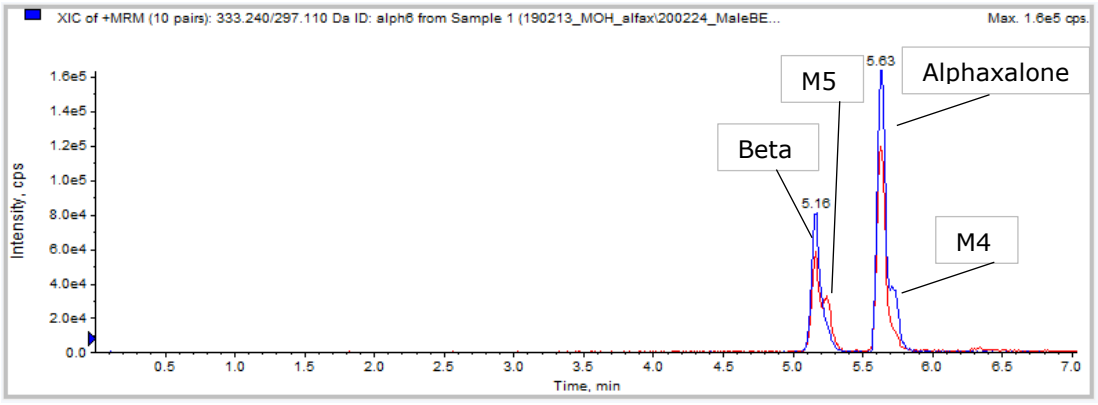

Figure 5.13. Alphaxalone chromatograph for male human. Two selective MS/MS channels for alphaxalone are shown. From the channels two new (M4 and M5) metabolites were detected.

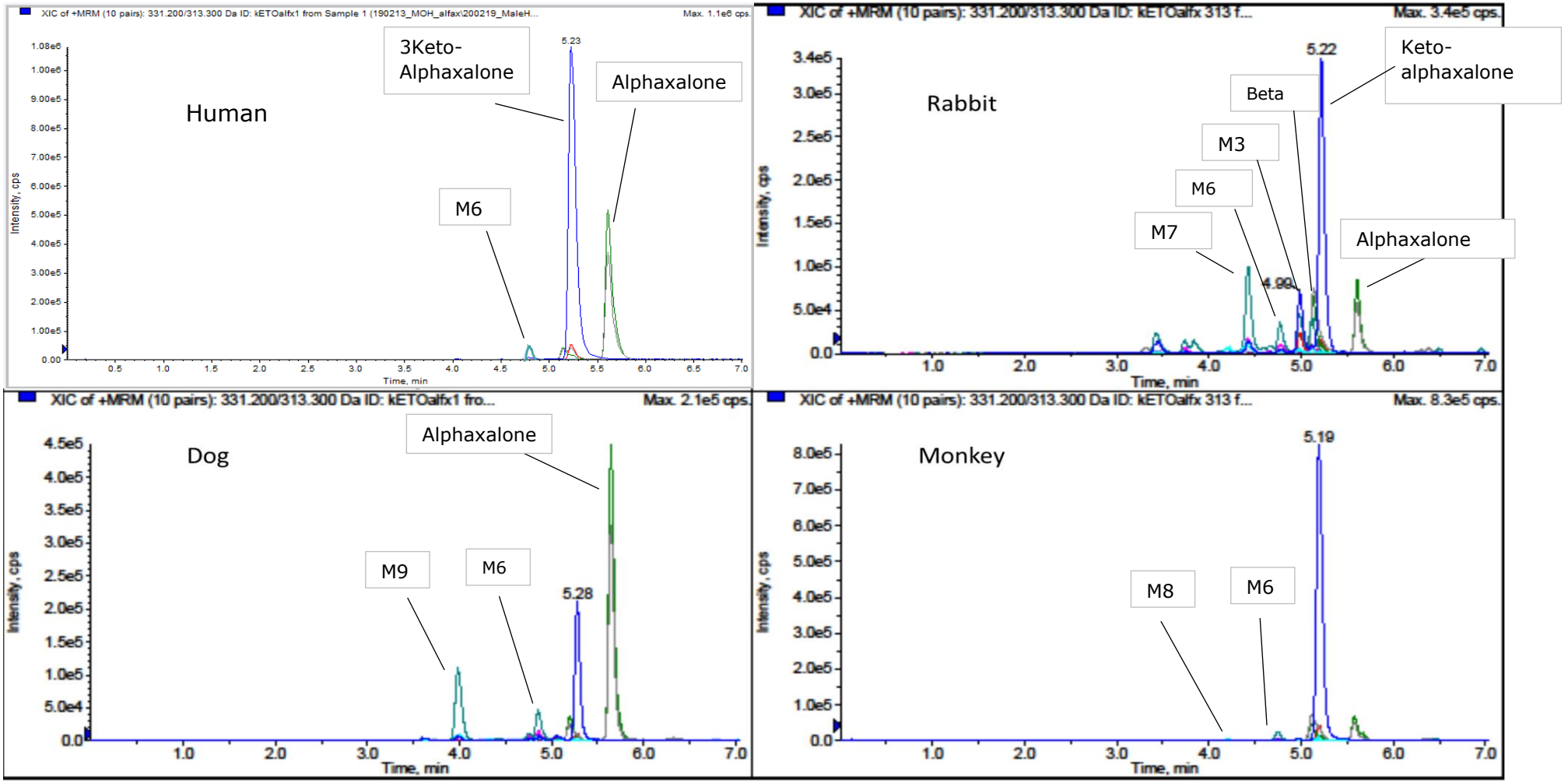

Figure 5.14: Comparison alphaxalone and its metabolites for male species. A Snapshot of the chromatography last time point of incubation. Different curve colours represent different ionisation channels (—) 331.2➔313.2, (—)331.2➔301.2, (—) 333.2➔297.2, (—) 333.2➔315.2, (—) 349.2➔331.2, (—) 349.2➔301.2.

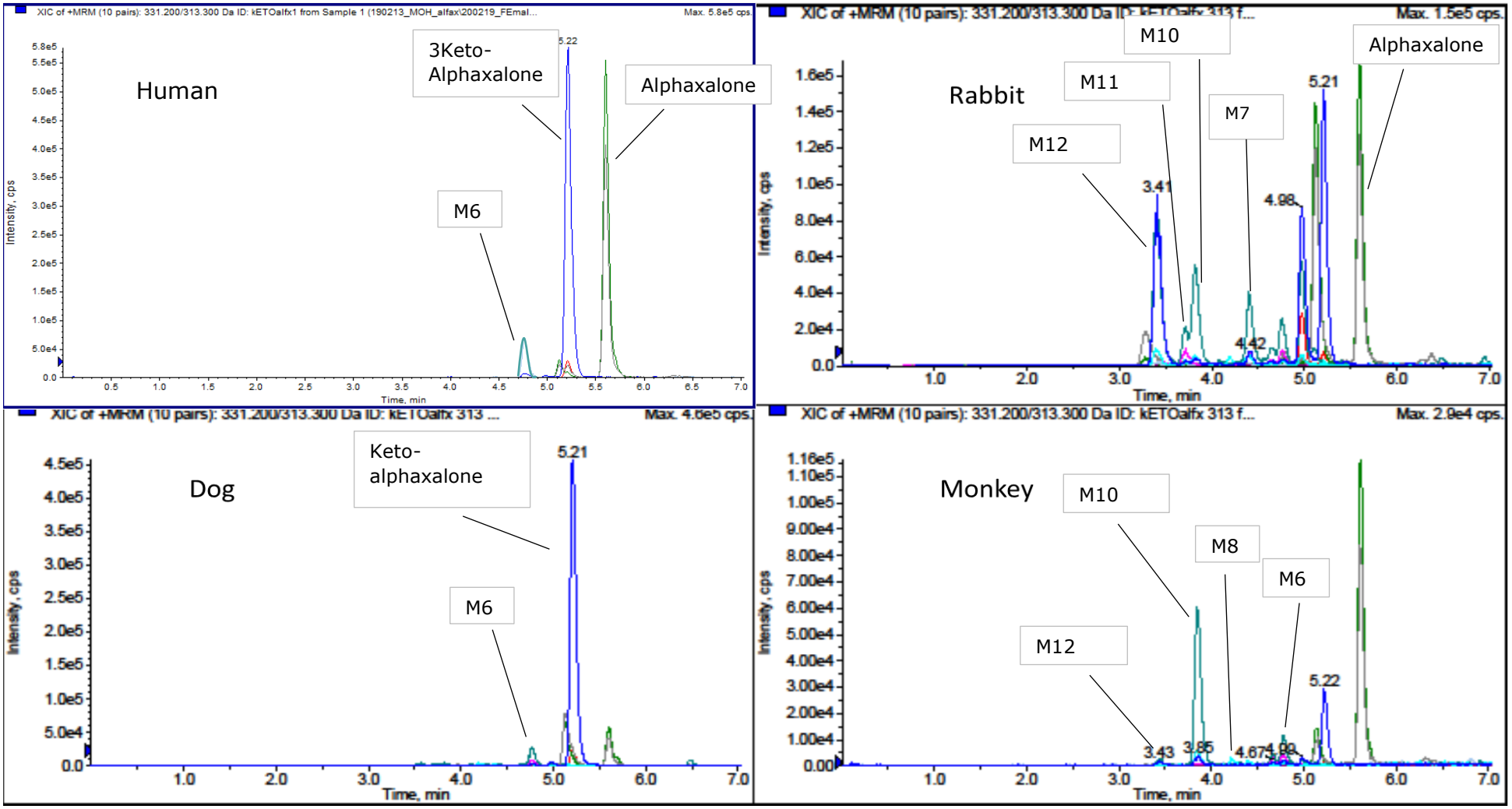

Figure 5.15: Comparison alphaxalone and its metabolites for female species. A Snapshot of the chromatography last time point of incubation. Different curve colours represent different ionisation channels (—) 331.2➔313.2, (—)331.2➔301.2, (—) 333.2➔297.2, (—) 333.2➔315.2, (—) 349.2➔331.2, (—) 349.2➔301.2.

Table 5.6: Alphaxalone and its metabolites in male and female of all species comparison.

Retention time	Alphaxalone and metabolites related	Male human	female human	Male rabbit	Female rabbit	Male dog	Female dog	Male Rhesus	Female rhesus
5.8, 5.7	alpha met (M4)	✔	-	✔	-	✔	-	✔	✔
5.6	alphaxalone	✔	✔	✔	✔	✔	✔	✔	✔
5.4	Keto met?	-	-	-	-	-	-	✔	✔
5.23?	beta met (M5)	✔	✔	✔	-	✔	✔	✔	✔
5.22	Keto-alphaxalone (M2)	✔	✔	✔	✔	✔	✔	✔	✔
5.1	Beta-alphaxalone (M1)	✔	✔	✔	✔	✔	✔	✔	✔
4.99	product X (M3)	small	small	✔	✔	✔	✔	✔	✔
4.74	M6 **MAJOR**	✔	✔✔	✔	✔	✔	✔	✔	✔
4.43	M7	-	-	✔✔	✔	-	-	-	-
4.31	M8	-	-	-	-	-	-	✔	✔
3.95	M9	-	-	-	-	✔	-	-	-
3.85	M10	-	-	✔	✔	-	✔	-	✔
3.7	M11	-	-	✔	✔	-	-	✔	✔
3.4	M12	-	-	✔	✔	-	✔	-	-

5.3. Discussion

Summary

The primary objective of the research was to investigate the alphaxalone metabolism pathway in liver microsomes across species in both genders. As seen from chapter 3 alphaxalone demonstrated sex-dependent PK in rats which consequently led to reducing the female administration dose in order to have similar plasma concentrations between genders and reduce the observed side effects (cardiovascular inhibition). In chapter 4, alphaxalone clearance was able to be closely extrapolated from *in vitro* to *in vivo* clearance, which indicates that alphaxalone metabolism occurs mainly in the liver. Understanding the metabolism pathway of alphaxalone is essential to deconvolute the sex bias in the metabolic pathway, if present, in other species as was observed in rats.

Kinetic Model

The alphaxalone metabolic pathway kinetic model was a simple model that fits concentration versus time data giving estimates of the conversion rate constants which ultimately determines the dominant direction of metabolite formation for the investigated species. The model accounts for alphaxalone, keto-alphaxalone and beta alphaxalone interconversion as well as elimination of these to any unidentified ones. Furthermore, it was based on the supposition that there is no noticeable species diversity as reported by Warne *et al.* (2015) group.

The model was able to fit most of the species data, however, there was poor fitting associated with beta-alphaxalone elimination. This was very apparent in male rabbit where beta-alphaxalone disappearance, produced from either alphaxalone or keto alphaxalone as initial substrates, was significantly greater than disappearance from beta-alphaxalone as initial substrate. This led to the model underestimating beta-alphaxalone disappearance when produced from either alphaxalone or keto alphaxalone as initial substrates. The slower rate of metabolism for beta-alphaxalone as initial substrate may be a result of metabolic

enzyme saturation as there was evidence that the beta-alphaxalone concentration was measured to be two-fold larger than the nominal starting concentration (15μM) for human and rabbit. This is more likely to be an error in the amount administered to the liver microsomes rather than an error in the quantification process as the remaining species did not have an extreme initial beta alphaxalone concentration.

Furthermore, due to the limited amount of liver microsomes for each species, all of the initial substrate concentrations used were selected based on a value below the alphaxalone K_m determined in rats. Studies in the literature often use a single substrate concentration without knowing the K_m of the substrate. A typical concentration of 1 μM is commonly used and assumed to be below the K_m concentration. However, alphaxalone and its metabolites do not have good sensitivity when analysed, and as the secondary objective was to observe alphaxalone metabolites produced for each species and sex, a higher initial nominal concentration of 15 μM was used.

Furthermore, surprisingly there was a hint of alphaxalone present as a product formed from beta-alphaxalone as the initial substrate ranged from 0.5-1 μM at time zero in human liver microsomes. This might be an endogenous peak present from the beta-alphaxalone substrate as the authentic sample of beta-alphaxalone was reported to have 90% purity. This may explain the presence of higher than expected alphaxalone concentrations due to the presence of alphaxalone in the beta-alphaxalone substrate for the human liver microsome experiment.

Alphaxalone metabolism

Male rats showed a faster conversion rate of alphaxalone to keto-alphaxalone and beta-alphaxalone compared to the females. In addition, the males demonstrated a significantly faster rate of alphaxalone elimination (K_0_a0) compared to female rats. Furthermore, both 3α-HSD and 3β-HSD showed directional preference for

each species. For example, in human and monkey experiments both species showed conversion preference of 3α-and 3β-HSD enzymes toward K_ak and K_bk (keto-alphaxalone formation), which was observed in both sexes. Furthermore, in rats, the conversion preference of those enzymes was sex dependent as male rats K_ak was the major conversional direction while in females it was the opposite (K_ka). This similar behaviour was only observed in dogs as 3β-HSD demonstrated sex dependent conversional direction. Sex differences in dog metabolism has been observed before (Chen et al., 2017) where female beagles showed slightly slower clearance and had higher plasma concentrations of metapristone compared to males. However, in our study the female dogs exhibited faster alphaxalone metabolism compared to the males.

Furthermore, the male rats had an overall faster conversion rate of 3α-HSD in both directions compared to females which was also apparent in female human. This was originally thought to be related to male rats having larger enzyme expression. However, this is unlikely as females have been reported to have 2-3 fold higher expression of 3α-HSD enzyme than male rats (Stolz et al., 1991); while 3β-HSD is 5.8 fold higher in male rats (Naville et al., 1991). Thus, it is more likely to be related to the enzyme isoform, as it has been shown that type -II and type-III of 3α-HSD can catalyse in a single direction and bidirectional respectively (Griffin & Mellon, 1999). This may be the case in some species as rabbits and dog were hardly able to form the beta-alphaxalone metabolite, but were able to convert beta-alphaxalone to keto-alphaxalone.

Species metabolism of alphaxalone

The formation of beta-alphaxalone was not as prominent in female rats compared to male. However, species who were not able to utilise 3β-HSD enzyme were able to eliminate alphaxalone by alternative pathways. For example, rabbits (both sexes) demonstrated quite an extensive ability to metabolise alphaxalone and create the most varied array of metabolites for the investigated species.

Furthermore, several metabolites of alphaxalone have been detected and were common in all species, whilst some of them were species specific such as metabolite M7 and M8 as each of them were exclusively detected in both sexes of rabbits and rhesus macaque liver microsomes, respectively. Alternatively, M10, M11, M12 were female dominant in female rabbits and rhesus macaque.

Metabolite identification issues

Identifying each metabolite formed from alphaxalone is quite a complicated objective. Due to alphaxalone sharing the steroid scaffold and all living beings are naturally adapted to metabolise these endogenous steroidal compounds, alphaxalone is prone to metabolism at similar sites. The major phase-I reactions for steroids are the interconversion of the hydroxy-keto groups by HSD enzymes (oxo-reductase enzymes) and additional hydroxylation by CYP450 enzymes (Schiffer et al., 2019).

With the exception of keto and beta-alphaxalone formation, most of the herein observed metabolites for each species were some type of alphaxalone hydroxylation product as evidenced by an increase of 16 mass units on the protonated alphaxalone mass ($M+H^+$+O). Using testosterone as an example of steroid metabolism, it was reportedly able to be hydroxylated in several places, such as, 2α, 2β, 6β, 7α, 15β, 16α, 16β positions (Pasanen, 2004; Schänzer, 1996). Alphaxalone has been reported to form keto-alphaxalone, 3β-alphaxalone, 20-hydroxy-alphaxalone and 20-hydroxy-3β-alphaxalone as well as 2α-hydroxy-alphaxalone in cats and dogs (Warne et al., 2015). However, based on the number of hydroxylated metabolites of testosterone, it is more likely that there are more hydroxylated forms of alphaxalone than currently reported.

Delta retention time and application to chromatography for identifying metabolites and diastereomers

For each oxidation/reduction reaction or hydroxylation process, the introduced functional group can be either in α or β position based on what enzyme is involved. Thus, there is a higher potential of more diastereoisomer metabolites of alphaxalone to be present. An example of an alphaxalone diastereoisomer is the interconversion of alphaxalone and 3β-alphaxalone by 3α-HSD and 3β-HSD enzymes via 3-keto-alphaxalone. Each different diastereomer can have different physio-chemical properties which can affect their retention time on a HPLC as observed for 3β-alphaxalone. This metabolite, although identical in structure to alphaxalone except for the spatiality of the 3-hydroxy group, has a different retention time and appeared at an earlier time point to alphaxalone. However, it is not feasible to extrapolate the difference in retention time (Δ Rt) between this diastereoisomer pair in this example and apply it to other potential alphaxalone diastereomers as the differences in physio-chemical properties may be different for each diastereomer metabolite (Kanie et al., 2016).

Stereochemistry may either enhance or inhibit enzyme activity

Another layer of complexity for identifying the alphaxalone metabolism pathway is that having the right stereochemical configuration can be either the final metabolism product or it can create the possibility of an additional oxidation process. For instance, the reduction of the 3-keto position is entirely dependent on the hydrogen configuration at the 5 position (α or β). Steroid metabolism enzymes are able to reduce the 3-keto to either 3α or 3β Hydroxy metabolites, however, only the 3α Hydroxy metabolite can be formed when the hydrogen is located at the 5β position as shown in Figure 5.16 (Schänzer, 1996; Schiffer et al., 2019). On the other hand, the unfavourable conformation 3β5β steroid structure does not allow binding in the 3β-HSD enzyme's active site making metabolism unfavourable to occur. This dual catalytic reaction may have happened for some

of the alphaxalone metabolites as retention times appeared at 1-2 minutes earlier than alphaxalone and the other metabolites, which may hint that they are more hydrophilic.

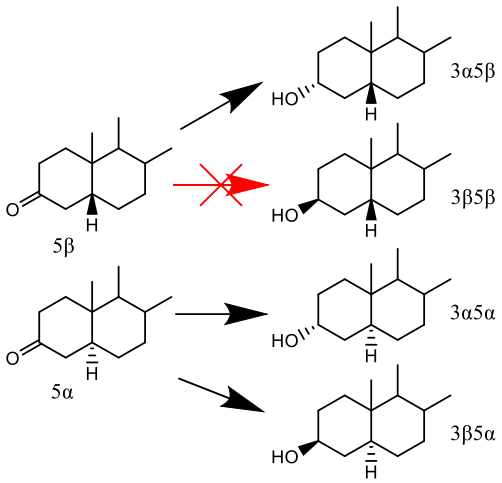

Figure 5.16: Steroid A-ring reduction scenarios. The formation of 3β,5β-tetrahydro metabolites is sterically unfavourable. While the other pathways can possibly occur.

The endogenous steroids can have hydroxylation reactions at several positions and in some cases, there can be more than one hydroxylation reaction for a single product. For instance, progesterone, which is a neurorsteroidal precursor, can metabolise and produce pregnanetriol, (5β-pregnan-3α,17α,20α-triol) which has two hydroxylations (Schiffer et al., 2019). Moreover, this change in compound polarity will affect the retention time and compound-column interaction. The detection of the new alphaxalone hydroxylated metabolites was inferred and based on a single hydroxylation alphaxalone mass ($M+H^+$+O). However, this does not preclude the presence of dual hydroxylated metabolites as there is the possibility of dual hydroxylated metabolites losing their second hydroxy group through loss of water if harsh conditions were used in the mass spectrometer. Steroids in general are known to be difficult to ionise due to the lack of acidic or basic groups in their structure, which makes them challenging for detection and quantification without an additional ionising adduct (Pozo et al., 2007). In addition, to improve the ionisation of alphaxalone and enhance its signal sensitivity a harsh mass spectrometry condition was used. Losing water from steroid compounds in the

mass spectrometer is common and was very noticeable for the alphaxalone analysis process as there were several mass fragments of alphaxalone with m/z associated with loss of water ($M+H^+$-H2O) using an aggressive method. This, however, should not affect the chromatographic separation as the retention time of each peak is affected by molecule lipophilicity before reaching the mass spectrometer. Hence, there is the possibility of dual hydroxylation occurring in alphaxalone metabolism.

Chapter 6:

General discussion

6. Chapter 6: General discussion

Brief introduction

There will be always a requirement for a new anaesthetic drug to be used in clinical practice. The ideal anaesthetic agent needs to have both anaesthetic (hypnotic) and analgesic effects as well as having a predictable outcome with minimum side effects. Unfortunately, drugs with dual characteristics are rare at present and typically two different administrations (analgesic and hypnotic) are required. Nevertheless, the search for the ideal agent is still in progress.

Alphaxalone is a neurorsteroidal agent, which is a unique drug class that binds to $GABA_A$ receptors. Alphaxalone resembles hormonal steroids but has negligible nuclear hormone receptor activation effects. It has been reported that alphaxalone does not exhibit severe side effects or tachyphylaxis in comparison to barbiturates and benzodiazepines agents. This may be due to its unique binding location in comparison to other drugs that bind to the same receptor type. Furthermore, the interest in alphaxalone has been rekindled with the introduction of a new safer formulation.

Alphaxalone has been reported to demonstrate sex dependent behaviour that was initially thought to be related to its pharmacodynamics (Fink et al., 1982). However, more recently it has been shown to be due to pharmacokinetic differences (White, *et al.*, 2017). This thesis aimed to identify the source of the pharmacokinetic sex differences observed in rats while also investigating any sex differences in other species where alphaxalone is licensed or being under investigation for licensing considerations.

PK modelling

The initial analysis of the alphaxalone PK data from the *in vivo* experiments was done by fitting a one compartmental model to individual animals. At this stage, the sample size was too small to be considered for a population PK model approach as the individual fitting is ideal for a small number of subjects. Population PK

modelling is a powerful analytical tool to understand a population as a whole but also individually. The model understands and shares the information between each subject and determines the population PK parameters and interindividual variability within the population (Mould & Upton, 2013). Therefore, utilising popPK modelling can help in understanding sub-group differences that have a limited number of samples in a population, when the data is incorporated in a larger group population PK model. For such reasons, other alphaxalone *in vivo* data publications were considered to be added to the present alphaxalone model. However, the popPK model requires accurate information on dosing and measurements as it is only as good as the data it is based on (Upton & Mould, 2014). Therefore, having access to the raw data from White, *et al.*, (2017) made it feasible to include, whereas adding additional subjects from other groups such as Visser and Lau groups, was not feasible due to the limited access to raw data.

Alphaxalone *in vivo* plasma samples were limited to 8 samples for each rat so as to not exceed 10% of the total rat blood volume. Furthermore, there was a considerable time gap for alphaxalone sampling between samples 6 and 7. The sampling decision was made based on the assumption that alphaxalone concentrations would reach steady state by 120 minutes of continuous infusion. In addition, there was an electrophysiological experiment that started after 120 min which limited the sampling afterwards. The male Lewis rats were behaving as expected, however, female Lewis rats were metabolising alphaxalone at a slower rate to their female SD counterparts as reported by (White, *et al.*, 2017). This made samples 6 and 7 the most impactful for an adequate individual fit and PK parameter estimates, while the last time point (sample 8) was less relevant due to the infusion reduction phase. Consequently, the presence of a quantification error on samples 6 and 7 or the absence of these samples will greatly impact the estimating capability of the individual fits. On the other hand, the population PK model will fit all of the rats simultaneously and supplement any missing samples using data from other subjects. The resulting functional model, with the lowest

objective function, will describe the influence of covariates on the typical parameter values within the population. The influence of time points 6 and 7 can be decreased by distributing alphaxalone plasma time points evenly. However, this approach would require the removal of the electrophysiological experiment component or will interfere with its reading. Alternatively, the approach taken herein was to remove the alphaxalone infusion reduction step which added more weight to the last sample (No. 8) in the PK model fit.

Furthermore, we were proud to comply to the guidelines of the three Rs: replacement, reduction and refinement that was first introduced by Russel and Burech in 1959 for the principles of humane experimental technique (Fenwick et al., 2009). According to the guidelines, scientists must replace the use of animals with other techniques, reduce the animals used and refine the way the experiments are carried in order to reduce animal suffering. Thus, in this perspective, we aimed to reduce the number of animals needed for the alphaxalone *in vivo* study and make the most of the animals for several research end points simultaneously. The three R's compliance was also accomplished for the preparation of rat hepatocytes, S9 fraction and liver microsomes by using the same animal to minimise the number of animal sacrifices.

popPK conclusion

The conclusion of the large population set model was that sex and weight were the most significant covariates that impacted on alphaxalone clearance in rats. Age of rats can also be considered as a covariate in popPK models as it has been reported to impact on the metabolic enzyme expression within the liver due to the effect of sex hormones on metabolic enzyme regulation (Waxman & Holloway, 2009). Sex and age are correlated with rat body weight; however, age and body weight correlate with each other in a continuous manner which makes them difficult to deconvolute. While sex and body weight have weaker correlation for each other, the presence of sex hormones can have influence on the overall

growing potential of the rats. However, the presence of either testosterone or progesterone can influence the expression of metabolic enzymes and is not dependent on body weight in a non-weight related behaviour (Martignoni et al., 2006). This was evident in our investigation as male Lewis rats and female SD rats did not have a significant weight difference. However, the male rats showed a faster rate of alphaxalone metabolism compared to the female SD rats.

Strain as covariate was considered significant in the small set pop pk model as the female Lewis rats had a significantly slower alphaxalone clearance compared to female SD rats. It has been reported that there are strain differences in the expression of metabolising enzymes in rat, with SD rats having higher expression of CYP450 enzymes compared to Lewis rats (Nishiyama et al., 2016). In fact, the female Lewis rats had the highest alphaxalone exposure compared to all rat groups and experienced a significant inhibition of arterial pressure. Furthermore, as alphaxalone clearance is significantly influenced by blood flow, a reduction in cardiovascular output could decrease liver blood flow further decreasing alphaxalone clearance and enhancing the cardiovascular inhibition effect due to higher plasma concentration. A possible alternative theory for the cause of the observable strain difference in female rats, is that alphaxalone plasma concentrations have reached the saturation concentration of the metabolism enzymes in the female Lewis rats. There is some evidence to support this as K_m values determined in female rat hepatocytes were comparable to the highest free alphaxalone plasma concentrations observed in section 3.2.1 above.

However, the conclusion of the large set popPK model was slightly different to the smaller set as more subjects were incorporated and resulted in body weight becoming more influential as a covariate than strain. The reason for this may be due to the larger set model having a wider body weight distribution range compared to the narrower range in the small set model. Furthermore, the larger population sample mainly consisted of SD rats while the contribution from Lewis

rats to the population was 2-3 fold lower (i.e. 8 vs 24 female Lewis and SD respectively). This may be an alternative factor that overshadowed the strain impact in favour of weight. Fortunately, PK population analysis can be enhanced with more rat subjects from later studies in the future to complement any imbalances. Moreover, the number of subjects is crucial for population modelling as the small model gave a very large SD for the outputted clearance values when compared to both the large set popPK model and the individual fit. Furthermore, the larger set model was more consistent with the parameters estimated by PK individual fits.

Optimisation of liver hepatocyte isolation in rats and IVIVE

It was crucial to develop a valid method for the isolation of hepatocytes in rat as the use of freshly isolated rat hepatocytes generally provides better *in vitro* data in comparison to sub-cellular fractions or liver slices for either quantitative or qualitative predictions of *in vivo* metabolism (Chiba et al., 2009).

As clearance prediction is a key component in drug discovery several groups have reported that IVIVE using either human or rat hepatocytes/liver microsomes has a tendency to under predict by 2-5 fold even with the use of empirical corrections (Wood, *et al.*, 2017). The exact reason for under-prediction is still not clear, however, explanations for this behaviour have focused on physiological scaling and plasma protein binding inaccuracies which mostly address *in vitro* methodological behaviour (Francesca L Wood et al., 2018). However, it has been reported that hepatocytes display spatial heterogeneity along the porto-central axis of the liver lobule between peripheral and pericentral sinusoids (liver zonation) (Kang et al., 2018). This in addition to the presence of hydrostatic pressure from blood flow, which is lacking *in vitro* causes morphological and CYP expression changes (Burton et al., 2020). These new findings contradict the main assumptions used for both the WS and PT models. For instance, the parallel tube

model, which assumes the liver is composed of parallel tubes surrounded by hepatocytes of equal metabolic capacity is inconsistent with liver zonation.

Nevertheless, both the WS and PT mathematical liver models generated good estimates of rat *in vivo* clearance with the PT model predicting slightly better than the WS model. This is not surprising as alphaxalone has a high extraction ratio and is in agreement with several reports where the PT model shows better accuracy than the WS model for highly cleared drugs (Ito & Houston, 2004). However, this may not be the case for drugs with low clearance.

Microsomal preparation and IVIVE

Due to the exotic nature of the chosen species the availability of cryopreserved hepatocytes were quite limited and present costs also limit the number of studies possible. While liver microsomes are cheaper and more widely available for exotic species compared to hepatocytes. As mentioned previously liver microsomes lack the presence of activating cofactors and therefore require external supplementation. However, using liver microsomes for *in vivo* clearance prediction is not quite reliable as it has been shown that the intrinsic clearance of several phase-I drugs and probes from liver microsomes can under-predict *in vivo* clearance by up to 4 fold in comparison with hepatocyte suspensions from the same donor (Foster et al., 2011). The reason for this may be due to the lack of cellular integrity and presence of certain enzymes and transporter activities as a result of the preparation process of the liver microsomal proteins which can influence the microsomes activity (Ito & Houston, 2004). Furthermore, the hydroxy group at C_3 of alphaxalone is able to be metabolised to both sulphated and glucuronidated metabolites in cats and dogs (Warne et al., 2015). Therefore, it is more than likely that other species are able to metabolise alphaxalone through phase II enzymes as well. Although, phase II conjugation metabolism can be carried out using microsomes, it was only applied for qualitative purposes for the

herein research in rat. Therefore, *in vivo* clearance predictions from liver microsomes for the investigated species (chapter 5) were not conducted.

Alphaxalone sex differences in liver microsomes

Rat and dog showed sex differences for the disappearance of alphaxalone in liver microsomes while the remaining species did not show apparent sex differences. The sex differences in dog were less profound in comparison to the rat. This may suggest that dogs will show sex differences in alphaxalone exposure level from *in vivo* clinical studies. However, the *in vitro* conclusion for dog is not in agreement with what has been reported for dog in the clinic where there was no sex difference observed for alphaxalone plasma exposure between male and female beagle dogs (Ferré et al., 2006).

The reason for no significant alphaxalone sex difference in the clinic for dog and possibly other larger species may be that for ultra-rapidly cleared drugs such as alphaxalone the rate of liver clearance will be limited by liver blood flow. Having a higher liver blood flow can give more leverage for the liver drug metabolism process compared to lower blood flow. The rate of liver blood flow varies from one species to another, as there is an inverse correlation between liver blood flow and species size. It ranges from 85, 60, 45, 30, 21 ml/min/kg for rat, monkey, dog and human respectively (Balabaud, *et al.*, 1975; Ward *et al.*, 2004).

Figure 6.1 below shows the relationship between liver blood clearance and liver intrinsic clearance for different species as described by the well stirred model (WSM). Initially, as the liver intrinsic clearance increases the liver blood clearance increases proportionally. However, blood flow restrictions start to limit liver clearance when intrinsic clearance becomes large. Human, has the smallest blood flow when expressed in ml/min/kg (21 ml/min/kg) among the species shown in Figure 6.1. Therefore, human liver blood clearance will restrict towards blood flow at a lower intrinsic clearance compared to species with larger blood flows such as rat. The vertical dashed lines in Figure 6.1 represent liver intrinsic clearance values

of 50 and 150 ml/min/kg. For, human the corresponding liver blood clearance for this intrinsic clearance range hardly changes and approximates to human blood flow. On the other hand, rat liver clearance almost doubles when intrinsic clearance increases from 50 to 150 ml/min/kg. Therefore, a difference in the *in vitro* intrinsic clearance for alphaxalone between male and female humans may not result in any significant *in vivo* clearance difference. As seen from Chapter 4, a 5 fold increase in intrinsic clearance for male compared to female rats resulted in only a 2.5 fold increase in the estimated blood clearance.

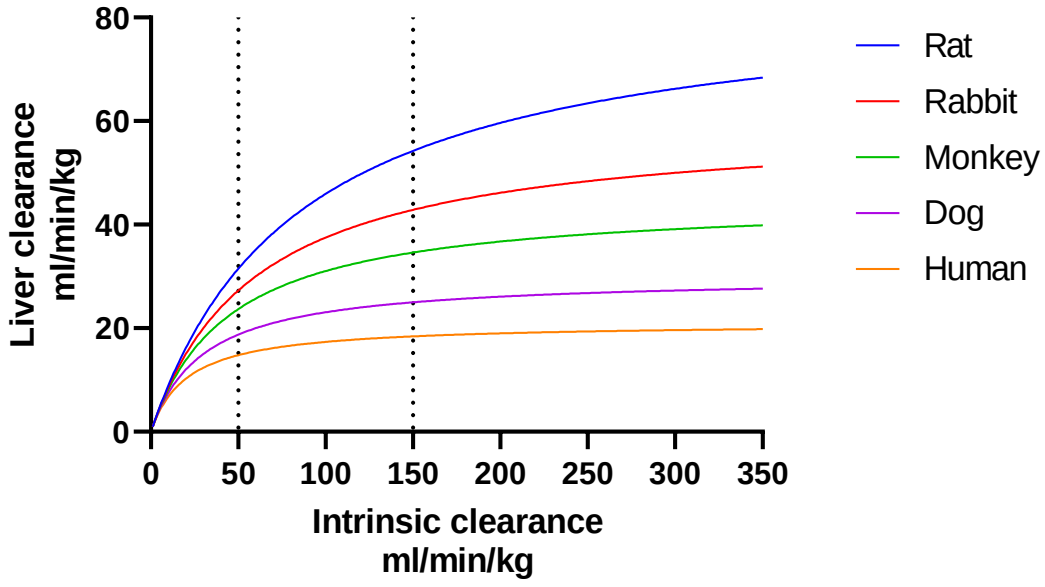

Figure 6.1. Representation of liver blood clearance across species based on different liver blood flows for the same liver intrinsic clearance.

Determining the alphaxalone metabolic pathway is important in understanding the mechanisms that lead to the sex differences for alphaxalone elimination. In addition, understanding the metabolic pathway can give clues to potential drug-drug interactions (DDI) that may happen if adjunct drugs were to be administered with it. Alphaxalone administration is typically administered in combination with pre-medication subjects and therefore, the chance of a DDI is higher. For instance, the diversity of alphaxalone metabolism pathways was limited in rats as not too many variations of metabolites were produced. The major product was an oxidised form of alphaxalone (M3) which was dominant in male compared to female rats.

This metabolite formation was inhibited using a specific CYP 3A1 enzyme inhibitor (Clotrimazole) which solidified the hypothesis of being formed by this enzyme. The use of adjunct agents that are mainly metabolised by CYP 3A1, such as fentanyl with alphaxalone, (Arenillas & Gomez de Segura, 2018; Feierman, 1996) can interfere in either/both of their metabolism pathways in males but may not be present in female rats.

The extent and variation of the metabolites formed from male and female of each species was different. Alphaxalone metabolites observed from rabbits in general and from female more specifically were the most diverse among the species. Since alphaxalone shares the steroidal scaffold, it is more likely to be metabolised in a similar manner to steroidal hormones. Unfortunately, there is limited data available for alphaxalone metabolism as well as endogenous steroid biosynthesis and metabolism in rabbits or monkeys. However, rabbits appear to be able to metabolise alphaxalone more profoundly in comparison to the other tested species.

Two major classes of enzymes are involved in the biosynthesis and metabolism of all steroidal hormones: the cytochrome p450 and hydroxysteroid dehydrogenase enzymes. Testosterone, which is closely similar in structure to alphaxalone, has been extensively used for metabolic and biosynthesis studies across species and showed several potential hydroxylation locations (Pasanen, 2004) which might also occur for alphaxalone. The hydroxylation process was shown to be occurred on many sites for testosterone in man, rat, rabbit, and dog, thus, these sites of hydroxylation may also be possible for alphaxalone. However, the rate and preferred pathway of steroid metabolism might range depending on sex and species (Bogaards et al., 2000). A proposed map for alphaxalone metabolism via the oxidation processes that testosterone undergoes is shown in Figure 6.2.

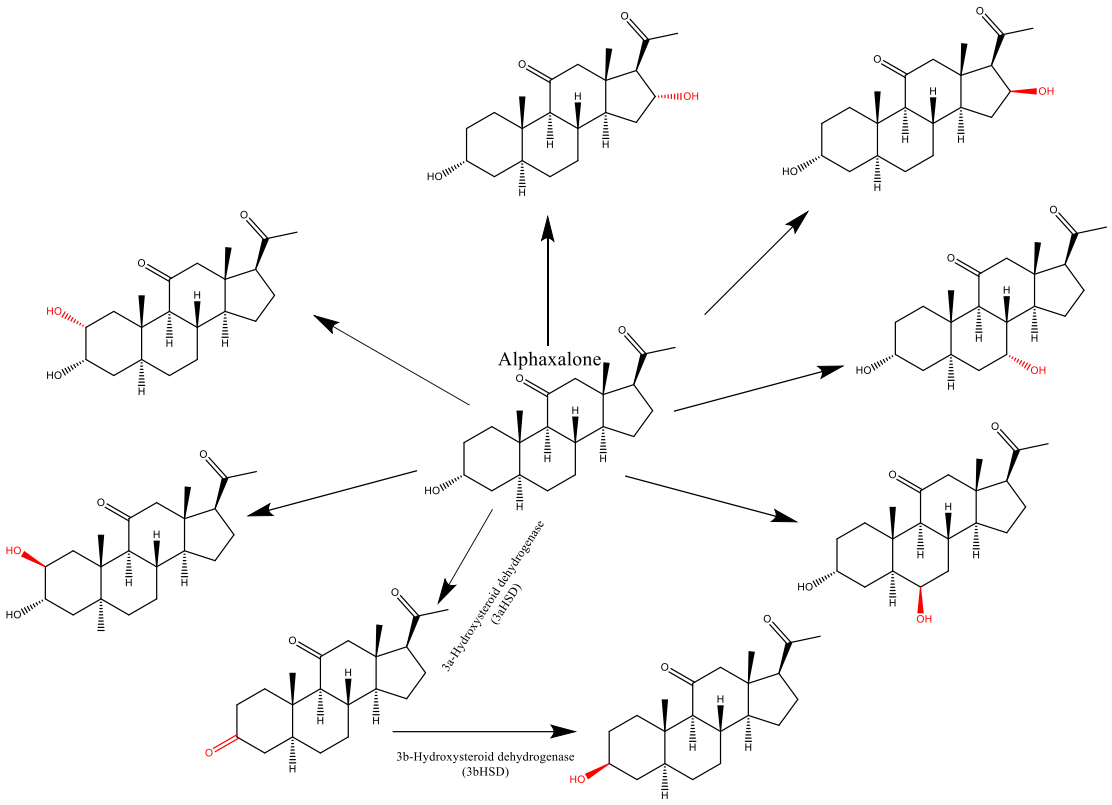

Figure 6.2. Alphaxalone metabolism pathway. A proposed metabolic pathway illustrates some of alphaxalone metabolites that can be formed.

Future work

Alphaxalone generated several significant metabolites which were present in several species. Estimating the relative metabolite pathway impact was not possible in the herein study, however, it can be done in the future if the observed metabolite appeared in a linear manner. In the present study the analytical process did not include a single ion scan, due time restrictions, which can help in identifying the total molecular mass of the metabolites that has not been identified. This analysis can be used for the purpose calculating the metabolite formation rate which can greatly enhance our knowledge of alphaxalone metabolism and to elucidate which metabolic pathways are used via each species. Furthermore, the use of individual recombinant enzymes can also help to determine which specific enzymes are associated with specific metabolites. Choosing which specific CYP450 recombinant enzymes for future experiments is difficult, however, selection based on what has been observed in steroidal hormone metabolism would be a good starting point. Furthermore, adjunct analytical techniques such as LC-NMR-MS (liquid chromatography – nuclear magnetic resonance – mass spectrometry) can be used affording a comprehensive structural analysis including the exact site of oxidation for the metabolites.

7. List of references

Aarons, L. (1991). Population pharmacokinetics: theory and practice. In *J. clin. Pharmac* (Vol. 32). https://doi.org/10.1111/j.1365-2125.1991.tb03971.x

Andaluz, A., Felez-Ocaña, N., Santos, L., Fresno, L., & García, F. (2012). The effects on cardio-respiratory and acid-base variables of the anaesthetic alfaxalone in a 2-hydroxypropyl-β-cyclodextrin (HPCD) formulation in sheep. *The Veterinary Journal*, *191*(3), 389–392. https://doi.org/10.1016/j.tvjl.2011.03.017

Anderson, G. D. (2002). Sex differences in drug metabolism: cytochrome P-450 and uridine diphosphate glucuronosyltransferase. *The Journal of Gender-Specific Medicine : JGSM : The Official Journal of the Partnership for Women's Health at Columbia*, *5*(1), 25–33. http://www.ncbi.nlm.nih.gov/pubmed/11859684

Anderson, G. D. (2005). Sex and racial differences in pharmacological response: where is the evidence? Pharmacogenetics, pharmacokinetics, and pharmacodynamics. *Journal of Women's Health (2002)*, *14*(1), 19–29. https://doi.org/10.1089/jwh.2005.14.19

Arenillas, M., & Gomez de Segura, I. A. (2018). Anaesthetic effects of alfaxalone administered intraperitoneally alone or combined with dexmedetomidine and fentanyl in the rat. *Laboratory Animals*, 1–11. https://doi.org/10.1177/0023677218764214

Arnold, A. P., & Burgoyne, P. S. (2004). Are XX and XY brain cells intrinsically different? *Trends in Endocrinology and Metabolism: TEM*, *15*(1), 6–11. http://www.ncbi.nlm.nih.gov/pubmed/14693420

Bakala, A., Karlik, W., & Wiechetek, M. (2003). Preparation of equine isolated hepatocytes. *Toxicology in Vitro*, *17*(5–6), 615–621. https://doi.org/10.1016/S0887-2333(03)00112-7

Balabaud, C., Roche, M. C., & Dangoumau, J. (1975). Measurement of hepatic blood flow in the unanesthetized rabbit using 198Au and 125I Rose Bengal clearance technique. *Biomedicine / [Publiee Pour l'A.A.I.C.I.G.]*, *23*(9), 353–355. http://www.ncbi.nlm.nih.gov/pubmed/1231933

Barter, Z. E., Bayliss, M. K., Beaune, P. H., Boobis, A. R., Carlile, D. J., Edwards, R. J., Houston, J. B., Lake, B. G., Lipscomb, J. C., Pelkonen, O. R., Tucker, G. T., & Rostami-Hodjegan, A. (2007). Scaling factors for the extrapolation of in vivo metabolic drug clearance from in vitro data: reaching a consensus on values of human microsomal protein and hepatocellularity per gram of liver. *Current Drug Metabolism*, *8*(1), 33–45. http://www.ncbi.nlm.nih.gov/pubmed/17266522

Becker, J. B., Prendergast, B. J., & Liang, J. W. (2016). Female rats are not more variable than male rats: a meta-analysis of neuroscience studies. *Biology of Sex Differences*, *7*(1), 34. https://doi.org/10.1186/s13293-016-0087-5

Beery, A. K. (2018). Inclusion of females does not increase variability in rodent research studies. *Current Opinion in Behavioral Sciences*, *23*, 143–149. https://doi.org/10.1016/j.cobeha.2018.06.016

Berardo, C., Ferrigno, A., Siciliano, V., Richelmi, P., Vairetti, M., & Di Pasqua, L.

G. (2020). Isolation of Rat Hepatocytes for Pharmacological Studies on Metabotropic Glutamate Receptor (mGluR) Subtype 5: A Comparison Between Collagenase I Versus Collagenase IV. *European Journal of Histochemistry*, *64*(2), 3123. https://doi.org/10.4081/ejh.2020.3123

Bertrand, H. G. M. J., Sandersen, C., Murray, J., & Flecknell, P. A. (2017). A combination of alfaxalone, medetomidine and midazolam for the chemical immobilization of Rhesus macaque (*Macaca mulatta*): Preliminary results. *Journal of Medical Primatology*, *46*(6), 332–336. https://doi.org/10.1111/jmp.12315

Billard, V. (2015). Pharmacokinetic-pharmacodynamic relationship of anesthetic drugs: from modeling to clinical use. *F1000Research*, *4*. https://doi.org/10.12688/f1000research.6601.1

Blix, H. S., Viktil, K. K., Moger, T. A., & Reikvam, A. (2010). Drugs with narrow therapeutic index as indicators in the risk management of hospitalised patients. *Pharmacy Practice (Internet)*, *8*(1). https://doi.org/10.4321/S1886-36552010000100006

Blomquist, C. H., Lima, P. H., & Hotchkiss, J. R. (2005). Inhibition of 3α-hydroxysteroid dehydrogenase (3α-HSD) activity of human lung microsomes by genistein, daidzein, coumestrol and C 18-, C19- and C21-hydroxysteroids and ketosteroids. *Steroids*, *70*(8), 507–514. https://doi.org/10.1016/j.steroids.2005.01.004

Bogaards, J. J. P., Bertrand, M., Jackson, P., Oudshoorn, M. J., Weaver, R. J., Van Bladeren, P. J., & Walther, B. (2000). Determining the best animal model for human cytochrome P450 activities: a comparison of mouse, rat, rabbit, dog, micropig, monkey and man. *Xenobiotica*, *30*(12), 1131–1152. https://doi.org/10.1080/00498250010021684

Bonate, P. L. (2001). A brief introduction to Monte Carlo simulation. In *Clinical Pharmacokinetics* (Vol. 40, Issue 1, pp. 15–22). Adis International Ltd. https://doi.org/10.2165/00003088-200140010-00002

Bormann, J. (2000). The "ABC" of GABA receptors. *Trends in Pharmacological Sciences*, *21*(1), 16–19. http://www.ncbi.nlm.nih.gov/pubmed/10637650

Boxenbaum, H. (1984). Interspecies Pharmacokinetic Scaling and the Evolutionary-Comparative Paradigm. *Drug Metabolism Reviews*, *15*(5–6), 1071–1121. https://doi.org/10.3109/03602538409033558

Brandon, E. F. A., Raap, C. D., Meijerman, I., Beijnen, J. H., & Schellens, J. H. M. (2003). An update on in vitro test methods in human hepatic drug biotransformation research: pros and cons. *Toxicology and Applied Pharmacology*, *189*(3), 233–246. http://www.ncbi.nlm.nih.gov/pubmed/12791308

Brian Houston, J. (1994). Utility of in vitro drug metabolism data in predicting in vivo metabolic clearance. *Biochemical Pharmacology*, *47*(9), 1469–1479. https://doi.org/10.1016/0006-2952(94)90520-7

Brown, N., Kerby, J., Bonnert, T. P., Whiting, P. J., & Wafford, K. A. (2002). Pharmacological characterization of a novel cell line expressing human alpha(4)beta(3)delta GABA(A) receptors. *British Journal of Pharmacology*, *136*(7), 965–974. https://doi.org/10.1038/sj.bjp.0704795

Burton, L., Scaife, P., Paine, S. W., Mellor, H. R., Abernethy, L., Littlewood, P., & Rauch, C. (2020). Hydrostatic pressure regulates CYP1A2 expression in human hepatocytes via a mechanosensitive aryl hydrocarbon receptor-dependent pathway. *Am J Physiol Cell Physiol*, *318*, 889–902. https://doi.org/10.1152/ajpcell.00472.2019.-Approximately

Byrns, M. C., Steckelbroeck, S., & Penning, T. M. (2008). An indomethacin analogue, N-(4-chlorobenzoyl)-melatonin, is a selective inhibitor of aldo-keto reductase 1C3 (type 2 3α-HSD, type 5 17β-HSD, and prostaglandin F synthase), a potential target for the treatment of hormone dependent and hormone independent malignancies. *Biochemical Pharmacology*, *75*(2), 484–493. https://doi.org/10.1016/j.bcp.2007.09.008

Carey, F. A., & Giuliano, R. M. (2011). *Organic chemistry* (8th ed.). McGraw-Hill.

Carver, C. M., & Reddy, D. S. (2013). Neurosteroid interactions with synaptic and extrasynaptic GABA(A) receptors: regulation of subunit plasticity, phasic and tonic inhibition, and neuronal network excitability. *Psychopharmacology*, *230*(2), 151–188. https://doi.org/10.1007/s00213-013-3276-5

Chen, W., Xiao, Y., Chen, J., Liu, J., Shao, J., Li, T., Zhu, Y., Ma, J., Gao, Y., Wang, J., Xu, J., Lu, Y., & Jia, L. (2017). Sex-related pharmacokinetic differences and mechanisms of metapristone (RU486 metabolite). *Scientific Reports*, *7*(1). https://doi.org/10.1038/s41598-017-17225-0

Chiba, M., Ishii, Y., & Sugiyama, Y. (2009). Prediction of Hepatic Clearance in Human From In Vitro Data for Successful Drug Development. *The AAPS Journal*, *11*(2), 262–276. https://doi.org/10.1208/s12248-009-9103-6

Ciccone, G. K., & Holdcroft, A. (1999). Drugs and sex differences: a review of drugs relating to anaesthesia. *British Journal of Anaesthesia Br J Anaesth*, *82*(82), 255–265. https://oup.silverchair-cdn.com/oup/backfile/Content_public/Journal/bja/82/2/10.1093_bja_82.2.255/2/255.pdf?Expires=1509130236&Signature=B5pg~8oFppxV2kaLu55YihRgKqp8ohnq7BaKcpu94uZPu6XpcYHdJPExithrQ3gbZGoUpw8iEITpyeIia-h5ioDIRiTSyN2THu~QVNxsPyrDoezIheX47h

Clarke, R. S., Dundee, J. W., & Carson, I. W. (1973). Proceedings: A new steroid anaesthetic-althesin. *Proceedings of the Royal Society of Medicine*, *66*(10), 1027–1030. http://www.ncbi.nlm.nih.gov/pubmed/4148526

Compagnone, N. A., & Mellon, S. H. (2000). Neurosteroids: Biosynthesis and Function of These Novel Neuromodulators. *Frontiers in Neuroendocrinology*, *21*(1), 1–56. https://doi.org/10.1006/FRNE.1999.0188

Consortium, I. T., Giacomini, K., Huang, S.-M., Tweedie, D., Benet, L., Brouwer, K., Chu, X., Dahlin, A., Evers, R., Fischer, V., Hillgren, K., Hoffmaster, K., Ishikawa, T., Keppler, D., Kim, R., Lee, C., Niemi, M., Polli, J., Sugiyama, Y., … Zhang, L. (2010). Membrane transporters in drug development. *Nature Reviews. Drug Discovery*, *9*(3), 215–236. https://doi.org/10.1038/nrd3028

Cornish-Bowden, A. (2012). Introduction to enzyme kinetics. In *Fundamentals of Enzyme Kinetics* (pp. 16–38). Elsevier. https://doi.org/10.1016/B978-0-408-10617-7.50007-9

Csajka, C., & Verotta, D. (2006). Pharmacokinetic–Pharmacodynamic Modelling:

History and Perspectives. *Journal of Pharmacokinetics and Pharmacodynamics*, *33*(3), 227–279. https://doi.org/10.1007/s10928-005-9002-0

Czerniak, R. (2001). Gender-based differences in pharmacokinetics in laboratory animal models. *International Journal of Toxicology*, *20*(3), 161–163. https://doi.org/10.1080/109158101317097746

Davis, A. M. (Chemist), & Ward, S. E. (Simon E. (2015). *The handbook of medicinal chemistry : principles and practice* (3rd ed.). https://books.google.co.uk/books?id=nGooDwAAQBAJ&pg=PA223&lpg=PA223&dq=blood+flow+for+liver+in+rats+is+72+ml/min/kg&source=bl&ots=FFz994qe2H&sig=UGAo6Cz_cYc8hfewpnQH79pTchY&hl=en&sa=X&ved=0ahUKEwiAyMD8lKDXAhWMPRoKHTQoDH4Q6AEIOTAD#v=onepage&q=blood flow fo

Derendorf, H., & Meibohm, B. (1999). Modeling of pharmacokinetic/pharmacodynamic (PK/PD) relationships: concepts and perspectives. *Pharmaceutical Research*, *16*(2), 176–185. https://doi.org/10.1023/A:1011907920641

Diczfalusy, U., Miura, J., Roh, H.-K., Mirghani, R. A., Sayi, J., Larsson, H., Bodin, K. G., Allqvist, A., Jande, M., Kim, J.-W., Aklillu, E., Gustafsson, L. L., & Bertilsson, L. (2008). 4Beta-hydroxycholesterol is a new endogenous CYP3A marker: relationship to CYP3A5 genotype, quinine 3-hydroxylation and sex in Koreans, Swedes and Tanzanians. *Pharmacogenetics and Genomics*, *18*(3), 201–208. https://doi.org/10.1097/FPC.0b013e3282f50ee9

Dimasi, J. A. (1994). Risks, Regulation, and Rewards in New Drug Development in the United States. *Regulatory Toxicology and Pharmacology*, *19*(2), 228–235. https://doi.org/10.1006/rtph.1994.1021

Do Rego, J. L., Seong, J. Y., Burel, D., Leprince, J., Luu-The, V., Tsutsui, K., Tonon, M.-C. C., Pelletier, G., & Vaudry, H. (2009). Neurosteroid biosynthesis: enzymatic pathways and neuroendocrine regulation by neurotransmitters and neuropeptides. *Frontiers in Neuroendocrinology*, *30*(3), 259–301. https://doi.org/10.1016/j.yfrne.2009.05.006

Dufort, I., Labrie, F., & Luu-The, V. (2001). *Human Types 1 and 3 3-Hydroxysteroid Dehydrogenases: Differential Lability and Tissue Distribution**. https://academic.oup.com/jcem/article/86/2/841/2841129

Edwards, R. J., Price, R. J., Watts, P. S., Renwick, A. B., Tredger, J. M., Boobis, A. R., & Lake, B. G. (2003). Induction of cytochrome P450 enzymes in cultured precision-cut human liver slices. *Drug Metabolism and Disposition: The Biological Fate of Chemicals*, *31*(3), 282–288. http://dmd.aspetjournals.org

Ekins, S., Ring, B. J., Grace, J., McRobie-Belle, D. J., & Wrighton, S. A. (2001). Present and future in vitro approaches for drug metabolism. *Journal of Pharmacological and Toxicological Methods*, *44*(1), 313–324. http://www.ncbi.nlm.nih.gov/pubmed/11274898

El-Kattan, A., & Varma, M. (2012). Preclinical Pharmacokinetics: Industrial Perspective. *Mass Spectrometry Handbook*, 107–118. https://doi.org/10.1002/9781118180730.ch5

Estes, K. S., Brewster, M. E., Webb, A. I., & Bodor, N. (1990). A non- surfactant

formulation for alfaxalone based on an amorphous cyclodextrin: Activity studies in rats and dogs. *International Journal of Pharmaceutics*, *65*(1–2), 101–107. https://doi.org/10.1016/0378-5173(90)90014-U

Feierman, D. E. (1996). Identification of cytochrome P450 3A1/2 as the major P450 isoform responsible for the metabolism of fentanyl by rat liver microsomes. *Anesthesia and Analgesia*, *82*(5), 936–941. https://doi.org/10.1097/00000539-199605000-00008

Fenwick, N., Griffin, G., & Gauthier, C. (2009). The welfare of animals used in science: How the "Three Rs" ethic guides improvements. *Canadian Veterinary Journal*, *50*(5), 523–530. https://www.ncbi.nlm.nih.gov/pmc/articles/PMC2671878/

Ferré, P. J., Pasloske, K., Whittem, T., Ranasinghe, M. G., Li, Q., & Lefebvre, H. P. (2006). Plasma pharmacokinetics of alfaxalone in dogs after an intravenous bolus of Alfaxan-CD RTU. *Veterinary Anaesthesia and Analgesia*, *33*(4), 229–236. https://doi.org/10.1111/j.1467-2995.2005.00264.x

Fink, G., Sarkar, D. K., Dow, R. C., Dick, H., Borthwick, N., Malnick, S., & Twine, M. (1982). Sex difference in response to alphaxalone anaesthesia may be oestrogen dependent. *Nature*, *298*(5871), 270–272. https://doi.org/10.1038/298270a0

Fisher, M. B., Campanale, K., Ackermann, B. L., VandenBranden, M., & Wrighton, S. A. (2000). In Vitro Glucuronidation Using Human Liver Microsomes and The Pore-Forming Peptide Alamethicin. *Drug Metabolism and Disposition*, *28*(5), 560–566. http://dmd.aspetjournals.org/content/28/5/560

Flecknell, P. (2016). Basic Principles of Anaesthesia. In *Laboratory Animal Anaesthesia* (4TH ed., pp. 1–75). Elsevier. https://doi.org/10.1016/B978-0-12-800036-6.00001-6

Fletcher, C. V., Acosta, E. P., & Strykowski, J. M. (1994). Gender differences in human pharmacokinetics and pharmacodynamics. *Journal of Adolescent Health*, *15*(8), 619–629. https://doi.org/10.1016/S1054-139X(94)90628-9

Foster, J. A., Houston, J. B., & Hallifax, D. (2011). Comparison of intrinsic clearances in human liver microsomes and suspended hepatocytes from the same donor livers: clearance-dependent relationship and implications for prediction of in vivo clearance. *Xenobiotica; the Fate of Foreign Compounds in Biological Systems*, *41*(2), 124–136. https://doi.org/10.3109/00498254.2010.530700

Gabrielsson, J., & Weiner, D. (2016). *Pharmacokinetic & pharmacodynamic data analysis : concepts and applications*. Apotekarsocieteten.

Gagez, A. L., Rouguieg-Malki, K., Sauvage, F. L., Marquet, P., & Picard, N. (2012). Simultaneous evaluation of six human glucuronidation activities in liver microsomes using liquid chromatography-tandem mass spectrometry. *Analytical Biochemistry*, *427*(1), 52–59. https://doi.org/10.1016/j.ab.2012.04.031

Galanopoulou, A. S. (2005). GABAA Receptors as Broadcasters of Sexually Differentiating Signals in the Brain. *Epilepsia*, *46*(s5), 107–112. https://doi.org/10.1111/j.1528-1167.2005.01007.x

Gandhi, M., Aweeka, F., Greenblatt, R. M., & Blaschke, T. F. (2004). Sex differences in pharmacokinetics and pharmacodynamics. *Annual Review of Pharmacology and Toxicology*, *44*(1), 499–523. https://doi.org/10.1146/annurev.pharmtox.44.101802.121453

Garcia, P. S., Kolesky, S. E., & Jenkins, A. (2010). General anesthetic actions on GABA(A) receptors. *Current Neuropharmacology*, *8*(1), 2–9. https://doi.org/10.2174/157015910790909502

Gonçalves, L. A., Vigário, A. M., & Penha-Gonçalves, C. (2007). Improved isolation of murine hepatocytes for in vitro malaria liver stage studies. *Malaria Journal*, *6*(1), 169. https://doi.org/10.1186/1475-2875-6-169

Goodchild, C. S., Serrao, J. M., Kolosov, A., & Boyd, B. J. (2015). Alphaxalone reformulated: A water-soluble intravenous anesthetic preparation in sulfobutyl-ether-β-cyclodextrin. *Anesthesia and Analgesia*, *120*(5), 1025–1031. https://doi.org/10.1213/ANE.0000000000000559

Goodchild, C. S., Serrao, J. M., Sear, J. W., & Anderson, B. J. (2020). Pharmacokinetic and Pharmacodynamic Analysis of Alfaxalone Administered as a Bolus Intravenous Injection of Phaxan in a Phase 1 Randomized Trial. *Anesthesia & Analgesia*, *130*(3), 704–714. https://doi.org/10.1213/ANE.0000000000004204

Goodwin, W., Keates, H. L., Pasloske, K., Pearson, M., Sauer, B., & Ranasinghe, M. G. (2011). The pharmacokinetics and pharmacodynamics of the injectable anaesthetic alfaxalone in the horse. *Veterinary Anaesthesia and Analgesia*, *38*(5), 431–438. https://doi.org/10.1111/j.1467-2995.2011.00634.x

Goodwin, W., Keates, H., Pasloske, K., Pearson, M., Sauer, B., & Ranasinghe, M. G. (2012). Plasma pharmacokinetics and pharmacodynamics of alfaxalone in neonatal foals after an intravenous bolus of alfaxalone following premedication with butorphanol tartrate. *Veterinary Anaesthesia and Analgesia*, *39*(5), 503–510. https://doi.org/10.1111/j.1467-2995.2012.00734.x

Griffin, L. D., & Mellon, S. H. (1999). Selective serotonin reuptake inhibitors directly alter activity of neurosteroidogenic enzymes. *Proceedings of the National Academy of Sciences of the United States of America*, *96*(23), 13512–13517. https://doi.org/10.1073/pnas.96.23.13512

Haworth, M., McEwen, M., Dixon, B., & Purcell, S. (2019). Anaphylaxis associated with intravenous administration of alphaxalone in a dog. *Australian Veterinary Journal*, *97*(6), 197–201. https://doi.org/10.1111/avj.12824

He, X.-Y., Wegiel, J., & Yang, S.-Y. (2005). Intracellular oxidation of allopregnanolone by human brain type 10 17beta-hydroxysteroid dehydrogenase. *Brain Research*, *1040*(1–2), 29–35. https://doi.org/10.1016/J.BRAINRES.2005.01.022

He, X. Y., Dobkin, C., & Yang, S. Y. (2019). 17β-Hydroxysteroid dehydrogenases and neurosteroid metabolism in the central nervous system. In *Molecular and Cellular Endocrinology* (Vol. 489, pp. 92–97). Elsevier Ireland Ltd. https://doi.org/10.1016/j.mce.2018.10.002

He, X. Y., Wegiel, J., Yang, Y. Z., Pullarkat, R., Schulz, H., & Yang, S. Y. (2005).

Type 10 17beta-hydroxysteroid dehydrogenase catalyzing the oxidation of steroid modulators of γ-aminobutyric acid type a receptors. *Molecular and Cellular Endocrinology*, *229*(1–2), 111–117. https://doi.org/10.1016/j.mce.2004.08.011

Hoffman, A., & Levy, G. (1989). Gender differences in the pharmacodynamics of barbiturates in rats. *Pharmaceutical Research*, *6*(11), 976–981. http://www.ncbi.nlm.nih.gov/pubmed/2574444

Holford, N. H. G., & Sheiner, L. B. (1982). Kinetics of pharmacologic response. *Pharmacology & Therapeutics*, *16*(2), 143–166. https://doi.org/10.1016/0163-7258(82)90051-1

Hulst, L. K., Fleishaker, J. C., Peters, G. R., Harry, J. D., Wright, D. M., & Ward, P. (1994). Effect of age and gender on tirilazad pharmacokinetics in humans. *Clinical Pharmacology and Therapeutics*, *55*(4), 378–384. https://doi.org/10.1038/clpt.1994.45

Inagaki, K., Inagaki, M., Kataoka, T., Sekido, I., Gill, M. A., & Nishida, M. (2002). A wide interindividual variability of urinary 6beta-hydroxycortisol to free cortisol in 487 healthy Japanese subjects in near basal condition. *Therapeutic Drug Monitoring*, *24*(6), 722–727. http://www.ncbi.nlm.nih.gov/pubmed/12451288

Ings, R. M. (1990). Interspecies scaling and comparisons in drug development and toxicokinetics. *Xenobiotica; the Fate of Foreign Compounds in Biological Systems*, *20*(11), 1201–1231. https://doi.org/10.3109/00498259009046839

Ito, K., & Houston, J. B. (2004). Comparison of the Use of Liver Models for Predicting Drug Clearance Using in Vitro Kinetic Data from Hepatic Microsomes and Isolated Hepatocytes. *Pharmaceutical Research*, *21*(5), 785–792. https://doi.org/10.1023/B:PHAM.0000026429.12114.7d

Kang, Y. B. A., Eo, J., Mert, S., Yarmush, M. L., & Usta, O. B. (2018). Metabolic Patterning on a Chip: Towards in vitro Liver Zonation of Primary Rat and Human Hepatocytes. *Scientific Reports*, *8*(1). https://doi.org/10.1038/s41598-018-27179-6

Kanie, O., Shioiri, Y., Ogata, K., Uchida, W., Daikoku, S., Suzuki, K., Nakamura, S., & Ito, Y. (2016). Diastereomeric resolution directed towards chirality determination focussing on gas-phase energetics of coordinated sodium dissociation. *Scientific Reports*, *6*(1), 1–9. https://doi.org/10.1038/srep24005

Kato, R., & Yamazoe, Y. (1992). Sex-specific cytochrome P450 as a cause of sex-and species-related differences in drug toxicity. *Toxicology Letters*, *64–65*(C), 661–667. https://doi.org/10.1016/0378-4274(92)90245-F

Keates, H. (2003). Induction of anaesthesia in pigs using a new alphaxalone formulation. *The Veterinary Record*, *153*(20), 627–628. http://www.ncbi.nlm.nih.gov/pubmed/14653343

Khan, K. S., Hayes, I., & Buggy, D. J. (2014). Pharmacology of anaesthetic agents I: Intravenous anaesthetic agents. *Continuing Education in Anaesthesia, Critical Care and Pain*, *14*(3), 100–105. https://doi.org/10.1093/bjaceaccp/mkt039

Kharasch, E. D., Mautz, D., Senn, T., Lentz, G., & Cox, K. (1999). Menstrual cycle variability in midazolam pharmacokinetics. *Journal of Clinical Pharmacology*, *39*(3), 275–280. http://www.ncbi.nlm.nih.gov/pubmed/10073327

Kilford, P. J., Gertz, M., Houston, J. B., & Galetin, A. (2008). Hepatocellular binding of drugs: Correction for unbound fraction in hepatocyte incubations using microsomal binding or drug lipophilicity data. *Drug Metabolism and Disposition*, *36*(7), 1194–1197. https://doi.org/10.1124/dmd.108.020834

Knights, K. M., Stresser, D. M., Miners, J. O., & Crespi, C. L. (2016). In Vitro Drug Metabolism Using Liver Microsomes. *Current Protocols in Pharmacology*, *September*, 7.8.1-7.8.24. https://doi.org/10.1002/cpph.9

Kola, I., & Landis, J. (2004). *Can the pharmaceutical industry reduce attrition rates? 3*(August), 1–5.

Korpi, E. R., & Sinkkonen, S. T. (2006). GABAA receptor subtypes as targets for neuropsychiatric drug development. *Pharmacology & Therapeutics*, *109*(1–2), 12–32. https://doi.org/10.1016/j.pharmthera.2005.05.009

Krueger, S. K., & Williams, D. E. (2005). Mammalian flavin-containing monooxygenases: structure/function, genetic polymorphisms and role in drug metabolism. *Pharmacology & Therapeutics*, *106*(3), 357–387. https://doi.org/10.1016/j.pharmthera.2005.01.001

Kwak, H. C., Kim, H. C., Oh, S. J., & Kim, S. K. (2015). Effects of age increase on hepatic expression and activity of cytochrome P450 in male C57BL/6 mice. *Archives of Pharmacal Research*, *38*(5), 857–864. https://doi.org/10.1007/s12272-014-0452-z

Lambert, J. J., Belelli, D., Peden, D. R., Vardy, A. W., & Peters, J. A. (2003). Neurosteroid modulation of GABAA receptors. *Progress in Neurobiology*, *71*(1), 67–80. http://www.ncbi.nlm.nih.gov/pubmed/14611869

Lanzino, G., & Kassell, N. F. (1999). Double-blind, randomized, vehicle-controlled study of high-dose tirilazad mesylate in women with aneurysmal subarachnoid hemorrhage. Part II. A cooperative study in North America. *Journal of Neurosurgery*, *90*(6), 1018–1024. https://doi.org/10.3171/jns.1999.90.6.1018

Lau, C., Ranasinghe, M. G., Shiels, I., Keates, H., Pasloske, K., & Bellingham, M. C. (2013). Plasma pharmacokinetics of alfaxalone after a single intraperitoneal or intravenous injection of Alfaxan?? in rats. *Journal of Veterinary Pharmacology and Therapeutics*, *36*(5), 516–520. https://doi.org/10.1111/jvp.12055

Lave, T., Dupin, S., Schmitt, M., Kapps, M., Meyer, J., Morgenroth, B., Chou, R. C., Jaeck, D., & Coassolo, P. (1996). Interspecies scaling of tolcapone, a new inhibitor of catechol-O-methyltransferase (COMT). Use of in vitro data from hepatocytes to predict metabolic clearance in animals and humans. *Xenobiotica; the Fate of Foreign Compounds in Biological Systems*, *26*(8), 839–851. http://www.ncbi.nlm.nih.gov/pubmed/8879148

Lavoie, A. M., Tingey, J. J., Harrison, N. L., Pritchett, D. B., & Twyman, R. E. (1997). Activation and deactivation rates of recombinant GABA(A) receptor channels are dependent on alpha-subunit isoform. *Biophysical Journal*, *73*(5), 2518–2526. https://doi.org/10.1016/S0006-3495(97)78280-8

Lees, J., Hallak, J. E. C., Deakin, J. F. W., & Dursun, S. M. (2004). Gender Differences and the Effects of Ketamine in Healthy Volunteers. *Journal of Psychopharmacology*, *18*(3), 337–339. https://doi.org/10.1177/026988110401800302

Lipinski, C. A. (2004). Lead- and drug-like compounds: the rule-of-five revolution. *Drug Discovery Today: Technologies*, *1*(4), 337–341. https://doi.org/10.1016/j.ddtec.2004.11.007

Liu, K. A., & Dipietro Mager, N. A. (2016). Women's involvement in clinical trials: Historical perspective and future implications. In *Pharmacy Practice* (Vol. 14, Issue 1). Grupo de Investigacion en Atencion Farmaceutica. https://doi.org/10.18549/PharmPract.2016.01.708

Loftsson, T., Jarho, P., Másson, M., & Järvinen, T. (2005). Cyclodextrins in drug delivery. In *Expert Opinion on Drug Delivery* (Vol. 2, Issue 2, pp. 335–351). Expert Opin Drug Deliv. https://doi.org/10.1517/17425247.2.1.335

Majewska, M. D., Harrison, N. L., Schwartz, R. D., Barker, J. L., & Paul, S. M. (1986). Steroid hormone metabolites are barbiturate-like modulators of the GABA receptor. *Science (New York, N.Y.)*, *232*(4753), 1004–1007. http://www.ncbi.nlm.nih.gov/pubmed/2422758

Marcos, R., Lopes, C., Malhão, F., Correia-Gomes, C., Fonseca, S., Lima, M., Gebhardt, R., & Rocha, E. (2016). Stereological assessment of sexual dimorphism in the rat liver reveals differences in hepatocytes and Kupffer cells but not hepatic stellate cells. *Journal of Anatomy*, *228*(6), 996–1005. https://doi.org/10.1111/joa.12448

Martignoni, M., Groothuis, G. M. M., & de Kanter, R. (2006). Species differences between mouse, rat, dog, monkey and human CYP-mediated drug metabolism, inhibition and induction. *Expert Opinion on Drug Metabolism & Toxicology*, *2*(6), 875–894. https://doi.org/10.1517/17425255.2.6.875

Martinez-Botella, G., Ackley, M. A., Salituro, F. G., & Doherty, J. J. (2014). Natural and synthetic neuroactive steroid modulators of GABAAand NMDA receptors. In *Annual Reports in Medicinal Chemistry* (1st ed., Vol. 49). Elsevier Inc. https://doi.org/10.1016/B978-0-12-800167-7.00003-1

Matsui, D., Sakari, M., Sato, T., Murayama, A., Takada, I., Kim, M., Takeyama, K., & Kato, S. (2002). Transcriptional regulation of the mouse steroid 5alpha-reductase type II gene by progesterone in brain. *Nucleic Acids Research*, *30*(6), 1387–1393. http://www.ncbi.nlm.nih.gov/pubmed/11884637

McCarthy, M. M., Arnold, A. P., Ball, G. F., Blaustein, J. D., & Geert, J. (2012). *Sex Differences in the Brain : The Not So Inconvenient Truth*. *32*(7), 2241–2247. https://doi.org/10.1523/JNEUROSCI.5372-11.2012.Sex

McMillan, M. W., & Leece, E. A. (2011). Immersion and branchial/transcutaneous irrigation anaesthesia with alfaxalone in a Mexican axolotl. *Veterinary Anaesthesia and Analgesia*, *38*(6), 619–623. https://doi.org/10.1111/j.1467-2995.2011.00660.x

Meibohm, B., Beierle, I., & Derendorf, H. (2002). How important are gender differences in pharmacokinetics? *Clinical Pharmacokinetics*, *41*(5), 329–342. https://doi.org/10.2165/00003088-200241050-00002

Meibohm, B., & Derendorf, H. (1997). Basic concepts of pharmacokinetic/pharmacodynamic (PK/PD) modelling. *International Journal of Clinical Pharmacology and Therapeutics*, *35*(10), 401–413. http://www.ncbi.nlm.nih.gov/pubmed/9352388

Meletiadis, J., Chanock, S., & Walsh, T. J. (2006). Human pharmacogenomic variations and their implications for antifungal efficacy. *Clinical Microbiology Reviews*, *19*(4), 763–787. https://doi.org/10.1128/CMR.00059-05

Mellon, S. H., & Deschepper, C. F. (1993). Neurosteroid biosynthesis: genes for adrenal steroidogenic enzymes are expressed in the brain. *Brain Research*, *629*(2), 283–292. https://doi.org/10.1016/0006-8993(93)91332-M

Mennecozzi, M., Landesmann, B., Palosaari, T., Harris, G., & Whelan, M. (2015). Sex Differences in Liver Toxicity—Do Female and Male Human Primary Hepatocytes React Differently to Toxicants In Vitro? *PLOS ONE*, *10*(4), e0122786. https://doi.org/10.1371/journal.pone.0122786

Miners, J. O., Smith, P. A., Sorich, M. J., McKinnon, R. A., & Mackenzie, P. I. (2004). Predicting Human Drug Glucuronidation Parameters: Application of In Vitro and In Silico Modeling Approaches. *Annual Review of Pharmacology and Toxicology*, *44*(1), 1–25. https://doi.org/10.1146/annurev.pharmtox.44.101802.121546

Mitchell, E. A., Gentet, L. J., Dempster, J., & Belelli, D. (2007). GABAA and glycine receptor-mediated transmission in rat lamina II neurones: relevance to the analgesic actions of neuroactive steroids. *The Journal of Physiology*, *583*(Pt 3), 1021–1040. https://doi.org/10.1113/jphysiol.2007.134445

Mitchell, E. A., Herd, M. B., Gunn, B. G., Lambert, J. J., & Belelli, D. (2008). Neurosteroid modulation of GABAA receptors: molecular determinants and significance in health and disease. *Neurochemistry International*, *52*(4–5), 588–595. https://doi.org/10.1016/j.neuint.2007.10.007

Mitev, Y. ., Darwish, M., Wolf, S. ., Holsboer, F., Almeida, O. F. ., & Patchev, V. . (2003). Gender differences in the regulation of 3α-hydroxysteroid dehydrogenase in rat brain and sensitivity to neurosteroid-mediated stress protection. *Neuroscience*, *120*(2), 541–549. https://doi.org/10.1016/S0306-4522(03)00287-2

Monaghan, E. P., Navalta, L. A., Shum, L., Ashbrook, D. W., & Lee, D. A. (1997). Initial human experience with ganaxolone, a neuroactive steroid with antiepileptic activity. *Epilepsia*, *38*(9), 1026–1031. https://doi.org/10.1111/j.1528-1157.1997.tb01486.x

Monagle, J., Siu, L., Worrell, J., Goodchild, C. S., & Serrao, J. M. (2015). A phase 1c trial comparing the efficacy and safety of a new aqueous formulation of alphaxalone with propofol. *Anesthesia and Analgesia*, *121*(4), 914–924. https://doi.org/10.1213/ANE.0000000000000856

Mordenti, J. (1986). Man versus beast: pharmacokinetic scaling in mammals. *Journal of Pharmaceutical Sciences*, *75*(11), 1028–1040. http://www.ncbi.nlm.nih.gov/pubmed/3820096

Mould, D. R., & Upton, R. N. (2012). Basic Concepts in Population Modeling, Simulation, and Model-Based Drug Development. *CPT: Pharmacometrics & Systems Pharmacology*, *1*(9), e6. https://doi.org/10.1038/psp.2012.4

Mould, D. R., & Upton, R. N. (2013). Basic Concepts in Population Modeling, Simulation, and Model-Based Drug Development—Part 2: Introduction to Pharmacokinetic Modeling Methods. *CPT: Pharmacometrics & Systems Pharmacology*, *2*(4), e38. https://doi.org/10.1038/psp.2013.14

Muir, W., Lerche, P., Wiese, A., Nelson, L., Pasloske, K., & Whittem, T. (2008). Cardiorespiratory and anesthetic effects of clinical and supraclinical doses of alfaxalone in dogs. *Veterinary Anaesthesia and Analgesia*, *35*(6), 451–462. https://doi.org/10.1111/j.1467-2995.2008.00406.x

Muir, W., Lerche, P., Wiese, A., Nelson, L., Pasloske, K., & Whittem, T. (2009). The cardiorespiratory and anesthetic effects of clinical and supraclinical doses of alfaxalone in cats. *Veterinary Anaesthesia and Analgesia*, *36*(1), 42–54. https://doi.org/10.1111/j.1467-2995.2008.00428.x

Naville, D., Keeney, D. S., Jenkin, G., Murry, B. A., Head, J. R., & Mason, J. I. (1991). Regulation of expression of male-specific rat liver microsomal 3β-hydroxysteroid dehydrogenase. *Molecular Endocrinology*, *5*(8), 1090–1100. https://doi.org/10.1210/mend-5-8-1090

Nebert, D. W., & Russell, D. W. (2002). Clinical importance of the cytochromes P450. *The Lancet*, *360*(9340), 1155–1162. https://doi.org/10.1016/S0140-6736(02)11203-7

Nicholas, J. S., & Barron, D. H. (1932). The use of sodium amytal in the production of anesthesia in the rat. *J Pharmacol Exp Ther*, *46*, 125–129.

NISHIYAMA, Y., NAKAYAMA, S. M. M., WATANABE, K. P., KAWAI, Y. K., OHNO, M., IKENAKA, Y., & ISHIZUKA, M. (2016). Strain differences in cytochrome P450 mRNA and protein expression, and enzymatic activity among Sprague Dawley, Wistar, Brown Norway and Dark Agouti rats. *Journal of Veterinary Medical Science*, *78*(4), 675–680. https://doi.org/10.1292/jvms.15-0299

Norman, W. M., Court, M. H., & Greenblatt, D. J. (1997). Age-related changes in the pharmacokinetic disposition of diazepam in foals. *American Journal of Veterinary Research*, *58*(8), 878–880. http://www.ncbi.nlm.nih.gov/pubmed/9256974

Obach, R. S. (1999). Prediction of Human Clearance of Twenty-Nine Drugs from Hepatic Microsomal Intrinsic Clearance Data: An Examination of In Vitro Half-Life Approach and Nonspecific Binding to Microsomes. *Drug Metabolism and Disposition*, *27*(11). http://dmd.aspetjournals.org/content/27/11/1350?ijkey=d609bb61063581f2a8195b04bb10c7612ecf51f6&keytype2=tf_ipsecsha

Obach, R. S., Baxter, J. G., Liston, T. E., Silber, B. M., Jones, B. C., MacIntyre, F., Rance, D. J., & Wastall, P. (1997). The prediction of human pharmacokinetic parameters from preclinical and in vitro metabolism data. *The Journal of Pharmacology and Experimental Therapeutics*, *283*(1), 46–58. https://doi.org/Animals Biological Availability Half-Life Human Metabolic Clearance Rate *Pharmacokinetics Retrospective Studies

Pang, K. S., & Rowland, M. (1977). Hepatic clearance of drugs. I. Theoretical considerations of a "well-stirred" model and a "parallel tube" model. Influence of hepatic blood flow, plasma and blood cell binding, and the hepatocellular enzymatic activity on hepatic drug clearance. *Journal of Pharmacokinetics and Biopharmaceutics*, *5*(6), 625–653. https://doi.org/10.1007/BF01059688

Pasanen, M. (2004). Species differences in CYP enzymes. In *Citocromo P450*. http://drnelson.utmem.edu/CytochromeP450.html;

Paul, S. M., & Purdy, R. H. (1992). Neuroactive steroids. *FASEB Journal : Official Publication of the Federation of American Societies for Experimental Biology*, *6*(6), 2311–2322. http://www.ncbi.nlm.nih.gov/pubmed/1347506

Pavel, M. A., Petersen, E. N., Wang, H., Lerner, R. A., & Hansen, S. B. (2018). Studies on the mechanism of membrane mediated general anesthesia. In *bioRxiv*. https://doi.org/10.1101/313973

Penning, T. M., Lin, H. K., Jez, J. M., & Ricigliano, J. W. (1997). Inhibition of type 3 3α-hydroxysteroid dehydrogenase (3α-HSD). *Expert Opinion on Therapeutic Targets*, *1*(1), 141–145. https://doi.org/10.1517/14728222.1.1.141

Pleym, H., Spigset, O., Kharasch, E. D., & Dale, O. (2003). Gender differences in drug effects: Implications for anesthesiologists. *Acta Anaesthesiologica Scandinavica*, *47*(3), 241–259. https://doi.org/10.1034/j.1399-6576.2003.00036.x

Porcu, P., Barron, A. M., Frye, C. A., Walf, A. A., Yang, S. Y., He, X. Y., Morrow, A. L., Panzica, G. C., & Melcangi, R. C. (2016). Neurosteroidogenesis Today: Novel Targets for Neuroactive Steroid Synthesis and Action and Their Relevance for Translational Research. In *Journal of Neuroendocrinology* (Vol. 28, Issue 2, pp. 1–19). Blackwell Publishing Ltd. https://doi.org/10.1111/jne.12351

Pozo, O. J., Van Eenoo, P., Deventer, K., & Delbeke, F. T. (2007). Ionization of anabolic steroids by adduct formation in liquid chromatography electrospray mass spectrometry. *Journal of Mass Spectrometry*, *42*(4), 497–516. https://doi.org/10.1002/jms.1182

Quinney, S. K., Haehner, B. D., Rhoades, M. B., Lin, Z., Gorski, J. C., & Hall, S. D. (2008). Interaction between midazolam and clarithromycin in the elderly. *British Journal of Clinical Pharmacology*, *65*(1), 98–109. https://doi.org/10.1111/j.1365-2125.2007.02970.x

Rane, A., Wilkinson, G. R., & Shand, D. G. (1977). INTRINSIC MEASUREMENT OF CLEARANCE1. *Journal of Pharmacology and Experimental Therapeutics*, *200*(2), 420–424. http://jpet.aspetjournals.org/content/jpet/200/2/420.full.pdf

Raven, P. W., & Taylor, N. F. (1996). Sex differences in the human metabolism of cortisol. *Endocrine Research*, *22*(4), 751–755. https://doi.org/10.1080/07435809609043772

Reddy, D. S., Castaneda, D. C., O'Malley, B. W., & Rogawski, M. A. (2004). Anticonvulsant Activity of Progesterone and Neurosteroids in Progesterone Receptor Knockout Mice. *Journal of Pharmacology and Experimental Therapeutics*, *310*(1), 230–239. https://doi.org/10.1124/jpet.104.065268

Reddy, D.S., & Kulkarnia, S. K. (1999). Sex and Estrous Cycle-Dependent Changes in Neurosteroid and Benzodiazepine Effects on Food Consumption and Plus-Maze Learning Behaviors in Rats. *Pharmacology Biochemistry and Behavior*, *62*(1), 53–60. https://doi.org/10.1016/S0091-3057(98)00126-9

Reddy, Doodipala S. (2003). Is there a physiological role for the neurosteroid

THDOC in stress-sensitive conditions? *Trends in Pharmacological Sciences*, *24*(3), 103–106. https://doi.org/10.1016/S0165-6147(03)00023-3

Reddy, Doodipala Samba. (2009). The role of neurosteroids in the pathophysiology and treatment of catamenial epilepsy. *Epilepsy Research*, *85*(1), 1–30. https://doi.org/10.1016/j.eplepsyres.2009.02.017

Reddy, Doodipala Samba. (2010). Neurosteroids: endogenous role in the human brain and therapeutic potentials. *Progress in Brain Research*, *186*(C), 113–137. https://doi.org/10.1016/B978-0-444-53630-3.00008-7

Rhéaume, E., Lachance, Y., Zhao, H.-F., Breton, N., Dumont, M., Launoit, Y. de, Trudel, C., Luu-The, V., Simard, J., & Labrie, F. (1991). Structure and Expression of a New Complementary DNA Encoding the almost Exclusive 3β-Hydroxysteroid Dehydrogenase/Δ^{5}-Δ^{4}-Isomerase in Human Adrenals and Gonads. *Molecular Endocrinology*, *5*(8), 1147–1157. https://doi.org/10.1210/mend-5-8-1147

Richardson, S., Bai, A., A. Kulkarni, A., & F. Moghaddam, M. (2016). Efficiency in Drug Discovery: Liver S9 Fraction Assay As a Screen for Metabolic Stability. *Drug Metabolism Letters*, *10*(2), 83–90. https://doi.org/10.2174/1872312810666160223121836

Ritschel, W. A., Vachharajani, N. N., Johnson, R. D., & Hussain, A. S. (1992). The allometric approach for interspecies scaling of pharmacokinetic parameters. *Comparative Biochemistry and Physiology. C, Comparative Pharmacology and Toxicology*, *103*(2), 249–253. http://www.ncbi.nlm.nih.gov/pubmed/1360380

Riviere, j. e., Martin-Jimenez, T., Sundlof, S. F., & Craigmill, A. L. (1997). Interspecies allometric analysis of the comparative pharmacokinetics of 44 drugs across veterinary and laboratory animal species. *Journal of Veterinary Pharmacology and Therapeutics*, *20*(6), 453–463. https://doi.org/10.1046/j.1365-2885.1997.00095.x

Rostami-Hodjegan, A. (2012). Physiologically Based Pharmacokinetics Joined With In Vitro–In Vivo Extrapolation of ADME: A Marriage Under the Arch of Systems Pharmacology. *Clinical Pharmacology & Therapeutics*, *92*(1), 50–61. https://doi.org/10.1038/clpt.2012.65

Rudolph, U, Crestani, F., & Möhler, H. (2001). GABA(A) receptor subtypes: dissecting their pharmacological functions. *Trends in Pharmacological Sciences*, *22*(4), 188–194. http://www.ncbi.nlm.nih.gov/pubmed/11282419

Rudolph, Uwe, & Antkowiak, B. (2004). Molecular and neuronal substrates for general anaesthetics. *Nature Reviews Neuroscience*, *5*(9), 709–720. https://doi.org/10.1038/nrn1496

Rupprecht, R. (2003). Neuroactive steroids: Mechanisms of action and neuropsychopharmacological properties. *Psychoneuroendocrinology*, *28*(2), 139–168. https://doi.org/10.1016/S0306-4530(02)00064-1

Santos González, M., Bertrán de Lis, B. T., & Tendillo Cortijo, F. J. (2013). Effects of intramuscular alfaxalone alone or in combination with diazepam in swine. *Veterinary Anaesthesia and Analgesia*, *40*(4), 399–402. https://doi.org/10.1111/vaa.12033

Schänzer, W. (1996). Metabolism of anabolic androgenic steroids. *Clinical*

Chemistry, *42*(7), 1001–1020.

Schiffer, L., Barnard, L., Baranowski, E. S., Gilligan, L. C., Taylor, A. E., Arlt, W., Shackleton, C. H. L., & Storbeck, K. H. (2019). Human steroid biosynthesis, metabolism and excretion are differentially reflected by serum and urine steroid metabolomes: A comprehensive review. In *Journal of Steroid Biochemistry and Molecular Biology* (Vol. 194). Elsevier Ltd. https://doi.org/10.1016/j.jsbmb.2019.105439

Sear, J. (1996). Steroid anesthetics: Old compounds, new drugs. *Journal of Clinical Anesthesia*, *8*(3 SUPPL.), S91–S98. https://doi.org/10.1016/S0952-8180(96)90021-5

Sear, J. W., & McGivan, J. D. (1981). Metabolism of alphaxalone in the rat: Evidence for the limitation of the anaesthetic effect by the rate of degradation through the hepatic mixed function oxygenase system. *British Journal of Anaesthesia*, *53*(4), 417–424. https://doi.org/10.1093/bja/53.4.417

Seglen, P. O. (1976). Preparation of Isolated Rat Liver Cells. *Methods in Cell Biology*, *13*(C), 29–83. https://doi.org/10.1016/S0091-679X(08)61797-5

Selye, H. (1941). Anesthetic Effect of Steroid Hormones. *Proceedings of the Society for Experimental Biology and Medicine*, *46*(1), 116–121. https://doi.org/10.3181/00379727-46-11907

Shafqat, N., Marschall, H. U., Filling, C., Nordling, E., Wu, X. Q., Björk, L., Thyberg, J., Mårtensson, E., Salim, S., Jörnvall, H., & Oppermann, U. (2003). Expanded substrate screenings of human and Drosophila type 10 17 β-hydroxysteroid dehydrogenases (HSDs) reveal multiple specificities in bile acid and steroid hormone metabolism: Characterization of multifunctional 3α/7α/7β/17β/20β/21-HSD. *Biochemical Journal*, *376*(1), 49–60. https://doi.org/10.1042/BJ20030877

Sheiner, L. B., Rosenberg, B., & Melmon, K. L. (1972). Modelling of individual pharmacokinetics for computer-aided drug dosage. *Computers and Biomedical Research*, *5*(5), 441–459. https://doi.org/10.1016/0010-4809(72)90051-1

Shen, L., Hillebrand, A., Wang, D. Q.-H. Q. H., & Liu, M. (2012). Isolation and Primary Culture of Rat Hepatic Cells. *Journal of Visualized Experiments*, *64*(64), e3917. https://doi.org/10.3791/3917

Shibany, K. A., Tötemeyer, S., Pratt, S. L., & Paine, S. W. (2016). Equine hepatocytes: isolation, cryopreservation, and applications to in vitro drug metabolism studies. *Pharmacology Research & Perspectives*, *4*(5), e00268. https://doi.org/10.1002/prp2.268

Soars, M. G. (2002). In Vitro Analysis of Human Drug Glucuronidation and Prediction of in Vivo Metabolic Clearance. *Journal of Pharmacology and Experimental Therapeutics*, *301*(1), 382–390. https://doi.org/10.1124/jpet.301.1.382

Soldatow, V. Y., Lecluyse, E. L., Griffith, L. G., & Rusyn, I. (2013). In vitro models for liver toxicity testing. In *Toxicology Research* (Vol. 2, Issue 1, pp. 23–39). Royal Society of Chemistry. https://doi.org/10.1039/c2tx20051a

Soldin, O. P., & Mattison, D. R. (2009). Sex Differences in Pharmacokinetics and

Pharmacodynamics. *Clinical Pharmacokinetics*, *48*(3), 143–157. https://doi.org/10.2165/00003088-200948030-00001

Sparreboom, A., & Figg, W. D. (2006). Identifying sources of interindividual pharmacokinetic variability with population modeling: Commentary on Joerger et al., p. 2150. In *Clinical Cancer Research* (Vol. 12, Issue 7 I, pp. 1951–1953). American Association for Cancer Research. https://doi.org/10.1158/1078-0432.CCR-06-0342

Stolz, A., Rahimi-Kiani, M., Ameis, D., Chan, E., Ronk, M., & Shively, J. E. (1991). Molecular structure of rat hepatic 3α-hydroxysteroid dehydrogenase: A member of the oxidoreductase gene family. *Journal of Biological Chemistry*, *266*(23), 15253–15257.

Suarez, M. A., Dzikiti, B. T., Stegmann, F. G., & Hartman, M. (2012). Comparison of alfaxalone and propofol administered as total intravenous anaesthesia for ovariohysterectomy in dogs. *Veterinary Anaesthesia and Analgesia*, *39*(3), 236–244. https://doi.org/10.1111/j.1467-2995.2011.00700.x

Sun, G.-C., Hsu, M.-C., Chia, Y.-Y., Chen, P.-Y., & Shaw, F.-Z. (2008). Effects of age and gender on intravenous midazolam premedication: a randomized double-blind study. *British Journal of Anaesthesia*, *101*(5), 632–639. https://doi.org/10.1093/bja/aen251

Tammisto, T., Takki, S., Tigerstedt, I., & Kauste, A. (1973). *A comparison of althesin and thiopentone in induction of anaesthesia*. *45*(1), 100–107. https://doi.org/10.1093/bja/45.1.100

Tamura, J., Ishizuka, T., Fukui, S., Oyama, N., Kawase, K., Itami, T., Miyoshi, K., Sano, T., Pasloske, K., & Yamashita, K. (2015). Sedative effects of intramuscular alfaxalone administered to cats. *The Journal of Veterinary Medical Science*, *77*(8), 897–904. https://doi.org/10.1292/jvms.14-0200

Tamura, J., Ishizuka, T., Fukui, S., Oyama, N., Kawase, K., Miyoshi, K., Sano, T., Pasloske, K., & Yamashita, K. (2015). The pharmacological effects of the anesthetic alfaxalone after intramuscular administration to dogs. *Journal of Veterinary Medical Science*, *77*(3), 289–296. https://doi.org/10.1292/jvms.14-0368

Tang, J., Qi, J., White, P. F., Wang, B., & Wender, R. H. (1997). Eltanolone as an alternative to propofol for ambulatory anesthesia. *Anesthesia and Analgesia*, *85*(4), 801–807. http://www.ncbi.nlm.nih.gov/pubmed/9322459

Tennant, J. R. (1964). EVALUATION OF THE TRYPAN BLUE TECHNIQUE FOR DETERMINATION OF CELL VIABILITY. *Transplantation*, *2*(6), 685–694. http://www.ncbi.nlm.nih.gov/pubmed/14224649

Toutain, P.-L. (2002). Pharmacokinetic/Pharmacodynamic Integration in Drug Development and Dosage-Regimen Optimization for Veterinary Medicine. *American Association of Pharmaceutical Scientists*, *4*(4), E38. https://doi.org/10.1208/ps040438

Tsunoda, S. M., Velez, R. L., Von Moltke, L. L., & Greenblatt, D. J. (1999). Differentiation of intestinal and hepatic cytochrome P450 3A activity with use of midazolam as an in vivo probe: Effect of ketoconazole. *Clinical Pharmacology and Therapeutics*, *66*(5), 461–471. https://doi.org/10.1016/S0009-9236(99)70009-3

Turner, J., & Simmonds, M. (1989). Modulation of the GABAA receptor complex by steroids in slices of rat cuneate nucleus. In *Br. J. Pharmacol* (Vol. 96).

Upton, R. N., & Mould, D. R. (2014). Basic Concepts in Population Modeling, Simulation, and Model-Based Drug Development: Part 3—Introduction to Pharmacodynamic Modeling Methods. *CPT: Pharmacometrics & Systems Pharmacology*, *3*(1), e88. https://doi.org/10.1038/psp.2013.71

Vaudry, H., Rego, J. L. Do, Burel, D., Luu-The, V., Pelletier, G., Vaudry, D., & Tsutsui, K. (2011). Neurosteroid biosynthesis in the brain of amphibians. In *Frontiers in Endocrinology* (Vol. 2, Issue NOV). Frontiers Media SA. https://doi.org/10.3389/fendo.2011.00079

Venkatakrishnan, K., von Moltke, L. L., & Greenblatt, D. J. (2001). Human Drug Metabolism and the Cytochromes P450: Application and Relevance of In Vitro Models. *The Journal of Clinical Pharmacology*, *41*(11), 1149–1179. https://doi.org/10.1177/00912700122012724

Vickers, A. E., & Lucier, G. W. (1996). Estrogen receptor levels and occupancy in hepatic sinusoidal endothelial and Kupffer cells are enhanced by initiation with diethylnitrosamine and promotion with 17alpha-ethinylestradiol in rats. *Carcinogenesis*, *17*(6), 1235–1242. http://www.ncbi.nlm.nih.gov/pubmed/8681437

Villaverde-Morcillo, S., Benito, J., García-Sánchez, R., Martín-Jurado, O., & de Segura, I. A. G. (2014). COMPARISON OF ISOFLURANE AND ALFAXALONE (ALFAXAN) FOR THE INDUCTION OF ANESTHESIA IN FLAMINGOS (PHOENICOPTERUS ROSEUS) UNDERGOING ORTHOPEDIC SURGERY. *Journal of Zoo and Wildlife Medicine*, *45*(2), 361–366. https://doi.org/10.1638/2012-0283R2.1

Visser, S. A. G., Smulders, C. J. G. M., Reijers, B. P. R., van der Graaf, P. H., Peletier, L. A., & Danhof, M. (2002). Mechanism-based pharmacokinetic-pharmacodynamic modeling of concentration-dependent hysteresis and biphasic electroencephalogram effects of alphaxalone in rats. *The Journal of Pharmacology and Experimental Therapeutics*, *302*(3), 1158–1167. https://doi.org/10.1124/jpet.302.3.1158

Wagner, J. G. (1968). Kinetics of Pharmacologic Response I. Proposed Relationships between Response and Drug Concentration in the Intact Animal and Man. *Biol*, *20*, 173–201. http://ac.els-cdn.com/0022519368901884/1-s2.0-0022519368901884-main.pdf?_tid=33b55308-5b31-11e7-875b-00000aab0f6c&acdnat=1498565433_040087b1e37d24b1e6b124bf2c65363b

Wang, M. (2011). Neurosteroids and GABA-A Receptor Function. *Frontiers in Endocrinology*, *2*, 44. https://doi.org/10.3389/fendo.2011.00044

Ward, K. W., Smith, B. R., Bondinell, W. E., Cousins, R. D., Huffman, W. F., Jakas, D. R., Keenan, R. M., Ku, T. W., Lundberg, D., Miller, W. H., Mumaw, J. A., Newlander, K. A., Pirhalla, J. L., Roethke, T. J., Salyers, K. L., Souder, P. R., Stelman, G. J., & Smith, B. R. (2004). A Comprehensive Quantitative And Qualitative Evaluation Of Extrapolation Of Intravenous Pharmacokinetic Parameters From Rat, Dog, And Monkey To Humans. I. Clearance. *Drug Metabolism and Disposition*, *32*(6), 603–611. https://doi.org/10.1124/dmd.32.6.603

Warne, L. N., Beths, T., Fogal, S., & Bauquier, S. H. (2014). The use of alfaxalone and remifentanil total intravenous anesthesia in a dog undergoing a craniectomy for tumor resection. *The Canadian Veterinary Journal*, *55*(11), 1083–1088. http://www.ncbi.nlm.nih.gov/pubmed/25392553

Warne, L. N., Beths, T., Whittem, T., Carter, J. E., & Bauquier, S. H. (2015). A review of the pharmacology and clinical application of alfaxalone in cats. *The Veterinary Journal*, *203*(2), 141–148. https://doi.org/10.1016/J.TVJL.2014.12.011

Waxman, D. J., & Holloway, M. G. (2009). Sex differences in the expression of hepatic drug metabolizing enzymes. *Molecular Pharmacology*, *76*(2), 215–228. https://doi.org/10.1124/mol.109.056705

West, J. A. (2017). Alfaxalone. *Journal of Exotic Pet Medicine*, *26*(2), 156–161. https://doi.org/10.1053/j.jepm.2017.01.001

White, K. L., Paine, S., & Harris, J. (2017). A clinical evaluation of the pharmacokinetics and pharmacodynamics of intravenous alfaxalone in cyclodextrin in male and female rats following a loading dose and constant rate infusion. *Veterinary Anaesthesia and Analgesia*, *44*(4), 865–875. https://doi.org/10.1016/j.vaa.2017.01.001

Whittem, T., Pasloske, K. S., Heit, M. C., & Ransinghe, M. G. (2008). The pharmacokinetics and pharmacodynamics of alfaxalone in cats after single and multiple intravenous administration of Alfaxan ® at clinical and supraclinical doses. *Journal of Veterinary Pharmacology and Therapeutics*, *31*(6), 571–579. https://doi.org/10.1111/j.1365-2885.2008.00998.x

Wood, F. L., Houston, J. B., & Hallifax, D. (2017). Clearance prediction methodology needs fundamental improvement: Trends common to rat and human hepatocytes/microsomes and implications for experimental methodology. In *Drug Metabolism and Disposition* (Vol. 45, Issue 11, pp. 1178–1188). American Society for Pharmacology and Experimental Therapy. https://doi.org/10.1124/dmd.117.077040

Wood, Francesca L, Houston, J. B., & Hallifax, D. (2018). Importance of the Unstirred Water Layer and Hepatocyte Membrane Integrity In Vitro for Quantification of Intrinsic Metabolic Clearance s. *DRUG METABOLISM AND DISPOSITION Drug Metab Dispos*, *46*, 268–278. https://doi.org/10.1124/dmd.117.078949

Yang, C., Chen, M. Y., Chen, T., & Cheng, C. (2014). Dose-dependent effects of isoflurane on cardiovascular function in rats. *Tzu Chi Medical Journal*, *26*(3), 119–122. https://doi.org/10.1016/j.tcmj.2014.07.005

Yawno, T., Miller, S. L., Bennet, L., Wong, F., Hirst, J. J., Fahey, M., & Walker, D. W. (2017). Ganaxolone: A new treatment for neonatal seizures. In *Frontiers in Cellular Neuroscience* (Vol. 11, p. 246). Frontiers Media S.A. https://doi.org/10.3389/fncel.2017.00246

Zambricki, E. A., & D'Alecy, L. G. (2004). Rat Sex Differences in Anesthesia. *Comparative Medicine*, *54*(1), 49–53.

Zhang, D., Luo, G., Ding, X., & Lu, C. (2012). Preclinical experimental models of drug metabolism and disposition in drug discovery and development. *Acta Pharmaceutica Sinica B*, *2*(6), 549–561.

https://doi.org/10.1016/j.apsb.2012.10.004

Zhang, L., Strong, J. M., Qiu, W., Lesko, L. J., & Huang, S. M. (2006). Scientific perspectives on drug transporters and their role in drug interaction. *Molecular Pharmaceutics*, *3*(1), 62–69. https://doi.org/10.1021/mp050095h

Zomorodi, K., Carlile, D. J., & Houston, J. B. (1995). Kinetics of diazepam metabolism in rat hepatic microsomes and hepatocytes and their use in predicting in vivo hepatic clearance. *Xenobiotica; the Fate of Foreign Compounds in Biological Systems*, *25*(9), 907–916. http://www.ncbi.nlm.nih.gov/pubmed/8553684

8. Appendix

Additional data for chapter 6

Rat liver microsomes

Individual concentration vs IPRED

Male

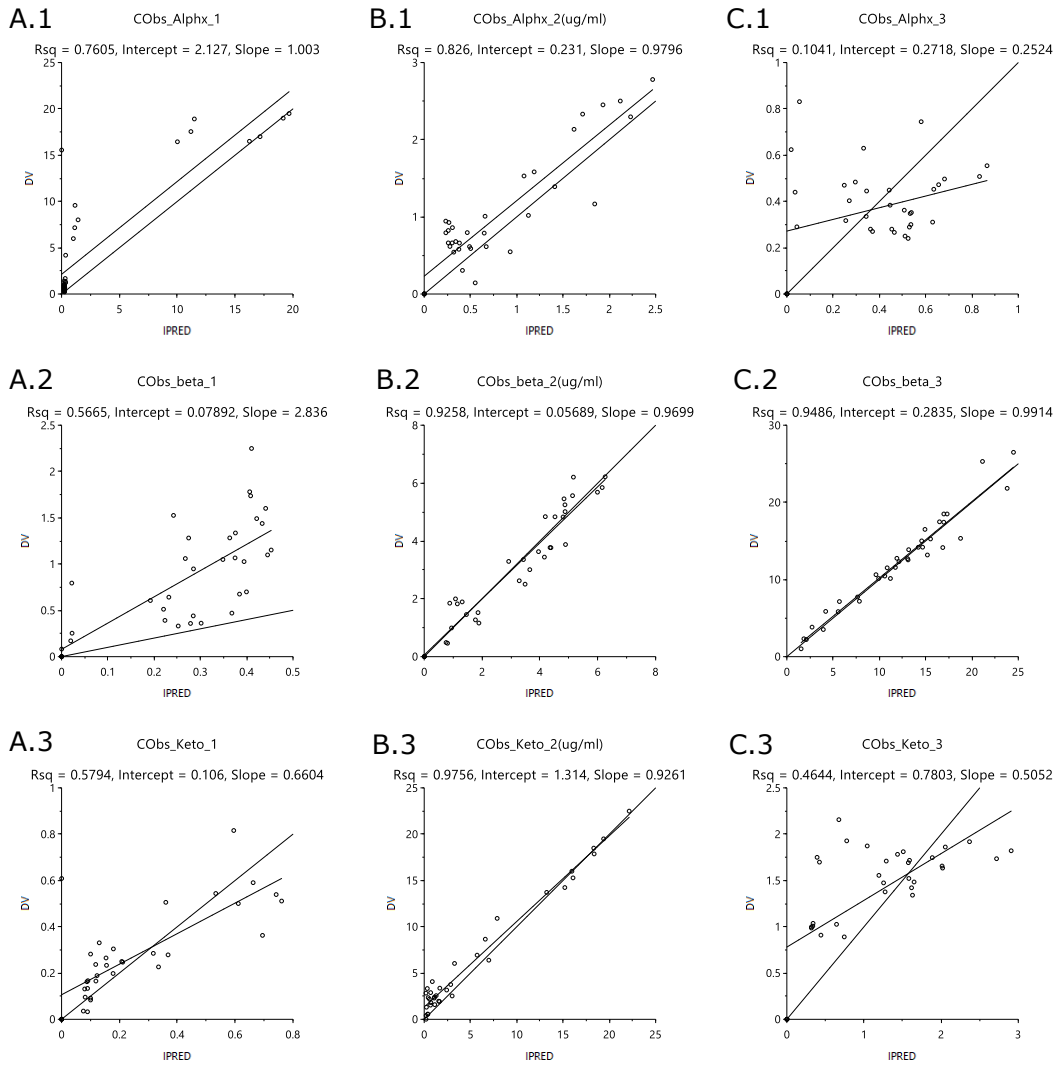

Figure 8.1. alphaxalone and metabolites model fit (DV vs IPRED). A, B, C groups represents a scenario of one substrate and the formation of two metabolites. A.1, 2, 3. Represents alphaxalone depletion as substrate (A.1) and beta (A.2) and keto (A.3) -alphaxalone formation from it. B.1, 2, 3 represents keto-alphaxalone depletion as substrate (B.3) and alphaxalone (B.1) and beta (B.2) -alphaxalone formation from it. C.1, 2, 3 represents beta-alphaxalone depletion as substrate (C.2) and alphaxalone (C.1) and keto-alphaxalone (C.3) formation from it.

Appendix

Female

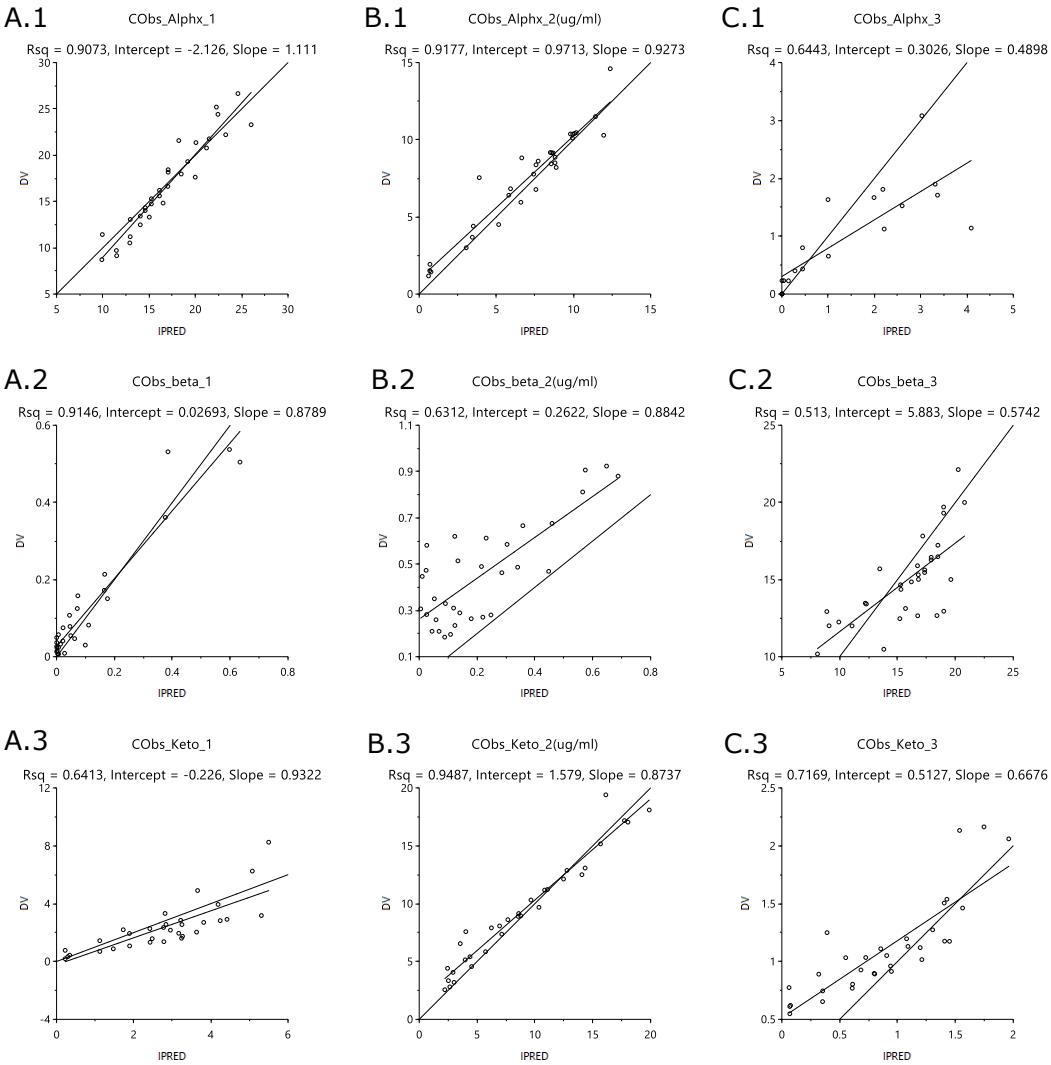

Figure 8.2. alphaxalone and metabolites model fit (DV vs IPRED). A, B, C groups represents a scenario of one substrate and the formation of two metabolites. A.1, 2, 3. Represents alphaxalone depletion as substrate (A.1) and beta (A.2) and keto (A.3) -alphaxalone formation from it. B.1, 2, 3 represents keto-alphaxalone depletion as substrate (B.3) and alphaxalone (B.1) and beta (B.2) -alphaxalone formation from it. C.1, 2, 3 represents beta-alphaxalone depletion as substrate (C.2) and alphaxalone (C.1) and keto-alphaxalone (C.3) formation from it.

Human liver microsomes

Individual concentration vs IPRED

Male

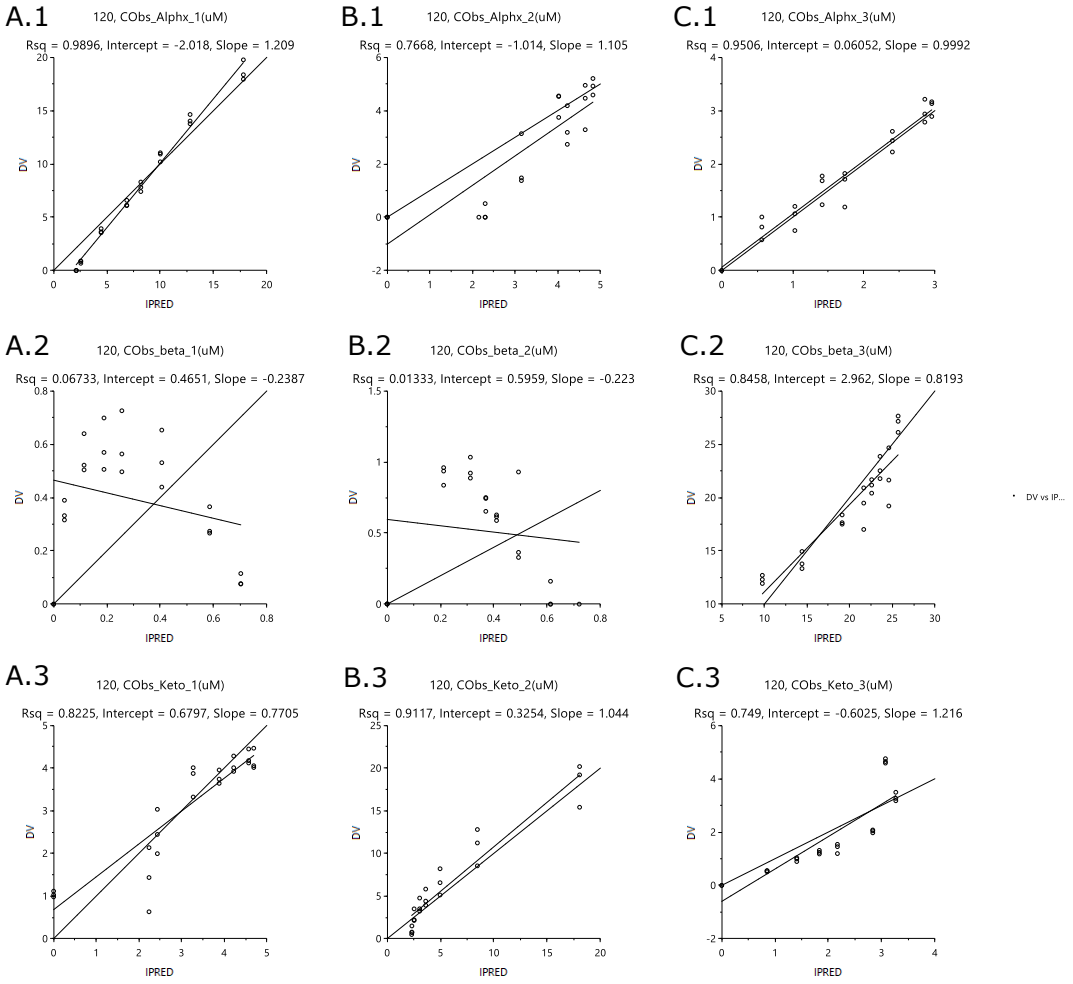

Figure 8.3. alphaxalone and metabolites model fit (DV vs IPRED). A, B, C groups represents a scenario of one substrate and the formation of two metabolites. A.1, 2, 3. Represents alphaxalone depletion as substrate (A.1) and beta (A.2) and keto (A.3) -alphaxalone formation from it. B.1, 2, 3 represents keto-alphaxalone depletion as substrate (B.3) and alphaxalone (B.1) and beta (B.2) -alphaxalone formation from it. C.1, 2, 3 represents beta-alphaxalone depletion as substrate (C.2) and alphaxalone (C.1) and keto-alphaxalone (C.3) formation from it.

Appendix

Female

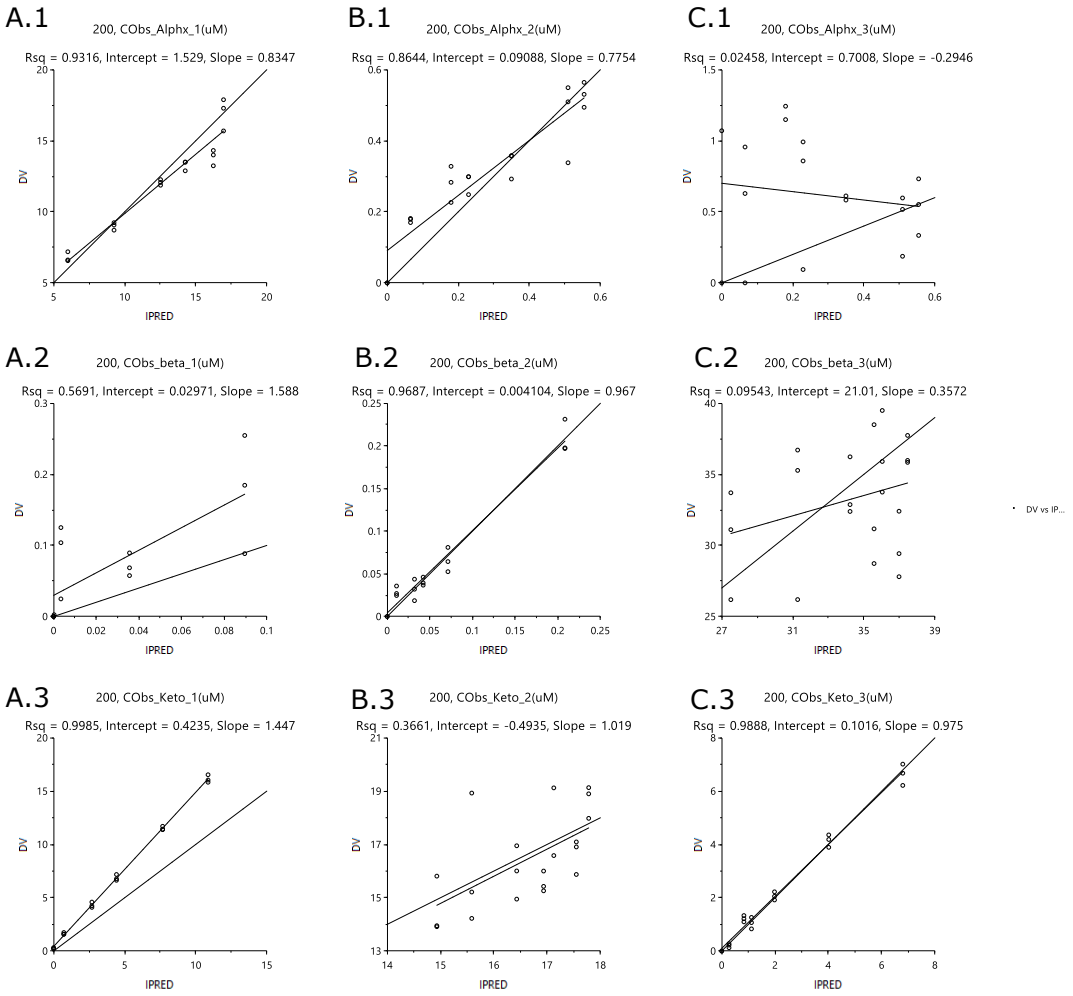

Figure 8.4. alphaxalone and metabolites model fit (DV vs IPRED). A, B, C groups represents a scenario of one substrate and the formation of two metabolites. A.1, 2, 3. Represents alphaxalone depletion as substrate (A.1) and beta (A.2) and keto (A.3) -alphaxalone formation from it. B.1, 2, 3 represents keto-alphaxalone depletion as substrate (B.3) and alphaxalone (B.1) and beta (B.2) -alphaxalone formation from it. C.1, 2, 3 represents beta-alphaxalone depletion as substrate (C.2) and alphaxalone (C.1) and keto-alphaxalone (C.3) formation from it.

Rabbit liver microsomes

Individual concentration vs IPRED

Male

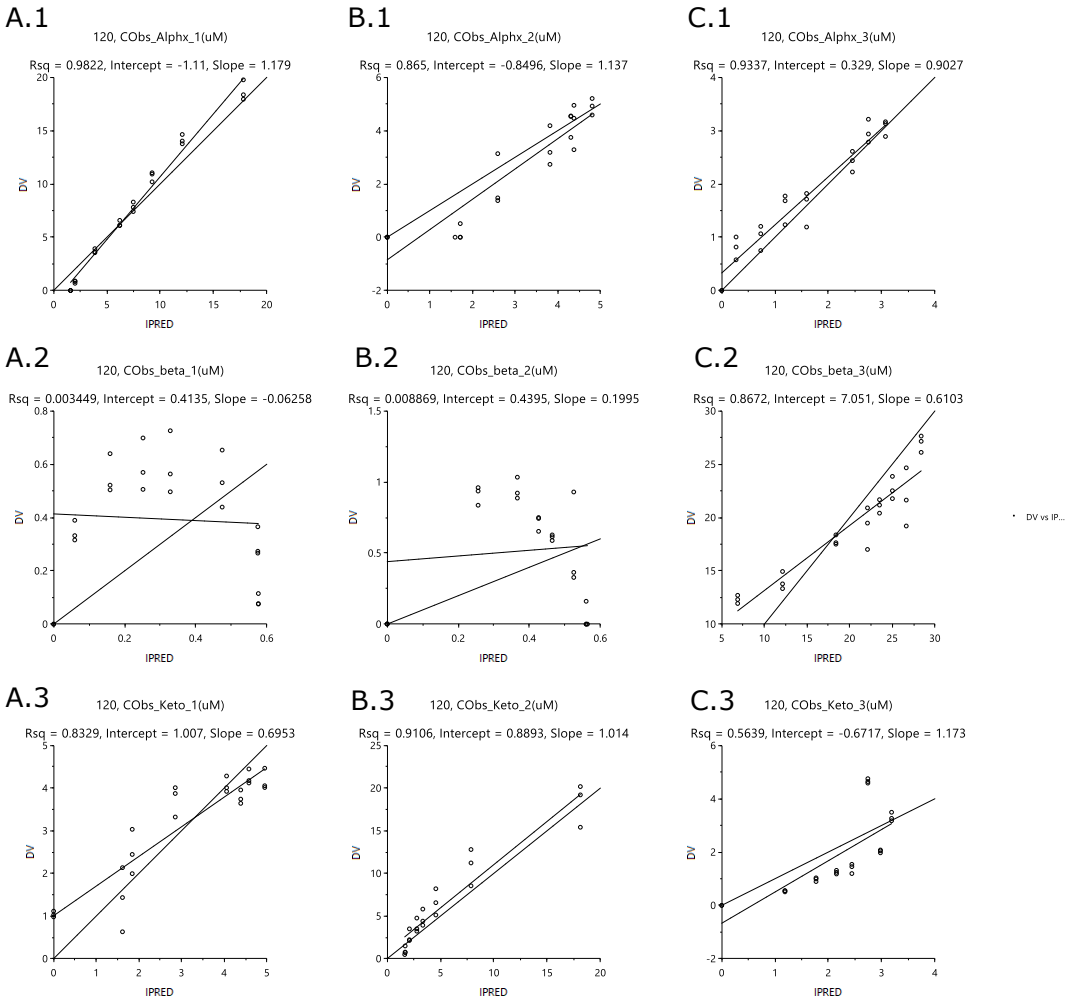

Figure 8.5. alphaxalone and metabolites model fit (DV vs IPRED). A, B, C groups represents a scenario of one substrate and the formation of two metabolites. A.1, 2, 3. Represents alphaxalone depletion as substrate (A.1) and beta (A.2) and keto (A.3) -alphaxalone formation from it. B.1, 2, 3 represents keto-alphaxalone depletion as substrate (B.3) and alphaxalone (B.1) and beta (B.2) -alphaxalone formation from it. C.1, 2, 3 represents beta-alphaxalone depletion as substrate (C.2) and alphaxalone (C.1) and keto-alphaxalone (C.3) formation from it.

Appendix

Female

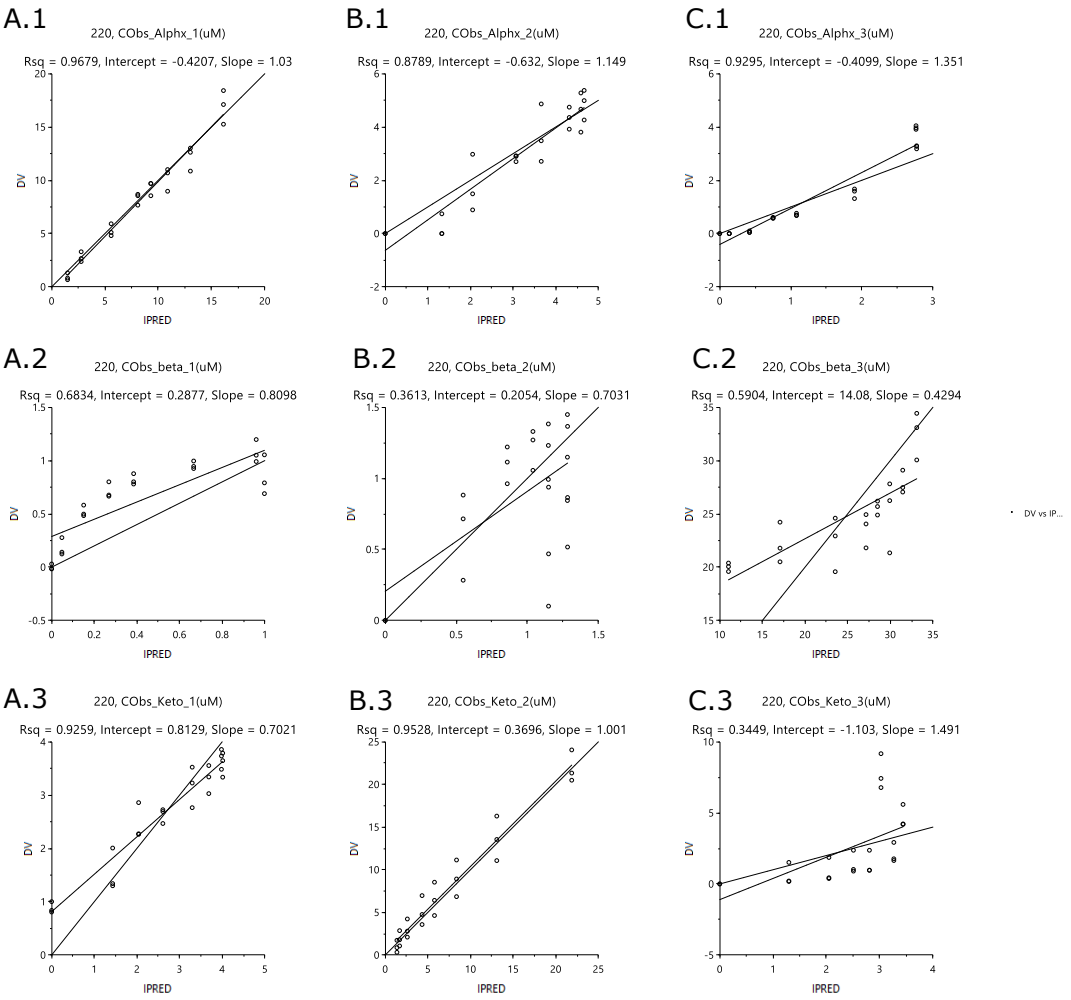

Figure 8.6. alphaxalone and metabolites model fit (DV vs IPRED). A, B, C groups represents a scenario of one substrate and the formation of two metabolites. A.1, 2, 3. Represents alphaxalone depletion as substrate (A.1) and beta (A.2) and keto (A.3) -alphaxalone formation from it. B.1, 2, 3 represents keto-alphaxalone depletion as substrate (B.3) and alphaxalone (B.1) and beta (B.2) -alphaxalone formation from it. C.1, 2, 3 represents beta-alphaxalone depletion as substrate (C.2) and alphaxalone (C.1) and keto-alphaxalone (C.3) formation from it.

Dog liver microsomes

Individual concentration vs IPRED

Male

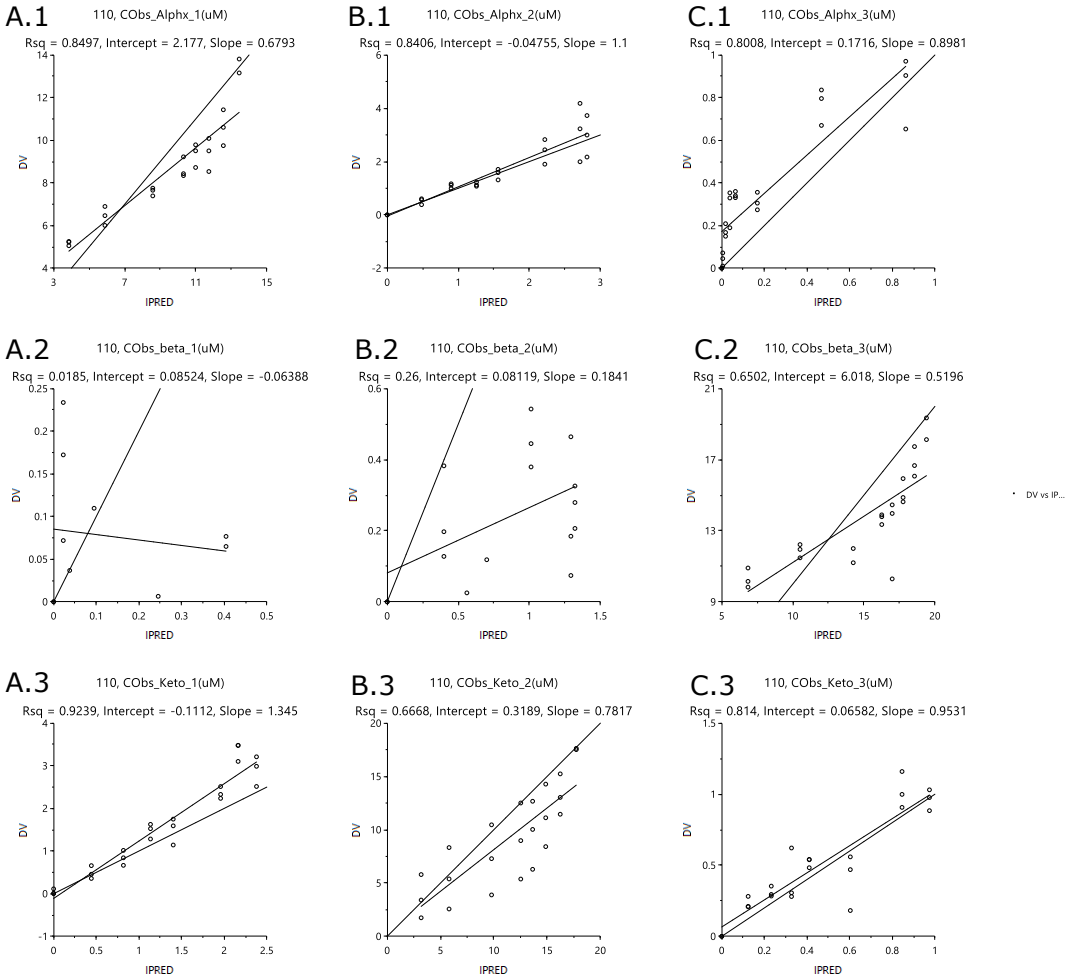

Figure 8.7. Alphaxalone and metabolites model fit (DV vs IPRED). A, B, C groups represents a scenario of one substrate and the formation of two metabolites. A.1, 2, 3. Represents alphaxalone depletion as substrate (A.1) and beta (A.2) and keto (A.3) -alphaxalone formation from it. B.1, 2, 3 represents keto-alphaxalone depletion as substrate (B.3) and alphaxalone (B.1) and beta (B.2) -alphaxalone formation from it. C.1, 2, 3 represents beta-alphaxalone depletion as substrate (C.2) and alphaxalone (C.1) and keto-alphaxalone (C.3) formation from it.

Appendix

Female

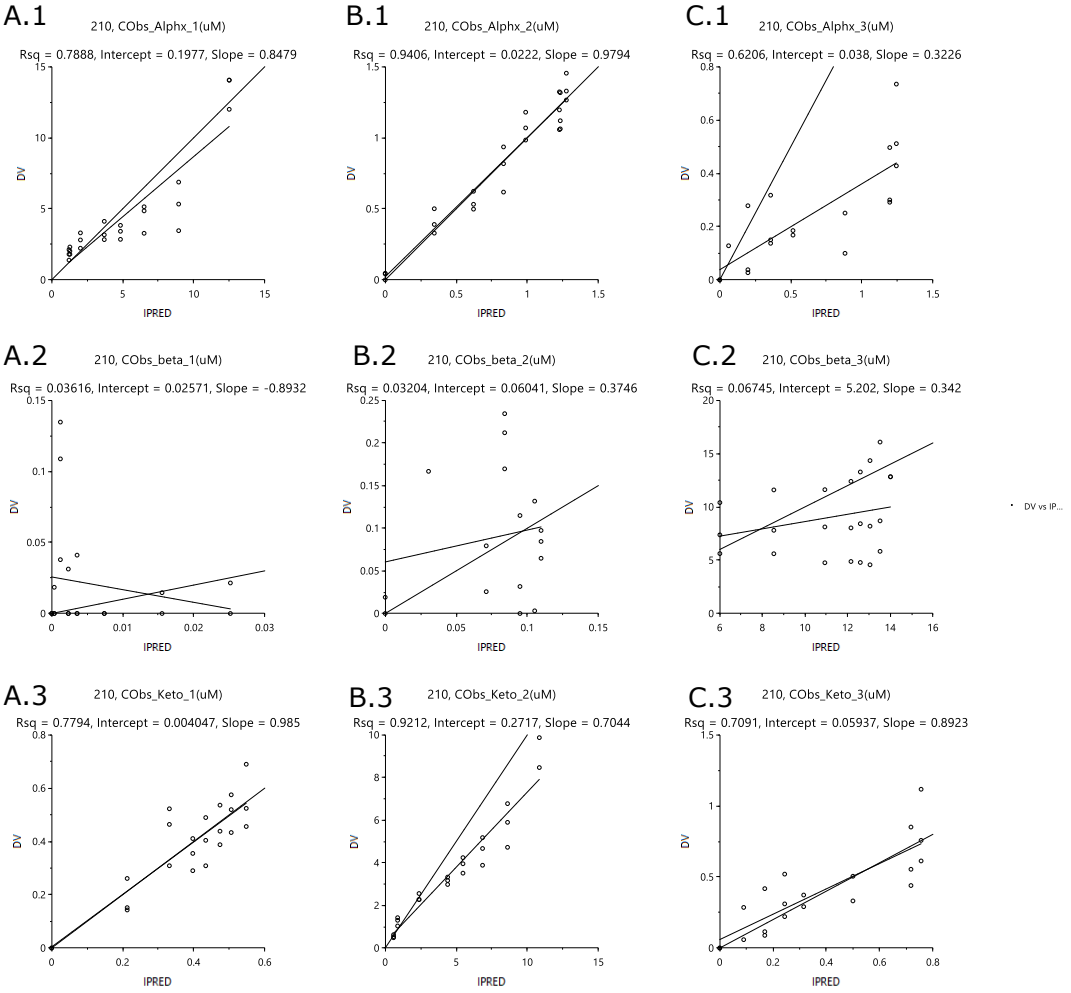

Figure 8.8. alphaxalone and metabolites model fit (DV vs IPRED). A, B, C groups represents a scenario of one substrate and the formation of two metabolites. A.1, 2, 3. Represents alphaxalone depletion as substrate (A.1) and beta (A.2) and keto (A.3) -alphaxalone formation from it. B.1, 2, 3 represents keto-alphaxalone depletion as substrate (B.3) and alphaxalone (B.1) and beta (B.2) -alphaxalone formation from it. C.1, 2, 3 represents beta-alphaxalone depletion as substrate (C.2) and alphaxalone (C.1) and keto-alphaxalone (C.3) formation from it.

Monkey liver microsomes

Individual concentration vs IPRED

Male

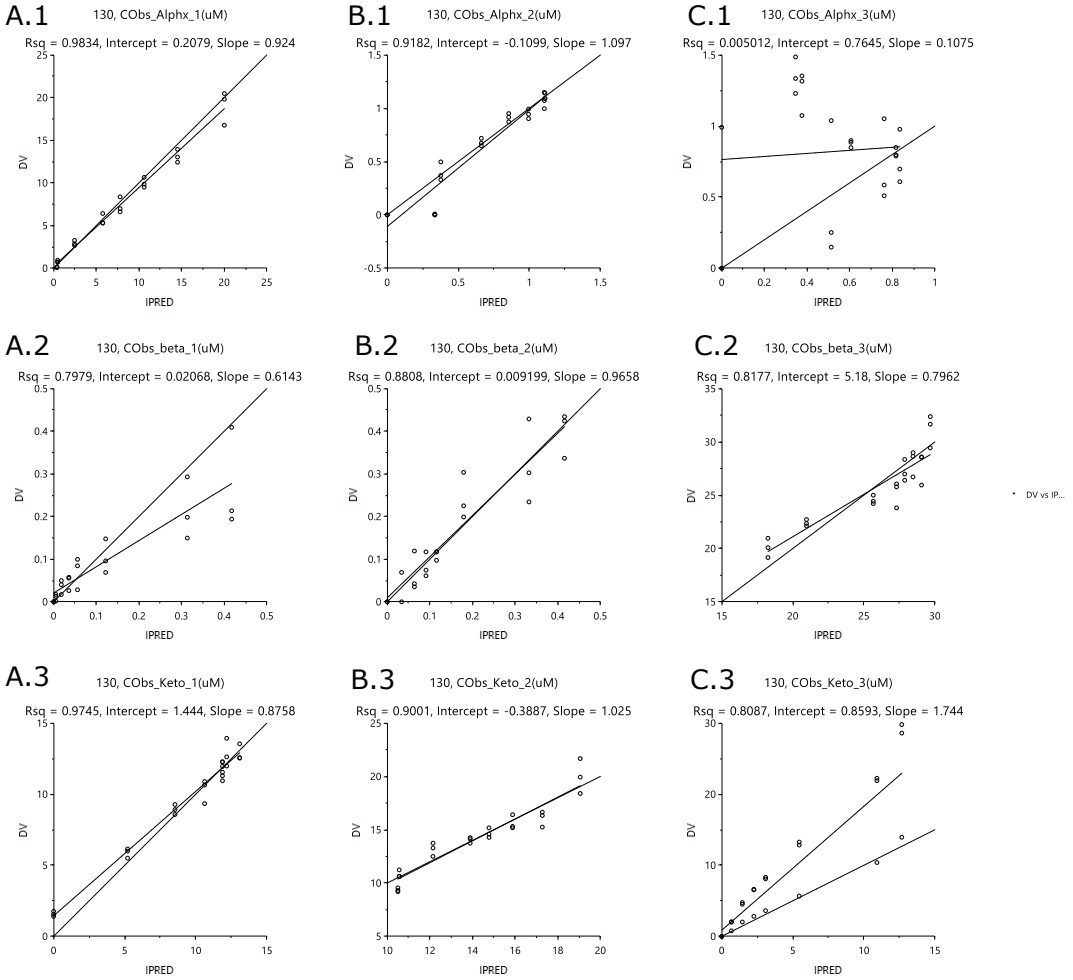

Figure 8.9. alphaxalone and metabolites model fit (DV vs IPRED). A, B, C groups represents a scenario of one substrate and the formation of two metabolites. A.1, 2, 3. Represents alphaxalone depletion as substrate (A.1) and beta (A.2) and keto (A.3) -alphaxalone formation from it. B.1, 2, 3 represents keto-alphaxalone depletion as substrate (B.3) and alphaxalone (B.1) and beta (B.2) -alphaxalone formation from it. C.1, 2, 3 represents beta-alphaxalone depletion as substrate (C.2) and alphaxalone (C.1) and keto-alphaxalone (C.3) formation from it.

Appendix

Female

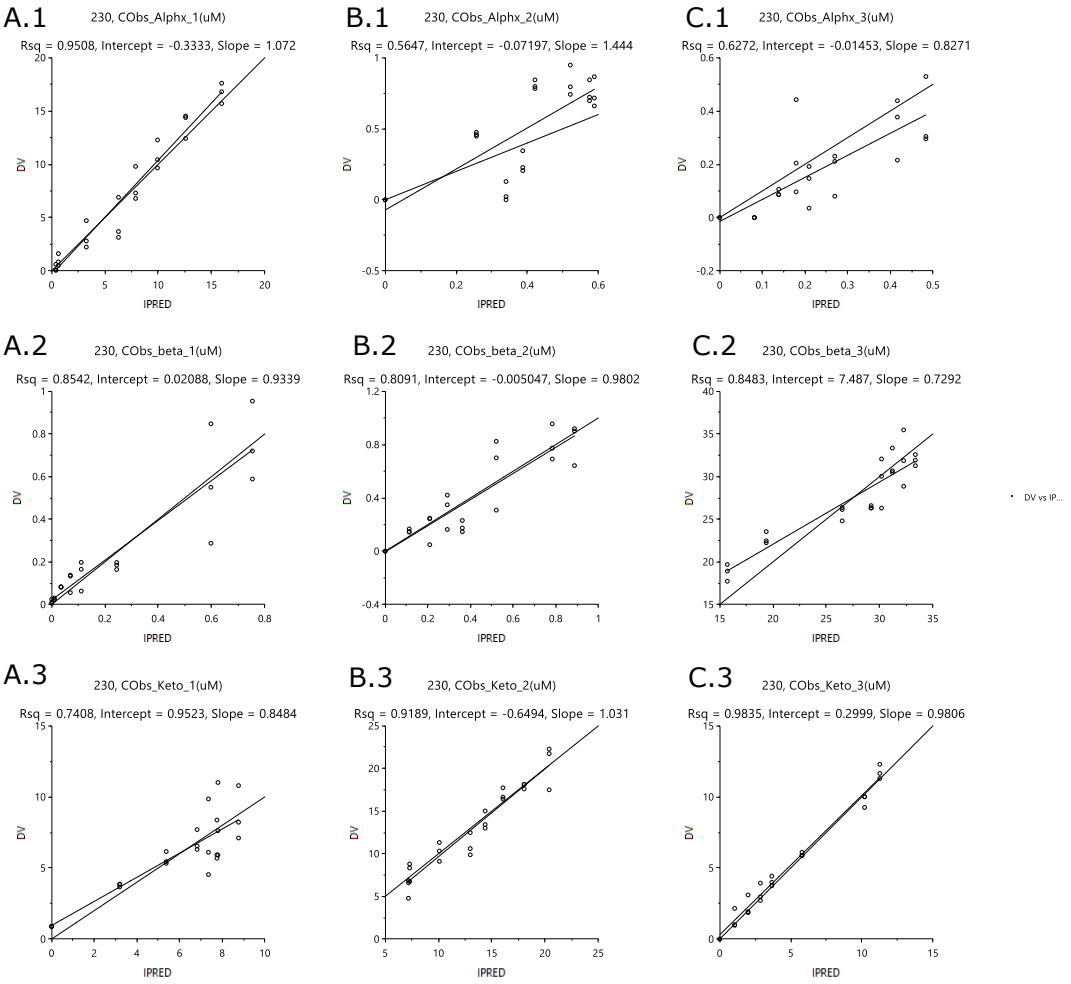

Figure 8.10. alphaxalone and metabolites model fit (DV vs IPRED). A, B, C groups represents a scenario of one substrate and the formation of two metabolites. A.1, 2, 3. Represents alphaxalone depletion as substrate (A.1) and beta (A.2) and keto (A.3) -alphaxalone formation from it. B.1, 2, 3 represents keto-alphaxalone depletion as substrate (B.3) and alphaxalone (B.1) and beta (B.2) -alphaxalone formation from it. C.1, 2, 3 represents beta-alphaxalone depletion as substrate (C.2) and alphaxalone (C.1) and keto-alphaxalone (C.3) formation from it.

Keto and beta metabolite formation

Keto-alphaxalone

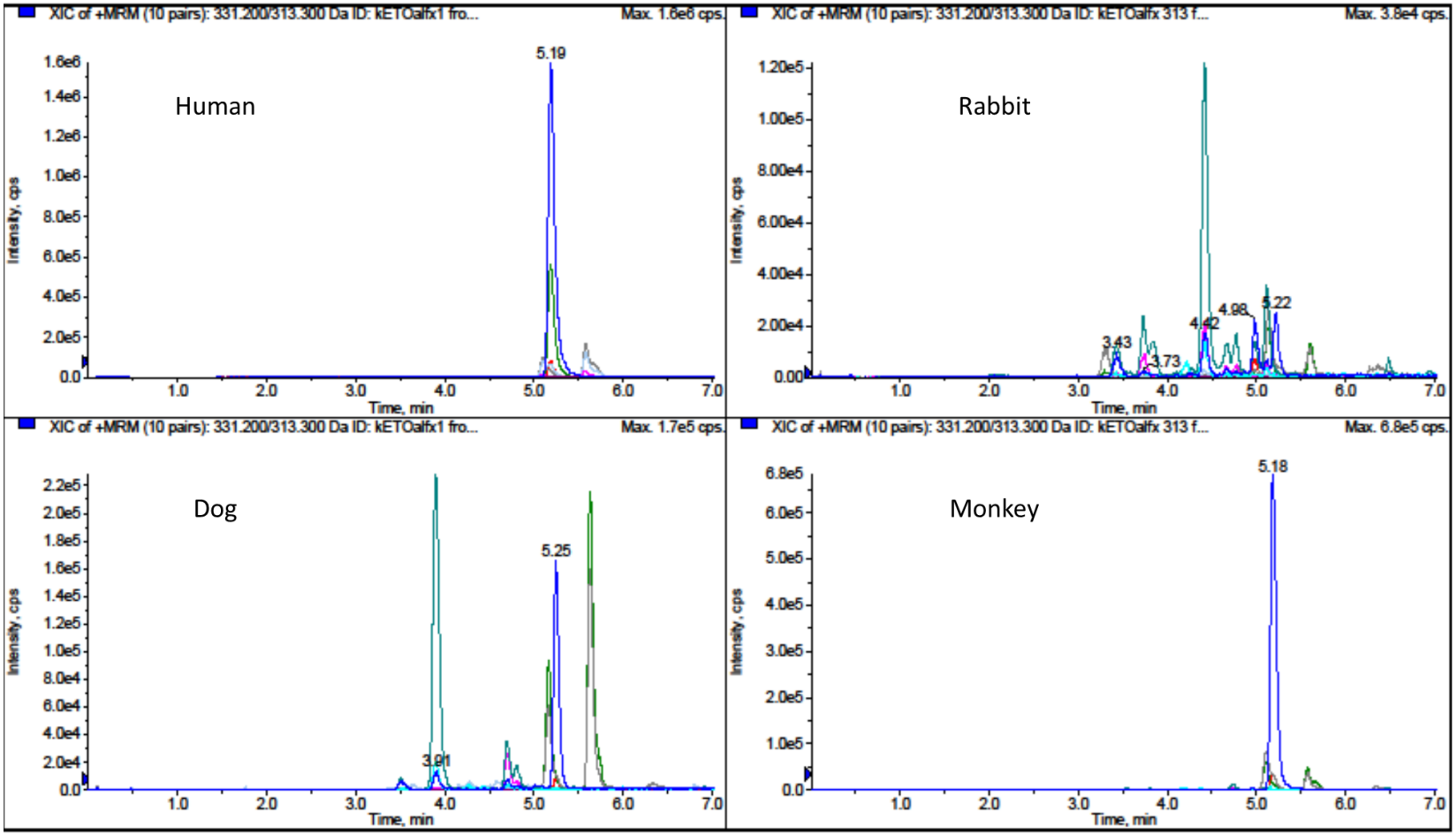

Figure 8.11: Metabolites formed when Keto-alphaxalone used as substrate in male human, rabbit, dog and monkey

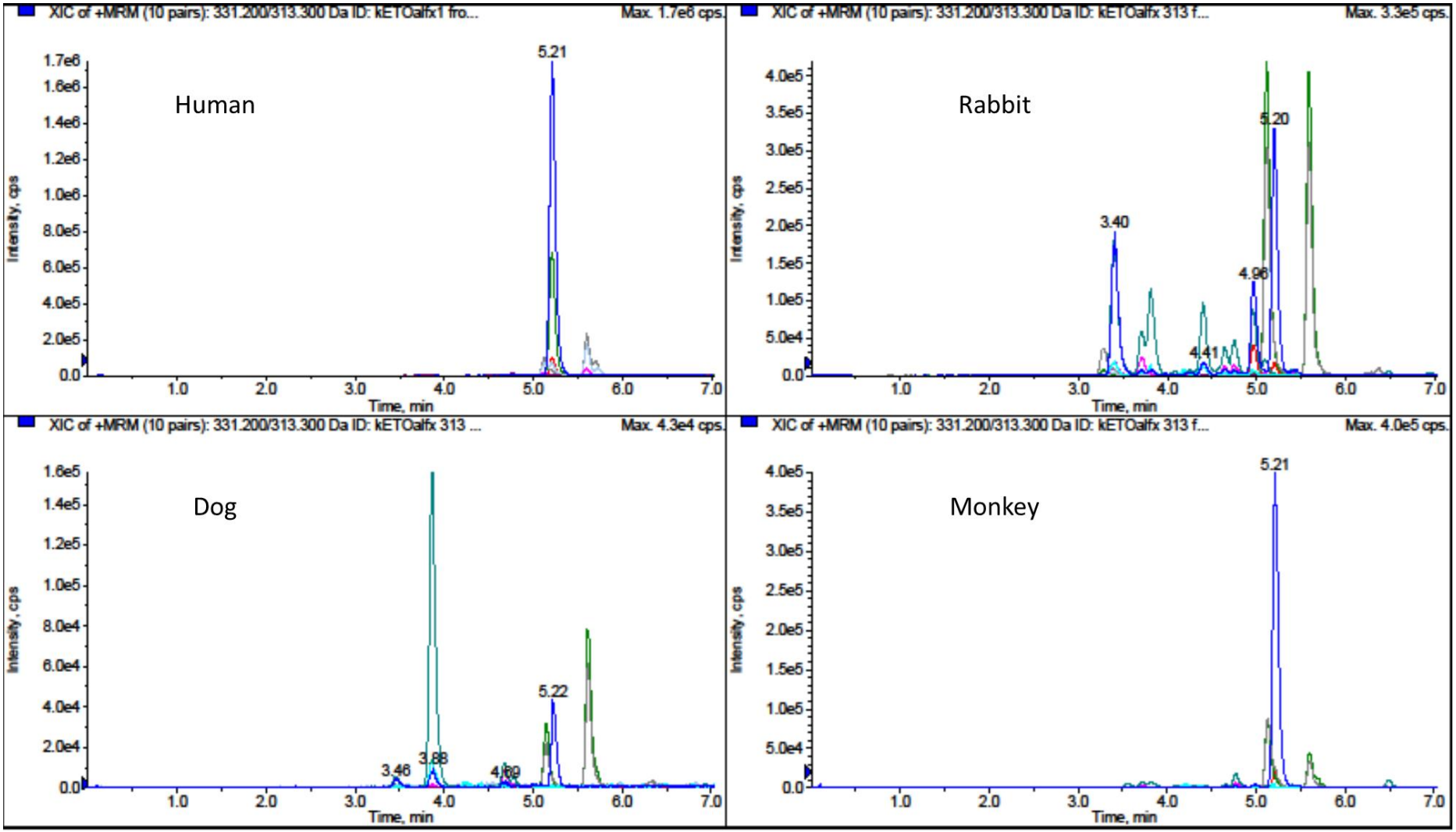

Figure 8.12: Metabolites formed when Keto-alphaxalone used as substrate in female human, rabbit, dog and monkey

Table 8.1: Table for metabolites detected in keto substrate for all species and gender

Keto substrate

Retintion time		Male human	female human	Male rabbit	Female rabbit	Male dog	Female dog	Male Rhesus	Female rhesus
6.45		small	✔	✔	✔	✔		✔	
5.8, 5.7	alpha met?	✔	✔	✔	-	✔	✔	✔	✔
5.6	alpha	✔	✔	✔	✔	✔	✔	✔	✔
5.45	Keto met?								
5.4	??	✔							✔
5.3?	beta met?	✔	✔	✔		✔		✔	
5.22	keto		✔	✔	✔	✔	✔	✔	✔
5.17		✔							
5.1	beta	✔	✔	✔	✔	✔	✔	✔	✔
5.11				✔				✔	✔
5.03	??		tiny?						
4.99	product X	no		✔	✔	✔		✔	✔
4.8	M4				✔	✔	✔		
4.74		✔	✔	✔	✔	✔	✔	✔	✔
4.65				✔	✔	✔			✔
4.59,4.57						✔			
4.4				✔ ✔ ✔	✔				✔
4.31								✔	✔
4.2									✔
4	M5								
3.95						✔			
3.86				✔			✔		✔
3.8	M6				✔			✔	
3.7			✔	✔	✔			✔	✔
3.57						✔		✔	✔
3.4				✔	✔		✔		

Species comparison for beta- alphaxalone metabolic pathway

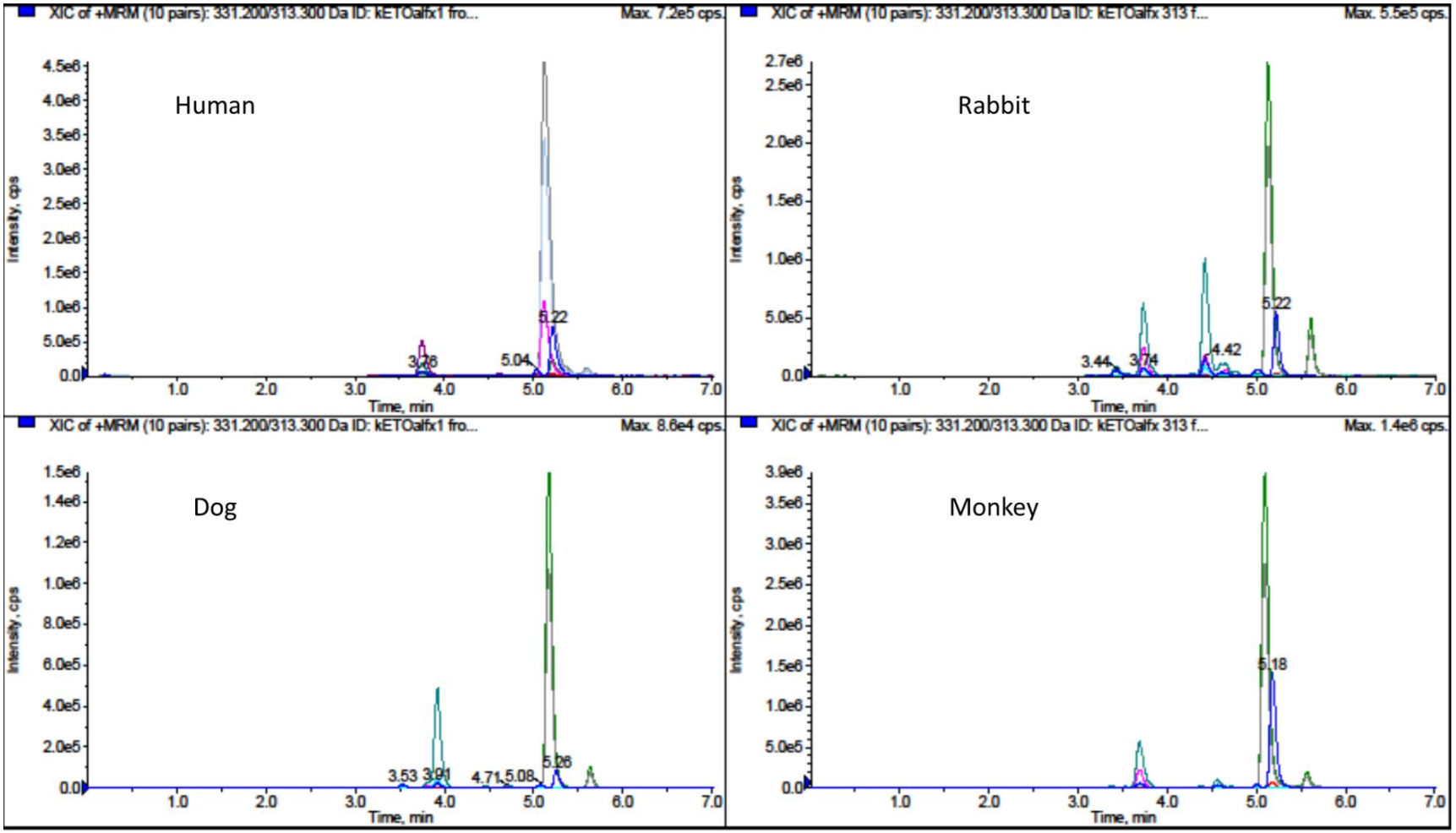

Figure 8.13: Metabolites formed when beta-alphaxalone used as substrate in male human, rabbit, dog and monkey.

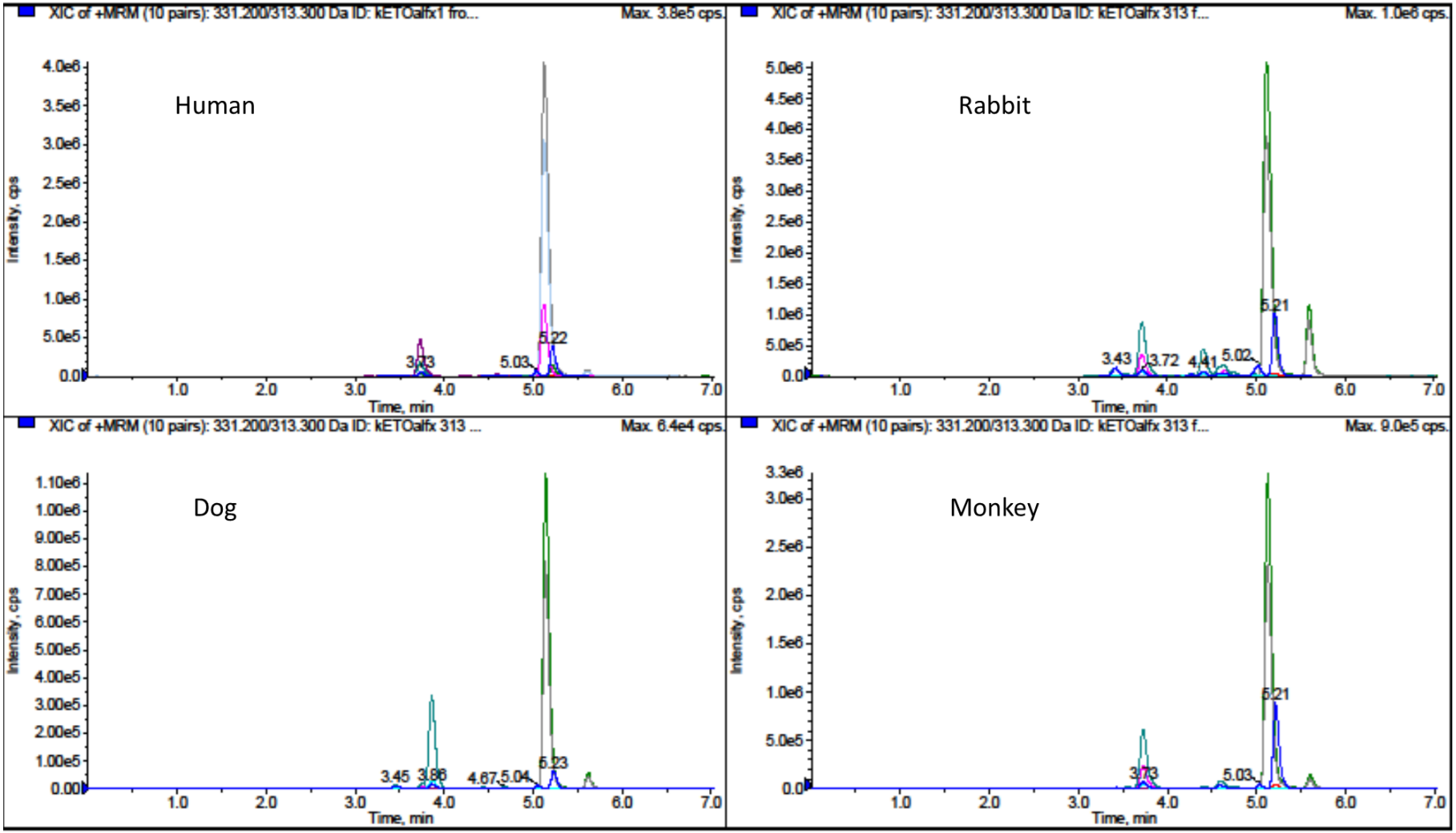

Figure 8.14: Metabolites formed when beta-alphaxalone used as substrate in male human, rabbit, dog and monkey

Table 8.2: Table of male and female other species interanad intra individual comparison

Retintion time		Male human	female human	Male rabbit	Female rabbit	Male dog	Female dog	Male Rhesus	Female rhesus
6.45									
5.8, 5.7	alpha met?								
5.6	alpha	✔	✔	✔	✔	✔	✔	✔	✔
5.45	Keto met?								
5.4	??								
5.3?	beta met?								
5.22	keto	✔	✔	✔	✔	✔	✔	✔	✔
5.1	beta	✔	✔	✔	✔	✔	✔	✔	✔
5.1								✔	
5.03	??	✔	✔	✔	✔		✔		✔
4.99	product X					✔	✔		
4.8	M4				✔				
4.74							✔	✔	✔
4.67					✔	✔			
4.65		✔		✔	✔		✔		
4.59,4.57				✔	✔	✔	✔		
4.4				✔		✔	✔		
4.31					✔			✔	
4.2									
4	M5								
3.95									
3.86								✔	✔
3.8	M6								
3.7		✔ ✔ ✔	✔ ✔ ✔	✔	✔	✔	✔		
3.57				✔	✔				
3.4				✔	✔	✔	✔		

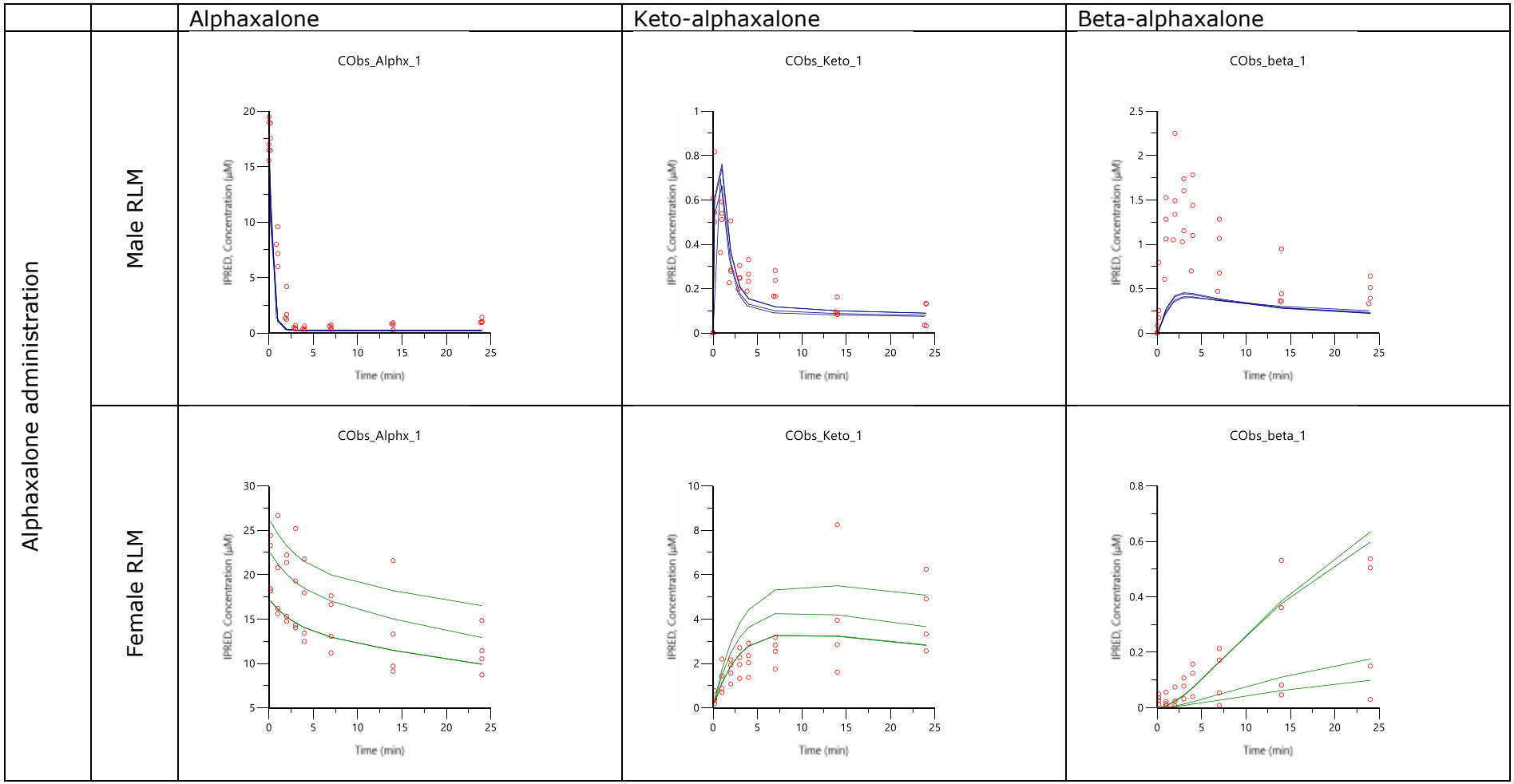

Figure 8.15. Model fit of alphaxalone substrate and keto-alphaxalone and beta-alphaxalone formation from male and female rat liver microsomes (RLM). The Y axis represent substrate concentration (µM) while the X axis represent time (minutes). n=4 representative.

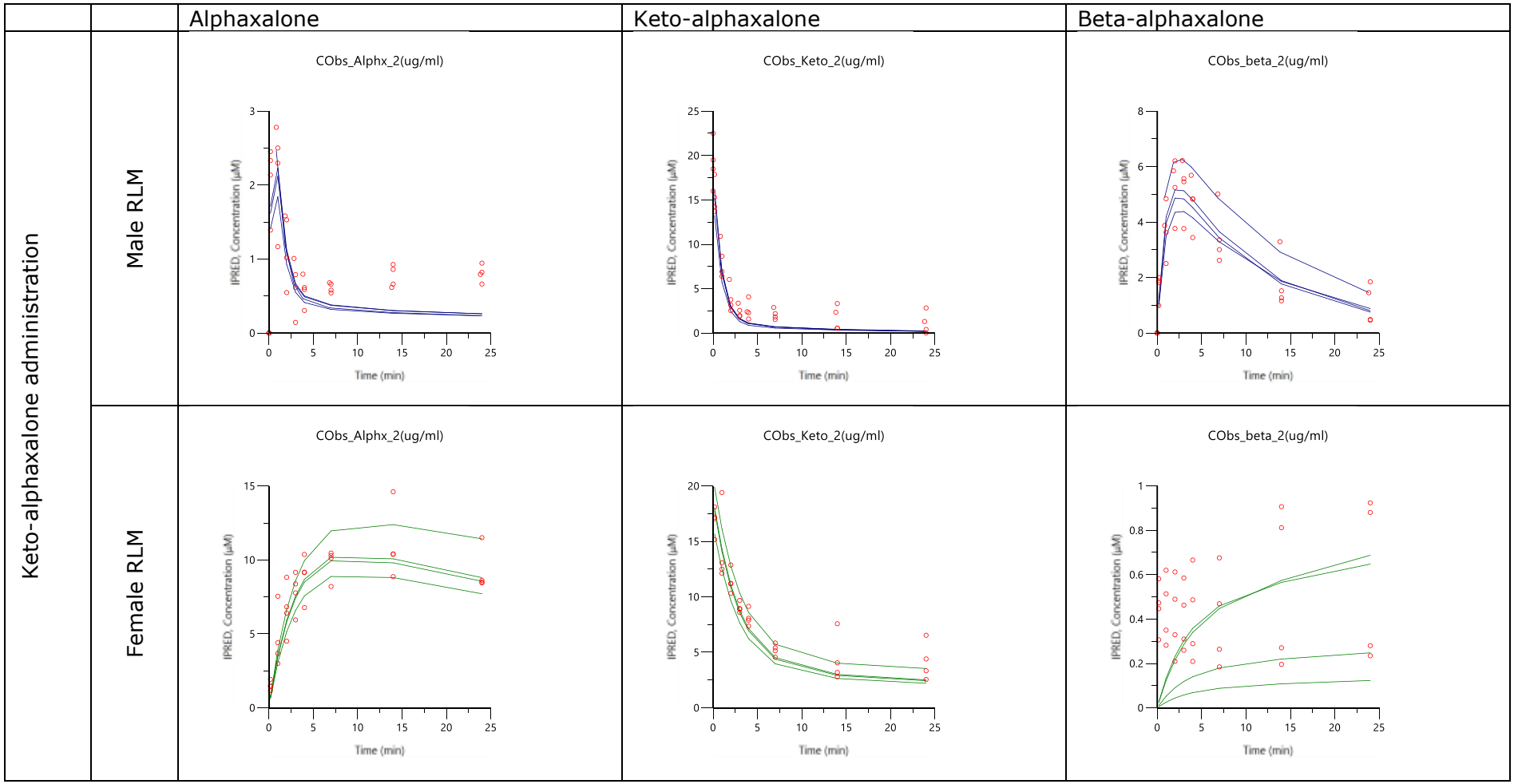

Figure 8.16. Model fit of keto-alphaxalone substrate and alphaxalone and beta-alphaxalone formation from male and female rat liver microsomes (RLM). The Y axis represent substrate concentration (µM) while the X axis represent time (minutes). n=4 representative.

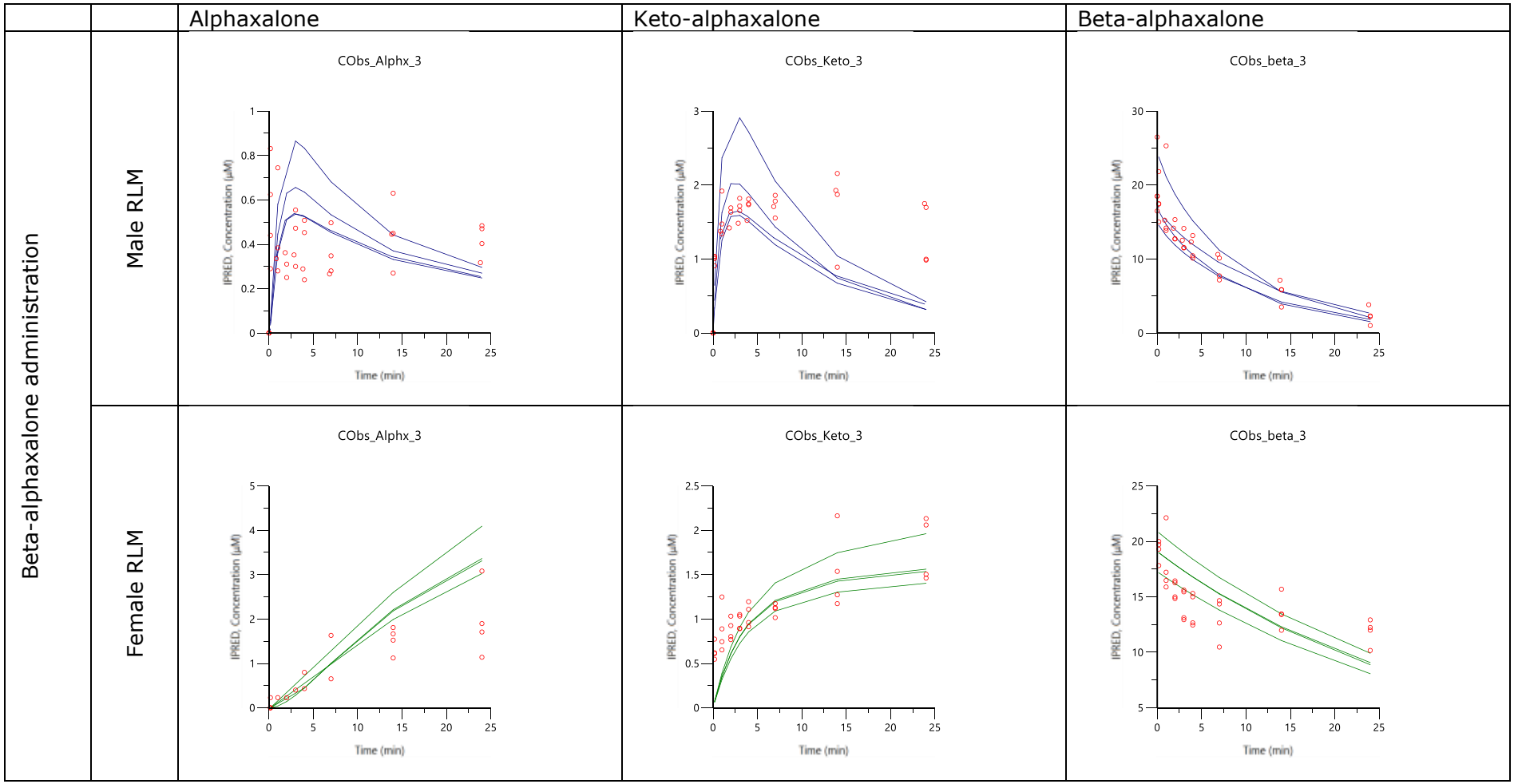

Figure 8.17. Model fit of beta-alphaxalone substrate and alphaxalone and keto-alphaxalone formation from male and female rat liver microsomes (RLM). The Y axis represent substrate concentration (µM) while the X axis represent time (minutes). n=4 representative.

		Alphaxalone	Keto-alphaxalone	Beta-alphaxalone
Alphaxalone administration	Male LM	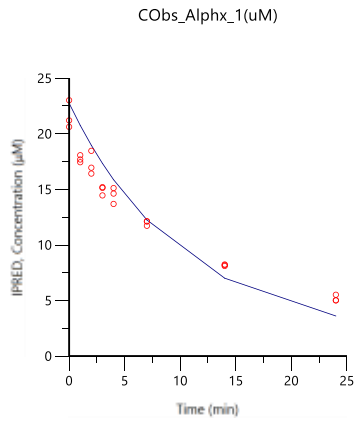	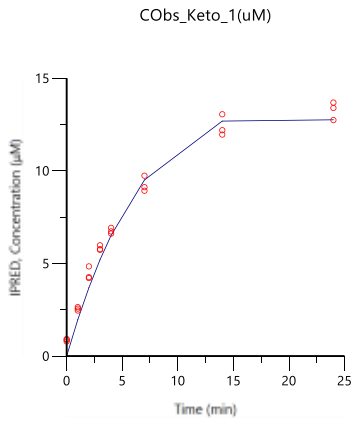	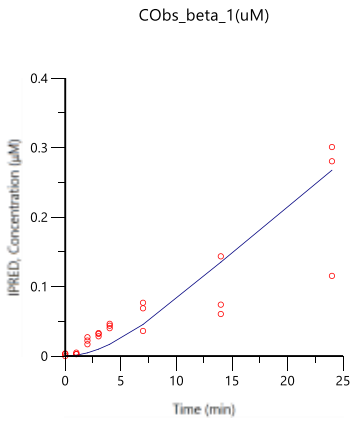
	Female LM	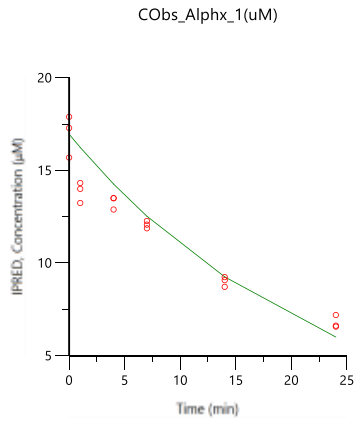	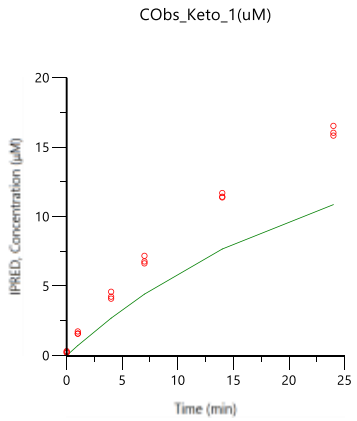	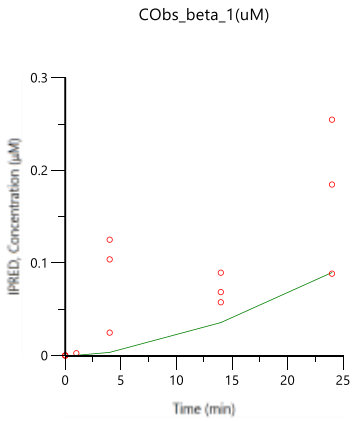

Figure 8.18 Model fit of alphaxalone substrate and keto-alphaxalone and beta-alphaxalone formation from male and female human liver microsomes (RLM). The Y axis represent substrate concentration (µM) while the X axis represent time (minutes).

		Alphaxalone	Keto-alphaxalone	Beta-alphaxalone
Keto-alphaxalone administration	Male LM	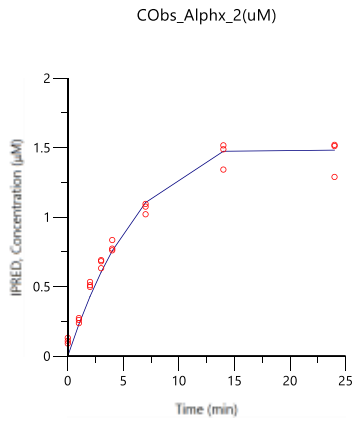	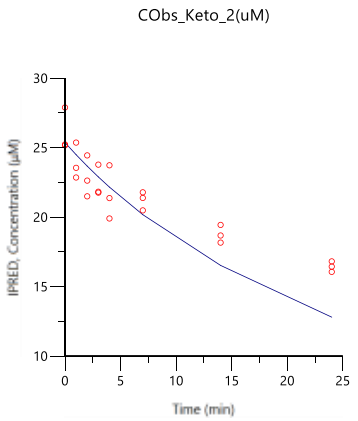	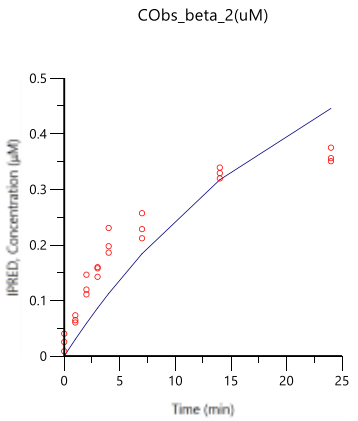
	Female LM	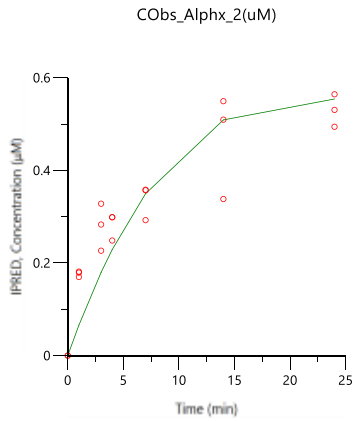	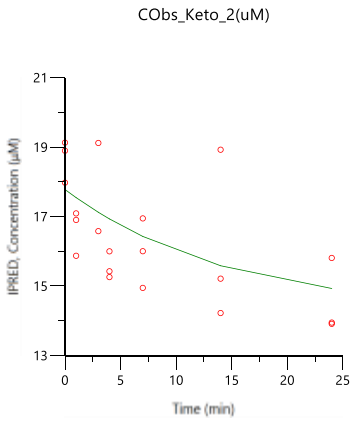	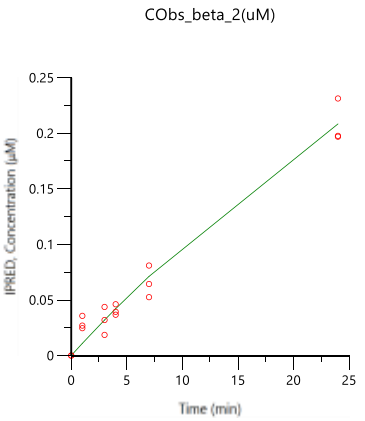

Figure 8.19. Model fit of keto-alphaxalone substrate and alphaxalone and beta-alphaxalone formation from male and female human liver microsomes. The Y axis represent substrate concentration (µM) while the X axis represent time (minutes).

		Alphaxalone	Keto-alphaxalone	Beta-alphaxalone
Beta-alphaxalone administration	Male LM	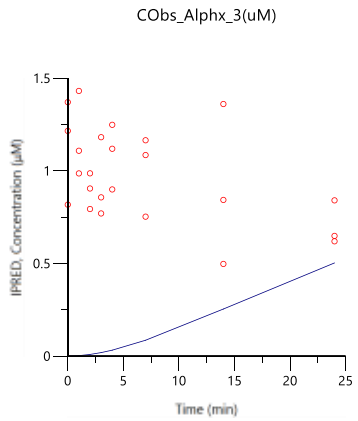	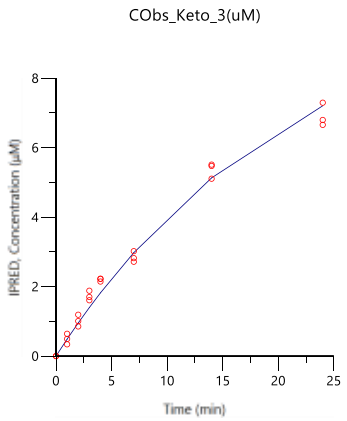	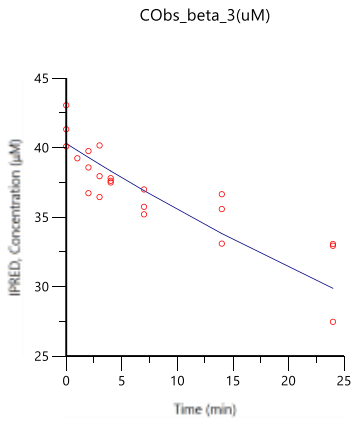
	Female LM	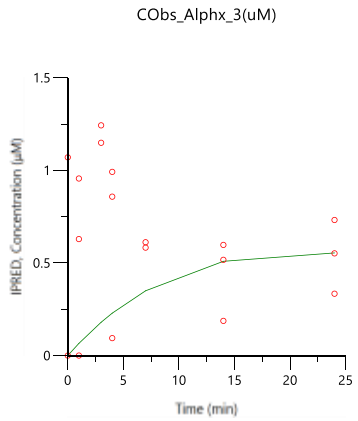	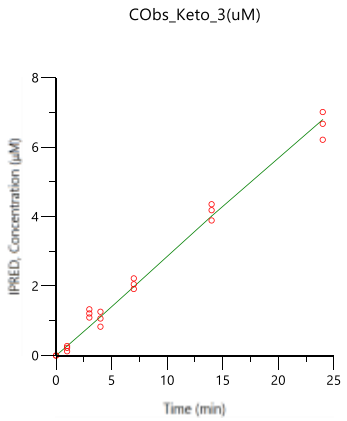	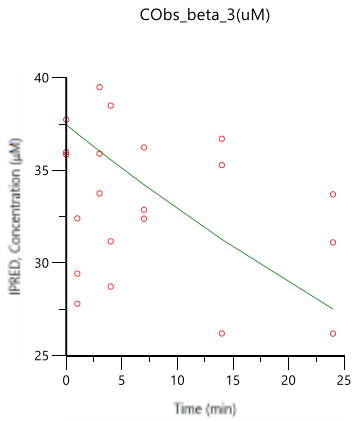

Figure 8.20. Model fit of beta-alphaxalone substrate and alphaxalone and keto-alphaxalone formation from male and female human liver microsomes. The Y axis represent substrate concentration (µM) while the X axis represent time (minutes).

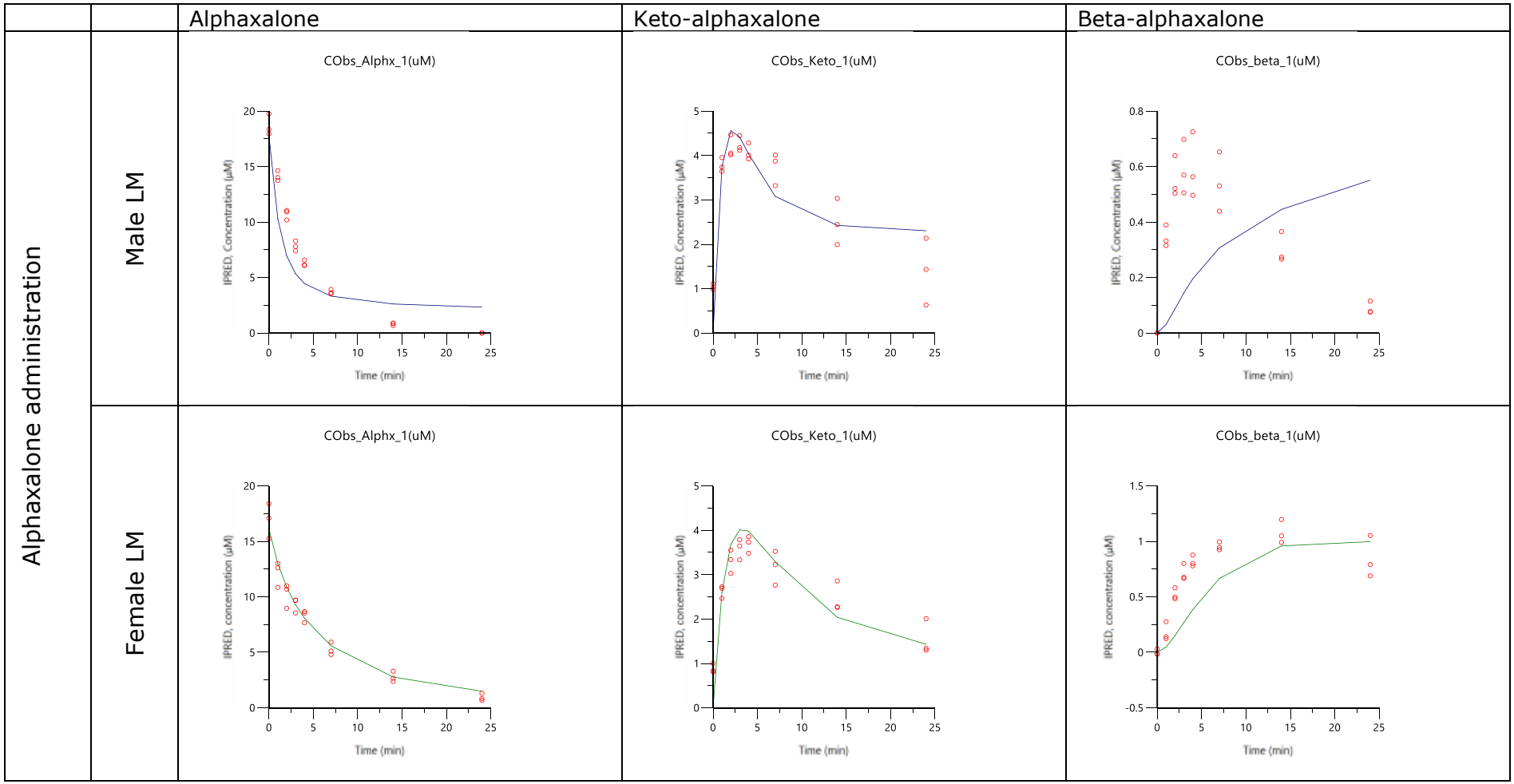

Figure 8.21. Model fit of alphaxalone substrate and keto-alphaxalone and beta-alphaxalone formation from male and female rabbit liver microsomes. The Y axis represent substrate concentration (µM) while the X axis represent time (minutes).

		Alphaxalone	Keto-alphaxalone	Beta-alphaxalone
Keto-alphaxalone administration	Male LM	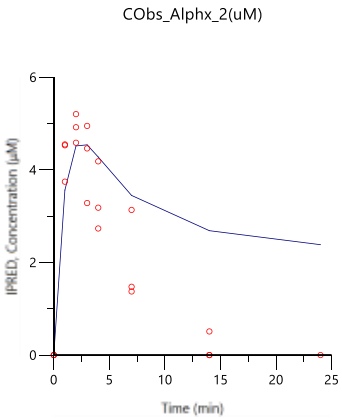	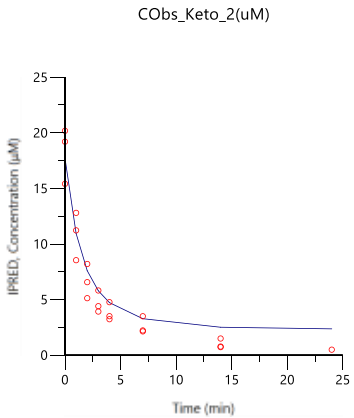	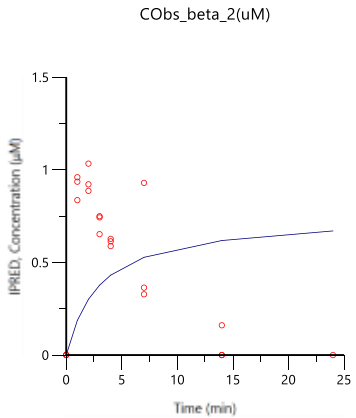
	Female LM	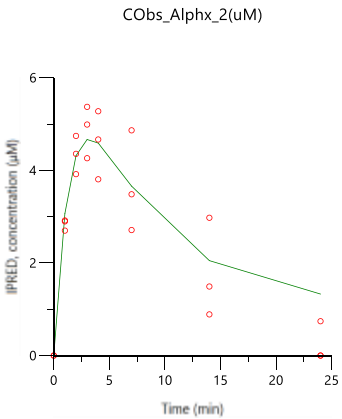	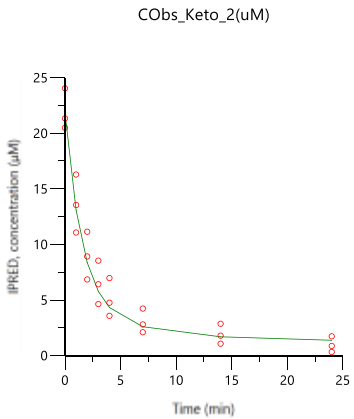	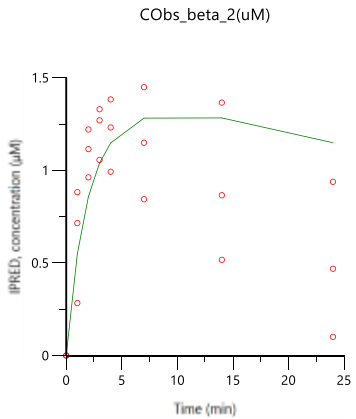

Figure 8.22. Model fit of keto-alphaxalone substrate and alphaxalone and beta-alphaxalone formation from male and female rabbit liver microsomes. The Y axis represent substrate concentration (µM) while the X axis represent time (minutes).

		Alphaxalone	Keto-alphaxalone	Beta-alphaxalone
Beta-alphaxalone administration	Male LM	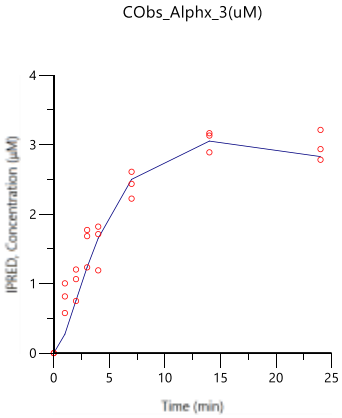	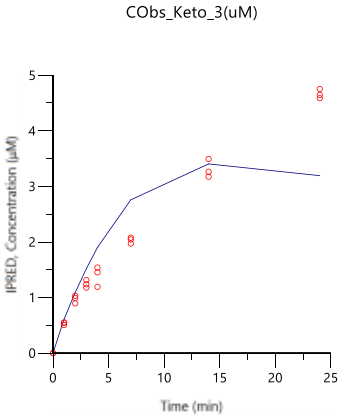	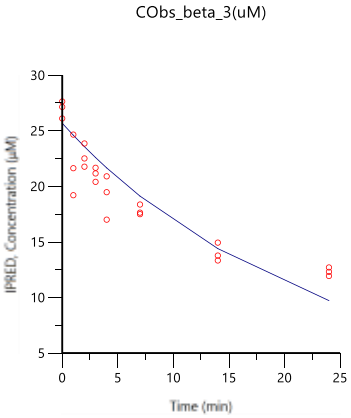
	Female LM	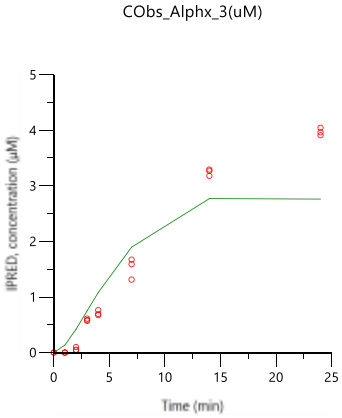	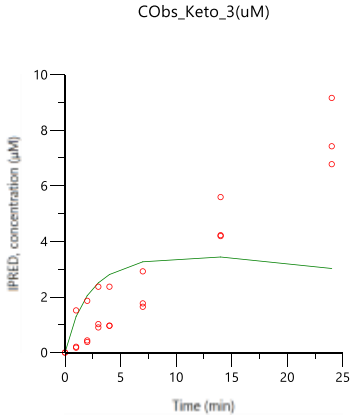	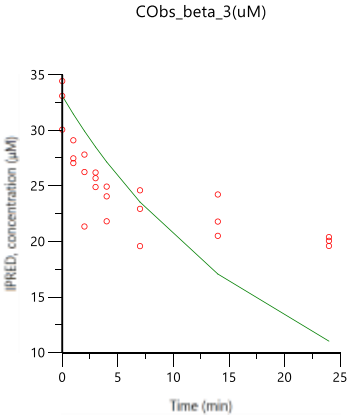

Figure 8.23. Model fit of beta-alphaxalone substrate and alphaxalone and keto-alphaxalone formation from male and female rabbit liver microsomes. The Y axis represent substrate concentration (µM) while the X axis represent time (minutes).

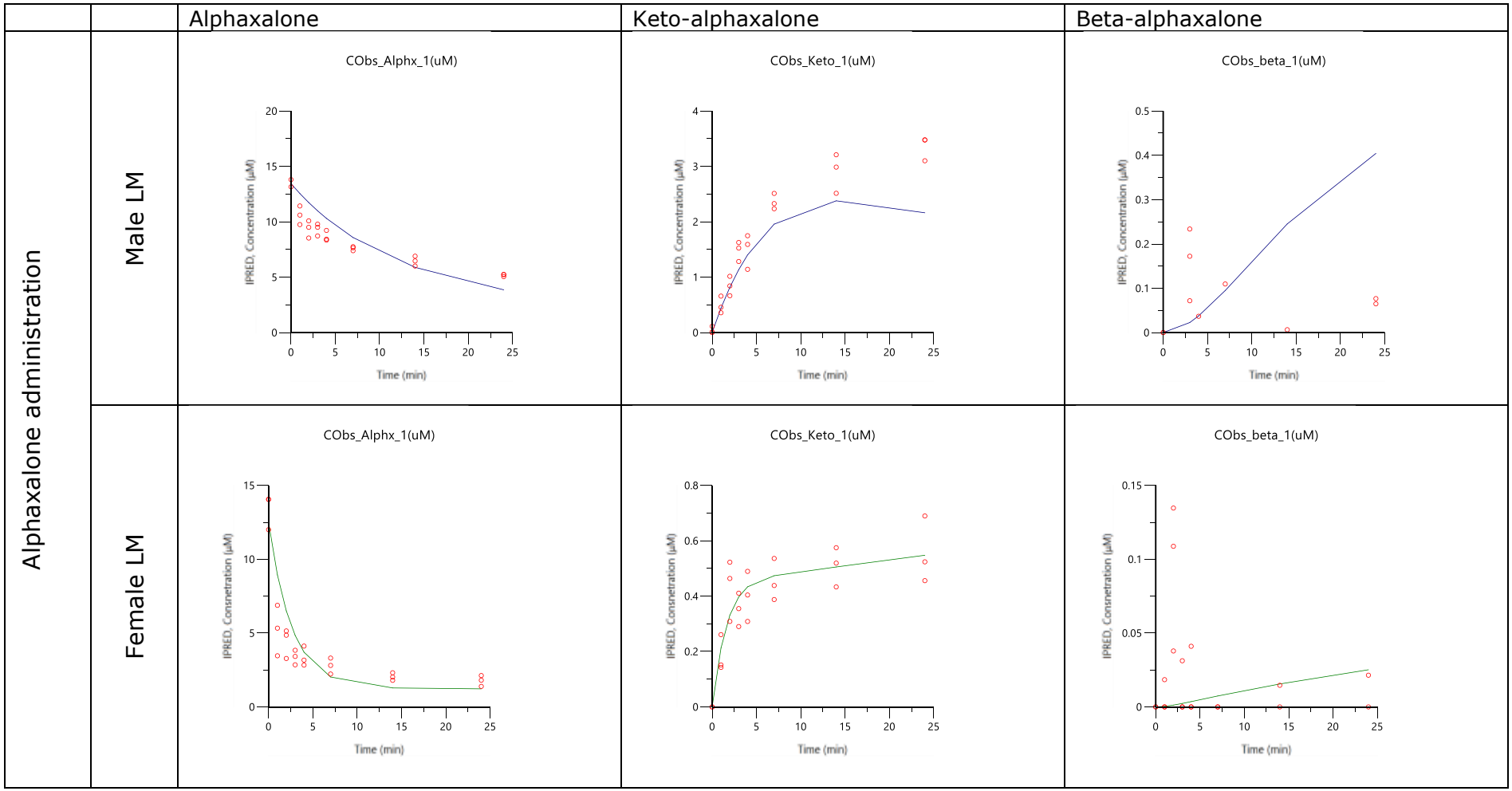

Figure 8.24. Model fit of alphaxalone substrate and keto-alphaxalone and beta-alphaxalone formation from male and female dog liver microsomes. The Y axis represent substrate concentration (µM) while the X axis represent time (minutes).

		Alphaxalone	Keto-alphaxalone	Beta-alphaxalone
Keto-alphaxalone administration	Male LM	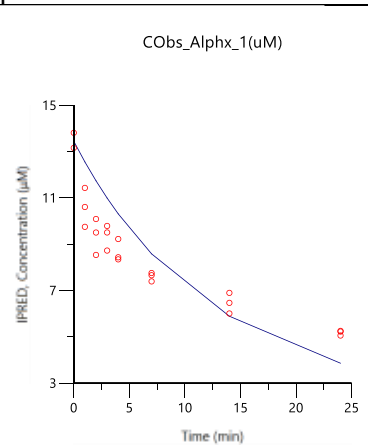	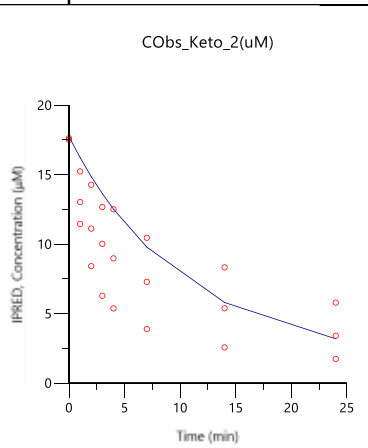	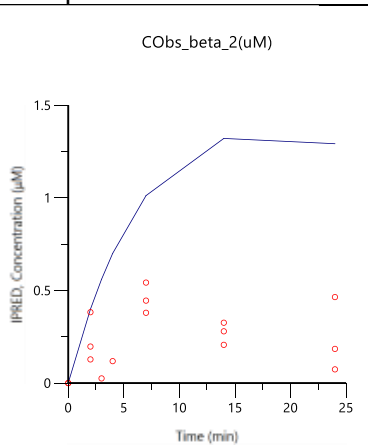
	Female LM	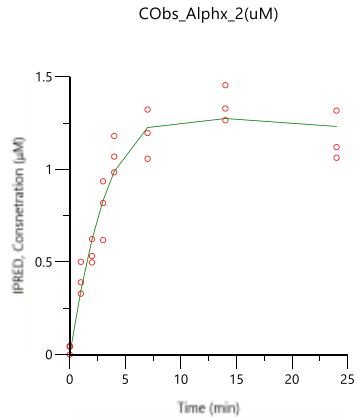	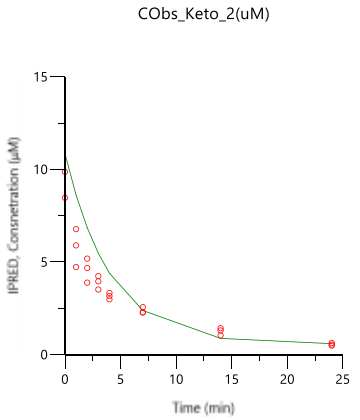	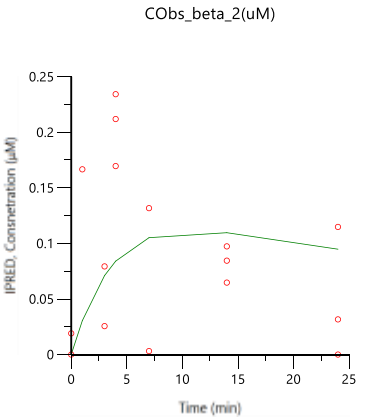

Figure 8.25. Model fit of keto-alphaxalone substrate and alphaxalone and beta-alphaxalone formation from male and female dog liver microsomes. The Y axis represent substrate concentration (µM) while the X axis represent time (minutes).

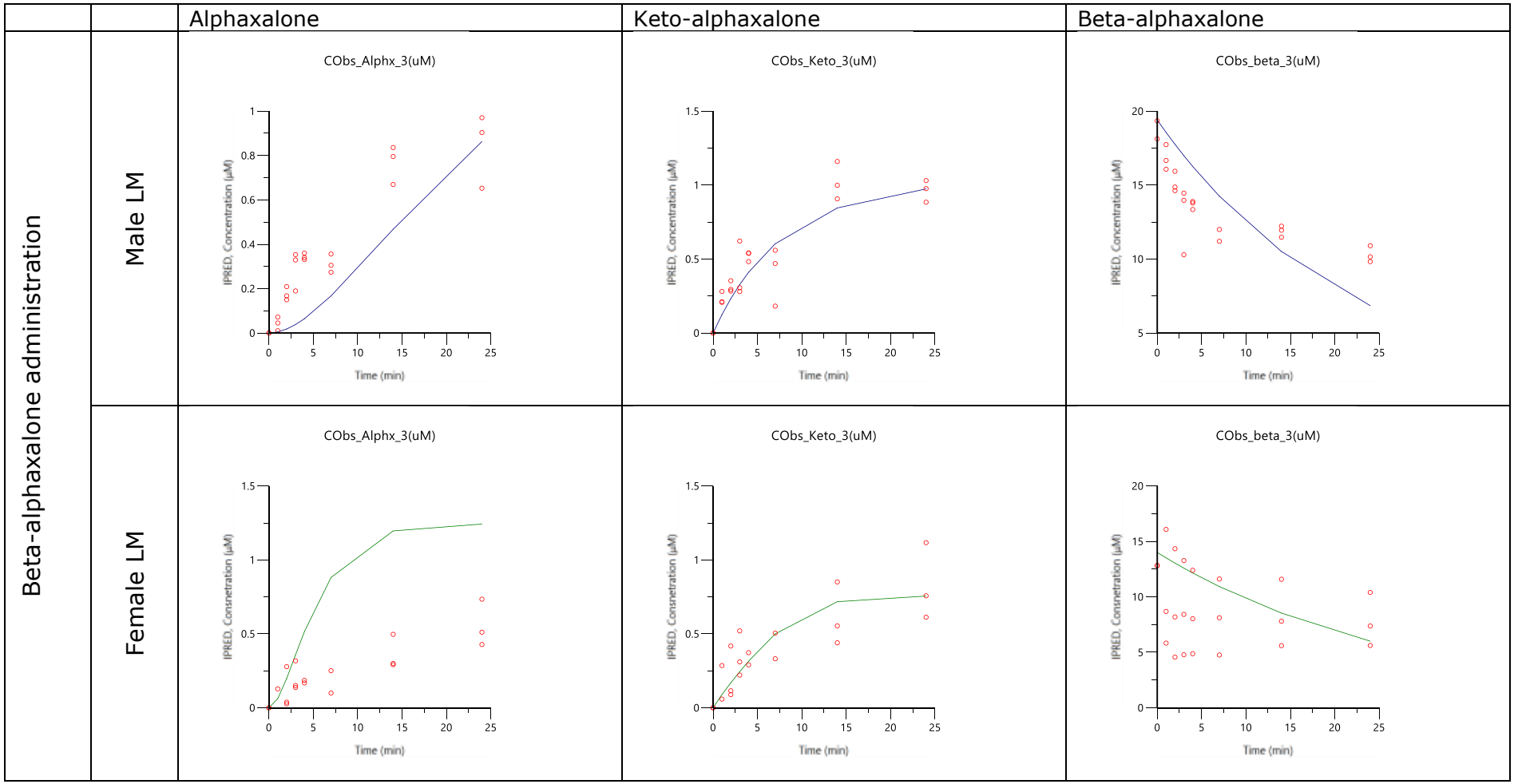

Figure 8.26. Model fit of beta-alphaxalone substrate and alphaxalone and keto-alphaxalone formation from male and female dog liver microsomes. The Y axis represent substrate concentration (µM) while the X axis represent time (minutes).

		Alphaxalone	Keto-alphaxalone	Beta-alphaxalone
Alphaxalone administration	Male LM	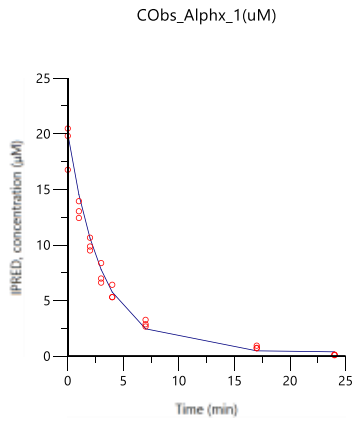	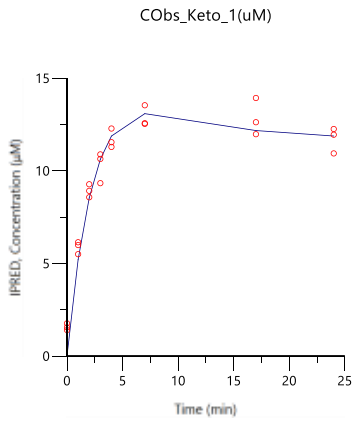	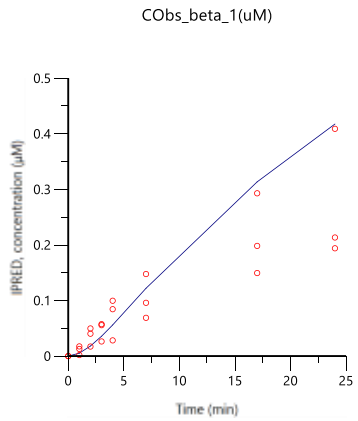
	Female LM	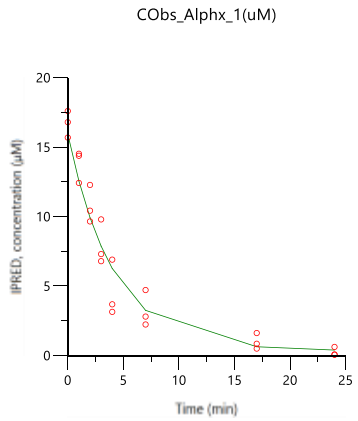	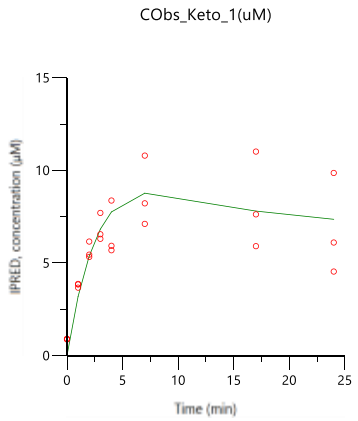	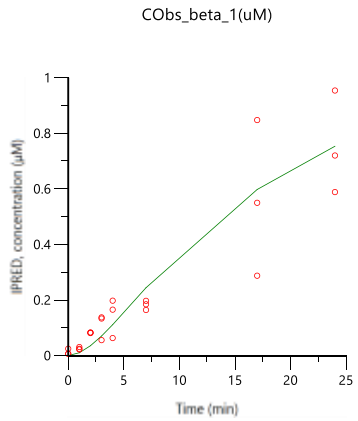

Figure 8.27. Model fit of alphaxalone substrate and keto-alphaxalone and beta-alphaxalone formation from male and female rhesus monkey liver microsomes. The Y axis represent substrate concentration (μM) while the X axis represent time (minutes).

		Alphaxalone	Keto-alphaxalone	Beta-alphaxalone
Keto-alphaxalone administration	Male LM	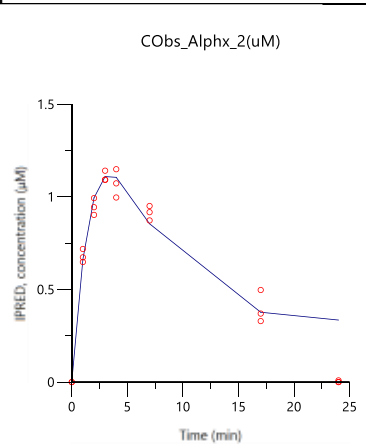	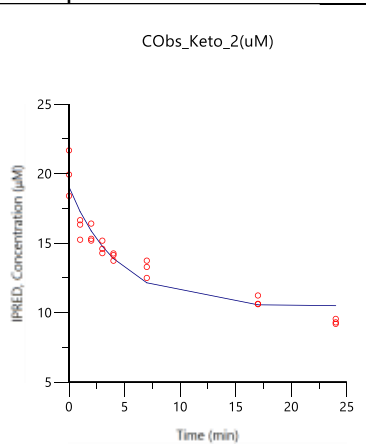	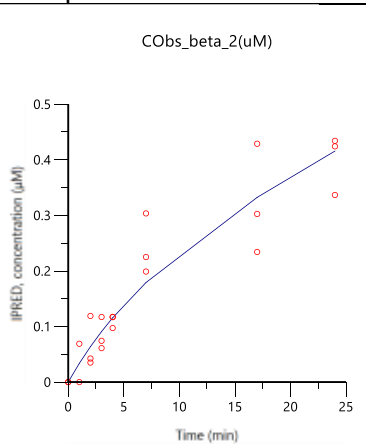
	Female LM	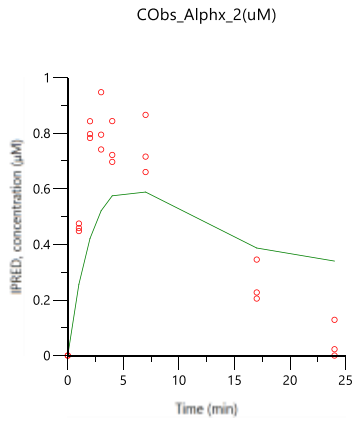	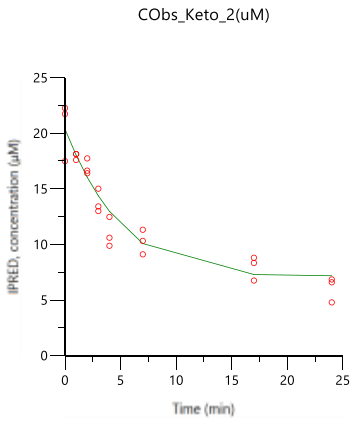	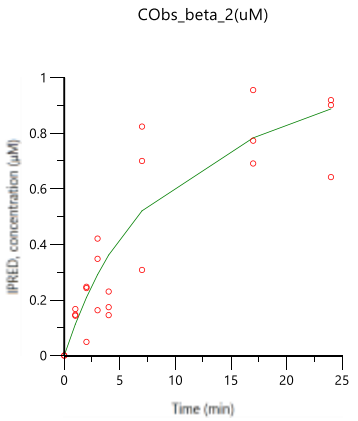

Figure 8.28. Model fit of keto-alphaxalone substrate and alphaxalone and beta-alphaxalone formation from male and female rhesus monkey liver microsomes. The Y axis represent substrate concentration (µM) while the X axis represent time (minutes).

		Alphaxalone	Keto-alphaxalone	Beta-alphaxalone
Beta-alphaxalone administration	Male LM	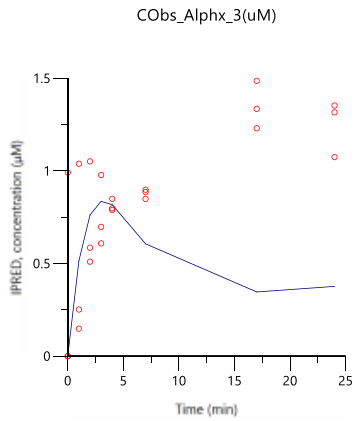	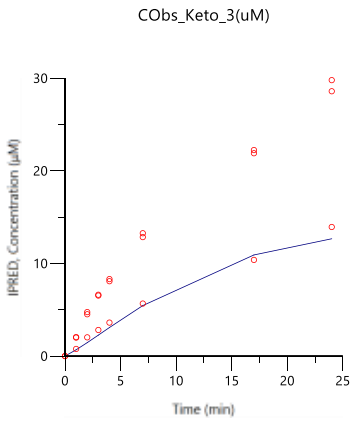	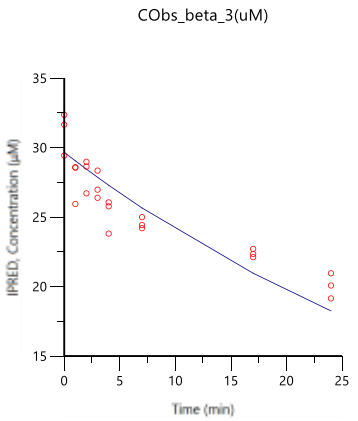
	Female LM	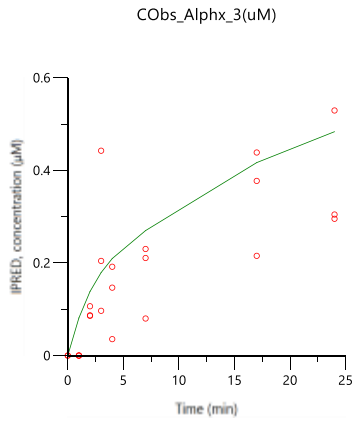	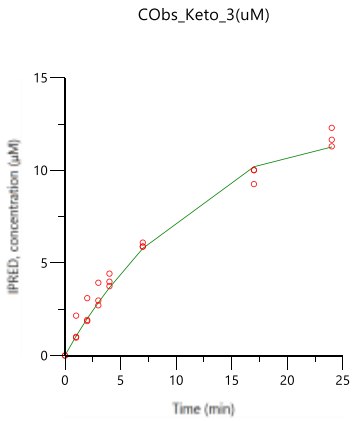	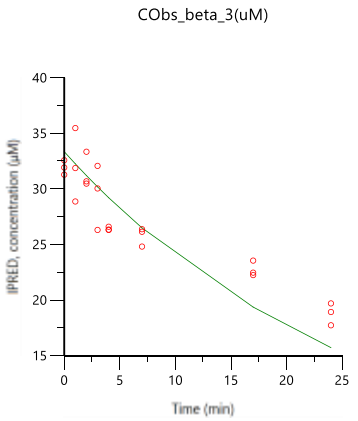

Figure 8.29. Model fit of beta-alphaxalone substrate and alphaxalone and keto-alphaxalone formation from male and female rhesus monkey liver microsomes. The Y axis represent substrate concentration (µM) while the X axis represent time (minutes).